

LONDON
SCHOOL of
HYGIENE
& TROPICAL
MEDICINE



LSHTM Research Online

Liaw, J; (2020) Investigation of the Role of the *Campylobacter jejuni* Type VI Secretion System in Bacterial Secretion of Virulence Factors and Interactions with Host Cells. PhD thesis, London School of Hygiene & Tropical Medicine. DOI: <https://doi.org/10.17037/PUBS.04657129>

Downloaded from: <https://researchonline.lshtm.ac.uk/id/eprint/4657129/>

DOI: <https://doi.org/10.17037/PUBS.04657129>

Usage Guidelines:

Please refer to usage guidelines at <https://researchonline.lshtm.ac.uk/policies.html> or alternatively contact researchonline@lshtm.ac.uk.

Available under license. To note, 3rd party material is not necessarily covered under this license: <http://creativecommons.org/licenses/by-nc-nd/3.0/>

<https://researchonline.lshtm.ac.uk>

LONDON
SCHOOL of
HYGIENE
& TROPICAL
MEDICINE



**Investigation of the Role of the
Campylobacter jejuni Type VI Secretion System
in Bacterial Secretion of Virulence Factors
and Interactions with Host Cells**

JANIE LIAW

Thesis submitted in accordance with the requirements for the degree of
Doctor of Philosophy
of the
University of London

April 2020

**Department of Infection Biology
Faculty of Infectious and Tropical Diseases
LONDON SCHOOL OF HYGIENE & TROPICAL MEDICINE**

Declaration

I, Janie Liaw, confirm that the work presented in this thesis is my own. Where information has been derived from other sources, I confirm that this has been indicated in the thesis.

Abstract

Campylobacter jejuni is a leading cause of bacterial gastroenteritis worldwide. An increasing number of *C. jejuni* strains possess a Type VI Secretion System (T6SS) capable of delivering bacterial effector proteins across a bacterial or host membrane. Despite this increasing prevalence of T6SS-positive *C. jejuni* isolates, the role of the T6SS is still not well understood. Phenotypic comparisons were performed between 488 (a T6SS-positive human clinical isolate from Brazil), a number of 488 isogenic defined mutants in genes encoding essential T6SS components and also 81-176 (a laboratory reference T6SS-negative strain). The T6SS serves a major role in bacterial competition in some bacteria. However in this study, competition assays performed with T6SS-positive against either T6SS-negative *C. jejuni* or *E. coli* did not reveal any significant differences. Expression of T6SS genes in the 488 strain by RT-PCR and secretion of the TssD needle-like component into the culture supernatant were indicative that the T6SS is functional. qRT-PCR analysis of T6SS gene expression demonstrated that *tssD* expression is up-regulated in the presence of 0.1% (w/v) sodium deoxycholate, a secondary bile salt. The 488 wild-type strain was significantly more resistant to the effects of oxidative stress, more interactive and invasive in a chicken cell line, more cytotoxic in the *Galleria mellonella* infection model and was able to colonise chickens in higher numbers compared to a 488 *tssD* mutant and the T6SS-negative 81-176 strain. Whole genome sequencing of the 488 strain was performed to analyse the T6SS cluster. Comparisons with previously sequenced strains identified a highly conserved T6SS cluster in strains isolated from humans and chickens. In order to identify potential T6SS effectors in *C. jejuni*, mass spectrometry was performed to compare the secretome of the 488 strain with that of a 488 *tssBC* contractile sheath double mutant. Bioinformatic analyses revealed the presence of multiple VgrGs in *C. jejuni* strains and identified a putative effector-immunity module associated with the *C. jejuni* T6SS. This study expanded on the knowledge of the function of the *C. jejuni* T6SS and highlighted the importance of the T6SS during *in vivo* survival of T6SS-positive *C. jejuni* strains.

Table of Contents

Declaration.....	2
Abstract.....	3
Table of Contents.....	4
Acknowledgements.....	10
CHAPTER ONE: Introduction	11
1.1 <i>Campylobacter jejuni</i>	11
1.1.1 General characteristics	11
1.1.2 History.....	12
1.1.3 Transmission.....	13
1.1.4 Disease	15
1.1.5 Epidemiology	15
1.2 <i>C. jejuni</i> Pathogenesis	17
1.2.1 Flagella.....	17
1.2.2 Capsular polysaccharide	18
1.2.3 Lipooligosaccharide.....	18
1.2.4 Glycosylation	19
1.2.5 Cytolethal distending toxin.....	19
1.2.6 Outer membrane vesicles	20
1.2.7 Oxidative stress response.....	20
1.3 Secretion systems in Gram-negative bacteria	22
1.3.1 General secretory (Sec) pathway	24
1.3.2 Twin-arginine translocation (Tat) pathway	26
1.3.3 Type I secretion system (T1SS).....	27
1.3.4 Type II secretion system (T2SS).....	28
1.3.5 Type III secretion system (T3SS)	29
1.3.6 Type IV secretion system (T4SS).....	31
1.3.7 Type V secretion system (T5SS)	32
1.4 Type VI secretion system (T6SS)	33
1.4.1 History of the T6SS	33
1.4.2 Structure of the T6SS.....	34
1.4.3 Role of the T6SS.....	38
1.5 Type VI secretion system in <i>C. jejuni</i>	42

1.5.1	Role of the Type VI secretion system in <i>C. jejuni</i>	42
1.5.2	Prevalence of the Type VI secretion system in <i>Campylobacter</i> spp.	43
1.6	Aims and Objectives	45
CHAPTER TWO: Materials and Methods		46
2.1	Chemicals and reagents	46
2.2	Bacterial strains and growth conditions	46
2.3	Assays.....	49
2.3.1	Growth kinetics	49
2.3.2	Motility	49
2.3.3	Biofilm formation	49
2.3.4	Oxidative stress assay	50
2.3.5	Haemolysis assay	50
2.3.6	Bacterial competition assay	51
2.3.7	Bicinchoninic acid (BCA) protein assay.....	51
2.3.8	Sodium taurocholate (ST) stress	52
2.3.9	Antimicrobial susceptibility – Disk diffusion.....	52
2.3.10	Antimicrobial susceptibility – Broth microdilution.....	53
2.4	Cell culture techniques	53
2.4.1	Cell culture.....	53
2.4.2	Interaction and invasion assays of T84 and HCT-8 colonic epithelial cells.....	54
2.4.3	Interaction and invasion with primary chicken intestinal epithelial cells.....	55
2.5	<i>In vivo</i> infection models	55
2.5.1	<i>Galleria mellonella</i> infection model.....	55
2.5.2	Chicken infection model	56
2.6	Molecular techniques	57
2.6.1	Primer design	57
2.6.2	Genomic DNA (gDNA) isolation	60
2.6.3	Polymerase chain reaction (PCR)	60
2.6.4	PCR purification	61
2.6.5	Gel electrophoresis.....	62
2.6.6	Mutagenesis strategy.....	62
2.6.7	Insertion of antibiotic resistance cassette into gene of interest.....	63
2.6.8	Transformation into <i>E. coli</i> competent cells	64
2.6.9	Screening for positive transformants	64
2.6.10	Isolation of plasmid DNA.....	65

2.6.11	Preparation of <i>C. jejuni</i> competent cells	65
2.6.12	Transformation via electroporation.....	66
2.6.13	Screening for positive <i>C. jejuni</i> mutants.....	66
2.6.14	Inverse PCR mutagenesis (IPCRM)	67
2.6.15	Double mutagenesis strategy	68
2.6.16	Complementation.....	68
2.6.17	Ribonucleic acid (RNA) isolation.....	70
2.6.18	Complementary DNA (cDNA) synthesis	71
2.6.19	Reverse transcription PCR (RT-PCR)	72
2.6.20	Quantitative real-time PCR (qRT-PCR)	72
2.6.21	Whole cell lysate (WCL) extraction	73
2.6.22	Protein secretion.....	74
2.6.23	Trichloroacetic acid (TCA) precipitation.....	74
2.6.24	OMV isolation	74
2.6.25	SDS-PAGE	75
2.6.26	Antibody production	75
2.6.27	Western blot.....	75
2.6.28	Silver staining	76
2.6.29	SYPRO Ruby protein staining	77
2.6.30	Imperial protein staining	77
2.6.31	Whole genome sequencing	77
2.6.32	Bioinformatic searches for known effector proteins.....	78
2.6.33	Mass spectrometry sample preparation.....	78
2.6.34	Liquid chromatography mass spectrometry.....	80
2.6.35	Functional enrichment	82
2.7	Statistical analysis.....	82
CHAPTER THREE: Characterisation of <i>Campylobacter jejuni</i> T6SS-positive strains and T6SS mutants		83
3.1	INTRODUCTION.....	83
3.2	RESULTS.....	84
3.2.1	Selection of T6SS-positive <i>C. jejuni</i> strains	84
3.2.2	Construction of <i>C. jejuni</i> 488 <i>tssC</i> mutant.....	86
3.2.3	Growth kinetics of <i>C. jejuni</i> 488 wild-type strain and 488 <i>tssC</i> mutant.....	88
3.2.4	Motility of <i>C. jejuni</i> 488 wild-type strain and 488 <i>tssC</i> mutant	89
3.2.5	Haemolysis of <i>C. jejuni</i> 488 wild-type strain and 488 <i>tssC</i> mutant.....	90

3.2.6	Construction of <i>C. jejuni</i> 488 <i>tssB</i> mutant	92
3.2.7	Construction of <i>C. jejuni</i> 488 <i>tssBC</i> double mutant	93
3.2.8	Construction of <i>C. jejuni</i> 488 <i>tssD</i> mutant.....	94
3.2.9	Growth kinetics of <i>C. jejuni</i> 488 wild-type strain, 488 <i>tssBC</i> double mutant and 488 <i>tssD</i> mutant	95
3.2.10	Motility of <i>C. jejuni</i> 488 wild-type strain, 488 <i>tssBC</i> double mutant and 488 <i>tssD</i> mutant	96
3.2.11	Biofilm formation of <i>C. jejuni</i> 488 wild-type strain, 488 <i>tssBC</i> double mutant, and 488 <i>tssD</i> mutant	97
3.2.12	Complementation of <i>C. jejuni</i> 488 <i>tssD</i> mutant.....	98
3.2.13	Bacterial competition with the 488 wild-type strain, 488 <i>tssD</i> mutant and 81-176 wild-type strain	99
3.2.14	Bacterial competition with the 488 wild-type strain and 11168H <i>kpsM</i> mutant 101	
3.2.15	Bacterial competition with the 488 wild-type strain and 43431 <i>tssD</i> mutant..	102
3.2.16	Bacterial competition with the 43431 wild-type strain and 488 <i>tssD</i> mutant..	103
3.2.17	Bacterial competition with the 488 wild-type strain, 488 <i>tssD</i> mutant and <i>E. coli</i> DHB10 GFP	104
3.3	DISCUSSION	105
3.4	CONCLUSION	110
CHAPTER FOUR: Investigation of the role of the Campylobacter jejuni Type VI Secretion System.....		111
4.1	INTRODUCTION.....	111
4.2	RESULTS.....	112
4.2.1	Analysis of T6SS gene expression in the 488 wild-type strain using RT-PCR 112	
4.2.2	Presence of TssD in whole cell lysates of <i>C. jejuni</i> wild-type strains	113
4.2.3	Secretion of TssD in <i>C. jejuni</i> wild-type strains and mutants.....	115
4.2.4	Presence of TssD in outer membrane vesicles from <i>C. jejuni</i> wild-type strains and mutants.....	117
4.2.5	Presence of VgrG in <i>C. jejuni</i> wild-type strains	118
4.2.6	Analysis of the effect of sodium taurocholate on T6SS gene expression in 488 wild-type strain	119
4.2.7	Analysis of the effect of sodium deoxycholate on T6SS gene expression in the 488 wild-type strain	121
4.2.8	Resistance to oxidative stress of the 488 wild-type strain, 488 <i>tssD</i> mutant, 488 <i>tssD</i> complement and 81-176 wild-type strain	124

4.2.9	Membrane integrity of the 488 wild-type strain, 488 <i>tssD</i> mutant and 488 <i>tssD</i> complement	126
4.2.10	Analysis of <i>katA</i> , <i>sodB</i> and <i>ahpC</i> expression in the 488 wild-type strain and 488 <i>tssD</i> mutant using qRT-PCR	128
4.2.11	The T6SS increases <i>C. jejuni</i> cytotoxicity in the <i>Galleria mellonella</i> model of infection	129
4.2.12	Interactions with and invasion of a human colonic epithelial cell line by the 488 wild-type strain, 488 <i>tssD</i> mutant and 81-176 wild-type strain	130
4.2.13	Interactions with and invasion of primary chicken intestinal epithelial cells by the 488 wild-type strain, 488 <i>tssD</i> mutant, and 81-176 wild-type strain.....	132
4.2.14	Chick infection with the 488 wild-type strain, 488 <i>tssD</i> mutant, and 81-176 wild-type strain	134
4.3	DISCUSSION	135
4.4	CONCLUSION	142
CHAPTER FIVE: Analysis of the <i>Campylobacter jejuni</i> T6SS secretome and identification of potential T6SS effectors		143
5.1	INTRODUCTION.....	143
5.2	RESULTS.....	144
5.2.1	Bioinformatics analysis of T6SS gene clusters in the <i>C. jejuni</i> 488 and other T6SS-positive strains reveals synteny	144
5.2.2	Bioinformatics searches identified no known effector proteins in the <i>C. jejuni</i> 488 and 43431 strains	146
5.2.3	Comparison of secretome profiles of the 488 wild-type strain and mutants ...	151
5.2.4	Mass spectrometry analysis identified proteins more abundant in the secretome of the 488 wild-type strain than the 488 <i>tssBC</i> double mutant.....	153
5.2.5	Mass spectrometry analysis identified proteins more abundant in the secretome of the 488 <i>tssBC</i> double mutant than the 488 wild-type strain.....	155
5.2.6	Curation of secreted proteins	167
5.2.7	Functional enrichment and domain analyses	168
5.2.8	Multiple VgrGs identified in T6SS-positive <i>C. jejuni</i> strains.....	175
5.3	DISCUSSION	184
5.4	CONCLUSION	191
CHAPTER SIX: Final Discussion		192
6.1	SUMMARY	192
6.2	FUTURE WORK	193
REFERENCES		196
APPENDICES		215
Appendix 1: <i>C. jejuni</i> 488 strain genome coordinates.....		215

Appendix 2: Amino acid sequences of known T6SS effector proteins	216
Appendix 3: List of secreted proteins and database predictions.....	224
Appendix 4: <i>C. jejuni</i> T6SS manuscript	244

Acknowledgements

My journey here would not have been possible without the support of many wonderful individuals.

First and foremost, I would like to express my sincere gratitude to my supervisors Professor Nick Dorrell and Dr Ozan Gundogdu for their constant guidance and support. Nick, thank you for all your advice, patience, and encouragement. Ozan, thank you for all your guidance, assistance, and for the endless coffee sessions.

I would like to thank members of the *Campylobacter* group – both past and present – for their assistance. I would like to thank Dr Abdi Elmi for his advice and support. I am very grateful for the encouragement and support from Cadi Davies and Geunhye (Gemma) Hong, and would also like to thank Zahra Omole, Coco Kerridge, Dr Fauzy Nasher, Dr Mahjanah Hussein, and Dr Daiani Teixeira da Silva for their assistance. I would like to acknowledge Gemma for her help with the oxidative stress and *Galleria* work, Zahra for her help with growth, motility and biofilm formation, and Coco for her help with mutant construction. I would like to thank Professor Brendan Wren and the Wren group for their support throughout my time here.

I would like to offer a sincere thank you to my collaborators: My advisory committee Dr Abdou Hachani at the University of Melbourne for his guidance and expertise. Professor Nicolae Corcionivoschi at the Agri-Food and Biosciences Institute for his support and assistance with the antibodies and chicken model study. Dr Dong Xia at the Royal Veterinary College for his guidance and help with proteomics and functional analysis. Dr Stuart Armstrong at the University of Liverpool for his assistance with the mass spectrometry. Dr Anna Grabowska for her help and advice with mutant construction.

I am forever grateful to my amazing family – Chi-Shyan, Lilan, Lily, and Frank – and to my partner – Tim – for their selflessness, wonderful words of encouragement and unwavering support throughout the years. Thank you for always being there for me.

CHAPTER ONE: Introduction

1.1 *Campylobacter jejuni*

1.1.1 General characteristics

Campylobacter jejuni is a Gram-negative bacterium that is the leading cause of foodborne gastroenteritis worldwide. *C. jejuni* is microaerophilic and prefers low oxygen environments, growing optimally in 85% nitrogen, 10% carbon dioxide and 5% oxygen (Park, 2002). The optimum growth temperature for *C. jejuni* is 42°C, the body temperature of avian species; however the bacterium is also capable of growth at 37°C, the body temperature of humans, and experiences significantly reduced levels of growth at temperatures lower than 30°C (Young et al., 2007, Park, 2002).

C. jejuni varies from 0.2 to 0.8 µm in width and 0.5 to 5.0 µm in length. The bacterium is motile with uni- or bi-polar flagella (Bolton, 2015). *C. jejuni* is typically spiral- or curved rod-shaped but can be pleomorphic dependent on phase of growth or environmental conditions, presenting as coccoid forms under nutrient-limiting conditions (Thomas et al., 1999). *C. jejuni* can enter a viable but non-culturable (VBNC) state when exposed to low-temperature and nutrient-depleted environments (Tholozan et al., 1999).

1.1.2 History

Campylobacter spp. were only recognised and isolated in recent decades, however their presence and ability to cause disease have been reported since the late 19th century. In 1886, Escherich described in a report of the presence of spiral-shaped bacteria that was unable to be cultured in the stool specimens of children and infants with diarrhoeal disease (Escherich, 1886); however his report was not known to the wider scientific community until it was presented at a conference by Kist in 1986 (Kist, 1986). In 1909, McFadyean and Stockman described the presence of a bacterium resembling a vibrio in the uterine mucus of sheep and were able to isolate the bacterium from aborted bovine foetuses in 1913 (McFadyean and Stockman, 1913). This bacterium was classified as *Vibrio fetus* by Smith and Taylor in 1919 (Smith and Taylor, 1919). *Vibrio jejuni* was described in bovine dysentery and named by Jones et al. in 1931 and *Vibrio coli* was later observed in swine dysentery by Doyle in 1944 (Jones et al., 1931, Doyle, 1944). These organisms were recognised to form a distinct genus and renamed from *Vibrio* spp. to *Campylobacter* spp. by Sebald and Véron in 1963 (Sebald and Véron, 1963).

Despite numerous attempts to culture *Campylobacter jejuni* since it was first identified, this proved to be difficult until 1968 when Butzler and Dekeyser isolated *C. jejuni* from blood and faecal samples from a patient with severe diarrhoea and high fever (Dekeyser et al., 1972). In 1977, Skirrow developed a selective culture medium with the addition of vancomycin, trimethoprim and polymyxin B that allowed for more straightforward isolation of *C. jejuni* from stool samples (Skirrow, 1977). Chickens were suggested to be the primary source of *C. jejuni* infection for humans by King in 1962, then Skirrow in 1977 postulated that *C. jejuni* must be widespread amongst poultry flocks and advocated proper food handling and hygiene to prevent infection (King, 1962, Skirrow, 1977).

1.1.3 Transmission

C. jejuni is most commonly transmitted through the handling and consumption of raw or undercooked poultry, but can also be spread through unpasteurised milk, contaminated water and cross contamination with other foods (Figure 1.1) (Young et al., 2007, Kaakoush et al., 2015). *C. jejuni* colonises chickens and other avian species and an estimated 70% of raw chicken sold in supermarkets in the United Kingdom will be contaminated with *C. jejuni* (Kaakoush et al., 2015). *C. jejuni* was previously regarded as a harmless commensal in the digestive tract of chickens, but recent studies indicate that colonisation by *C. jejuni* is not asymptomatic, resulting in weight loss and slow growth of the infected poultry (Hermans et al., 2012, Wigley, 2015). The spread of *C. jejuni* through chicken flocks in farms can have a vast economic impact on the poultry industry and an increased spread of *C. jejuni* in chickens can subsequently affect the rates of infection in humans (Newell and Fearnley, 2003, Skarp et al., 2016).

Wild birds are suggested to be a reservoir for *C. jejuni* to infect humans via faecal contamination of surfaces or drinking water (Cody et al., 2015). It was proposed that wild birds can contaminate food or drinking water of farmed poultry, particularly on free-range or organic farms where poultry have more access to the outdoors; however this link has not been demonstrated (Colles et al., 2008). *C. jejuni* can also infect other animals such as cattle, sheep, dogs and cats. Transmission of multidrug-resistant strains of *C. jejuni* through puppies in pet stores to humans has led to recent outbreaks in the United States (Montgomery et al., 2018).

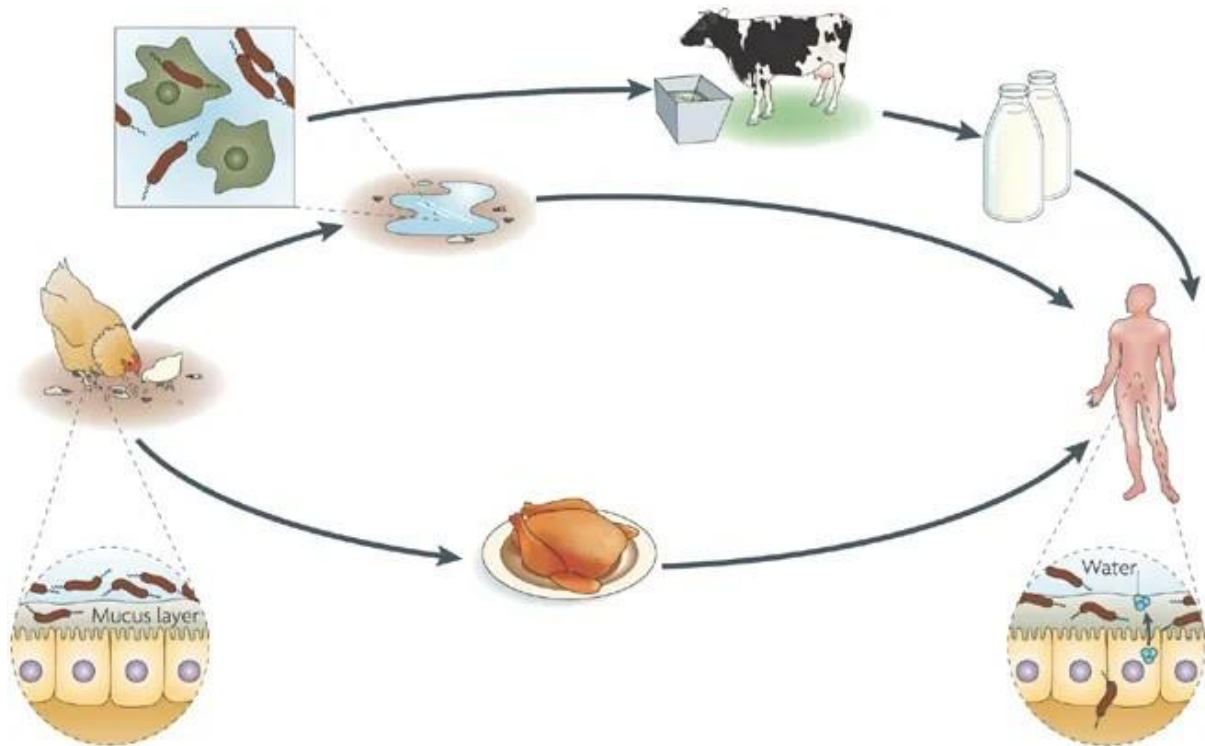


Figure 1.1. Transmission of *C. jejuni*. Human infection of *C. jejuni* can be through consumption of raw or undercooked chicken or through the drinking of contaminated milk. *C. jejuni* can also contaminate the water supply and are associated with freshwater amoebae. Image obtained from Young et al. (2007).

1.1.4 Disease

C. jejuni infection in humans can lead to diarrhoea, vomiting, abdominal pain, fever, with symptoms generally appearing 2 to 5 days following exposure to an infectious dose as low as 500-900 bacteria (Kaakoush et al., 2015, Robinson, 1981). Disease presentation can vary depending on geographical region, with infections in low- and middle-income countries typically presenting with watery, non-inflammatory diarrhoea whilst infections in high income countries display more severe disease, presenting with bloody inflammatory diarrhoea (Coker et al., 2002). *C. jejuni* infection can lead to bacteraemia and septicaemia, often in young, elderly or immunocompromised patients and resulting in poor prognosis.

Campylobacteriosis is generally self-limiting, however around 1 in 1,000 cases can develop severe auto-immune complications such as Guillain-Barré syndrome or Miller Fisher syndrome (Ang et al., 2001). *C. jejuni* infection can also cause other post-infection sequelae such as Reiter syndrome, inflammatory bowel diseases, irritable bowel syndrome and oesophageal diseases (Kaakoush et al., 2015).

1.1.5 Epidemiology

C. jejuni is the leading cause of foodborne gastroenteritis, resulting annually in more than 400 million cases worldwide, with an estimated 500,000 cases in the United Kingdom and an economic burden of £900 million (FSA, 2014). Cases of campylobacteriosis are likely to be severely underreported due to the self-limiting nature of the disease (Young et al., 2007). The number of laboratory-confirmed cases of campylobacteriosis in England and Wales is reported by Public Health England to be between 50,000 and 60,000 annually from 2008 to 2017 (Figure 1.2) (PHE, 2017a). Surveillance by Health Protection Scotland revealed 6,096 laboratory-confirmed cases in 2018 (Scotland, 2019). Public Health England and Health Protection Scotland reported a rise in the number of cases in recent years following a decrease in 2015-2016. In the United States, surveillance by CDC revealed the number of laboratory-confirmed cases to be 9,723 in 2018 (Tack et al., 2019). Due to most cases remaining undiagnosed or unreported, CDC estimates approximately 1.5 million people per year in the United States suffer from campylobacteriosis (CDC, 2019).

Data from Public Health England indicate a seasonal trend associated with *Campylobacter* infections, with the number of reported cases peaking in the summer. Gender and age group also factors, with the number of reported cases highest in men between 50 and 59 years old. Foodborne outbreaks caused by *Campylobacter* spp. is most commonly associated with the consumption of improperly prepared chicken liver pate or parfait (PHE, 2017a). Infection with *Campylobacter* spp. can also be travel-associated, with 2 to 3% of cases annually associated with foreign travel (PHE, 2017b).

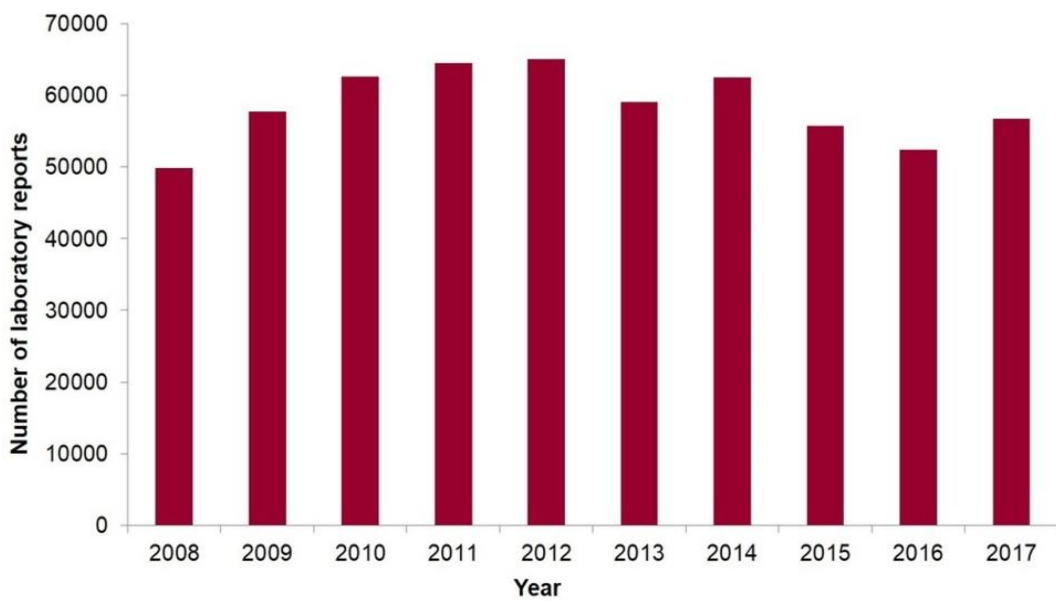


Figure 1.2. Laboratory-confirmed cases of *Campylobacter* infection in England and Wales from 2008 to 2017. Figure obtained from Public Health England (2017a).

1.2 *C. jejuni* Pathogenesis

1.2.1 Flagella

The uni- or bi-polar flagellum of *C. jejuni* is a crucial virulence determinant, required not only for motility and chemotaxis but also proposed to be involved in the secretion of virulence and colonisation factors and evasion of the immune response (Young et al., 2007, Guerry, 2007). The *C. jejuni* flagellum consists of three primary structural components – a basal body and a hook spanning both inner and outer membranes, and also an extracellular filament (Lertsethtakarn et al., 2011). The flagella filament is composed of highly homologous flagellins, with FlaA as the major flagellin and FlaB as the minor flagellin (Guerry, 2007). Regulation of the flagella is via sigma factors σ^{54} and σ^{28} , encoded by *rpoN* and *fliA* respectively (Jagannathan et al., 2001). The phase-variable FlgSR two-component regulatory system is also involved in flagellar gene regulation (Hendrixson, 2006, Joslin and Hendrixson, 2009).

The flagellum is crucial for *C. jejuni* to colonise host intestines and is particularly important for the movement of *C. jejuni* in highly viscous solutions, such as the mucus lining of the intestinal tract (Lee et al., 1986, Black et al., 1988). Chemotaxis is the movement of a bacterium towards an increased gradient of favourable chemicals or stimuli or away from noxious substances, allowing the bacterium to efficiently respond to and survive in a rapidly changing environment (Bren and Eisenbach, 2000). *C. jejuni* is chemotactic towards amino acids such as L-aspartate, L-cysteine, L-glutamate and L-serine, as well as organic acids such as citrate, fumarate, malate, pyruvate, succinate and alpha-ketoglutarate (Hugdahl et al., 1988). In addition, *C. jejuni* is attracted to constituents of mucus but repelled by components of bile except for L-fucose. Chemoattractants for *C. jejuni* are demonstrated to be beneficial to the growth of the bacterium (Vegge et al., 2009).

C. jejuni lacks the Type III and Type IV secretion systems typically associated with enteric pathogens and it is proposed that the *C. jejuni* flagellum is capable of the secretion of virulence factors (Guerry, 2007). Studies indicate that the flagellum functions similarly to a Type III secretion system (T3SS), with components homologous to the T3SS such as FlhA, FlhB, FliO, FliP, FliQ and FliR present in the flagellar base (Lertsethtakarn et al., 2011). The *C. jejuni* flagellum is required for the secretion of *Campylobacter* invasion antigens (Cia proteins), FlaC, and FspA (Konkel et al., 2004, Song et al., 2004, Poly et al., 2007).

CiaB is proposed to be important in mediating the invasion and translocation of *C. jejuni* into epithelial cells (Konkel et al., 1999). FlaC is a flagellin-like protein with roles in cell invasion and modulation of the host immune response (Song et al., 2004, Faber et al., 2016). FspA is heterogenous amongst *C. jejuni* strains and can be present in two different variants – FspA1 and FspA2; FspA2 enhances *C. jejuni* interaction with epithelial cells and induces apoptosis of epithelial cells, whilst the role of FspA1 remains unknown. Heterogeneity of FspA is suggested as a potential explanation for the differences in disease severity produced by different *C. jejuni* strains (Poly et al., 2007).

1.2.2 Capsular polysaccharide

The presence of a polysaccharide capsule in *C. jejuni* was first demonstrated by Karlyshev et al. (Karlyshev et al., 2000, Karlyshev et al., 2001). The capsular polysaccharide (CPS) is the primary serodeterminant of the Penner serotyping system which differentiates *C. jejuni* isolates into 47 recognised serotypes (Penner et al., 1983, Pike et al., 2013). Extensive variation in the capsular structure due to differences in the composition and linkage of the sugars in addition to modifications with glycerol, ethanolamine and *O*-methyl phosphoramidate are a result of widespread horizontal gene transfer and phase variation (Karlyshev et al., 2005, Guerry et al., 2012). The polysaccharide capsule of *C. jejuni* is involved in serum resistance, modulation of the host immune response, adherence and invasion of host epithelial cells, host colonisation and virulence in *in vivo* mammalian, avian and insect models (Bacon et al., 2001, Maue et al., 2013, Jones et al., 2004, Champion et al., 2010).

1.2.3 Lipooligosaccharide

Lipooligosaccharides (LOS) are major phosphorylated glycolipids located in the outer membrane of Gram-negative bacteria and play an important role in virulence (Preston et al., 1996). The LOS of *C. jejuni* consists of a lipid A component, a conserved inner core and a highly variable outer core region, A high degree of variation is present in the structures of the LOS encoded by the LOS biosynthesis loci as a result of differences in the composition and linkages of monosaccharide components (Parker et al., 2008). The *C. jejuni* LOS is responsible for Guillain-Barré syndrome and Miller-Fisher syndrome due to molecular

mimicry of human gangliosides (Houliston et al., 2011). Extensive variation of the LOS is important in the ability of *C. jejuni* to avoid the host immune response (Young et al., 2007).

1.2.4 Glycosylation

Two protein glycosylation systems – O-linked glycosylation and N-linked glycosylation – are found to be present in *C. jejuni* (Szymanski et al., 2003). The O-linked flagellin glycosylation system extensively modifies the surface-exposed region of the *C. jejuni* flagellar filament with pseudaminic acid, with glycosylation of 19 serine and threonine residues of the central domain of the flagellin (Thibault et al., 2001). Studies have indicated that O-linked glycosylation of the flagellin may be involved in autoagglutination and virulence in a ferret diarrhoeal disease model (Guerry et al., 2006). The precise mechanisms and functions of the O-linked flagellin glycosylation system remains to be elucidated.

The N-linked general glycosylation system links glycans to proteins by attaching to asparagine residues located in potential glycosylation sites with the sequon Asn-Xaa-Ser/Thr (Young et al., 2002). The N-linked glycosylation pathway is utilised by eukaryotes and archaea and was subsequently identified to be present also in *C. jejuni* (Szymanski et al., 1999). The highly-conserved genes in the locus are termed *pgl* for protein glycosylation and are involved in the N-linked glycosylation of over 60 periplasmic and membrane-bound proteins (Nothaft and Szymanski, 2013). Defects in N-linked glycosylation in *C. jejuni* lead to reduction in adherence and invasion of intestinal epithelial cells and host colonisation in animal models (Szymanski et al., 2003). The PglB oligosaccharyltransferase is essential for transferring heptasaccharides to the asparagine residues and has been exploited for the generation of glycoconjugate vaccines (Cuccui and Wren, 2015).

1.2.5 Cytolethal distending toxin

The cytolethal distending toxin (CDT) is a heat-labile toxin first identified in *Campylobacter* spp. by Johnson and Lior; CDT was also described in *Escherichia coli* and *Shigella dysenteriae* (Johnson and Lior, 1988). The CDT toxin is composed of three subunits – CdtA, CdtB and CdtC – all of which are crucial for toxicity (Lara-Tejero and Galan, 2001). The active subunit CdtB is delivered into host cells by carrier subunits CdtA and CdtC which bind to receptors in the plasma membrane (Young et al., 2007); CdtA and CdtC contain a

cholesterol-binding motif and are associated with lipid rafts (Boesze-Battaglia et al., 2009). The enzymatic subunit CdtB is internalised and the DNase I activity of CdtB leads to DNA double-strand breaks and cell-cycle arrest at G₁/S transition or G₂/M damage checkpoint phases, resulting in targeted cell death (Lai et al., 2016); CdtB also has PIP3 phosphatase activity that leads to T-cell apoptosis (Shenker et al., 2014). CDT secreted by *C. jejuni* is associated with inducing secretion of pro-inflammatory chemokine interleukin-8 (IL-8) via activation of NF- κ B in human intestinal epithelial cells (Zheng et al., 2008).

1.2.6 Outer membrane vesicles

Outer membrane vesicles (OMVs) play an important role in many bacterial pathogens for the delivery of virulence factors into host cells (Elmi et al., 2012). In *C. jejuni*, OMVs have been shown to secrete a range of virulence factors including CDT and three serine proteases – HtrA, Cj0511 and Cj1365c (Lindmark et al., 2009, Elmi et al., 2016). *C. jejuni* OMVs induce pro-inflammatory cytokine responses in intestinal epithelial cells and mediate cleavage of the tight and adherens junction proteins E-cadherin and occludin, enhancing the ability of *C. jejuni* to adhere to and invade intestinal epithelial cells (Elmi et al., 2012, Elmi et al., 2016). OMV production is mediated by physiological concentrations of the primary bile salt sodium taurocholate and is regulated by the maintenance of lipid asymmetry (MLA) pathway (Elmi et al., 2018, Davies et al., 2019).

1.2.7 Oxidative stress response

During host colonisation and infection, *C. jejuni* is exposed to conditions in the host gastrointestinal tract that present as physical and chemical stresses, including oxidative stress (Flint et al., 2016, Kim et al., 2015). Oxidative stress involves the generation of reactive oxygen species (ROS) that cause damage to nucleic acids, membranes and proteins of bacteria. In order to survive in this hostile environment, *C. jejuni* must defend against oxidative stress with enzymes that degrade ROS, such as SodB (superoxide dismutase), KatA (catalase) and AhpC (hydroperoxide reductase) (Kim et al., 2015). KatA is a catalase that breaks down H₂O₂ to H₂O and O₂, SodB is an iron-co-factored superoxide dismutase that detoxifies superoxide and AhpC is an alkyl hydroperoxide reductase that scavenges endogenous H₂O₂ (Seaver and Imlay, 2001, Hwang et al., 2013, Kim et al., 2015). Regulation of the *C. jejuni* oxidative stress response is

controlled by multiple regulatory mechanisms involving PerR, Fur and CosR to respond to fluctuating levels of ROS. Two MarR-type transcriptional regulators, RrpA and RrpB, also play a role in oxidative stress response regulation (Gundogdu et al., 2015).

1.3 Secretion systems in Gram-negative bacteria

Bacteria possess an extensive and diverse array of machineries for the secretion of substrates such as proteins, DNA, and other small molecules across the phospholipid membrane (Figure 1.3). Secretion of substrates can occur in either a single or two-step process. The general secretory (Sec) and twin-arginine translocation (Tat) pathways can be utilised by both Gram-negative and Gram-positive bacteria, whilst the other systems are more specific. The Type I Secretion System (T1SS), T2SS, T3SS, T4SS, T5SS, T6SS and T8SS are found in Gram-negative bacteria; the T7SS is found only in *Mycobacteria* and the T9SS is found only in the *Bacteroidetes* phylum. Secretion systems and the mechanisms for secretion of substrates are discussed below with the focus on systems present in Gram-negative bacteria.

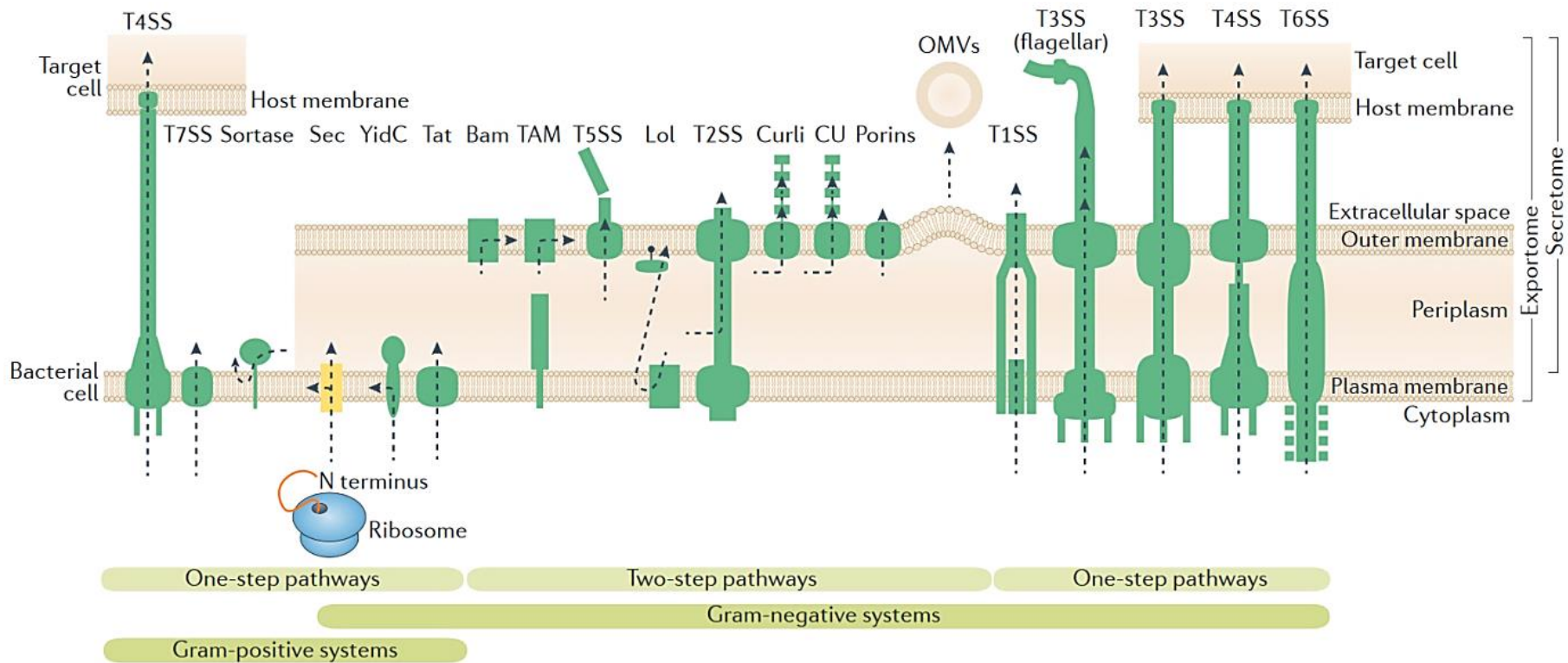


Figure 1.3. Secretion pathways of Gram-positive and Gram-negative bacteria. Major secretion pathways present in Gram-negative bacteria include the Sec- and Tat-secretion pathways, T1SS, T2SS, T3SS, T4SS, T5SS and T6SS. Image obtained from Tsirigotaki et al. (2017).

1.3.1 General secretory (Sec) pathway

The Sec pathway is present in all domains of life and translocates proteins in an unfolded state across the cytoplasmic membrane in Gram-negative bacteria (Tsirigotaki et al., 2017). Unfolded proteins with a hydrophobic N-terminal signal peptide can be translocated via two different routes – the SecB pathway or the signal recognition particle (SRP) pathway – dependent on the signal sequence present (Green and Meccas, 2016). In the SecB pathway, the SecB chaperone protein recognises the signal sequence, binds to the protein to prevent folding, then delivers the protein to the ATPase motor SecA. SecA directs the protein to the SecYEG channel and the protein is translocated across the periplasm, where the protein then becomes folded (Figure 1.4A) (Tsirigotaki et al., 2017). In the SRP pathway, the signal sequence is recognised by SRP and the membrane receptor FtsY and delivered to the SecYEG channel; instead of translocating proteins across to the periplasm, the SRP pathway is more commonly used in bacteria to integrate proteins into the cytoplasmic membrane (Figure 1.4B) (Natale et al., 2008). The Sec pathway is used by *E. coli*, *V. cholerae*, *K. pneumoniae* and many other bacteria for the translocation of virulence factors across the cytoplasmic membrane (Crane and Randall, 2017, Green and Meccas, 2016).

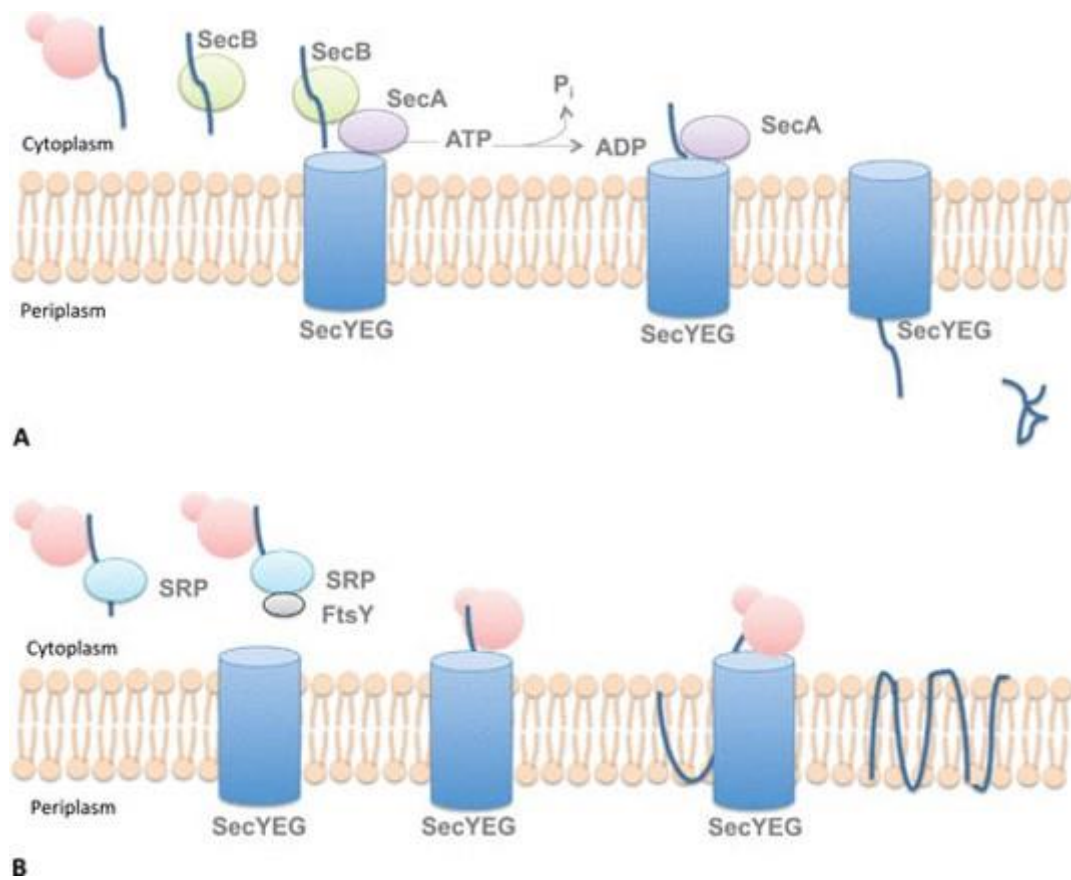


Figure 1.4. Secretion of proteins through the Sec pathway. (A) In the SecB pathway, SecB binds to the unfolded protein and delivers the protein to SecA. SecA directs the protein to the SecYEG channel and the protein is translocated to the periplasm where folding then occurs. (B) In the SRP pathway, signal sequence on the unfolded protein is recognised by SRP and FtsY and the protein is delivered to the SecYEG channel. The protein is then integrated into the cytoplasmic membrane. Image obtained from Green and Mecsas (2016).

1.3.2 Twin-arginine translocation (Tat) pathway

The Tat pathway translocates folded proteins across the cytoplasmic membrane (Figure 1.5). TatB and TatC subunits of the Tat system recognise and bind to proteins with an N-terminal Tat signal sequence consisting of a 'twin-arginine' motif (Lee et al., 2006). TatA is recruited by TatB and TatC and forms a channel, allowing translocation of the protein across the cytoplasmic membrane into the periplasm (Green and Mecsas, 2016). The Tat system is important in the transport of phospholipase C and other virulence factors in *P. aeruginosa*, *L. pneumophila* and other pathogens (Ochsner et al., 2002).

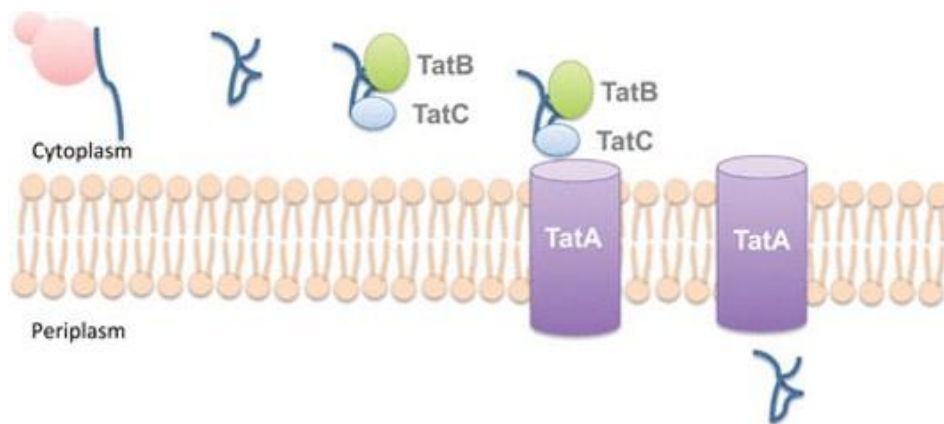


Figure 1.5. Secretion of proteins through the Tat pathway. Folded proteins with an N-terminal Tat signal sequence are recognised by and bind to TatB and TatC. TatB and TatC recruit TatA and form a channel, allowing translocation of the protein across the cytoplasmic membrane into the periplasm. Image obtained from Green and Mecsas (2016).

1.3.3 Type I secretion system (T1SS)

The T1SS spans across both the inner and outer membranes and transports protein substrates from the cytoplasm to the extracellular space in a single-step process (Figure 1.6). The T1SS is formed of three components – an inner-membrane-spanning ABC transporter protein, a periplasmic membrane fusion protein (MFP) and an outer-membrane factor TolC. Protein substrates bind to the ATP transporter and are transferred into the cavity of the MFP in the periplasm. Binding of the substrates to the ATP transporter and MFP results in TolC forming a channel in the outer membrane, subsequently allowing transport of the substrates into the extracellular space (Lee et al., 2012). T1SS substrates are frequently associated with virulence or nutrient acquisition, examples include haemolysin A (HlyA) of *E. coli*, iron scavenging protein HasA of *S. marcescens* and multifunctional autoprocessing repeats-in-toxin (MARTX) toxins of *V. cholerae* (Thomas et al., 2014, Masi and Wandersman, 2010, Dolores et al., 2015).

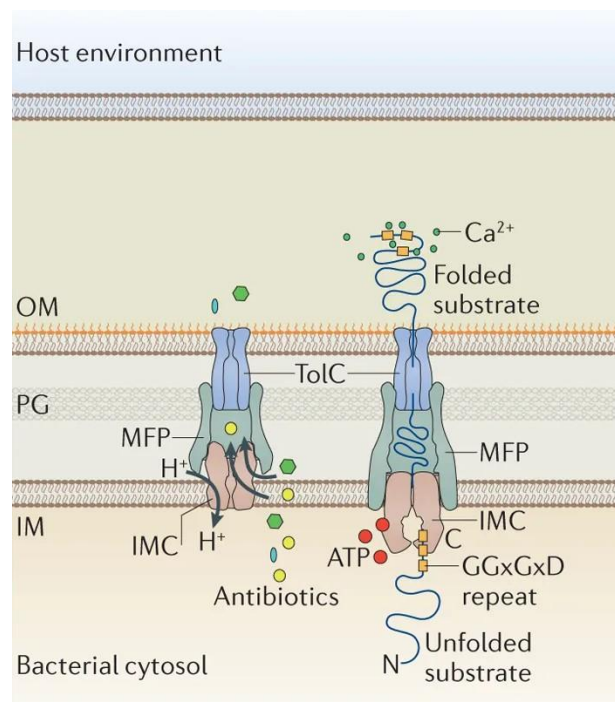


Figure 1.6. Secretion of proteins through the T1SS. The T1SS (shown on right) is formed of an inner-membrane-spanning ABC transporter protein (IMC), a periplasmic membrane fusion protein (MFP) and an outer-membrane factor TolC. The T1SS shares structural similarities with resistance-nodulation-division (RND) pumps (shown on left). T1SS substrates are translocated from the cytoplasm to the extracellular space in a single-step process. Image adapted from Costa et al. (2015).

1.3.4 Type II secretion system (T2SS)

The T2SS transports protein substrates across both membranes in a two-step process (Figure 1.7). The T2SS is formed of four components – a cytoplasmic ATPase, an inner-membrane platform, a periplasmic pseudopilus and an outer-membrane complex (Cianciotto, 2005). The first step requires the Sec pathway to translocate an unfolded protein or the Tat-pathway to translocate a folded protein from the cytoplasm into the periplasm (Green and Meccas, 2016). In the periplasm, the protein substrate is inserted into the secretin channel of the outer-membrane complex; the pseudopilus then retracts and pushes the substrate in a piston-like manner through the secretin channel into the extracellular space (Douzi et al., 2012). The T2SS is used by pathogens for the secretion of toxins and enzymes into the extracellular environment. Examples of T2SS substrates include the cholera toxin of *V. cholerae*, exotoxin A of *P. aeruginosa* and pullulanase of *K. pneumoniae* (Reichow et al., 2010, Durand et al., 2003, Korotkov et al., 2012).

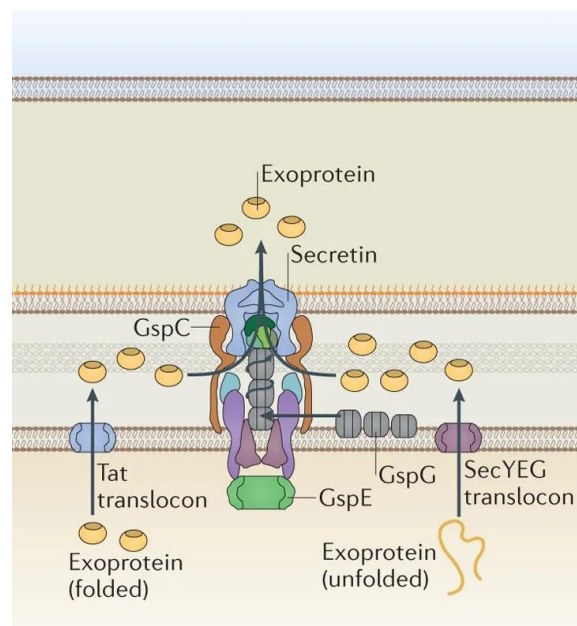


Figure 1.7. Secretion of proteins through the T2SS. The T2SS is formed of a cytoplasmic ATPase, an inner-membrane platform, a periplasmic pseudopilus and an outer-membrane complex. T2SS substrates are translocated in a two-step process. The Sec pathway is required to translocate an unfolded protein into the periplasm. Alternatively, the Tat pathway is required to translocate a folded protein into the periplasm. The protein is inserted into the secretin channel and pushed out into the extracellular space by the pseudopilus. Image adapted from Costa et al. (2015).

1.3.5 Type III secretion system (T3SS)

The T3SS, also known as an 'injectisome' machinery, spans both the inner and outer membranes (Figure 1.8). T3SSs are utilised by Gram-negative pathogens and symbionts for the secretion of protein substrates across both bacterial membranes and in some cases, the host membrane for the delivery of effector proteins into the cytosol of the host cells (Cornelis, 2006). The structure of the T3SS is evolutionarily related to the bacterial flagellum, sharing eight out of nine core proteins (Troisfontaines and Cornelis, 2005). The T3SS is formed of three main components – a basal complex with concentric rings and a central rod that span both membranes, a needle-like structure with a secretion channel and a tip component and a pore-forming translocon. In response to host cell contact, the translocon forms a pore through the host membrane and allows protein substrates to be secreted through the needle-like structure and into the cytosol of the host cells (Coburn et al., 2007). The T3SS can be categorised into seven different families, examples of the T3SS include the SPI-1 (*Salmonella* pathogenicity island 1) of *Salmonella enterica* subsp. *enterica* serovar Typhimurium, SPI-2 of *E. coli* and Ysc of *Yersinia* spp (Cornelis, 2006).

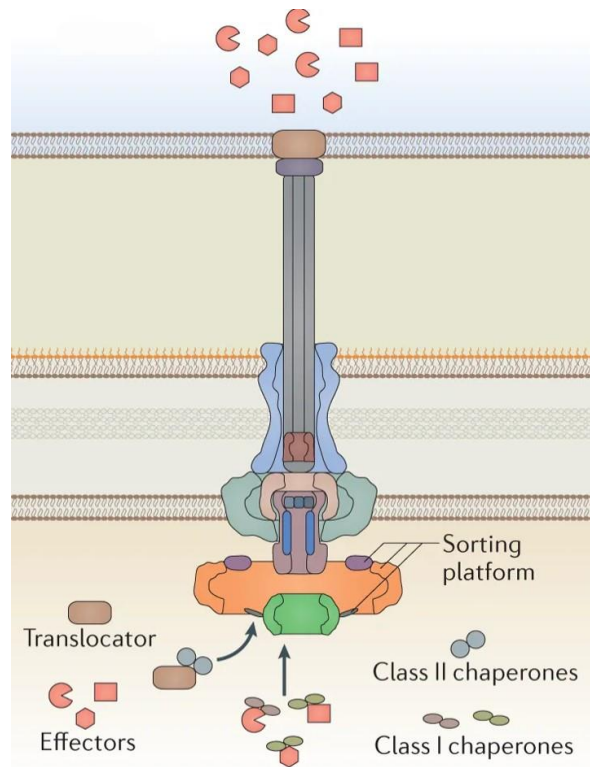


Figure 1.8. Secretion of proteins through the T3SS. The T3SS is formed of a basal complex with concentric rings and a central rod that span both membranes, a needle-like structure with a secretion channel and a tip component and a pore-forming translocon. The translocon forms a pore through the host membrane and T3SS substrates are secreted through the needle-like structure into the host cytosol. Image adapted from Costa et al. (2015).

1.3.6 Type IV secretion system (T4SS)

Capable of secreting both DNA and protein substrates, the T4SS is important in mediating the conjugation of plasmid DNA and secretion of effector proteins (Figure 1.9) (Wallden et al., 2010). The T4SS spans both membranes and consist of 12 proteins forming a core-inner membrane complex, an outer membrane complex and a pili. The nucleic acid or protein substrate is transferred from an inner membrane channel complex to an outer membrane complex. The extracellular pili can have differing functions, including functioning as a channel during conjugation or in cell-to-cell adhesion (Costa et al., 2015). The T4SS is involved in the spread of antibiotic resistance due to the ability to transfer DNA and also has a role in the secretion of effector proteins in pathogens; examples of T4SS secreted effectors include CagA of *Helicobacter pylori*, VirB of *A. tumefaciens*, Dot of *Legionella pneumophila* and TraS/TraB of *P. aeruginosa* (Green and Mecsas, 2016, Tseng et al., 2009).

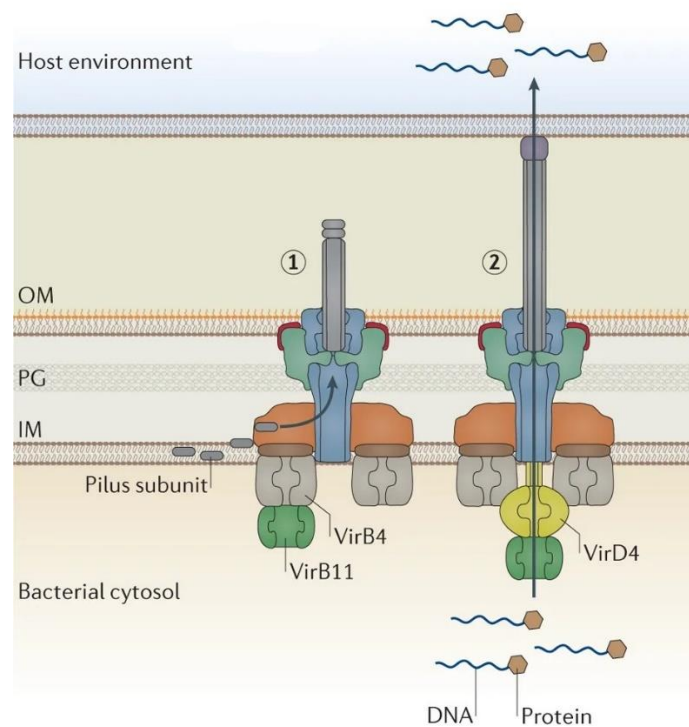


Figure 1.9. Secretion of proteins through the T4SS. The T4SS consist of a core-inner membrane complex, an outer membrane complex and a pili. T4SS substrates are transferred from the inner membrane complex to the outer membrane complex. The pili can function as a conduit for T4SS substrates to pass through or as an attachment device. Image adapted from Costa et al. (2015).

1.3.7 Type V secretion system (T5SS)

The T5SS only spans the outer membrane and requires the Sec machinery to translocate substrates across the inner membrane (Figure 1.10) (Leo et al., 2012). The N-terminal signal sequence present in T5SS substrates is recognised by the Sec pathway which then directs transport of the N-terminal passenger domain through the periplasm, with the assistance of a helper protein in some instances (Tseng et al., 2009). Substrates of the T5SS, also known as ‘auto-transporters’, contain a C-terminal β -barrel domain that can insert into the outer membrane. T5SSs are divided into five sub-classes – types Va to Ve – with the secreted passenger domains varying in structural features and functions. The N-terminal passenger domain can be cleaved from the C-terminal β -barrel domain, which often occurs for passenger domains with enzymatic activities. Alternatively, often in the case of adhesins, the N-terminal passenger domain remains attached to the C-terminal β -barrel domain and outer membrane following translocation (Meuskens et al., 2019). T5SS-secreted proteins are often virulence factors in pathogenic bacteria; examples include VacA and Hsr of *H. pylori*, Hia of *Haemophilus influenzae*, SepA of *Shigella flexneri* and PrtS of *S. marcescens* (Costa et al., 2015, Leo et al., 2012).

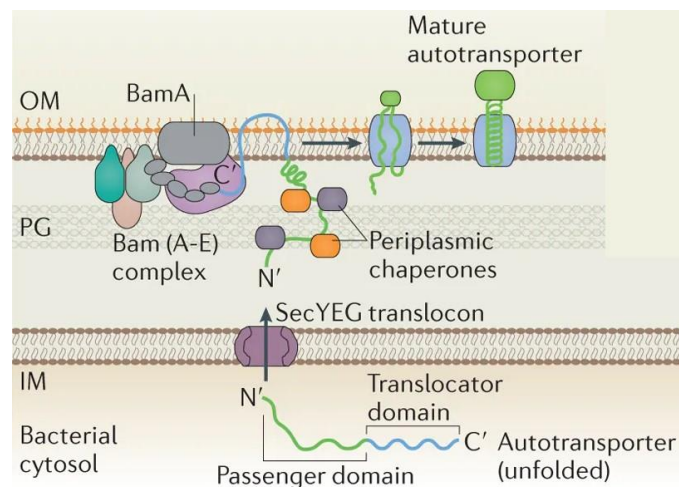


Figure 1.10. Secretion of proteins through the T5SS. T5SS substrates require the Sec pathway for translocation across the inner membrane. The N-terminal passenger domain of the T5SS substrate is recognised by the Sec pathway and transported into the periplasm, where the unfolded structure is stabilised by periplasmic chaperones. The C-terminal β -barrel domain is inserted into the outer membrane by BamA. The N-terminal passenger domain is then either cleaved off or remains attached to the C-terminal β -barrel domain following translocation. Image adapted from Costa et al. (2015).

1.4 Type VI secretion system (T6SS)

1.4.1 History of the T6SS

The T6SS is a contact-dependent secretion machinery capable of delivering effector proteins to both prokaryotic and eukaryotic cells. The T6SS was first identified in 2006 in *Vibrio cholerae* and *Pseudomonas aeruginosa*. Pukatzki et al. discovered a unique secretion mechanism that could translocate proteins lacking signal peptides in *V. cholerae* and named the genes *vas* (for ‘virulence-associated secretion’); these genes were proposed to encode for a novel T6SS that secretes virulence factors targeting eukaryotic cells (Pukatzki et al., 2006). The Vas proteins were found to be secreted in a contact-dependent manner and their presence was required for cytotoxicity towards *Dictyostelium discoideum* amoebae and a murine macrophage cell line. In *P. aeruginosa*, a similar virulence-associated apparatus termed ‘HIS-I’ was identified by Mougous et al.; this novel secretion system was found to secrete Hcp1, which was detected in the sputum of cystic fibrosis patients (Mougous et al., 2006). Since it was discovered, T6SS has been identified to be present in 25% of sequenced Gram-negative bacteria (Dong et al., 2013).

1.4.2 Structure of the T6SS

The structure of the T6SS resembles an inverted bacteriophage tail with homologous components (Figure 1.11). The T6SS consists of 13 core components (TssA-TssM) and accessory proteins such as the T6SS-associated gene (Tag) proteins (see Table 1.1). A functioning T6SS complex requires essential components such as the membrane-anchoring complex (TssJLM), a baseplate structure (TssEFGK), a contractile sheath (TssBC) wrapped around a needle-like tube (Hcp/TssD) and a puncture tip (VgrG/TssI) further sharpened by a spike (PAAR/TagD) (Cianfanelli et al., 2016b). In this study, the T6SS components will primarily be referred to using their names under the ‘Tss’ nomenclature; however there will be occasions where names utilised more extensively in the literature (labelled in red in Table 1.1) are used instead.

The membrane-anchoring complex is composed of three subunits – TssJ, TssL and TssM (Ho et al., 2014). TssJ is an outer-membrane lipoprotein and interacts with TssM in the periplasm. TssM is attached to the inner membrane and interacts with another inner-membrane subunit TssL. The TssJLM complex appears to function as a docking platform for the rest of the T6SS machinery; conformational change in the TssJLM complex is proposed to lead to transient pore formation, allowing the movement of the TssD tube and TssI tip through the outer membrane (Durand et al., 2015).

The baseplate structure – formed of TssE, TssF, TssG and TssK – is proposed to act as a platform for T6SS assembly and for attachment of the tube and sheath structures (Zoued et al., 2014). TssE is homologous to the gp25 baseplate component of the T4 phage; TssE along with TssK are crucial for polymerisation of the TssBC contractile sheath (Leiman et al., 2009). TssA was previously proposed to be a component of the T6SS baseplate structure. However, it is now known that TssA forms dodecameric complexes that are crucial to every step of the T6SS assembly process – from assembly of the membrane complex to co-ordination of the contractile sheath assembly (Zoued et al., 2016).

The needle-like tube structure is formed of hexamers of TssD, which is structurally homologous to the gp19 tail component of the T4 phage (Cianfanelli et al., 2016b). TssD hexamers stack to form a tube with a central channel large enough to accommodate a small protein, with the tube stabilised by polymerisation of the TssBC contractile sheath (Zoued et

al., 2014). VgrG/TssI is similar to the gp5 component of the T4 phage and is required for assembly of the TssD tube. VgrG/TssI is the cell-puncturing device and is further sharpened by a PAAR/TagD tip, which is proposed to play a role in linking effector proteins to VgrG/TssI (Shneider et al., 2013, Cianfanelli et al., 2016a).

The contractile sheath – composed of TssB and TssC subunits – resembles the contractile tail of the T4 phage which is formed of gp18 subunits (Zoued et al., 2016). TssB and TssC are interlocking subunits that form cogwheel-like structures assembling into a tubular structure with a central channel sufficiently large to accommodate the TssD tube. TagA, which is closely associated with TssA, stops the polymerisation of the contractile sheath (Santin et al., 2018). The contractile sheath is responsible for producing enough energy to force the TssD needle-like structure through the inner membrane out into the extracellular space and puncture a host membrane to deliver effector proteins (Cianfanelli et al., 2016b, Salih et al., 2018). In enteroaggregative *E. coli* (EAEC), Szwedziak and Pilhofer demonstrated that the contractile sheath of the T6SS is attached to opposite ends of the bacterial cell and is capable of bidirectional contraction (Szwedziak and Pilhofer, 2019). Whether this bidirectional contraction allows for bidirectional secretion of effectors from both ends is yet unknown. The extended contractile sheath is broken down and the components recycled by the ClpV/TssH ATPase for further sheath assembly (Kapitein et al., 2013).

Table 1.1. Components of the bacterial Type VI Secretion System.

Tss System	Orthologues*	Putative function/location
TssA	VasJ / ImpA	Docks to membrane complex, recruits baseplate complex, initiates/coordinates polymerisation of TssD with sheath
TssB	VipA / ImpB	Contractile sheath
TssC	VipB / ImpC	Contractile sheath
TssD	Hcp	Secreted tube, effector
TssE	HsiF	Baseplate
TssF	VasA / ImpG	Baseplate
TssG	VasB / ImpH	Baseplate
TssH	ClpV / VasG	AAA+ ATPase, sheath recycling
TssI	VgrG	Expelled spike, effector
TssJ	VasD / Lip / SciN	Membrane complex
TssK	VasE / ImpJ	Baseplate
TssL	IcmH / DotU / VasF	Membrane complex
TssM	IcmF / VasK	Membrane complex
TagA	-	Termination of sheath elongation
TagD	PAAR	Tip of expelled spike

* T6SS components will primarily be referred to using their names under the ‘Tss’ nomenclature. However, names utilised extensively in the literature are labelled in red.

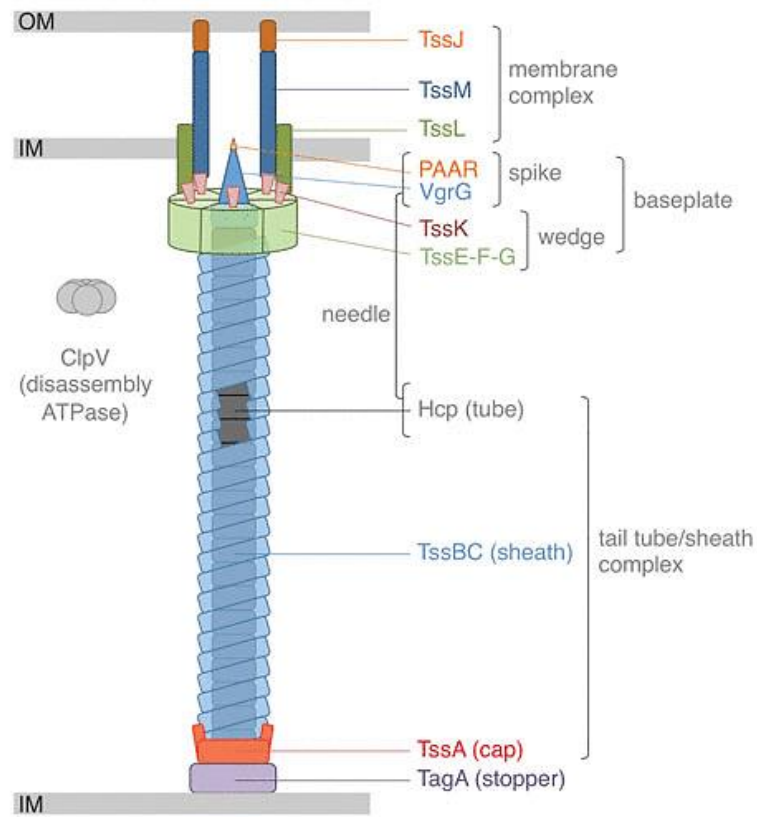


Figure 1.11. Structure of the Type VI Secretion System. The T6SS is formed of a membrane-anchoring complex (TssJLM), a baseplate structure (TssEFGK), a contractile sheath (TssBC) wrapped around a needle-like tube (Hcp/TssD) and a puncture tip (VgrG/TssI) further sharpened by a spike (PAAR/TagD). Image obtained from Cherrak et al. (2019).

1.4.3 Role of the T6SS

The primary role of T6SS was originally assumed to be solely for the delivery of effector proteins into eukaryotic host cells and promotion of virulence; however a role for T6SS in interbacterial interactions was proposed due to the similarity of T6SS components to bacteriophage proteins (Schwarz et al., 2010). A study by Hood et al. in 2010 revealed that in *P. aeruginosa* the haemolysin co-regulated protein secretion island I (HSI-I)-encoded T6SS (H1-T6SS) is responsible for targeting Tse2, a toxin, towards bacterial rather than eukaryotic cells (Hood et al., 2010). The T6SS has since been established to have widely diverse roles in mediating antagonism against microbial competitors, conferring colonisation advantage through niche establishment and promoting virulence through interactions with host cells (Russell et al., 2014, Chen et al., 2019).

1.4.3.1 Competition against microbes

The T6SS has a crucial role in mediating bacterial antagonism and can be involved in both interbacterial and intrabacterial competition. An example of T6SS mediating both types of bacterial antagonism could be observed in *A. tumefaciens*, a soil bacterium that causes crown gall disease in plants; *A. tumefaciens* uses a T6SS to compete *in planta* with neighbouring sister cells and with *P. aeruginosa*, another soil-dwelling bacterium (Ma et al., 2014).

Antibacterial effectors can target the peptidoglycan cell wall, phospholipids, nucleic acids, cytoplasmic co-factors and cell-division proteins through a diverse range of mechanisms (Durand et al., 2014, Chen et al., 2019). Peptidoglycan hydrolases such as Tse1 and Tse3 of *P. aeruginosa* target the cross-linking peptide bonds of the cell wall, whilst PldA is a phospholipase that degrades phosphatidylethanolamine in the bacterial membrane (Russell et al., 2011, Russell et al., 2013). Nucleic acids are targeted by T6SS effectors such as the DNase Tde1 in *A. tumefaciens* and Rhs-CT5 in enterohemorrhagic *E. coli* (Ma et al., 2014, Ma et al., 2017). NADase effectors Tse6/Tne1 in *P. aeruginosa* and Tne2 in *Pseudomonas protegens* hydrolyse NAD(P)⁺ (Tang et al., 2018). ADP-ribosylating effector Tre1 in *Serratia proteamaculans* modifies FtsZ, a tubulin-like protein critical for cell division (Ting et al., 2018). To prevent self-intoxication by effector proteins, bacteria with the T6SS possess cognate immunity proteins to neutralise the effects of the toxins (Ringel et al., 2017, Kirchberger et al., 2017, Fitzsimons et al., 2018). Immunity proteins are located in the same

cellular compartment as the target for their cognate effectors and neutralise the action of the effectors via binding (Figure 1.12) (Durand et al., 2014).

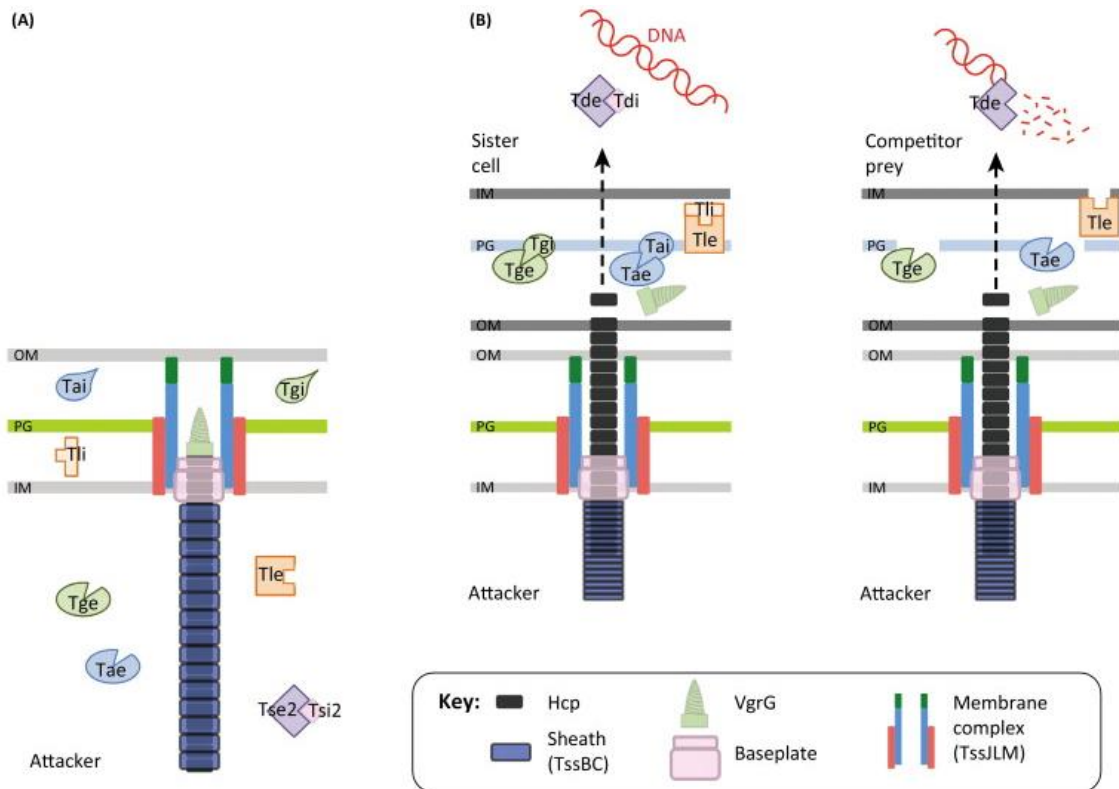


Figure 1.12. T6SS antibacterial effectors, cognate immunity proteins and sites of action.

(A) T6SS effector proteins target different features of the bacterial cell. To prevent self-intoxication, immunity proteins are located at the site of action. (B) Cognate immunity proteins are present in sister cells and the effects of the effector proteins are neutralised. Amidases Tae targets the peptidoglycan cell wall and is neutralised by immunity protein Tai. Glycoside hydrolase Tge acts by cleaving the backbone glycan chain in the cell wall and is neutralised by immunity protein Tgi. Lipase Tle targets the membrane and is neutralised by immunity protein Tli. DNase Tde is neutralised by immunity protein Tdi. However, in other strains or species, the absence of cognate immunity proteins results in degradation of target by effector proteins. Image obtained from Durand et al. (2014).

In competition with prokaryotic targets, a T6SS can act either defensively or offensively. The use of T6SS as a weapon between bacterial species both with a T6SS is known as ‘T6SS duelling’ (Basler and Mekalanos, 2012). Upon sensing an attack from a neighbouring cell’s T6SS, a *P. aeruginosa* bacterium under attack will initiate T6SS assembly in order to retaliate in a defensive strategy known as ‘tit-for-tat’ (Basler et al., 2013). Basler et al. suggested that organisms such as *P. aeruginosa* may be able to pinpoint the location of the initial assault and respond effectively by firing their own T6SS in the precise direction of the attacker (Basler et al., 2013). In contrast to the efficient tit-for-tat response of *P. aeruginosa*, the T6SS of *V. cholerae* and *Serratia marcescens* are used as an offensive weapon, apparently firing constantly and indiscriminately into the surrounding space (Basler et al., 2012).

In addition to mediating bacterial antagonism, T6SS effectors can also target and eliminate single-cell eukaryotic competitors such as fungi and amoebae. The initial identification of the T6SS by Pukatzki et al. occurred due to the observation of the ability of *V. cholerae* to kill *Dictyostelium discoideum* amoebae, with the T6SS effector VasX subsequently identified to cause cytotoxicity by binding to host membrane lipids and disrupting host cell signalling in the amoebae (Pukatzki et al., 2006, Miyata et al., 2011). Recently, Trunk et al. identified two T6SS effectors in *S. marcescens* that target fungal cells; anti-fungal effector Tfe1 triggers plasma membrane depolarisation whilst Tfe2 disrupts crucial nutrient transport and metabolic pathways and induces autophagy (Trunk et al., 2018).

1.4.3.2 Virulence in host

During infection, T6SS effectors can subvert host cell processes by manipulating the host cytoskeleton, hindering host defence mechanisms, modulating the host inflammatory response and modifying host membrane structure (Hachani et al., 2016). Examples of T6SS effectors manipulating the actin cytoskeleton and thereby preventing phagocytosis include the *V. cholerae* VgrG1^{VC} and the *Aeromonas hydrophila* VgrG1^{AH}; VgrG1^{VC} causes cell death by promoting an accumulation of highly toxic polymers, whereas VgrG1^{AH} does so through preventing F-actin polymerisation (Heisler et al., 2015, Suarez et al., 2010). To modulate the host inflammatory response, the T6SS effector VgrG-5 of *Burkholderia pseudomallei*, *Burkholderia mallei* and *Burkholderia thailandensis* is required for membrane fusion of macrophages to form multinucleated giant cells (Schwarz et al., 2014). T6SS effectors can

also target cell membranes and alter their structure, such as the toxin VasX of *V. cholerae*, which can cause pore formation in the phospholipid bilayers (Miyata et al., 2011).

The T6SS can also defend against the production of reactive oxygen species (ROS) through the secretion of effectors. For example, the T6SS-4 of *Yersinia pseudotuberculosis* secretes the effector YezP, which is able to bind to and sequester zinc ions and protect the bacteria from the effects of oxidative stress (Wang et al., 2015). The T6SS-4 of *B. thailandensis* also secretes effectors TseM for the uptake of manganese ions and TseZ for the uptake of zinc ions to mitigate the effects of oxidative stress. Similarly, enterohemorrhagic *E. coli* secretes a T6SS effector, the catalase KatN, which facilitates survival of the bacteria in macrophages through decreasing the level of intracellular ROS (Wan et al., 2017). *Burkholderia cenocepacia* decreases the assembly of NADPH oxidase complex and production of ROS through T6SS activity (Rosales-Reyes et al., 2012).

1.4.3.3 Colonisation and niche establishment

The presence of a T6SS in bacteria such as *P. aeruginosa*, *A. tumefaciens*, *Bacteroides fragilis* and *V. cholerae* can have a significant impact on the ability of the bacteria to colonise and establish a niche. The T6SS has been shown to be important in quorum sensing in *P. aeruginosa*. Russell et al. hypothesised that the T6SS may also play a role in contact-dependent signalling (Sana et al., 2012, Russell et al., 2014). Possession of a T6SS can benefit a bacterial community through the ability to restructure biofilms and also enable horizontal gene transfer through the lysis of sister cells, as observed in *V. cholera* (Russell et al., 2014, Borgeaud et al., 2015). In addition, the T6SS favours a homogenous population as this protects bacterial populations from bacterial adversaries and could also potentially defend against bacteriophages via the intoxication of infected sister cells (Russell et al., 2014).

1.5 Type VI secretion system in *C. jejuni*

1.5.1 Role of the Type VI secretion system in *C. jejuni*

In *C. jejuni*, components of a T6SS were first identified by Lertpiriyapong et al. in 2012 (Lertpiriyapong et al., 2012). A cluster of 13 genes was identified in *C. jejuni* 43431 (a human isolate from Canada) and in *C. jejuni* 414 (a bank vole isolate from the United Kingdom). The secretion of TssD (Hcp) was detected and the *C. jejuni* T6SS was found to be modulated during exposure to physiologically relevant concentrations of deoxycholic acid. Lertpiriyapong et al. also found that the *C. jejuni* T6SS is required for adhesion and invasion of T84 human colonic epithelial cells and RAW 264.7 murine macrophage cells, as well as for persistent colonisation in IL-10-deficient mice.

Concurrently, Bleumink-Pluym et al. also discovered a TssD ortholog in *C. jejuni* 108 (a human isolate from the United States) and subsequently identified a 17-kb cluster with the same 13 conserved genes (Bleumink-Pluym et al., 2013). The absence of the TssH (ClpV) component was observed by both Lertpiriyapong et al. and Bleumink-Pluym et al. in *C. jejuni* strains and other *Campylobacter* species. In *C. jejuni* 108, the T6SS cluster was located on *C. jejuni* integrative element 3 (CJIE3) and was inserted between two rearrangement hot-spot (Rhs) elements. The *C. jejuni* T6SS was found to cause cytotoxicity towards red blood cells and the presence of the *C. jejuni* surface capsule polysaccharide impaired T6SS function.

A recent study examined the structure of the TssD effector protein in *C. jejuni* and found that TssD is cytotoxic towards HepG2 human liver carcinoma cells (Noreen et al., 2018). However, in contrast to the well-studied T6SSs of *P. aeruginosa*, *V. cholerae* and *S. marcescens*, a more detailed understanding of the roles of the T6SS in *C. jejuni* requires further investigation.

1.5.2 Prevalence of the Type VI secretion system in *Campylobacter* spp.

Prevalence of the T6SS in *C. jejuni* and other *Campylobacter* species appears to vary widely depending on the region of origin, the sample size studied and the detection method employed in various studies. *C. jejuni* strains can also harbour incomplete T6SS clusters that are probably non-functional but may be identified if PCR detection techniques are used; to mitigate this some studies utilise genome sequencing as either the primary or secondary detection method to screen for a complete T6SS cluster.

Sainato et al. analysed 615 stool samples collected from children with diarrhoea caused by *Campylobacter* spp. during an active surveillance program in Egypt from 1995 to 2003 (Sainato et al., 2018). Of the 441 isolates analysed, PCR detection of the *tssD* gene revealed that 57.6% of *C. jejuni* isolates and 18.0% of *C. coli* isolates were positive for the presence of *tssD*. However this study did not find a correlation between the presence of the T6SS and more severe clinical disease.

Samples from humans, animals and environmental sources were collected between 2010 and 2013 in Pakistan and examined by Siddiqui et al. (Siddiqui et al., 2015). The presence of T6SS genes *tssD*, *tssI* and *tssM* were detected by PCR in 4.43% of 158 chicken isolates, 1.64% of 122 cattle isolates, 15% of wildlife isolates and 15.6% of wastewater isolates. The T6SS genes were absent in all of the 34 human diarrhoeal isolates, half of which were bloody diarrhoeal isolates, suggesting a lack of association between the presence of the T6SS in *C. jejuni* and disease severity.

Bleumink-Pluym et al. in 2013 examined eighty *Campylobacter* strains from human and animal sources worldwide using PCR detection of *tssD* (*hcp*) and 8 (10%) of the *C. jejuni* strains and 2 (2.5%) of the *C. coli* strains were T6SS-positive (Bleumink-Pluym et al., 2013). Two of the eight T6SS-positive *C. jejuni* strains were from patients with *C. jejuni* bacteraemia, indicating a potential link of T6SS-positive strains to more severe disease.

Harrison et al. in 2014 focused on genome sequencing 181 *C. jejuni* isolates from human, chicken and environmental sources and compared samples from the United Kingdom, Vietnam, Pakistan and Thailand (Harrison et al., 2014). The prevalence of T6SS-positive isolates was 7.6%, 54.4%, 22.2% and 33.3% respectively, suggesting that the T6SS may be more widespread amongst strains in Asia than in the United Kingdom. Harrison et al. also found an increased prevalence of T6SS-positive strains in patients experiencing bloody diarrhoea and more severe disease, with bloody diarrhoea experienced by 6 of 19 patients

infected with T6SS-positive strains and 1 of 17 patients infected with T6SS-negative strains. Results by Bleumink-Pluym et al. and Harrison et al. indicated that the presence of the T6SS may correlate to more severe clinical disease; however it is possible this correlation is due to the small sample numbers used in both studies.

The link between T6SS-positive *C. jejuni* strains and more severe disease was investigated more comprehensively by Agnetti et al. in 2019, using PCR to detect the presence of *hcp* with confirmation by whole genome sequencing (Agnetti et al., 2019). A prevalence of 16.8% was found in 119 isolates from adults with a *C. jejuni* infection in a hospital in Switzerland; however similar to the findings of Sainato et al. and Siddiqui et al., there was also no correlation found between the T6SS-positive isolates and more severe clinical disease. Interestingly, there appeared to be an association between immunocompromised patients and T6SS-positive strains which requires further investigation.

Despite a high prevalence of T6SS-positive isolates present in domestic poultry, few studies thus far have investigated the prevalence amongst wild birds which could potentially provide an environmental reservoir for these strains. Kovanen et al. examined *C. jejuni* isolates from western jackdaws and game birds in Finland and found that 49% of the western jackdaw isolates and 72% of the mallard duck isolates were T6SS-positive (Kovanen et al., 2018).

T6SS-positive *C. jejuni* strains are now observed to be considerably more prevalent than T6SS-negative strains in chickens in commercial poultry farms, in raw chicken in the supermarket and even in hospital patients in Northern Ireland (Carmel Kelly, Agri-Food and Biosciences Institute, Belfast, Personal Communication). There is an observable increase in the prevalence of T6SS-positive strains in human isolates in the United Kingdom over the past decade (Arnoud van Vliet, University of Surrey, Personal Communication). Due to the lack of data from outside of Europe, it is difficult to draw any conclusions on whether the recent increased prevalence of T6SS-positive isolates observed in Europe is due to a shift towards a higher prevalence of T6SS-strains in this region only or if this forms part of a globally occurring pattern.

1.6 Aims and Objectives

The aim of this study was to investigate the role of the Type VI Secretion System in *Campylobacter jejuni* interactions with host and bacterial cells.

Objectives:

1. To characterise T6SS-positive *C. jejuni* strains and T6SS mutants;
2. To investigate the role of the *C. jejuni* T6SS;
3. To analyse the *C. jejuni* T6SS secretome and identify potential T6SS effectors.

CHAPTER TWO: Materials and Methods

2.1 Chemicals and reagents

All chemicals and reagents were obtained from Oxoid (Basingstoke, UK), Sigma-Aldrich (Gillingham, UK), or Thermo Fisher Scientific (Loughborough, UK) unless otherwise stated.

2.2 Bacterial strains and growth conditions

C. jejuni strains used in this study are listed in Table 2.1. *C. jejuni* strains were grown at 37°C under microaerobic conditions (85% N₂, 10% CO₂ 5% O₂) in a variable atmosphere chamber (Don Whitley Scientific, Bingley, UK). Unless otherwise stated, *C. jejuni* were grown either on Columbia agar with 7% (v/v) horse blood in Alsever's (TCS Biosciences, Buckingham, UK) with the addition of Skirrow *Campylobacter* selective supplement (Oxoid) or in Brucella broth (BD Diagnostics, Wokingham, UK) shaking at 75 revolutions per minute (rpm).

Escherichia coli strains listed in Table 2.2 were grown on lysogeny broth (LB) agar plates or in LB broth at 37°C shaking at 200 rpm in an incubator (Sanyo, Loughborough, UK). The appropriate antibiotics were added as required at concentrations of 50 µg/ml kanamycin, 100 µg/ml ampicillin or 10 µg/ml chloramphenicol for *C. jejuni* growth, with the concentration of chloramphenicol for *E. coli* growth increased to 50 µg/ml.

Glycerol stocks for *C. jejuni* were prepared from cultures grown overnight on blood agar (BA) plates. Bacterial cells were resuspended in 10% (v/v) glycerol, 10% (v/v) foetal calf serum (FCS) and 80% (v/v) Brucella broth, snap frozen in a dry ice and 100% (v/v) ethanol slurry, then stored in a -80°C freezer. Glycerol stocks for *E. coli* were prepared from cultures grown overnight in LB broth. Broth cultures were mixed with 15% (v/v) glycerol and stored in a -80°C freezer.

Table 2.1. *Campylobacter jejuni* strains used in this study.

<i>C. jejuni</i> strains	Description	Source/Reference
T6SS-positive		
488	Wild-type human isolate from Brazil.	Kindly provided by Dr Daiani Teixeira da Silva.
488 <i>tssB</i>	488 <i>tssB::Km</i>	This study
488 <i>tssC</i>	488 <i>tssC::Km</i>	This study
488 <i>tssBC</i>	488 <i>tssB::Km tssC::Km</i>	This study
488 <i>tssD</i>	488 <i>tssD::Km</i>	This study
488 <i>tssD</i> complement	488 <i>tssD::Km</i> complemented with a copy of <i>tssD</i> using the pRRC complementation vector	This study
43431	Wild-type human isolate from Canada.	Purchased from ATCC (Penner et al., 1983).
43431 <i>tssD</i>	43431 <i>tssD::Km</i>	Kindly provided by Chloe Kerridge.
RC039	Wild-type chicken isolate from Northern Ireland.	Kindly provided by Professor Nicolae Corcionivoschi (Corcionivoschi et al., 2015).
Cj1	Wild-type human isolate from Thailand.	Kindly provided by Dr Olivia Champion. (Harrison et al., 2014)
Cj5	Wild-type human isolate from Thailand.	Kindly provided by Dr Olivia Champion. (Harrison et al., 2014)

414	Wild-type bank vole isolate from the United Kingdom.	(Hepworth et al., 2011)
T6SS-negative		
81-176	Wild-type human isolate from the United States.	(Korlath et al., 1985)
11168H <i>kpsM</i>	Capsule mutant of the 11168H hypermotile strain.	(Karlyshev et al., 2000)

Table 2.2. *Escherichia coli* strains used in this study.

<i>E. coli</i> strains	Description	Source/Reference
SCS110	Competent cells deficient in Dam and Dcm methylases.	Agilent Technologies (Cheadle, UK)
XL2-Blue MRF	Competent cells for cloning methylated DNA.	Agilent Technologies
DH10B GFP	Strain with GFP plasmid.	Kindly provided by Dr Abderrahman Hachani (Ma et al., 2014)

Table 2.3. Plasmids used in this study.

Plasmids	Description	Source/Reference
pGEM-T Easy	Cloning vector.	Promega (Southampton, UK)
pCJC1	Complementation vector. (Also known as pDENNIS.)	(Jervis et al., 2015)
pRRC	Complementation vector.	(Karlyshev and Wren, 2005)

2.3 Assays

2.3.1 Growth kinetics

C. jejuni strains were restreaked on blood agar plates and grown for 24 hours at 37°C under microaerobic conditions. Flasks with 10 ml Brucella broth was also pre-incubated for 24 hours at 37°C under microaerobic conditions, with shaking at 75 rpm. Bacterial cells were harvested and resuspended in 1 ml Brucella broth. 100 µl of bacterial suspension was mixed with 900 µl Brucella broth in a cuvette and OD₆₀₀ readings were taken using a Spectronic spectrophotometer (Thermo Fisher Scientific, Waltham, USA). The following calculations were carried out to determine the volume of bacterial suspension required to inoculate 10 ml Brucella broth to an OD₆₀₀ of 0.1:

$$\frac{\text{Required OD}_{600}}{\text{Suspension OD}_{600} \times 10} \times 10 \text{ ml} \times 1000 = \text{Volume required } (\mu\text{l})$$

The volume required was added to the pre-incubated flasks and the cultures were incubated at 37°C, under microaerobic conditions, shaking at 75 rpm. At the desired timepoints, 1 ml of bacterial culture was removed from the flask and the OD₆₀₀ readings were recorded.

2.3.2 Motility

Brucella motility plates were prepared with 0.4% (w/v) bacteriological agar (Sigma-Aldrich). *C. jejuni* strains from 24 hour plate cultures were resuspended in phosphate-buffered saline (PBS) and adjusted to an OD₆₀₀ of 1.0. 5 µl of bacterial suspensions were pipetted into the centre of a motility plate and plates were incubated un-inverted at 37°C under microaerobic conditions. At time points 24 hours, 48 hours and 72 hours the diameters of the halos were measured.

2.3.3 Biofilm formation

Bacterial cells from 24 hour plates were inoculated to an OD₆₀₀ of 0.1 into pre-incubated flasks with 10 ml of Muller Hinton (MH) broth. Cultures were incubated for 5 hours at 75 rpm under microaerobic conditions. The OD₆₀₀ of the cultures were readjusted to 0.1, then 1 ml of culture was added to each well of a 24-well polystyrene plate (Corning, Amsterdam,

Netherlands) which was incubated at 37°C under either aerobic or microaerobic conditions, stationary, for 24, 48 and 72 hours. Following incubation, the liquid culture was removed and the wells were washed twice with 1.2 ml of PBS per well then left to air dry for 20 minutes at 37°C. 1.1 ml of 1% (w/v) crystal violet (Sigma-Aldrich) was added to each well and incubated for 15 minutes. The wells were washed three times with 1.2 ml of PBS per well, then de-stained with 1.2 ml of 80% (v/v) ethanol and 20% (v/v) acetone per well for 20 minutes at 400 rpm on shaker. The absorbance (A_{595}) was measured using a SpectraMax M3 microplate reader (Molecular Devices, San Jose, USA).

2.3.4 Oxidative stress assay

C. jejuni strains from 24 hour plate cultures were resuspended in PBS and adjusted to an OD_{600} of 1.0. Bacterial suspensions were exposed to 25 mM or 50 mM hydrogen peroxide (H_2O_2) (Acros Organics, Geel, Belgium) for 15 minutes or 30 minutes at 37°C under microaerobic conditions. Serial dilutions were performed on the bacterial suspensions and dilutions were plated onto blood agar plates, incubated for 48 hours at 37°C under microaerobic conditions and the CFUs/ml were counted.

2.3.5 Haemolysis assay

7-day old cultures of *C. jejuni* were grown on blood agar plates at 37°C under microaerobic conditions. 10 ml of Brain Heart Infusion (BHI) broth was pre-incubated for 24 hours at 37°C under microaerobic conditions, with shaking at 75 rpm. The bacterial cultures were resuspended in PBS, inoculated in the pre-incubated BHI broth to an OD_{600} of 1.0 and incubated for 16 hours at 37°C under microaerobic conditions with shaking. OD_{600} measurements were taken and calculations were performed to inoculate 1 ml PBS to OD_{600} of 1.0:

$$\frac{\text{Required } OD_{600}}{\text{Suspension } OD_{600} \times 10} \times 1 \text{ ml} \times 1000 = \text{Volume required } (\mu\text{l})$$

1 ml bacterial suspensions were prepared in 1.5 ml sterile Eppendorf tubes then centrifuged at 4,000 rpm for 10 minutes. The supernatant was discarded and the pellet was resuspended in 750 μl PBS. The bacterial suspension was added to 4 ml of pre-incubated PBS. To prepare red blood cells (RBCs), 1 ml of horse blood in Alsever's was added to an Eppendorf and centrifuged at 13,000 rpm for 2 minutes. The supernatant was discarded and the RBCs were

resuspended in 1 ml of PBS. 250 µl of prepared RBCs were added to the bacterial suspension for 5% (v/v) concentration of RBCs. Flasks for positive control with Milli-Q water (Millipore, Burlington, USA) and RBCs and a negative control with PBS only were also prepared. The suspensions were incubated for 6 hours, at 37°C, under microaerobic conditions, stationary. The suspensions were transferred to universal tubes and centrifuged at 1,000 rpm for 5 minutes. The OD₄₂₀ was measured and cytotoxicity scored as a percentage of cell lysis relative to the positive control:

$$\% \text{ Haemolysis} = \frac{\text{OD}_{420} \text{ of sample}}{\text{OD}_{420} \text{ of RBCs incubated in water}}$$

2.3.6 Bacterial competition assay

This methodology was adapted from protocols published by Hachani et al. and Diniz et al. (Alcoforado Diniz et al., 2017, Hachani et al., 2013). Bacterial strains were restreaked onto blood agar plates and incubated at 37°C under microaerobic conditions overnight. Bacterial cells were harvested and resuspended in 500 µl Brucella broth. OD₆₀₀ readings were taken and suspensions were adjusted to OD₆₀₀ 0.5. Two sets of blood agar plates were prepared. The first set (input plates) with 25 µl of each strain in triplicate. The second set (output plates) with 50 µl of mixed suspension of the predator and prey strains mixed in the desired ratios spotted in triplicate. The plates were allowed to dry and incubated for 16 hours at 37°C under microaerobic conditions to allow killing to take place. Each spot was harvested, resuspended in 1 ml PBS and serial dilutions were performed in PBS. Dilutions were spotted with 10 µl in each spot in triplicates onto blood agar plates and also blood agar plates with the addition of the appropriate antibiotic to screen for the prey strain. Dilution plates were incubated for 48 hours at 37°C under microaerobic conditions and the CFUs/ml were counted.

2.3.7 Bicinchoninic acid (BCA) protein assay

Pierce BCA Protein Assay Kit (Thermo Fisher Scientific) was used to measure protein concentration. BSA standards were prepared from Pierce Bovine Serum Albumin standards (Thermo Fisher Scientific) using PBS as a diluent. The working reagent was prepared from reagent A and reagent B in a ratio of 50:1 and stored in the dark. 10 µl of each BSA standard

was added in triplicate into the wells of a 96-well plate. Each protein sample was diluted to a desired dilution (e.g. 10 µl protein sample to 90 µl PBS) and 10 µl of diluted protein sample was added in triplicates to the 96-well plate. 200 µl of working reagent was added to each standard and sample in the 96-well plate and the plate was wrapped in foil and incubated at 37°C for 30 minutes. The absorbance (A_{595}) was measured on the ELx800 Absorbance Microplate Reader (BioTek, Swindon, UK) and the absorbance readings were plotted against the standards to generate a standard curve from which the protein concentration of the samples could be calculated.

2.3.8 Sodium taurocholate (ST) stress

To prepare 2% (w/v) sodium taurocholate in Brucella broth, 10% (w/v) sodium taurocholate was prepared in sterile Brucella broth and 2 ml added to pre-incubated flasks containing 8 ml Brucella broth. Bacterial suspensions were prepared from 24 hour plate cultures and flasks were inoculated to OD_{600} of 0.1. Inoculated flasks were incubated at 37°C under microaerobic conditions for 7.5 hours. Following incubation, OD_{600} readings were taken and serial dilutions were performed and plated onto blood agar plates. The plates were incubated at 37°C under microaerobic conditions for 24 hours and the CFU/ml were counted.

2.3.9 Antimicrobial susceptibility – Disk diffusion

The disk diffusion assay was performed with ampicillin (10 µg), amoxycillin/clavulonic acid (2:1, 30 µg), tetracycline (30 µg) and polymyxin B (300 units) disks following the method published by the European Society of Clinical Microbiology (EUCAST) (EUCAST, 2019). Briefly, the inocula were prepared from 24 hour plate cultures in sterile Milli-Q water and adjusted to 0.5 McFarland Standard (equivalent to approximately OD_{600} 0.1 or 1.5×10^8 CFU/ml). A sterile cotton-wool swab was dipped into the prepared suspension and excess liquid was removed. The inoculum was spread evenly over the entire surface of a blood agar plate by swabbing in three different directions. The inoculated plate was then allowed to dry before antibiotic discs were applied to the dried surface. Plates were incubated at 37°C under microaerobic conditions for 24 hours. Zones of growth inhibition were measured in millimetres and sensitivity (S) determined based on EUCAST guidelines.

2.3.10 Antimicrobial susceptibility – Broth microdilution

Broth microdilution was performed with vancomycin (Sigma) and the minimum inhibitory concentration (MIC, $\mu\text{g/ml}$) was determined according to a method published by Wiegand et al. (Wiegand et al., 2008). Briefly, a range of dilutions were prepared with vancomycin diluted in sterile MH broth to obtain concentrations of 128, 64, 32, 16, 8, 4, 2, 1, 0.5 and 0.25 mg/L. A 96-well plate was labelled with the antibiotic concentrations and the corresponding dilutions of vancomycin were pipetted into each column. One column was filled with sterile MH broth only to act as the sterility control and a second column was to be filled with only the bacterial inoculum to act as the growth control. The inocula were prepared from 24 hour plate cultures in sterile Milli-Q water and adjusted to 0.5 McFarland Standard (equivalent to approximately OD_{600} 0.1 or 1.5×10^8 CFU/ml). 50 μl of prepared inoculum was added to each well containing antibiotic solution and also the growth control well for a final inoculum of approximately 5×10^5 CFU/ml. The CFU/ml of the inoculum was measured by performing serial dilutions with 10 μl of inoculum from the growth control well and plating onto blood agar plates. The microtitre plate and the blood agar plates were both incubated at 37°C under microaerobic conditions for 24 hours. Growth on the microtitre plate was observed and CFU/ml were counted from the blood agar plates.

2.4 Cell culture techniques

2.4.1 Cell culture

All cells were cultured in complete media, composed of the following:

Dulbecco's Modified Eagle's Medium (DMEM) + GlutaMAX

10% (v/v) Foetal bovine serum (FBS)

1% (v/v) Non-essential amino acids

1% (v/v) Penicillin-Streptomycin

Frozen stocks of T84 and HCT-8 cells were maintained in liquid nitrogen. To culture cells, a vial of frozen cells was resuspended in 10 ml of complete media pre-warmed to 37°C and placed in a 5% CO_2 incubator (Sanyo, Osaka, Japan).

Cells were split weekly once they reached a confluent state. Cells were washed three times with 10 ml of pre-warmed PBS, then incubated with 3 ml of pre-warmed trypsin-EDTA for 10 minutes at 37°C. Following incubation, the flask was tapped lightly to detach the cells and the contents were resuspended in 10 ml of complete media and transferred to a falcon tube. The resuspended cells were centrifuged for 10 minutes at 1,500 rpm, the supernatant was discarded and the cells were resuspended in 1 ml of complete media. To split the cells without counting, 24 ml of complete media was added to the resuspended cells and the total volume was transferred to a 75cm³ flask. The flask was incubated at 37°C in a CO₂ incubator.

To seed the wells of a 24-well plate to 1 x 10⁵ cells/ml for interaction and invasion assays, the number of cells present was first calculated. 100 µl of resuspended cells were added to 100 µl of Trypan blue and 800 µl of complete media to perform a 1:10 dilution. 100 µl of the suspension was applied to a haemocytometer (Weber Scientific, Teddington, UK) and the number of live (unstained) cells were counted under a DM1000 light microscope (Leica, Milton Keynes, UK). To seed wells to 1 x 10⁵ cells/ml, cells were diluted in complete media and 1 ml of diluted cell suspension is pipetted into each well of a 24-well plate. The plate was placed in a CO₂ incubator at 37°C and the media was replaced with fresh pre-warmed complete media every 2 days. The number of cells would reach 1 x 10⁶ cells per well after 7 days. The media was replaced with infection media (complete media without the addition of penicillin-streptomycin) a day prior to the interaction and invasion assay.

2.4.2 Interaction and invasion assays of T84 and HCT-8 colonic epithelial cells

Interaction and invasion assays of T84 and HCT-8 cells were performed as previously described (Corcionivoschi et al., 2009). *C. jejuni* strains were grown for 24 hours on Muller-Hinton agar under microaerobic conditions. Bacterial cells were washed and resuspended in tissue culture medium to an OD₆₀₀ of 0.4, then added to cells grown in tissue culture plates to yield a multiplicity of infection of 1000:1. Plates were centrifuged and incubated for 3 hours at 37°C in a CO₂ incubator.

For interaction assays, infected monolayers were washed with PBS three times and treated with 0.5 ml 0.1% v/v Triton X-100 for 20 minutes at room temperature under normal atmospheric conditions. The suspension in each well was mixed by pipetting for one minute

and the lysate was transferred to an Eppendorf. Serial dilutions were performed in PBS and the CFUs/ml were enumerated on blood agar plates.

For invasion assays, infected monolayers were washed with PBS three times and treated with 3 µl gentamicin (150 µg/ml) for 2 hours at 37°C in a CO₂ incubator. Cells were then washed with PBS three times and treated with 0.5 ml 0.1% v/v Triton X-100 for 20 minutes at room temperature under normal atmospheric conditions. The suspension in each well was mixed by pipetting for one minute and the lysate was transferred to an Eppendorf. Serial dilutions were performed in PBS and the CFUs/ml were enumerated on blood agar plates.

2.4.3 Interaction and invasion with primary chicken intestinal epithelial cells

Interaction and invasion with primary chicken intestinal epithelial cells were performed in collaboration with Professor Nicolae Corcionivoschi at the Agri-Food and Biosciences Institute (Belfast, UK). Isolation of primary chicken intestinal cells were performed as described previously (Byrne et al., 2007). Briefly, biopsies from sections of small intestines from 6 12 week-old broiler chickens (Cobb 500) were placed in cell culture medium and primary cells were isolated. Interaction and invasion of primary chicken intestinal cells were performed as described above in Section 2.4.2.

2.5 *In vivo* infection models

2.5.1 *Galleria mellonella* infection model

Galleria mellonella (greater wax moth) larvae were obtained from Livefoods Direct (Sheffield, UK) and maintained at room temperature in a well-ventilated container in the dark. TruLarv research-grade *G. mellonella* larvae were also obtained from BioSystems Technology (Exeter, UK). Larvae were weighed and larvae weighing 0.18 g to 0.26 g were selected for this assay. *C. jejuni* from 24 hour plate cultures were harvested in 1 ml PBS and diluted to OD₆₀₀ of 0.1 or OD₆₀₀ of 1.0. The 25 µl gastight syringe (Hamilton, Giarmata, Romania) was washed with 100% (v/v) ethanol four times and PBS four times prior to and in-between injections with different *C. jejuni* strains. 10 µl of bacterial suspension was inoculated in the right foremost leg of the larvae and 10 larvae were inoculated per strain. 10 larvae were also inoculated with 10 µl PBS and 10 larvae were un-inoculated as controls. The

larvae were incubated at 37°C and counts of alive or dead larvae were recorded every 24 hours over a duration of 5 days. Larvae were recorded as dead if they no longer responded to touch.

2.5.2 Chicken infection model

The chicken infection experiment was performed in the laboratory of Professor Nicolae Corcionivoschi (under the supervision of Dr Lavinia Stef) at the Banat University of Agricultural Sciences and Veterinary Medicine - King Michael I of Romania (Timișoara, Romania). Thirty male broiler chickens (Ross 308) were housed in isolation units on wood shaving bedding. The temperature in the isolation unit was kept between 22-25°C and thermostatically controlled. Broilers were fed *ad libitum* with a standard diet. *C. jejuni* strains were grown on Muller Hinton plates for 24 hours under microaerobic conditions and resuspended in sterile distilled water. At 15 days old, ten broilers were inoculated with approximately 1×10^8 CFU/ml of either the 488 wild-type strain, the 488 *tssD* mutant or the 81-176 wild-type strain. The different batches of infected broilers were kept separated in sterile isolation units. After 3 days of infection, broilers were euthanised and *C. jejuni* numbers were enumerated by analysing the cecum contents using the ISO17025 methodology for plate counting. All broilers were confirmed using cloacal swabs as being *Campylobacter* free at the time of infection. These experiments were performed in triplicate on three separate occasions. The experiments were performed according to the legislation in place (Law 471/2002 and government ordinance 437/2002) and under the supervision of National Sanitary Veterinary Agency. This work was approved by the Ethics Committee of Banat University of Agricultural Sciences and Veterinary Medicine - King Michael I of Romania.

2.6 Molecular techniques

2.6.1 Primer design

Primers used in this study are listed in Table 2.4. Primers were designed and checked for the presence of self-dimers, heterodimers and hairpin loops using the OligoAnalyzer Tool (Integrated DNA Technologies, Coralville, USA).

Table 2.4. Primers used in this study.

Primer Name	Sequences	Source
Mutagenesis		
<i>tssB</i> F	TGACAAAGAACATACTACAAG	This study
<i>tssB</i> R	AATCTAAGTCCACGCC	This study
<i>tssB</i> IPCRM F	GGGAGATCTGAACAGGAGCTGAAGAGC	This study
<i>tssC</i> IPCRM R	GGGAGATCTTTGTTGTTATATTGAGTTTTTC	This study
<i>tssC</i> F	AAGCAGTTGATATGCC	This study
<i>tssC</i> R	AATGAGGTCGGACAC	This study
<i>tssC</i> IPCRM F	GGGAGATCTGACTGTTAAGGATCTGCCTAC	This study
<i>tssC</i> IPCRM R	GGGAGATCTTCCACACCATCTATATTTAGC	This study
<i>tssD</i> F	ATTGAAGGTTCCACACAAGG	This study
<i>tssD</i> R	GTTGATAATCTCCAAT	This study
<i>tssD</i> complement F	CCCTCTAGAATGAAGCGAGTAGATTTTGCCA AGCATTAAATA	This study
<i>tssD</i> complement R	CCCTCTAGATTAAATTCACGATAACAATCC	This study
Kan ^R F out	TGGGTTTCAAGCATTAGTCCATGCAAG	(Gundogdu et al., 2016)
Kan ^R R out	GTGGTATGACATTGCCTTCTGCG	(Gundogdu et al., 2016)
Cam ^R F out	CGATTGATGATCGTTGTA	(Gundogdu et al., 2016)
Cam ^R R out	TACAGCAGACTATACTG	(Gundogdu et al., 2016)
RT-PCR		
<i>tssB</i> F	TGAGGATGTGGAGTTG	This study
<i>tssB</i> R	ATTACCCATAGGACCT	This study
<i>tssC</i> F	TTGATGAAATGATAGC	This study
<i>tssC</i> R	GTTGATAATCTCCAAT	This study
<i>tssD</i> F	TGAAGGTTCCACACAAGG	This study
<i>tssD</i> R	CACTTGTTGCGGTTCTAA	This study

qRT-PCR		
<i>katA</i> F	AACAAGCTGCCTTTAGTCCAAG	This study
<i>katA</i> R	CATAGCACCAGCGACATTGTAAG	This study
<i>sodB</i> F	GTGGCTGTGGCGGTTTCATGTC	This study
<i>sodB</i> R	CTGCGTTTGAAGTACCTACA	This study
<i>ahpC</i> F	ATCAAGGTGGTATTGGTCAG	This study
<i>ahpC</i> R	TAACCACAGCATGGCGAACTG	This study
<i>gyrA</i> F	GTTATTATAGGTCGTGCTTT	This study
<i>gyrA</i> R	CTATGAGGTGGGATGTTTGT	This study

(IPCRM = Inverse PCR mutagenesis. Kan = Kanamycin. Cam = Chloramphenicol.)

2.6.2 Genomic DNA (gDNA) isolation

Genomic DNA isolation was performed using the PureLink Genomic DNA Kit (Invitrogen, Loughborough, UK). *C. jejuni* strains were grown on blood agar plates for 16 hours and the bacterial cells were suspended in 180 µl PureLink Genomic Digestion buffer. To lyse the cells, 20 µl Proteinase K (20 mg/ml) was added and incubated at 55°C with frequent vortexing until lysis was complete (approximately 1-2 hours). 20 µl RNase A (20 mg/ml) was added to the lysate, mixed by vortexing and incubated for 2 minutes at room temperature. 200 µl PureLink Genomic Lysis/Binding Buffer was added to the lysate, mixed by vortexing, followed by the addition of 200 µl of 100% (v/v) ethanol then vortexing for 5 seconds. To bind the DNA, the lysate was loaded onto a PureLink Spin Column in a collection tube and centrifuged at 13,000 rpm for 1 minute at room temperature. The spin column was placed into a new collection tube and washed with 500 µl Wash Buffer 1. The column was centrifuged at 13,000 rpm for 1 minute at room temperature and placed in a new collection tube. The column was then washed with 500 µl Wash Buffer 2, centrifuged at 13,000 rpm for 3 minutes at room temperature. To elute the DNA, the spin column was transferred into a 1.5 ml Eppendorf tube. 50 µl sterile Milli-Q water was added onto the membrane and incubated for 1 minute at room temperature. The column was centrifuged at 13,000 rpm for 1 minute at room temperature, then to increase the concentration of DNA recovered, the sample in the collection tube containing purified DNA was reapplied to the membrane. The column was centrifuged at 13,000 rpm for 1 minute at room temperature. The purified gDNA was checked for concentration and quality on the NanoDrop ND-1000 spectrophotometer (Thermo Fisher Scientific) and stored at -20°C.

2.6.3 Polymerase chain reaction (PCR)

For typical PCR reactions, the following were pipetted into and mixed in a 0.6 µl Eppendorf tube:

MyTaq Red 1X master mix (Bioline)	24 µl
Forward primer (100 pmol/µl)	0.75 µl
Reverse primer (100 pmol/µl)	0.75 µl
Genomic DNA (10-100 ng/µl)	1 µl

Tubes containing mixtures of the above were placed into a DNA Engine Tetrad 2 Peltier Thermal Cycler (Bio-Rad, Watford, UK) and the appropriate PCR program was selected.

A typical PCR program involved the following steps:

Denaturing	94°C for 15 seconds
Annealing	50°C for 1 minute
Extension	72°C for 1 minute

The three steps above were repeated 34 times and followed by:

Final extension	72°C for 7 minutes
-----------------	--------------------

The program conditions above were optimised for each reaction: The annealing temperature (T_a) was altered depending on the melting temperatures (T_m) of the primers. The optimal T_a was calculated by averaging the T_m of the forward and reverse primers and subtracting 5°C from the average. The extension time was adjusted to suit the expected size of the PCR product, with an additional minute for each 1 kb of product.

2.6.4 PCR purification

Purification of PCR products was performed using QIAquick PCR Purification Kit (QIAGEN, Manchester, UK) according to the manufacturer's instructions. Buffer PB was added to PCR products in a 5:1 ratio, mixed by vortexing, then transferred to a QIAquick column in a 2 ml collection tube. To bind DNA, the sample was centrifuged at 13,000 rpm for 60 seconds, the flow-through discarded and the column was placed back in the tube. To wash the column, 750 μ l of Buffer PE was added to the column and centrifuged for 60 seconds. The flow-through was discarded and the column was placed back in the tube. To remove any remaining wash buffer, the column was centrifuged for an additional 60 seconds. To elute DNA, the column was placed in a clean 1.5 ml Eppendorf tube, 50 μ l of sterile Milli-Q water was carefully added to the membrane and allowed to stand for 60 seconds. The column was centrifuged for 60 seconds. To increase the DNA concentration, the eluted DNA at the bottom of the tube was reapplied to the membrane and centrifuged again for 60 seconds. DNA concentration was measured using the NanoDrop spectrophotometer and stored at -20°C.

2.6.5 Gel electrophoresis

1% (w/v) agarose gels with addition of GelRed nucleic acid stain (10,000X) (Biotium, Fremont, USA) were used for gel electrophoresis. Agarose gels were prepared by adding 1.0 g of agarose powder to 100 ml of TAE (1X) buffer and dissolved by heating in a microwave until all the agarose had dissolved. The mixture was allowed to cool until comfortable to touch and 10 µl of GelRed stain was added and mixed. A UV-transparent gel tray (Bio-Rad) with the appropriate comb was placed and secured in a gel caster (Bio-Rad). The gel was cast by pouring the mixture into the gel tray and allowed to set. Once solidified, the gel along with the gel tray was placed in a Sub-Cell Electrophoresis Cell System (Bio-Rad) and submerged in TAE (1X) buffer.

20 µl of PCR products were added to each lane and 5 µl of HyperLadder (1 kb) (Bioline) was used as a molecular weight marker. Gel electrophoresis was performed with PowerPac Basic Power Supply (Bio-Rad) and typical settings used were 100 V, 500 mA, for 45 minutes. The voltage and duration of time were adjusted depending on the PCR product size expected. Following gel electrophoresis, gels were imaged using the GeneGenius Gel Imaging System (Syngene, Cambridge, UK).

2.6.6 Mutagenesis strategy

Isogenic mutants of the *C. jejuni* 488 wild-type strain were constructed via insertion of a chloramphenicol resistance cassette into *tssB* for the 488 *tssB* mutant or insertion of a kanamycin resistance cassette into *tssC* for the 488 *tssC* mutant and *tssD* for the 488 *tssD* mutant.

Firstly, the gene of interest was checked for the presence of BamHI, BclI, or BglII restriction sites. If none of the above sites were present then inverse PCR mutagenesis (IPCRM) would be required. Forward and reverse primers were designed as described in Section 2.6.1 and used to amplify the gene of interest from gDNA. The amplified gene of interest was purified, cloned into the pGEM-T Easy vector and transformed into *E. coli* competent cells. *E. coli* XL2 Blue was used if the unique restriction site was either BamHI or BglII and *E. coli* SCS110 was used if the unique restriction site was BclI. Positive transformants were selected.

Plasmid DNA from the positive transformants were isolated and digested with either BamHI, BclI, or BglII restriction enzymes. The digested products were purified and the antibiotic resistance cassette of choice was ligated into the digested plasmid DNA. The ligated products were transformed into *E. coli* competent cells and positive transformants were screened by PCR using gene-specific primers. Plasmid DNA was isolated from positive transformants and confirmed via sequencing.

Once confirmed, the plasmid DNA were transformed into *C. jejuni* competent cells by electroporation and screened for positive transformants by PCR and sequencing. Glycerol stocks of positive mutants were prepared and stored at -80°C as described in Section 2.2.

2.6.7 Insertion of antibiotic resistance cassette into gene of interest

Genomic DNA of the 488 wild-type strain was isolated as described in Section 2.6.2. Forward and reverse primers were designed as described in Section 2.6.1 and used to amplify the gene of interest from the gDNA by setting up a PCR reaction as described in Section 2.6.3. Amplified PCR products were checked via gel electrophoresis for the correct size. Once confirmed, PCR products were purified using the QIAQuick PCR Purification Kit (see Section 2.6.4).

PCR products were ligated into the pGEM-T Easy vector using the pGEM-T Easy Vector System (Promega, Southampton, UK). The following were added to the ligation reaction:

PCR product	(See below for calculation of volume)
pGEM-T Easy vector (50 ng/μl)	1 μl
T4 DNA ligase (3 Weiss units/μl)	1 μl
2X Rapid Ligation buffer	5 μl
Milli-Q water	up to 10 μl

The volume of PCR product to be added was calculated using the equation below:

$$\text{ng of insert} = \frac{(\text{ng of vector}) \times (\text{kb size of insert})}{(\text{kb size of vector})} \times (\text{insert: vector molar ratio})$$

The manufacturer suggested using insert:vector molar ratios between 3:1 to 1:3 as a good starting parameter. The ligation reaction was mixed by gentle pipetting and incubated at 4°C overnight.

2.6.8 Transformation into *E. coli* competent cells

The appropriate *E. coli* competent cells were selected for transformation dependent on the restriction site present in the gene of interest. The competent cells were thawed on ice and 100 µl of cells were gently aliquoted into a pre-chilled Eppendorf. 1.7 µl of β-mercaptoethanol (1.22 M) was added to each 100 µl aliquot of cells to improve transformation efficiency. The mixture of competent cells and β-mercaptoethanol was incubated on ice for 10 minutes, with gentle swirling every 2 minutes. 0.1-50 ng of ligated DNA (see Section 2.6.7) was added to each aliquot of cells, swirled gently and incubated on ice for 30 minutes. The mixture was heat-pulsed in a 42°C water bath for 45 seconds and this timing was crucial to achieve maximum efficiency. The mixture was incubated on ice for 2 minutes, followed by addition of 900 µl SOC medium (pre-warmed to 42°C) and incubation at 37°C for 1 hour with shaking at 225-250 rpm. 200 µl of the transformation mixture was plated onto LB plates with the addition of ampicillin and other appropriate antibiotics as required. The plates were incubated at 37°C overnight and stored at 4°C.

2.6.9 Screening for positive transformants

A number of colonies were selected from the transformants plate (see Section 2.6.8) and restreaked onto LB plates with the addition of ampicillin and other appropriate antibiotics as required. The plates were incubated at 37°C overnight. Colonies were dabbed with a 1 µl loop and resuspended in 100 µl Milli-Q water. The suspension was vortexed thoroughly and incubated at 95°C for 10 minutes. The boilate was centrifuged at 13,000 rpm for 5 minutes and 1 µl of the supernatant was used in the standard PCR reaction mixture. Gel electrophoresis was performed with the PCR products and successful transformants were screened by sequencing. Once confirmed, positive transformants were stored in glycerol at -80°C as described in Section 2.2.

2.6.10 Isolation of plasmid DNA

Plasmid DNA was isolated using the QIAprep Spin Miniprep Kit (QIAGEN) according to the manufacturer's instructions. Overnight cultures of *E. coli* in 10 ml LB were pelleted by centrifuging at 4,000 rpm for 10 minutes at 4°C. Pelleted *E. coli* were resuspended in 250 µl Buffer P1 and transferred to a 1.5 ml Eppendorf tube. 250 µl Buffer P2 was added and the tube was inverted 5 times to mix the solution. 350 µl Buffer N3 was immediately added and again the tube was inverted 5 times to mix the solution. The solution was centrifuged at 13,000 rpm for 10 minutes at room temperature and the supernatant was transferred to the QIAprep spin column. The column was centrifuged for 60 seconds and the flow-through was discarded. 500 µl Buffer PB was applied to wash the column and the column was centrifuged for 60 seconds and the flow-through was discarded. 750 µl Buffer PE was applied to wash the column and the column was centrifuged for 60 seconds and the flow-through was discarded. To remove residual buffer, the column was centrifuged for an additional 60 seconds. To elute DNA, 50 µl of sterile Milli-Q water was added to the membrane, allowed to stand for 60 seconds and centrifuged for 60 seconds. To increase DNA concentration, the eluted DNA at the bottom of the tube was reapplied to the membrane and centrifuged again for 60 seconds. DNA concentration was measured using the NanoDrop spectrophotometer and stored at -20°C.

2.6.11 Preparation of *C. jejuni* competent cells

Competent cells were prepared by growing *C. jejuni* strains on blood agar plates for 16 hours. EBF buffer was prepared by adding 15 ml of 100% (v/v) glycerol and 10 ml of 10% (w/v) sucrose to 75 ml Milli-Q water. The buffer was filter sterilised and stored at 4°C until use. Bacterial cells were harvested from 3-4 plates and resuspended in 10 ml ice cold EBF buffer. The bacterial suspension was centrifuged at 4,000 rpm at 4°C for 10 minutes and the supernatant was discarded. To wash the bacterial cells, the pellet was resuspended in 1 ml EBF buffer, centrifuged at 13,000 rpm for 2 minutes, the supernatant was discarded and the washing process repeated again. The final pellet was resuspended in 250 µl EBF buffer and stored at -80°C.

2.6.12 Transformation via electroporation

Ice-cold plasmid DNA (see Section 2.6.10) and *C. jejuni* competent cells (see Section 2.6.11) were mixed in a range of desired ratios, for example 10 µl plasmid DNA (1-5 µg) added to 30 µl competent cells, then incubated on ice for 10 minutes. The suspension was pipetted into a cold 2 mm electroporation cuvette (Bio-Rad, UK) and gently tapped to eliminate any bubbles. The cuvette was placed in the ShockPod cuvette chamber of a Gene Pulser Xcell electroporation system (Bio-Rad) and electroporated using settings 25 uFD, 2.5 KV and 200Ω. 100 µl room temperature SOC broth (Invitrogen) was added immediately to the cuvette and the contents of the cuvette was pipetted onto a blood agar plate and incubated at 37°C under microaerobic conditions for 18 hours. The cells on the blood plate were harvested and resuspended in 400 µl Brucella broth. The suspension was spread onto a blood plate containing 50 µg/ml kanamycin or 10 µg/ml chloramphenicol and incubated at 37°C under microaerobic conditions for 2-7 days.

2.6.13 Screening for positive *C. jejuni* mutants

Colonies grown on blood agar plates containing the appropriate antibiotic were harvested and restreaked onto fresh blood agar plates with antibiotics. Plates were incubated at 37°C under microaerobic conditions for 24 hours. A small amount of each colony was harvested with a 1 µl loop and resuspended in 100 µl Milli-Q water. The suspensions were vortexed, heated to 95°C for 10 minutes and centrifuged at 13,000 rpm for 5 minutes. PCR screening was performed with 1 µl of the boilate supernatant and appropriate primers as described in Section 2.6.9. Positive mutants were checked by sequencing and stored as glycerol stocks at -80°C as described in Section 2.2.

2.6.14 Inverse PCR mutagenesis (IPCRM)

For mutagenesis, inverse PCR was performed when the gene of interest lacks the restriction sites BamHI, BclI or BglII in order to insert an antibiotic resistance cassette. A 10-15 nucleotide region was selected in the centre of the gene of interest to be replaced by a restriction site. IPCRM primers were designed as followed (with BglII chosen as an example):

IPCRM forward – 5' **GGG**AGATCTXXXXXXXXXXXXXXXXX 3'
IPCRM reverse – 5' **GGG**AGATCTYYYYYYYYYYYYYYYYY 3'

The sequence of the BglII restriction site (AGATCT) was preceded by three extra guanine residues (GGG) to increase the efficiency of the primers. For the forward primer, XXXXXXXXXXXXXXXXXXXX denote the 5' flanking sequence of the selected region and YYYYYYYYYYYYYYYYYY denote the reverse complement of the 3' flanking sequence of the selected region.

The BglII restriction site was inserted into the selected region and the products were amplified by performing PCR using the IPCRM forward and reverse primers as described above. The amplified product was purified with QIAquick PCR Purification Kit and the concentration was measured using a Nanodrop spectrophotometer. Digestion of the product was performed as followed:

Purified amplified IPCRM product (10-500 ng/μl)	20 μl
BglII (20 units)	2 μl
DpnI (20 units) (to reduce methylated template DNA)	2 μl
NEBuffer 3.1	10 μl
Milli-Q water	up to 100 μl

Digestion was performed at 37°C for 3 hours, then the digested IPCRM products were purified with QIAquick PCR Purification Kit and the concentration was measured using a Nanodrop spectrophotometer. Digestion of the desired antibiotic resistance cassette (kanamycin^R or chloramphenicol^R) with BamHI was also performed.

The digested antibiotic resistance cassette was re-ligated into the digested IPCRM product as followed and incubated at 4°C overnight:

Digested IPCRM product (250 ng/μl)	2 μl
Digested antibiotic resistance cassette (20 ng/μl)	5 μl
T4 DNA ligase (3 Weiss units/μl)	2 μl
10X ligase buffer	1 μl

The IPCRM product ligated with the antibiotic resistance cassette was transformed into *E. coli* competent cells as described in Section 2.6.8. Plasmid DNA was isolated from positive transformants as described in Section 2.6.10 and transformed into *C. jejuni* competent cells by electroporation as described in Section 2.6.12.

2.6.15 Double mutagenesis strategy

The 488 *tssBC* double mutant was constructed by transforming the plasmid containing *tssC::Km* into the 488 *tssB* mutant as described in Section 2.6.12. Positive mutants were screened on blood agar plates containing kanamycin and chloramphenicol as described in Section 2.6.13 and checked by sequencing.

2.6.16 Complementation

To complement a mutant strain, the gene of interest was amplified by PCR and the following PCR pre-mix prepared per sample:

Buffer II (for gDNA)	10 μl
Accuprime Taq polymerase (2U/ μl)	0.2 μl
Milli-Q water	89.6 μl

PCR reactions were prepared with a total volume of 100 μl:

Pre-mix (as above)	98.4 μl
gDNA (10-100 ng/μl)	1.0 μl
Forward and reverse primers (100 pmol/μl)	0.6 μl

The PCR program was optimised to the annealing temperature (T_a) of the primers. PCR products were checked by gel electrophoresis. PCR products were purified by QIAQuick PCR purification (see Section 2.6.4) and purified inserts were checked on the NanoDrop spectrophotometer. Digestion reactions were set up to digest the purified inserts and the pCJC1 or pRRC complementation vector plasmids:

Purified PCR product (10-500 ng/ μ l)	10 μ l
Buffer (NEB buffer 2)	2 μ l
NcoI (20 units)	1 μ l
NheI (20 units)	1 μ l
BSA (100 mg/ml)	1 μ l
Milli-Q water	up to total volume of 100 μ l

And the above digestion reaction was incubated for 3 hours at 37°C, purified by QIAQuick PCR purification again and checked on the NanoDrop. To ligate the insert into pCJC1 or pRRC complementation vectors, the following ligation reaction was set up:

2X ligation buffer	5 μ l
Digested complementation vector	(See below)
Digested insert	(See below)
T4 DNA ligase (3 Weiss units/ μ l)	1 μ l
Milli-Q water	up to total volume of 10 μ l

To calculate the amount of insert and vector to add:

$$\frac{(\text{ng of vector} \times \text{kb size of insert})}{(\text{kb size of vector})} \times \text{insert: vector molar ratio} = \text{ng of insert}$$

The manufacturer recommended an insert: vector ratio of 3:1. The ligation reaction was incubated overnight at 4°C and the concentration was checked using the NanoDrop. The ligation mixture was transformed into XL2 cells as described in Section 2.6.8 and plated onto LB plates with the addition of ampicillin and chloramphenicol. Positive transformants were selected and screened as described in Section 2.6.9. The plasmid DNA of the positive transformants were isolated as described in Section 2.6.10 and transformed via

electroporation into *C. jejuni* mutant strains as described in Section 2.6.12. The electroporation mixture was plated onto blood agar plates with the addition of kanamycin and chloramphenicol and positive transformants were screened and confirmed as described in Section 2.6.13.

2.6.17 Ribonucleic acid (RNA) isolation

C. jejuni strains from 24 hour plates were inoculated into 10 ml pre-incubated Brucella broth to an OD₆₀₀ of 0.1. If required, bile salts such as sodium taurocholate and sodium deoxycholate were prepared and added to the Brucella broth for a total concentration of 0.05%, 0.1% and 0.2% (w/v) 15 minutes prior to inoculation. Bacterial cultures were grown for 6 or 16 hours at 37°C under microaerobic conditions. To stabilise RNA prior to RNA isolation, 4 ml RNAprotect bacteria reagent (Qiagen) was added to 2 ml of bacterial cultures and vortexed for 5 seconds. The suspension was incubated for 5 minutes at room temperature, centrifuged at 4,000 rpm at 4°C for 10 minutes, then the supernatant was discarded.

The isolation of RNA was performed using the PureLink RNA Mini Kit (Invitrogen). 600 µl of Lysis buffer and 6 µl of β-mercaptoethanol (14.3 M) was added to the pellet. The lysis mixture was pipetted vigorously for 2 minutes until frothy to resuspend the pellet and suspension was vortexed for 2 minutes. 550 µl of 70% (v/v) ethanol was added to 550 µl of sample and vortexed immediately. To purify, the sample was transferred to a spin cartridge in a collection tube and centrifuged at 13,000 rpm for 15 seconds. The flow through was discarded and a further 550 µl of 70% (v/v) ethanol was added and centrifuged at 13,000 rpm for 15 seconds. To dry out the membrane, the flow through was discarded and the tube was centrifuged at 13,000 rpm for 1 minute. To elute the RNA, 30 µl of RNase-free water was added to the centre of the spin cartridge and incubated for 1 minute at room temperature. The tube was centrifuged at 13,000 rpm for 2 minutes. For higher yield, the resulting sample was pipetted back onto the membrane and centrifuged at 13,000 rpm for a further 2 minutes. DNA contamination was removed from the RNA using the TURBO DNA-free kit (Invitrogen). The concentration of RNA was measured on the NanoDrop 1000 spectrophotometer (Thermo Fisher Scientific) and RNA normalised to 2000 ng:

$$\frac{2000 \text{ ng}}{\text{Concentration measured on Nanodrop}} = \text{required RNA volume } (\mu\text{l})$$

Reactions were set up as follows:

10X TURBO DNase buffer	5 μ l
TURBO DNase (2 U/ μ l)	1 μ l
RNA	2000 ng
Made up to 50 μ l total volume with nuclease-free water	

The mixture was vortexed gently and incubated at 37°C for 45 minutes. To inactivate the DNase, 5 μ l of DNase inactivation reagent was added to the mixture and incubated at room temperature for 5 minutes with occasional vortexing. The mixture was centrifuged at 10,000 rpm for 90 seconds and the supernatant containing RNA was transferred to a new tube and the concentration checked by the NanoDrop spectrophotometer.

2.6.18 Complementary DNA (cDNA) synthesis

cDNA synthesis was performed using the SuperScript III First-Strand Synthesis System (Invitrogen). The following reaction was set up:

Random hexamers (50 ng/ μ l)	1 μ l
dNTP mix (10 mM)	1 μ l
RNA (2000 ng)	2.5 μ l

The reaction was incubated at 65°C for 5 minutes and immediately transferred onto ice for at least 1 minute. The following cDNA synthesis mix was prepared in the following order:

10X RT buffer	2 μ l
MgCl ₂ (25 mM)	4 μ l
DTT (0.1 M)	2 μ l
RNaseOUT (40 U/ μ l)	1 μ l
SuperScript III RT (200 U/ μ l)	1 μ l

To ensure DNA is no longer present in samples, a negative control was also prepared by omitting the SuperScript III RT from the synthesis mix before adding to samples.

10 µl of cDNA synthesis mix was added to each reaction from above and mixed gently and collected by brief centrifugation. The mixture was incubated at 25°C for 10 minutes, at 50°C for 50 minutes, at 85°C for 5 minutes and allowed to chill on ice for at least 1 minute. The mixture was collected by brief centrifugation, then 1 µl RNase H (2 U/µl) was added and incubated at 37°C for 20 minutes. The concentration of the cDNA synthesis reaction was checked using the NanoDrop and either stored at -20°C or used for RT-PCR or qRT-PCR immediately.

2.6.19 Reverse transcription PCR (RT-PCR)

RNA was isolated from 24 hour plate cultures grown on blood agar plates or 16 hour cultures grown in Brucella broth with shaking at 75 rpm under microaerobic conditions. RNA was converted to cDNA as described in Section 2.6.18 and RT-PCR was performed with primers listed in Table 2.4. PCR was performed as according to Section 2.6.3. Gel electrophoresis with PCR products were performed at 90 V for 1 hour 15 minutes and the gel was imaged with the GeneGenius Gel Imaging System. Relative intensity of the bands were analysed using the ImageJ software (National Institutes of Health, USA) (Schneider et al., 2012).

2.6.20 Quantitative real-time PCR (qRT-PCR)

qRT-PCR was performed using primers listed in Table 2.4, with SYBR Green PCR Master Mix (Applied Biosystems, Loughborough, UK) on the ABI 7500 Real-Time PCR System machine (Applied Biosystems). The concentration of the cDNA was standardised during the synthesis reaction. The mixture was prepared as below for each well:

SYBR Green PCR Master Mix (2X)	10 µl
Forward primer (10 pmol/µl)	0.5 µl
Reverse primer (10 pmol/µl)	0.5 µl
Nuclease free water	10 µl
cDNA (concentration standardised)	1 µl

20 µl of the mixture above was mixed thoroughly and loaded into each well on a MicroAmp Fast Optical 96-Well Reaction Plate (Thermo Fisher). Each reaction was loaded in triplicate. The plate was sealed tightly with MicroAmp Optical Adhesive Film and loaded onto the ABI 7500 Real-Time PCR System machine. The following settings were selected:

7500 Fast (96 wells)

Quantitation – Comparative CT ($\Delta\Delta CT$)

SYBR Green reagents

Standard (approximately 2 hours to complete a run)

qRT-PCR data was analysed by the comparative C_T method using the *gyrA* gene as an internal control (Schmittgen and Livak, 2008).

2.6.21 Whole cell lysate (WCL) extraction

For extraction of whole cell lysates, *C. jejuni* from 24 hour plate cultures were inoculated into 50 ml Brucella broth and incubated at 37°C with shaking at 75 rpm under microaerobic conditions until late exponential phase. Bacterial cultures were centrifuged at 4,000 rpm at 4°C for 30 minutes and the supernatant was discarded. Cell pellet samples were resuspended in the appropriate sample buffer, placed on ice and sonicated for 10 minutes (cycles of 1 minute on / 30 seconds off) on high setting using the Bioruptor Plus sonication device (Diagenode, Liège, Belgium) or 3 minutes (cycles of 30 seconds on / 30 seconds off) using the Fisherbrand 120 sonic dismembrator (Thermo Fisher Scientific). Samples were centrifuged at 14,000 rpm for at 4°C for 5 minutes and the supernatant with lysed cell content was transferred to a new Eppendorf. Samples were boiled at 95°C for 10 minutes, centrifuged at 13,000 rpm for 5 minutes and stored at -20°C. Protein concentration of the whole cell lysate samples was measured using the BCA assay as described in Section 2.3.7.

2.6.22 Protein secretion

For isolation of secretome, *C. jejuni* from 24 hour plate cultures were inoculated into 50 ml Brucella broth to starting OD₆₀₀ of 0.1 and incubated at 37°C with shaking at 75 rpm under microaerobic conditions until late exponential phase. Bacterial cultures were centrifuged at 4,000 rpm at 4°C for 30 minutes and the supernatant was then filtered using 0.22 µm-pore-size filters (Millipore). The titrate was concentrated using an Amicon Ultra-15 centrifugal filter (10 kDa) (Millipore) at 4,000 rpm at 4°C until all the supernatant had been concentrated. Concentrated titrate was further concentrated via TCA precipitation as described in Section 2.6.23. Samples were resuspended in 100 µl of the appropriate sample buffer, boiled at 95°C for 10 minutes, centrifuged at 13,000 rpm for 5 minutes and stored at -20°C. Protein concentration of the supernatant samples was measured using the BCA assay as described in Section 2.3.7.

2.6.23 Trichloroacetic acid (TCA) precipitation

The TCA precipitation method was adapted from a protocol published by Link & LaBaer (Link and LaBaer, 2011). Following concentration via centrifugal filter, samples were divided into smaller volumes (approximately 500 µl) per Eppendorf. 55 µl of ice-cold 100% (v/v) TCA (6.1 N) was gently added to each 500 µl of sample and incubated on ice for 10 minutes. 500 µl of ice-cold 10% (v/v) TCA was then added to each sample and incubated on ice for 1 hour. Samples were centrifuged at 14,000 rpm at 4°C for 30 minutes. 500 µl of 90% (v/v) acetone was added to the samples, mixed by gently inverting the tubes twice and centrifuged at 14,000 rpm at 4°C for 30 minutes. The supernatant was carefully removed and the pellets were allowed to air dry with the tubes inverted for 15 minutes. Samples were resuspended in 100 µl of the appropriate sample buffer.

2.6.24 OMV isolation

For isolation of OMVs, *C. jejuni* from 24 hour plate cultures were inoculated at OD₆₀₀ 0.1 into 50 ml Brucella broth and incubated at 37°C with shaking at 75 rpm under microaerobic conditions until late exponential phase. Bacterial cultures were adjusted to the same OD₆₀₀, centrifuged at 4,000 rpm at 4°C for 30 minutes and the supernatant was then filtered using 0.22 µm-pore-size filters (Millipore). The titrate was concentrated using an Amicon Ultra-15 centrifugal filter (10 kDa) (Millipore) at 4,000 rpm at 4°C until all the supernatant had been

filtered. Filtered samples were centrifuged at 45,000 rpm at 4°C for 3 hours with a TLA 100.4 rotor (Beckman Instruments, U.S.A.). OMVs in the pellet were re-suspended in PBS and stored at -20°C. Protein concentration of the OMV samples was measured using the BCA assay as described in Section 2.3.7.

2.6.25 SDS-PAGE

NuPAGE 12% Bis-Tris protein gel (1.0 mm, 10 wells) (Thermo Fisher Scientific) was slotted into an XCell SureLock Mini-Cell Electrophoresis System (Thermo Fisher Scientific) and MOPS (1X) running buffer was used. To prepare samples for loading onto SDS-PAGE gels, Laemmli (2X) sample buffer was added in equal volume to samples if samples were not already resuspended in Laemmli buffer. Samples were boiled at 95°C for 10 minutes, centrifuged at 13,000 rpm for 5 minutes and 10 µl of samples were loaded per well. 5 µl of PageRuler Plus Pre-stained Protein Ladder (Thermo Fisher Scientific) was loaded as a molecular weight marker. The gel was run at 150 V for 50-60 minutes and removed carefully from the case. SDS-PAGE gels were stained with SYPRO Ruby or used for Western blotting.

2.6.26 Antibody production

The polyclonal TssD antibody and recombinant TssD protein were kindly provided by Professor Nicolae Corcionivoschi at the Agri-Food and Biosciences Institute (Belfast, UK). The polyclonal VgrG antibody was produced by Capra Science Antibodies AB (Ängelholm, Sweden). The *vgrG* gene was cloned into an expression vector and the recombinant VgrG protein was isolated and purified. For production of the VgrG antiserum, purified VgrG was immunised into a rabbit. Two boosts with the antigen were performed, followed by the first bleed. A further boost with the antigen was performed followed by the second bleed; the process was repeated for a third bleed. Antiserum collected from the third bleed was affinity purified using a peptide-coupled column for the VgrG antibody.

2.6.27 Western blot

The iBlot 2 Dry Blotting System (Thermo Fisher Scientific) was used to transfer the proteins to the membrane. The gel was placed into the iBlot 2 Transfer Stack (nitrocellulose, mini) according to the manufacturer's instructions and a roller was used to ensure all bubbles were eliminated between the layers. The P1 program (25 V for 6 minutes) was selected to perform

the blotting. To block, the membrane was placed in a square petri dish and submerged in blocking solution made from 2% (w/v) dried skimmed milk in PBS for either 1 hour shaking at room temperature or overnight stationary at 4°C. The blocking solution was decanted and the primary antibody was added to a dilution of 1:5000 in PBS, 0.1% (v/v) TWEEN 20 and 2% (w/v) dried skimmed milk. The membrane was incubated with the primary antibody for either 1 hour shaking at room temperature or overnight stationary at 4°C. Four washes were then performed with PBS and 0.1% (v/v) TWEEN 20 and the membrane was placed in a dark box. The secondary antibody (Goat anti-rabbit 680) (Sigma-Aldrich) was added at a dilution of 1:10,000 in PBS and 0.1% (v/v) TWEEN 20, 2% (w/v) dried skimmed milk and 0.02% (v/v) SDS. The membrane was incubated for 1 hour shaking at room temperature. Three washes were performed with PBS and 0.1% (v/v) TWEEN 20 and a further wash was performed with PBS only. The membrane was kept in PBS at 4°C until imaged on the Odyssey Imaging System (Li-Cor, Cambridge, UK).

2.6.28 Silver staining

The basic staining protocol for the SilverQuest Silver Staining Kit (Thermo Fisher Scientific) was used. Following electrophoresis, the SDS-PAGE gel was placed in a square petri dish and rinsed with Milli-Q water. The gel was fixed in 100 ml fixative solution for 20 minutes on an orbital shaker. The fixative solution was then decanted and the gel was then washed with 30% (v/v) ethanol for 10 minutes. The ethanol was decanted and 100 ml of sensitising solution (30 ml 100% (v/v) ethanol, 10 ml sensitiser solution and 70 ml Milli-Q water) was added and incubated for 10 minutes. The sensitising solution was decanted and the gel was washed with 100 ml of 30% (v/v) ethanol for 10 minutes. A further wash was performed with 100 ml of Milli-Q water for 10 minutes. To stain, 100 ml of staining solution (1 ml stainer and 99 ml Milli-Q water) was added for 15 minutes. The staining solution was decanted and the gel was washed with 100 ml of Milli-Q water for 20-60 seconds. To develop the bands, 100 ml of developing solution (10 ml developer, 1 drop of developer enhancer and 90 ml of Milli-Q water) was added for 4-8 minutes until the desired band intensity is achieved. Once the band intensity was reached, 10 ml of stopper solution was added and the gel was placed on a shaker for 10 minutes until the colour changed from pink to colourless. The stopper solution was decanted and the gel was washed with 100 ml of Milli-Q water for 10 minutes. The gel was imaged in the GeneGenius Gel Imaging System.

2.6.29 SYPRO Ruby protein staining

The basic manufacturer's protocol for the SYPRO Ruby Protein Gel Stain (Invitrogen) was followed. The SDS-PAGE gel was placed in a square petri dish following electrophoresis and fixed with 100 ml of 50% (v/v) methanol and 7% (v/v) acetic acid for 30 minutes on an orbital shaker. This solution was decanted and 100 ml fix solution was added for a further 30 minutes. This solution was decanted and 60 ml SYPRO Ruby gel stain was added and incubated overnight on the shaker. The gel was transferred to a clean container and washed with 100 ml 10% (v/v) methanol and 7% (v/v) acetic acid for 30 minutes on the shaker. The wash solution was decanted and 100 ml Milli-Q water was added for 5 minutes, decanted and a further 100 ml Milli-Q water was added for 5 minutes. The gel was stored in Milli-Q water before imaging on the Typhoon Trio (Amersham Biosciences, Amersham, UK). For imaging the following settings were used: Fluorescence, green 532 nm, emission filter 520 nm bandpass (520 BP 40).

2.6.30 Imperial protein staining

Following gel electrophoresis, the SDS-PAGE gel was placed in a square petri dish and washed four times with 100 ml Milli-Q water for 5 minutes. To stain the gel, Imperial Protein Stain (Thermo Fisher Scientific) was added to cover the gel and incubated for 2 hours on a shaker. To wash and reduce the background, the staining reagent was decanted and 200 ml Milli-Q water was added then incubated overnight on a shaker. The gel was imaged using the GeneGenius Gel Imaging System.

2.6.31 Whole genome sequencing

Genome sequencing of the *C. jejuni* 488 and 43431 (Poly et al., 2004) wild-type strains was performed as previously described by Ugarte-Ruiz et al. (Ugarte-Ruiz et al., 2014). Briefly, sequencing was performed using the Illumina MiSeq 2 x 301 bp paired-end sequencing. To analyse the data quality, FastQC was used (S, 2010) followed by read trimming using Trimmomatic (v0.32) (leading' and 'trailing' setting of 3, a 'slidingwindow' setting of 4:20 and a 'minlength' of 36 nucleotides) (Bolger et al., 2014). Reads were mapped using BWA-MEM (v0.7.7-r441) against the genome sequence of *C. jejuni* NCTC 11168 (AL111168) (Li and Durbin, 2009). Assembly on unmapped regions was performed using Velvet Optimiser (v2.2.5) using n50 optimization (Gladman S, 2012, Zerbino and Birney, 2008). Contigs were

ordered against *C. jejuni* NCTC 11168 (AL111168) strains using ABACAS (v1.3.1) (Assefa et al., 2009). Genome annotation was performed using Prokka (Seemann, 2014). Genomes were visualized using Artemis and ACT software (Carver et al., 2012). T6SS open reading frames (ORFs) were identified using BLAST (Altschul et al., 1990, Gish and States, 1993). The 488 and 43431 genome sequences were uploaded to the EBI ENA database (Accession number PRJEB31331).

2.6.32 Bioinformatic searches for known effector proteins

Bioinformatic searches were performed to identify *C. jejuni* known effector proteins found in other bacteria. A list was generated of known effector proteins and the amino acid sequences of known effector proteins were retrieved from GenBank and added to this list as query sequences. The sequences from this list were queried against the genome sequence of the 488, 43431 and RC039 strains using Blastall scripts on UNIX. No matches were found with expectation values of $-e0.01$ and $-e0.1$. Positive controls were performed with TssD from *C. jejuni* 414 and Hcp1 from *P. aeruginosa* PAO1 as the query sequences.

2.6.33 Mass spectrometry sample preparation

Ammonium bicarbonate (AmBic) buffer was prepared by adding 0.395 g of ammonium bicarbonate (Honeywell Fluka, Mexico City, USA) to 50 ml Milli-Q water for a 100 mM AmBic buffer stock. The stock solution was prepared fresh and filter sterilised prior to diluting to 25 mM for use in sample preparation.

cOmplete Mini, EDTA-free tablets (Sigma) were added as a protease inhibitor to prevent protein degradation. A stock solution (7x concentration) was prepared by dissolving one tablet in 1.5 ml Milli-Q water and stored at -20°C for 12 weeks.

Rapigest-SF (Waters, Milford, USA) was added as a denaturant. A 1% (w/v) stock solution was prepared by adding 100 μl 25 mM AmBic buffer to 1 mg of pre-measured powder in a vial and stored at 4°C for 1 week.

Bacterial suspensions were prepared by inoculating *C. jejuni* strains from 24 hour plate cultures at OD_{600} 0.1 into 50 ml of pre-incubated Brucella broth. Bacterial cultures were incubated at 37°C with shaking at 75 rpm under microaerobic conditions for 12 hours.

Cultures were transferred to falcon tubes and centrifuged at 4,000 rpm for 30 minutes at 4°C to separate the pellet and supernatant.

Pellets were resuspended in 10 ml AmBic buffer and centrifuged at 4,000 rpm for 10 minutes at 4°C. The supernatant from the wash was discarded and a further wash was performed with 10 ml AmBic buffer with the supernatant again discarded. The pellets were re-suspended in 1 ml AmBic buffer and transferred to a 1.5 ml Eppendorf tube. Samples were sonicated using the FB120 Sonic Dismembrator (Thermo Fisher Scientific) at 50% amplitude, 30 seconds on and 30 seconds off for 5 minutes total. Sonicated samples were centrifuged at 13,000 rpm for 5 minutes and 400 µl of supernatant with lysed cell content was transferred to a new 1.5 ml tube. 20 µl Rapigest and 57.1 µl cOmplete were added to each 400 µl sample and samples were boiled at 90°C for 10 minutes, centrifuged for 5 minutes at 13,000 rpm and the supernatant were transferred to a new tube.

For the supernatant samples containing the secretome, any remaining cells were filtered out using a 0.22 µm-pore-size filter with a 50 ml syringe. The titrate was concentrated using an Amicon Ultra-15 centrifugal filter (10 kD). 15 ml of supernatant were transferred to the filter and centrifuged at 4,000 rpm, 4°C for 30 minutes. The flow through was discarded, another 15 ml of supernatant was transferred to the filter and centrifuged. This was repeated until all supernatants were filtered. The samples were centrifuged for an additional 20 minutes to further concentrate the samples to less than 1 ml. 1 ml of 25 mM AmBic buffer was added and centrifuged four times at 4,000 rpm, 4°C for 20 minutes. The remaining concentrated samples (approximately 400 µl remaining) were transferred to 1.5 ml Eppendorf tubes. 20 µl Rapigest and 57.1 µl cOmplete were added to each 400 µl sample and samples were boiled at 90°C for 10 minutes, centrifuged for 5 minutes at 13,000 rpm and the supernatant were transferred to a new tube. The protein concentration of pellet and supernatant samples were measured using the BCA assay as described in Section 2.3.7 and samples were stored at -20°C.

2.6.34 Liquid chromatography mass spectrometry

Pellet and supernatant samples prepared in Section 2.6.33 were sent for liquid chromatography mass spectrometry (LC-MS) which were performed by Dr Stuart Armstrong at the University of Liverpool. LC-MS was performed as described by Dubourg et al. (2018). Analysis of the LC-MS data was performed by Dr Stuart Armstrong at the University of Liverpool and Dr Dong Xia at the Royal Veterinary College using Mascot Server (Matrix Science), PEAKS DB (Bioinformatics Solutions Inc.) and Progenesis QI (Nonlinear Dynamics).

A list of proteins was generated from analysis of the LC-MS data, then the following criteria were applied to select for proteins of interest:

Unique peptides ≥ 2

q-value < 0.05

Anova p-value < 0.05

Max fold change > 2

The protein sequences of the proteins of interest were compiled and searched using the databases list in Table 2.5 to predict protein family (Pfam), subcellular location (PSORTb and SOSUIGramN), presence of transmembrane domains (TMHMM), presence of signal peptides (SignalP), secretion method (SecretomeP and Bastion6), protein structure and domains (Phyre2) and to search for orthologues in other bacteria (BlastP). Volcano plot of the secretome data was generated using RStudio with ggplot2, a data visualisation package.

Table 2.5. Databases used in the analysis of LC-MS data.

Database	Description	Reference
Pfam	Database of protein families.	(El-Gebali et al., 2019)
PSORTb	Protein subcellular localisation tool.	(Yu et al., 2010)
SOSUIGramN	Protein subcellular localisation tool with a focus on Gram-negative bacteria.	(Imai et al., 2008)
TMHMM	Predictor of transmembrane helices in proteins.	(Moller et al., 2001)
SignalP	Predictor for the presence of signal peptides and cleavage sites.	(Almagro Armenteros et al., 2019)
SecretomeP	Predictor for non-classically secreted proteins.	(Bendtsen et al., 2005)
Bastion6	Predictor for effectors of the T6SS.	(Wang et al., 2018)
Phyre2	Predictor of protein structure and domains.	(Kelley et al., 2015)
BLASTp	An algorithm that allows the comparison of a query sequence against a sequence database.	(Altschul et al., 1990)

2.6.35 Functional enrichment

Functional enrichment of the secretome data was performed by Dr Dong Xia at the Royal Veterinary College. Secreted proteins were identified and selected as described in Section 2.6.34 and enrichment analyses were performed using Blast2GO to identify gene ontology and Pfam to identify domains.

2.7 Statistical analysis

All experiments were performed with at least three biological replicates and three technical replicates, unless otherwise stated. Statistical analyses were performed using GraphPad Prism 8 (GraphPad Software, San Diego, USA) data were presented as mean \pm SEM. Results were compared using unpaired *t*-test with * indicating $p \leq 0.05$, ** indicating $p \leq 0.01$, *** indicating $p \leq 0.001$ and **** indicating $p \leq 0.0001$.

CHAPTER THREE: Characterisation of *Campylobacter jejuni* T6SS-positive strains and T6SS mutants

3.1 INTRODUCTION

The structure and role of the T6SS machinery in *Campylobacter jejuni* has remained relatively unexplored. Two studies have thus far examined the *C. jejuni* T6SS where 43431 (a human clinical strain from Canada) and 414 (a bank vole isolate from the United Kingdom) were studied by Lertpiriyapong et al. and Bleumink-Pluym et al. respectively (Lertpiriyapong et al., 2012, Bleumink-Pluym et al., 2013). Both studies examined the impact of mutating the genes encoding the TssD needle-like component and the TssM baseplate component.

In this chapter, our aim was to identify a number of T6SS-positive *C. jejuni* strains and construct isogenic mutants to study the role of the T6SS. For mutagenesis, the focus was particularly on the genes encoding the TssBC contractile sheath components, which are crucial to the functioning of the T6SS and have yet to be studied in *C. jejuni*, and also the gene encoding the TssD needle-like component as mutated in the previous studies.

Phenotypic analysis of the *C. jejuni* 488 wild-type strain and isogenic mutants was then performed. The T6SS serves an important role in inter- and intra-bacterial competition in *V. cholerae*, *S. marcescens*, *P. aeruginosa*, *Bacteriodes fragilis* and many others (Ho et al., 2014, Sana et al., 2017). Whether the *C. jejuni* T6SS played a role in bacterial competition was also examined in this chapter.

3.2 RESULTS

3.2.1 Selection of T6SS-positive *C. jejuni* strains

In order to study the T6SS in *C. jejuni*, a number of strains harbouring the complete T6SS locus were required. *C. jejuni* 488, a recent human clinical isolate from Brazil kindly provided by Dr Daiani Teixeira da Silva (a previous PhD student at LSHTM), was identified as having the complete T6SS locus. This strain became the primary focus for this study.

For comparison, *C. jejuni* 43431 was obtained from the American Type Culture Collection. The 43431 strain, previously known as TGH9011, was isolated by Penner et al. from a human diarrheic patient in Canada in the 1980s (Penner et al., 1983). The 43431 strain was also used by Lertpiriyapong et al. in their study (Lertpiriyapong et al., 2012). *C. jejuni* RC039, a T6SS-positive strain isolated from retail raw chicken in Northern Ireland, was kindly provided by Professor Nicolae Corcionivoschi (Agri-Food and Biosciences Institute, Belfast) (Corcionivoschi et al., 2015). *C. jejuni* Cj1 and Cj5 were isolated from human patients in Thailand and were identified by Harrison et al. to have the complete T6SS locus; these strains were kindly provided by Dr Olivia Champion (University of Exeter) (Harrison et al., 2014). The *C. jejuni* 414 strain was used by Bleumink-Pluym et al. in their study (Bleumink-Pluym et al., 2013).

C. jejuni 81-176, a lab reference strain originally isolated from a human patient in the United States, was selected for comparison in phenotypic assays as this strain lacks the T6SS (Korlath et al., 1985).

Table 3.1. *C. jejuni* strains obtained for this study.

<i>C. jejuni</i> strains	Description	Source/Reference
T6SS-positive		
488	Wild-type human isolate from Brazil.	Kindly provided by Dr Daiani Teixeira da Silva.
43431	Wild-type human isolate from Canada.	Purchased from ATCC. (Penner et al., 1983)
RC039	Wild-type chicken isolate from Northern Ireland.	Kindly provided by Professor Nicolae Corcionivoschi. (Corcionivoschi et al., 2015)
Cj1	Wild-type human isolate from Thailand.	Kindly provided by Dr Olivia Champion. (Harrison et al., 2014)
Cj5	Wild-type human isolate from Thailand.	Kindly provided by Dr Olivia Champion. (Harrison et al., 2014)
414	Wild-type bank vole isolate from the United Kingdom.	(Hepworth et al., 2011)
T6SS-negative		
81-176	Wild-type human isolate from the United States.	(Korlath et al., 1985)

3.2.2 Construction of *C. jejuni* 488 *tssC* mutant

The contractile sheath structure is composed of two interlocking components – TssB and TssC – that have been shown to be crucial in T6SS function. Inactivation of either component in *V. cholerae* results in a defective T6SS that is unable to secrete effectors (Basler et al., 2012). The structure and role of the contractile sheath of *C. jejuni* T6SS has yet to be examined. For this study, single and double mutants were constructed for the two contractile sheath components.

The mutagenesis strategy and methodology are described in Chapter 2. Briefly, forward and reverse primers were designed and used to amplify the gene of interest from gDNA. The amplified gene of interest was purified, cloned into the pGEM-T Easy vector and then transformed into *E. coli* XL2 Blue or SCS110 competent cells. Plasmid DNA from positive transformants was isolated and digested with restriction enzymes. The digested products were purified and the antibiotic resistance cassette of choice was inserted and re-ligated into the digested plasmid DNA. The ligated products were transformed into *E. coli* competent cells and positive transformants were screened by PCR. Plasmid DNA was isolated from positive transformants and confirmed via Sanger sequencing. Once confirmed, the plasmid DNA was transformed into *C. jejuni* competent cells by electroporation and screened for positive transformants by PCR and Sanger sequencing.

The *C. jejuni* 488 *tssC* mutant was constructed via insertion of a kanamycin resistance cassette (Kan^R) into the *tssC* gene to disrupt gene function. PCR with *tssC* forward and reverse primers were used to check that the 488 *tssC* mutant clones were of the correct size (2,809 bp) to indicate successful homologous recombination. PCR with the gene-specific primers and kanamycin resistance cassette primers were also used to check that the kanamycin resistance cassette had inserted in the correct orientation into the 488 *tssC* mutant clones (Figure 3.1). 488 *tssC* mutant clones were confirmed by Sanger sequencing.

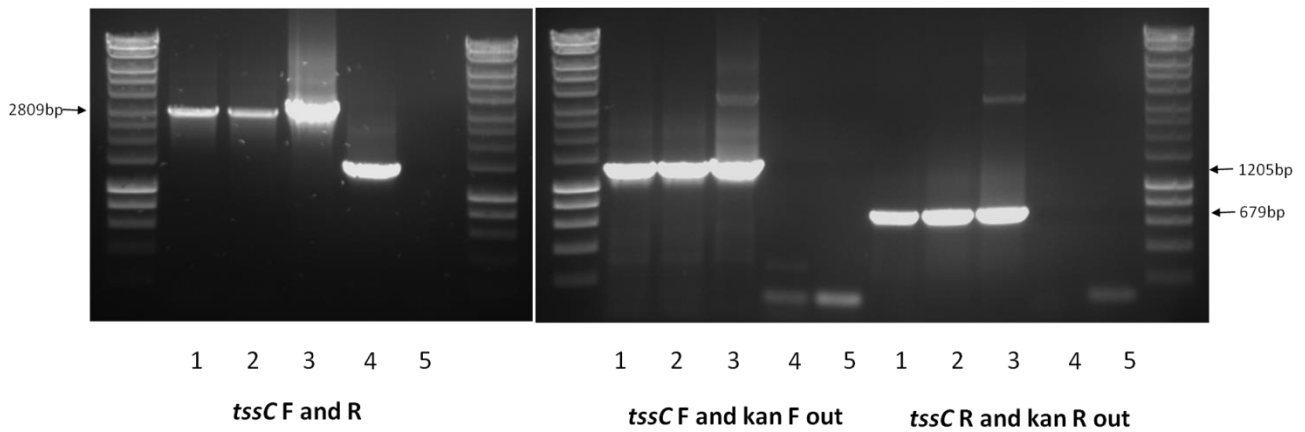


Figure 3.1. PCR checks confirming *C. jejuni* 488 *tssC* mutant clones. Primers specific to *tssC* (*tssC* F and R) and the kanamycin resistance cassette (kan F out and kan R out) were used. Ladder used was HyperLadder 1 kb. Lanes 1 and 2: gDNA of 488 *tssC* mutant clones. Lane 3: Positive control (plasmid DNA with insertion of Kan^R into *tssC*). Lane 4: gDNA of the 488 wild-type strain. Lane 5: Negative control (no DNA).

3.2.3 Growth kinetics of *C. jejuni* 488 wild-type strain and 488 *tssC* mutant

Phenotypic comparisons between the 488 wild-type strain and the 488 *tssC* mutant were performed for growth kinetics, motility and haemolysis of red blood cells. There were no observable differences in growth between the 488 wild-type strain and the 488 *tssC* mutant (Figure 3.2).

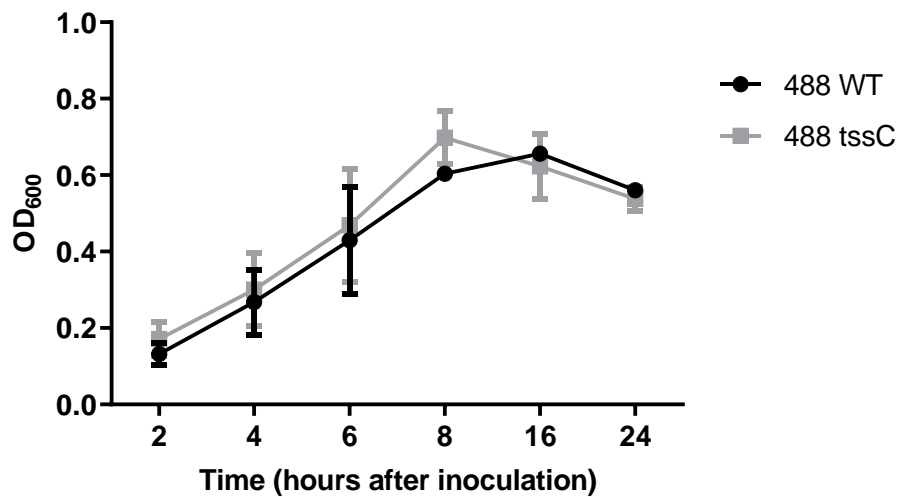


Figure 3.2. Growth of *C. jejuni* 488 wild-type strain and 488 *tssC* mutant in Brucella broth. Strains were harvested from 24 hour plate cultures, inoculated to OD₆₀₀ of 0.1 in Brucella broth, then incubated at 37°C, shaking at 75 rpm under microaerobic conditions. OD₆₀₀ readings were recorded at 2, 4, 6, 8, 16 and 24 hours.

3.2.4 Motility of *C. jejuni* 488 wild-type strain and 488 *tssC* mutant

Motility of the 488 wild-type strain and the 488 *tssC* mutant were assessed over 24, 48 and 72 hours following inoculation on Brucella motility plates with 0.4% (w/v) bacteriological agar as described in Chapter 2. The 488 *tssC* mutant was more motile than the 488 wild-type at 24 hours following inoculation, however no significant differences in motility were observed between the two strains at 48 and 72 hours (Figure 3.3).

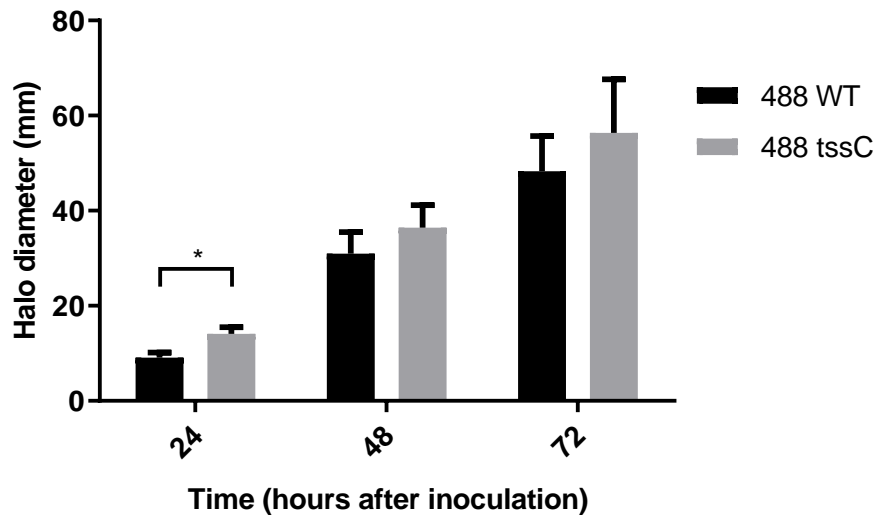


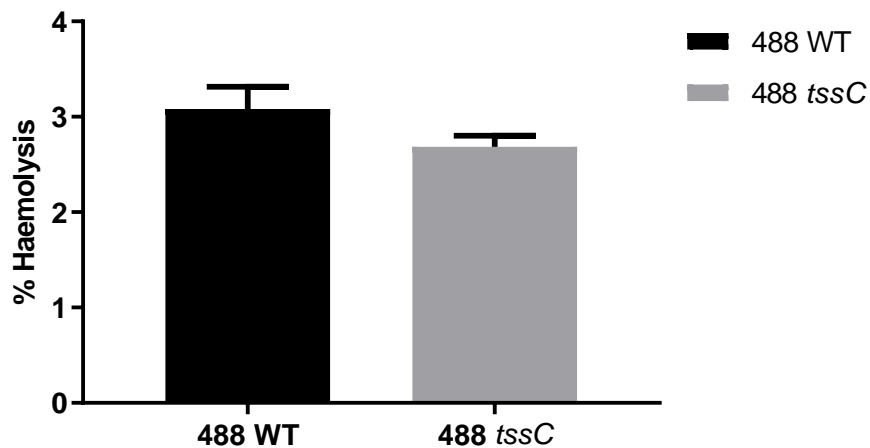
Figure 3.3. Motility assay for *C. jejuni* 488 wild-type strain and 488 *tssC* mutant.

C. jejuni strains from 24 hour plate cultures were resuspended in PBS and adjusted to an OD₆₀₀ of 1.0. 5 µl of bacterial suspensions were pipetted into the centre of Brucella plates with 0.4% (w/v) bacteriological agar. Motility plates were incubated un-inverted at 37°C under microaerobic conditions. Diameter of the haloes were measured at 24, 48 and 72 hours. Asterisks denote a statistically significant difference (* indicating $p \leq 0.05$).

3.2.5 Haemolysis of *C. jejuni* 488 wild-type strain and 488 *tssC* mutant

The T6SS of the *C. jejuni* 108 strain is capable of causing cytotoxicity towards red blood cells (Bleumink-Pluym et al., 2013). To investigate whether the T6SS of the *C. jejuni* 488 strain is also able to cause cytotoxicity towards red blood cells, the 488 wild-type strain and the 488 *tssC* mutant were incubated with red blood cells for 6 hours and 24 hours as described in Chapter 2. At both time points, the 488 wild-type strain appeared to cause more cytotoxicity than the 488 *tssC* mutant; however these differences were not significant (Figure 3.4).

A



B

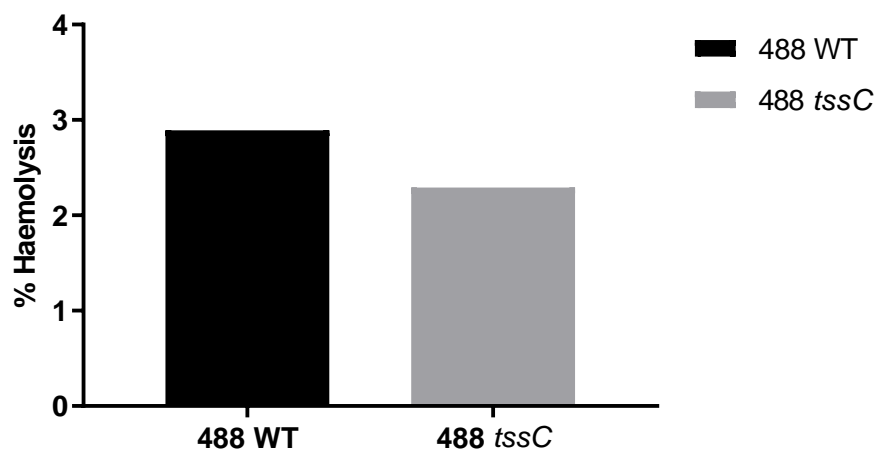


Figure 3.4. Cytotoxicity of the 488 wild-type strain and 488 *tssC* mutant towards red blood cells. Bacterial suspensions were prepared from 7 day old plate cultures of *C. jejuni*, inoculated into BHI broth to an OD₆₀₀ of 1.0, and cultured for 16 hours at 37°C under microaerobic conditions. The cultures were centrifuged and resuspended in PBS to an OD₆₀₀ of 1.0. 250 µl of prepared horse RBCs were added to the bacterial suspension for 5% (v/v) concentration of RBCs and incubated for 6 hours (Figure 3.4A) or 24 hours (Figure 3.4B) at 37°C under microaerobic conditions. A positive control with water incubated with red blood cells was also included. The OD₄₂₀ was measured and cytotoxicity was scored as a percentage of cell lysis of the positive control. Data for Figure 3.4B represents a single biological replicate only.

3.2.6 Construction of *C. jejuni* 488 *tssB* mutant

The *C. jejuni* 488 *tssB* mutant was constructed via insertion of a chloramphenicol resistance cassette (Cam^R) into the *tssB* gene to disrupt gene function. PCR with *tssB* forward and reverse primers were used to check that the 488 *tssB* mutant clones were of the correct size (1,881 bp) to indicate successful homologous recombination. PCR with the gene-specific primers and chloramphenicol resistance cassette primers were also used to check that the chloramphenicol resistance cassette had inserted in the correct orientation into the 488 *tssB* mutant clones (Figure 3.5). 488 *tssB* mutant clones were confirmed by Sanger sequencing.

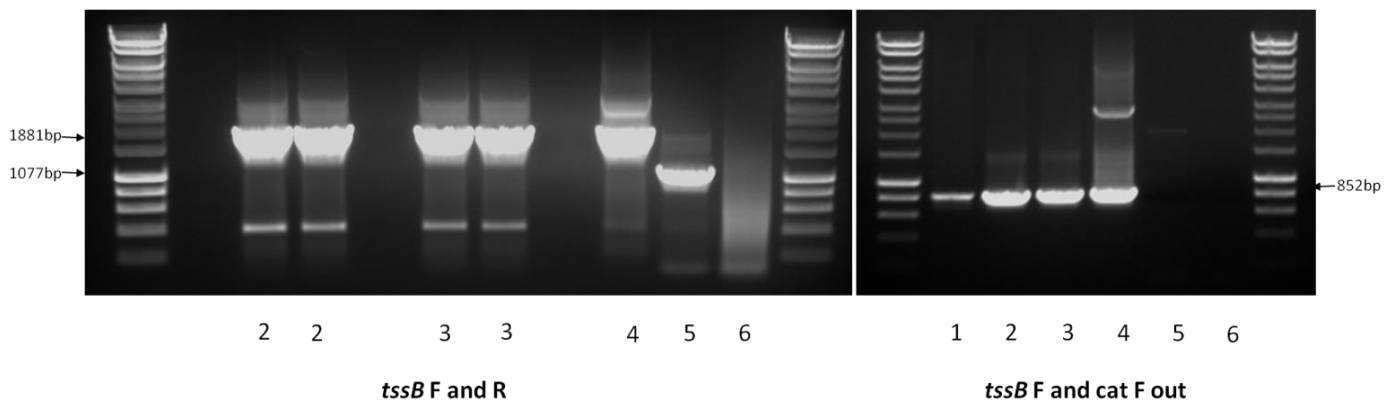


Figure 3.5. PCR checks confirming *C. jejuni* 488 *tssB* mutant clones. Primers specific to *tssB* and the chloramphenicol resistance cassette were used. Ladder used was HyperLadder 1 kb. Lanes 1-3: gDNA of 488 *tssB* mutant clones. Lane 4: Positive control (plasmid DNA with insertion of Cam^R into *tssB*). Lane 5: gDNA of the 488 wild-type strain. Lane 6: Negative control (no DNA).

3.2.7 Construction of *C. jejuni* 488 *tssBC* double mutant

The plasmid with insertion of the kanamycin resistance cassette into *tssC* was transformed into the 488 *tssB* mutant to construct a 488 *tssBC* double mutant. PCR with *tssB* forward and reverse primers and *tssC* forward and reverse primers were used to check that the 488 *tssBC* mutant clones were of the correct size (1,881 bp with *tssB* forward and reverse primers and 2,809 bp with *tssC* forward and reverse primers) to indicate successful homologous recombination (Figure 3.6). 488 *tssBC* mutant clones were confirmed by Sanger sequencing.

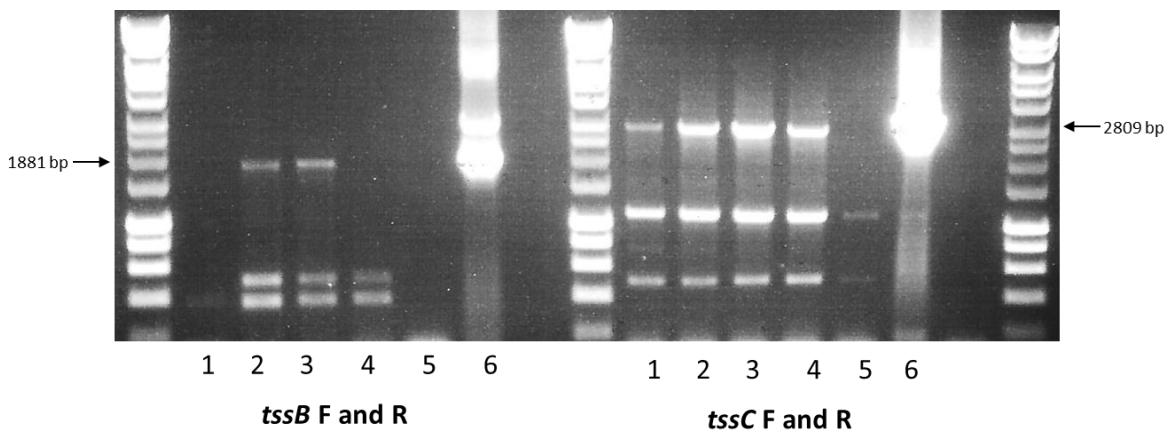
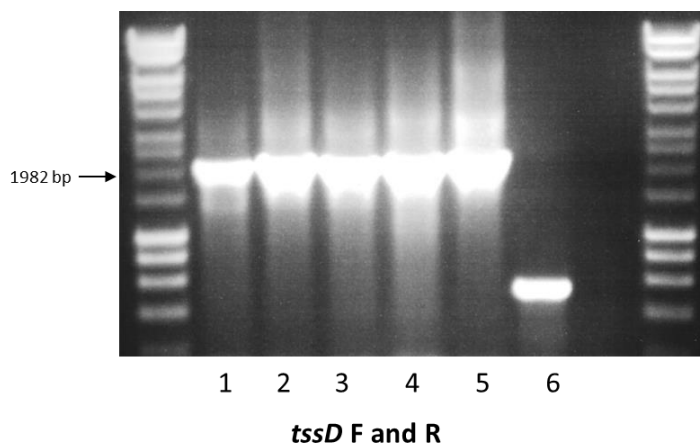


Figure 3.6. PCR checks confirming *C. jejuni* 488 *tssBC* mutant clones. Primers specific to *tssB* and *tssC* were used. Ladder used was HyperLadder 1 kb. Lanes 1-5: gDNA of 488 *tssBC* mutant clones. Lane 6: Positive control (Left: plasmid DNA with insertion of Cam^R into *tssB*. Right: plasmid DNA with insertion of Kan^R into *tssC*).

3.2.8 Construction of *C. jejuni* 488 *tssD* mutant

The *C. jejuni* 488 *tssD* mutant was constructed via insertion of a kanamycin resistance cassette (Kan^R) into the *tssD* gene to disrupt gene function. PCR with *tssD* forward and reverse primers were used to check that the 488 *tssD* mutant clones were of the correct size (1,982 bp) to indicate successful homologous recombination. PCR with the gene-specific primers and kanamycin resistance cassette primers were also used to check that the kanamycin resistance cassette had inserted in the correct orientation into the 488 *tssD* mutant clones (Figure 3.7). 488 *tssD* mutant clones were confirmed by Sanger sequencing.

A



B

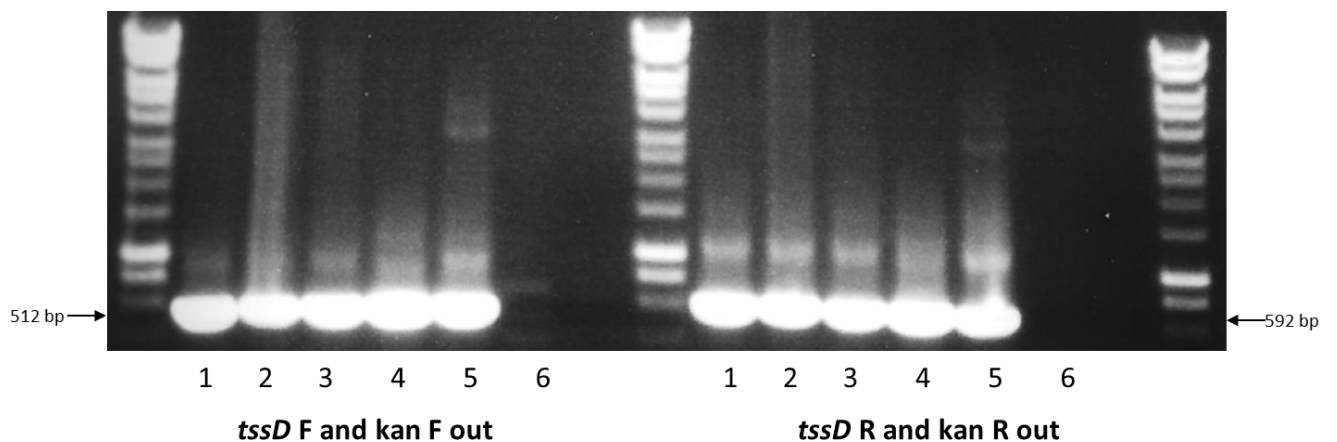


Figure 3.7. PCR checks confirming *C. jejuni* 488 *tssD* mutant clones. Primers specific to *tssD* (A) and the kanamycin resistance cassette (B) were used. Ladder used was HyperLadder 1 kb. Lanes 1-4: gDNA of 488 *tssD* mutant clones. Lane 5: Positive control (plasmid DNA with insertion of Kan^R into *tssD*). Lane 6: gDNA of the 488 wild-type strain.

3.2.9 Growth kinetics of *C. jejuni* 488 wild-type strain, 488 *tssBC* double mutant and 488 *tssD* mutant

Phenotypic comparisons between the 488 wild-type strain, the 488 *tssBC* mutant and the 488 *tssD* mutant were performed for growth kinetics, motility, and biofilm formation. The 488 *tssBC* mutant and the 488 *tssD* mutant exhibited significantly reduced levels of growth compared to the 488 wild-type strain at 8, 10, 12, 14, and 16 hours (Figure 3.8).

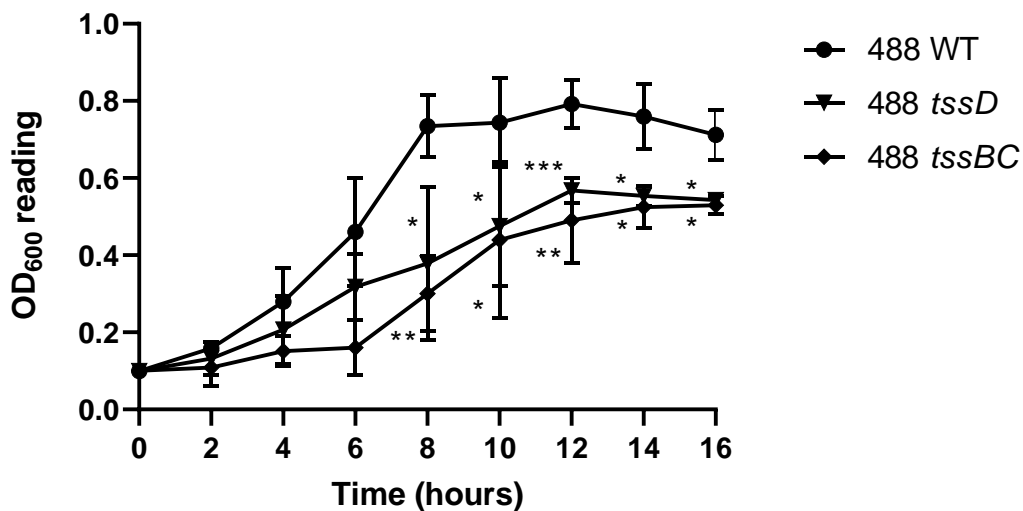


Figure 3.8. Growth of *C. jejuni* 488 wild-type strain, 488 *tssBC* double mutant and 488 *tssD* mutant in Brucella broth. Strains were harvested from 24 hour plate cultures, inoculated to OD₆₀₀ of 0.1 in Brucella broth, and incubated at 37°C, shaking at 75 rpm under microaerobic conditions. OD₆₀₀ readings were recorded at 2, 4, 6, 8, 10, 12, 14 and 16 hours. Asterisks denote a statistically significant difference (* indicating $p \leq 0.05$, ** indicating $p \leq 0.01$, *** indicating $p \leq 0.001$).

3.2.10 Motility of *C. jejuni* 488 wild-type strain, 488 *tssBC* double mutant and 488 *tssD* mutant

The motility of the 488 wild-type strain, 488 *tssBC* mutant and 488 *tssD* mutant were assessed over a duration of 24, 48 and 72 hours. There were no significant differences in motility observed between the 488 wild-type strain, 488 *tssBC* mutant and 488 *tssD* mutant (Figure 3.9).

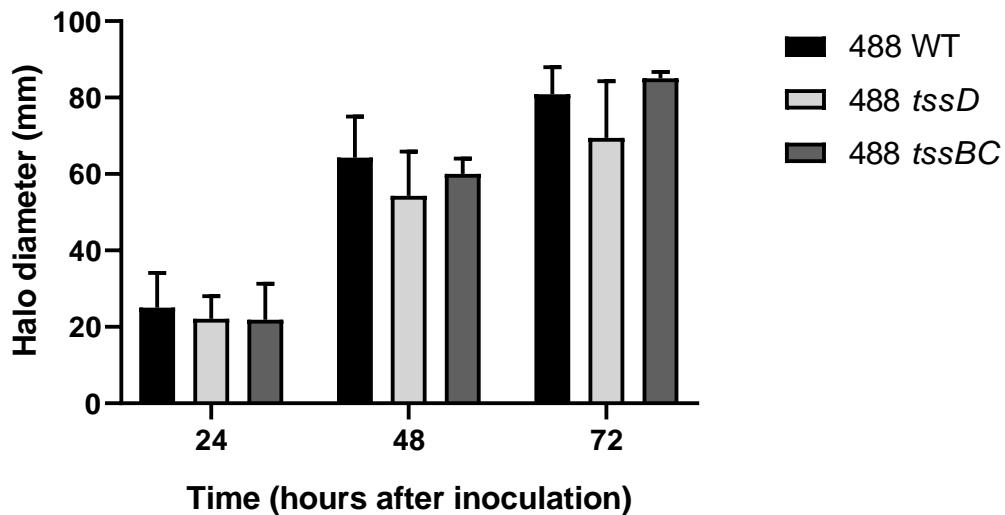


Figure 3.9. Motility assay for *C. jejuni* 488 wild-type strain, 488 *tssBC* double mutant and 488 *tssD* mutant. *C. jejuni* strains from 24 hour plate cultures were resuspended in PBS and adjusted to an OD₆₀₀ of 1.0. 5 µl of bacterial suspensions were pipetted into the centre of Brucella plates with 0.4% (w/v) bacteriological agar. Motility plates were incubated un-inverted at 37°C under microaerobic conditions. Diameter of the haloes were measured at 24, 48 and 72 hours.

3.2.11 Biofilm formation of *C. jejuni* 488 wild-type strain, 488 *tssBC* double mutant, and 488 *tssD* mutant

C. jejuni is capable of forming three types of biofilms – attached, aggregates and pellicles (Joshua et al., 2006). The ability of *C. jejuni* to form pellicles at the air-surface interface was assessed in this study. The ability of both the 488 *tssD* mutant and the 488 *tssBC* double mutant were significantly reduced compared to the 488 wild-type strain to form biofilms, indicating that the presence of the T6SS is involved in biofilm formation (Figure 3.10).

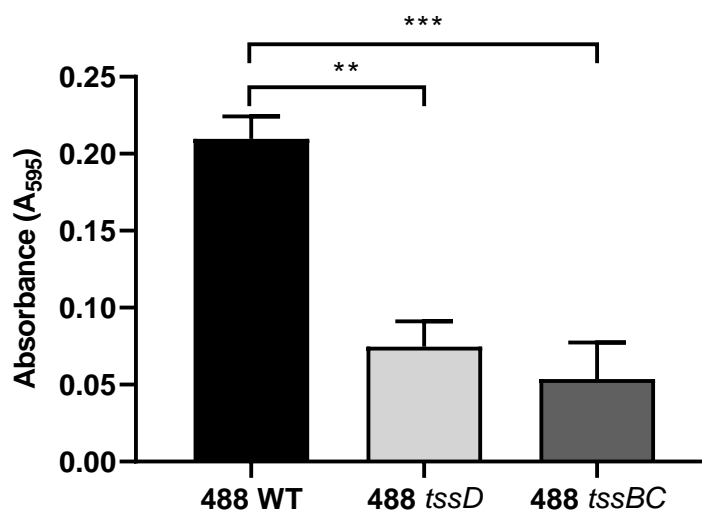


Figure 3.10. Biofilm formation with the *C. jejuni* 488 wild-type strain, 488 *tssBC* double mutant and 488 *tssD* mutant. Bacterial cells from 24 hour plates were inoculated to an OD_{600} of 0.1 into pre-incubated flasks with 10 ml of Muller Hinton (MH) broth. Cultures were incubated for 5 hours at 75 RPM under microaerobic conditions. The OD_{600} of the cultures were readjusted to 0.1, and 1 ml of culture were added to the wells of a 24-well plate and incubated at 37°C, stationary under microaerobic conditions for 72 hours. The inoculated wells were washed with PBS, stained with 1% (w/v) crystal violet, further washed with PBS, and de-stained with 80% (v/v) ethanol and 20% (v/v) acetone. Absorbance (A_{595}) readings were recorded using a SpectraMax M3 microplate reader. Asterisks denote a statistically significant difference (** indicating $p \leq 0.01$, *** indicating $p \leq 0.001$).

3.2.12 Complementation of *C. jejuni* 488 *tssD* mutant

The 488 *tssD* complement was constructed via insertion of a copy of the *tssD* gene into the pRRC delivery plasmid (Karlyshev and Wren, 2005). The construct was then transformed via electroporation into the 488 *tssD* mutant. PCR with *tssD* forward and reverse primers were used to check that the 488 *tssD* complement clones were of the correct size to indicate that a copy of the *tssD* gene was successfully inserted (Figure 3.11). 488 *tssD* complement clones were confirmed by Sanger sequencing.

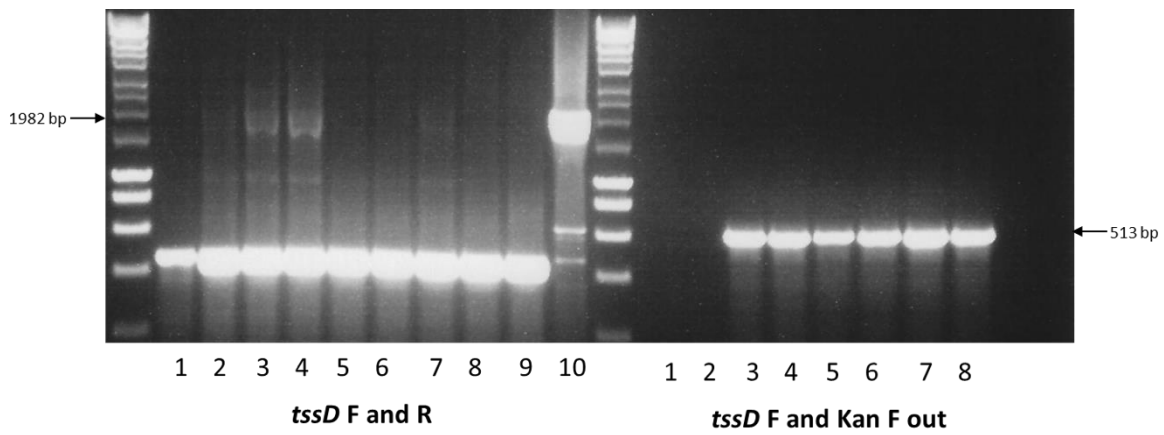


Figure 3.11. PCR checks confirming *C. jejuni* 488 *tssD* complement clones. Primers specific to *tssD* and the kanamycin resistance cassette were used. Ladder used was HyperLadder 1 kb. Lanes 1-8: gDNA of 488 *tssD* complement clones. Lane 9: gDNA of the 488 wild-type strain. Lane 10: gDNA of the 488 *tssD* mutant.

3.2.13 Bacterial competition with the 488 wild-type strain, 488 *tssD* mutant and 81-176 wild-type strain

The T6SS is a contact-dependent machinery that requires close cell-to-cell contact for the delivery of effector proteins (Hachani et al., 2013, Sana et al., 2017, Chen et al., 2019).

Predator and prey strains were co-cultured on solid agar plates to allow for closer contact between bacterial cells to examine whether contact-dependent killing takes place.

The T6SS-negative 81-176 wild-type strain was used as the prey strain to assess differences between the 488 wild-type strain and the 488 *tssD* mutant in bacterial killing. Two different ratios of predator-to-prey strains were examined. At 1:1 predator-to-prey ratio, 50% of the co-culture mixture were the 488 wild-type strain or the 488 *tssD* mutant as the predator strains and the other 50% were the T6SS-negative 81-176 wild-type strain. At 5:1 predator-to-prey ratio, 83.3% of the co-culture mixture were the 488 wild-type strain or the 488 *tssD* mutant as the predator strains and the remaining 16.7% were the 81-176 wild-type strain. The control consisted of 100% of the 81-176 wild-type strain.

Co-culture of the 488 wild-type strain or the 488 *tssD* mutant as the predator strains and the 81-176 wild-type strain as the prey strain did not appear to demonstrate any bacterial killing (Figure 3.13). Differences in the ability of the 488 wild-type strain and the 488 *tssD* mutant to kill the 81-176 wild-type strain at either the 5:1 or 1:1 predator-to-prey ratios were not statistically significant.

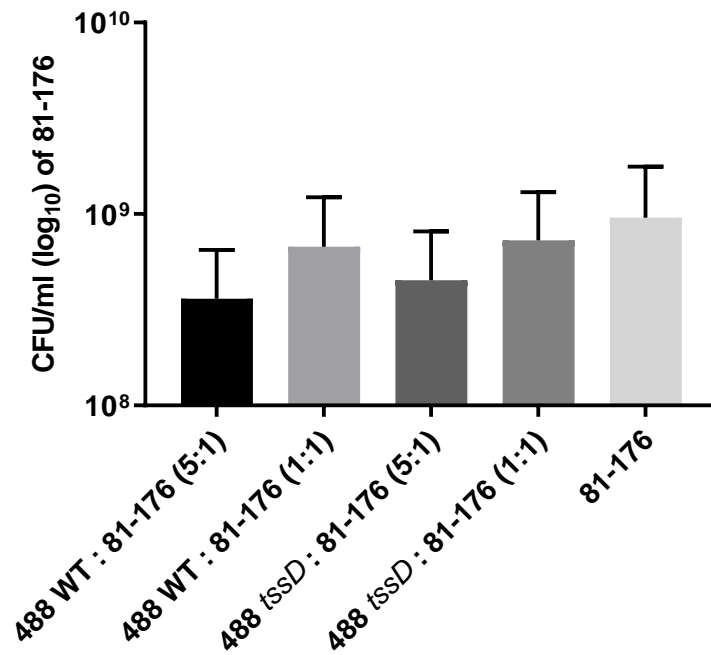


Figure 3.13. Bacterial competition with *C. jejuni* 488 wild-type strain or 488 *tssD* mutant as the predator strain and *C. jejuni* 81-176 wild-type strain as the prey strain. Predator and prey strains were co-cultured at 5:1 and 1:1 ratios on blood agar plates for 16 hours at 37°C under microaerobic conditions. Serial dilutions were performed and dilutions were plated on blood agar with tetracycline to select for the *C. jejuni* 81-176 wild-type strain. CFU/ml of the *C. jejuni* 81-176 wild-type strain were counted after 48 hours at 37°C under microaerobic conditions.

3.2.14 Bacterial competition with the 488 wild-type strain and 11168H *kpsM* mutant

Bleumink-Pluym et al. demonstrated that the presence of the polysaccharide capsule in *C. jejuni* impairs T6SS function (Bleumink-Pluym et al., 2013). Similarly, in *V. cholerae* the exopolysaccharide functions as a barrier to protect the bacterium from T6SS attacks (Toska et al., 2018). Co-culture of the 488 wild-type strain as the predator strain and the 11168H *kpsM* mutant as the prey strain did not demonstrate any significant bacterial killing (Figure 3.14). No statistical analysis was performed as the percentage of the 11168H *kpsM* mutant differed at each predator-to-prey strain ratio and were therefore not comparable.

The 488 *tssD* mutant was not used as a predator strain as both the 488 *tssD* mutant and the 11168H *kpsM* mutant are resistant to kanamycin. This results in an inability to differentiate between the two mutants on kanamycin selection plates.

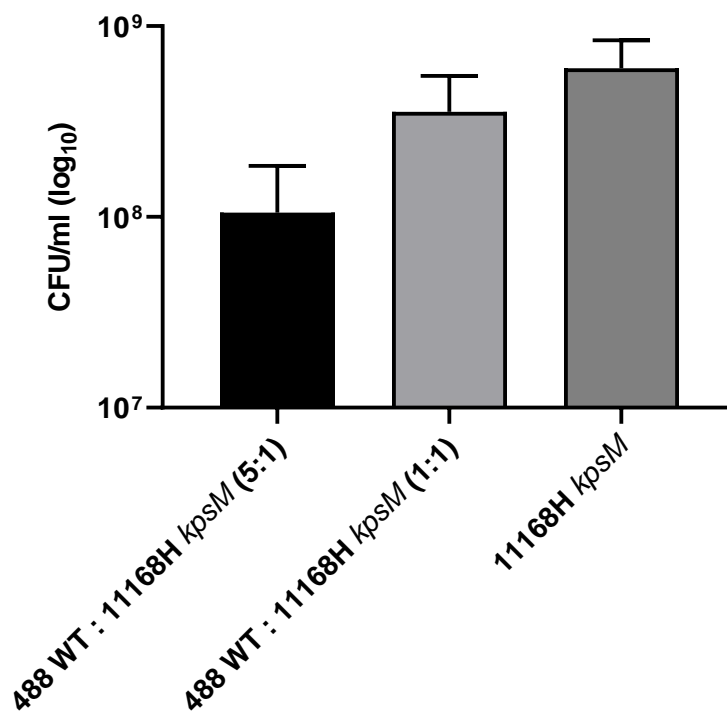


Figure 3.14. Bacterial competition with *C. jejuni* 488 wild-type strain as the predator strain and *C. jejuni* 11168H *kpsM* mutant as the prey strain. Predator and prey strains were co-cultured at 5:1 and 1:1 ratios on blood agar plates for 16 hours at 37°C under microaerobic conditions. Serial dilutions were performed and dilutions were plated on blood agar with kanamycin to select for the *C. jejuni* 11168H *kpsM* mutant. CFU/ml of the *C. jejuni* 11168H *kpsM* mutant were counted after 48 hours at 37°C under microaerobic conditions.

3.2.15 Bacterial competition with the 488 wild-type strain and 43431 *tssD* mutant

Co-culturing of the 488 wild-type strain with the 43431 *tssD* mutant at ratios of 5:1 and 1:1 did not appear to result in any killing (Figure 3.15). No statistical analysis was performed as the percentage of the 43431 *tssD* mutant differed at each predator-to-prey strain ratio and were therefore not comparable.

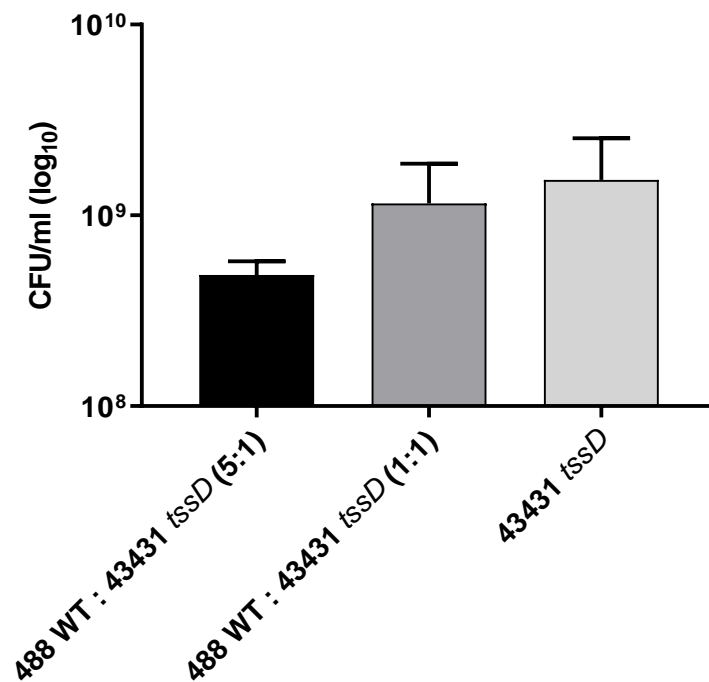


Figure 3.15. Bacterial competition with *C. jejuni* 488 wild-type strain as the predator strain and *C. jejuni* 43431 *tssD* mutant as the prey strain. Predator and prey strains were co-cultured at 5:1 and 1:1 ratios on blood agar plates for 16 hours at 37°C under microaerobic conditions. Serial dilutions were performed and dilutions were plated on blood agar with kanamycin to select for the *C. jejuni* 43431 *tssD* mutant. CFU/ml of the *C. jejuni* 43431 *tssD* mutant were counted after 48 hours at 37°C under microaerobic conditions.

3.2.16 Bacterial competition with the 43431 wild-type strain and 488 *tssD* mutant

The 43431 wild-type strain was also co-cultured with the 488 *tssD* mutant and bacterial killing was not observed (Figure 3.16).

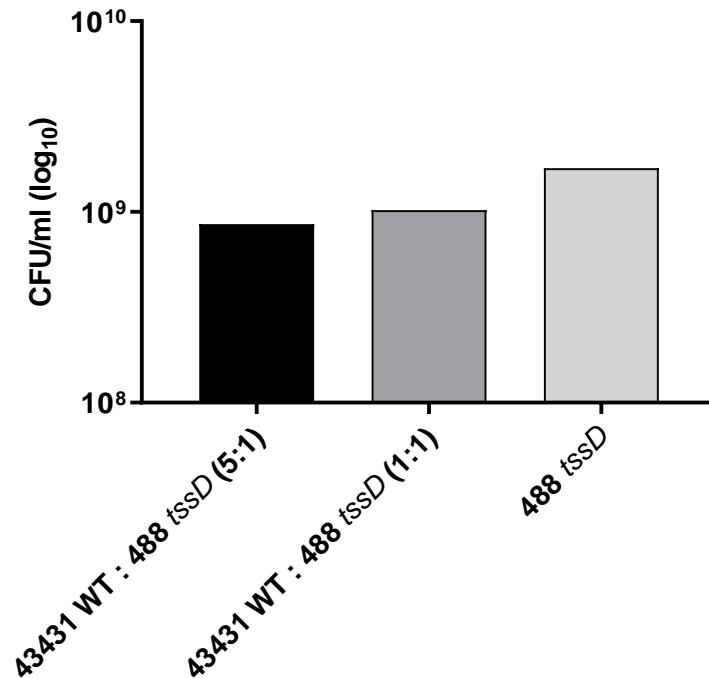


Figure 3.16. Bacterial competition with *C. jejuni* 43431 wild-type strain as the predator strain and *C. jejuni* 488 *tssD* mutant as the prey strain. Predator and prey strains were co-cultured at 5:1 and 1:1 ratios on blood agar plates for 16 hours at 37°C under microaerobic conditions. Serial dilutions were performed and dilutions were plated on blood agar with kanamycin to select for the *C. jejuni* 488 *tssD* mutant. CFU/ml of the *C. jejuni* 488 *tssD* mutant were counted after 48 hours at 37°C under microaerobic conditions. Data represents a single biological replicate only.

3.2.17 Bacterial competition with the 488 wild-type strain, 488 *tssD* mutant and *E. coli* DHB10 GFP

E. coli is frequently utilised as the prey strain in bacterial competition studies (Hachani et al., 2013, Hachani et al., 2014, Sana et al., 2016, Alcoforado Diniz et al., 2017). To test whether the presence of the T6SS plays a role in competition between *C. jejuni* and *E. coli*, the 488 wild-type strain or 488 *tssD* mutant were used as the predator strain against *E. coli* DHB10 GFP as the prey strain. No bacterial killing was observed when the predator and prey strains were co-incubated at 10:1, 5:1 and 1:1 ratios (Figure 3.17). Differences in the ability of the 488 wild-type strain and the 488 *tssD* mutant to kill *E. coli* DHB10 GFP at either the 5:1 or 1:1 predator-to-prey ratios were not statistically significant.

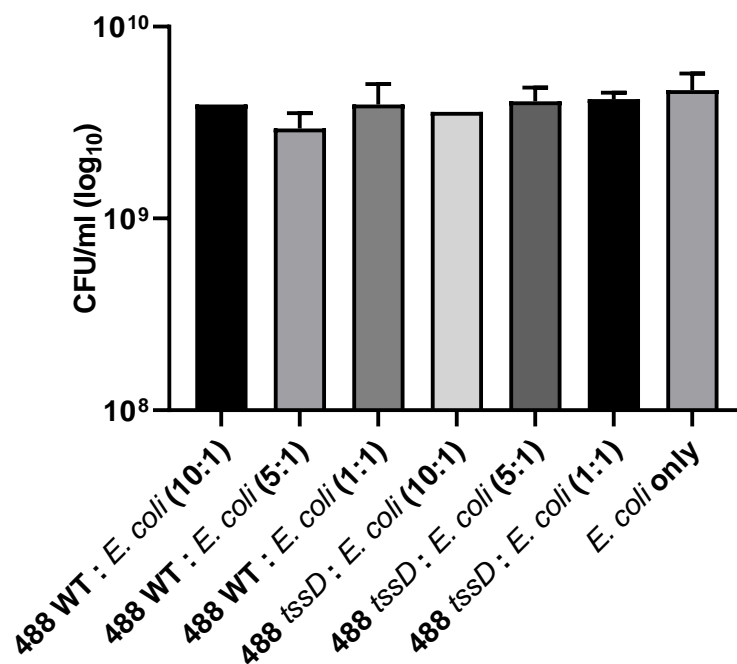


Figure 3.17. Bacterial competition with *C. jejuni* 488 wild-type strain or *C. jejuni* 488 *tssD* mutant as the predator strain and *E. coli* DHB10 GFP as the prey strain. Predator and prey strains were co-cultured at 10:1, 5:1, and 1:1 ratios on Brucella agar plates for 16 hours at 37°C under microaerobic conditions. Serial dilutions were performed and dilutions were plated on Brucella agar with gentamicin to select for *E. coli*. CFU/ml of the *E. coli* were counted after 16 hours at 37°C under aerobic conditions.

3.3 DISCUSSION

Mutagenesis and phenotypic assays

T6SS-positive *C. jejuni* strains were obtained from a variety of sources and countries to represent strains that may be found in different regions from around the world. The 488 strain, a novel human clinical isolate from Brazil, was selected for mutagenesis and became the focus of this study. Previous studies have used 43431 (a human clinical strain isolated in the 1980s in Canada) and *C. jejuni* 414 (a bank vole isolate from the United Kingdom) (Lertpiriyapong et al., 2012, Bleumink-Pluym et al., 2013). The 488 strain was selected for this study as it was recently isolated and came from a region geographically distinct from the 43431 and 414 strains.

Isogenic 488 mutants were constructed by mutating the genes that encode the TssBC contractile sheath components and the TssD needle-like structure primarily in the 488 wild-type strain. Mutagenesis of *tssD* has frequently been used to inactivate the T6SS in *C. jejuni* and other bacteria (Lertpiriyapong et al., 2012, Bleumink-Pluym et al., 2013). The hypothesis is that mutagenesis of either the TssB or TssC contractile sheath components would also lead to complete inactivation of the T6SS.

Phenotypic assays were performed with the 488 wild-type strain and the 488 *tssC* mutant whilst work was ongoing to construct other T6SS mutants. However, results presented in Chapter 4 indicate that mutation of *tssC* reduces but does not completely abolish secretion of TssD, suggesting that the T6SS in the 488 *tssC* mutant is still partially functional. Therefore, this could provide an explanation for the lack of phenotypic differences observed with the 488 *tssC* mutant.

The T6SS of *C. jejuni* was demonstrated by Bleumink-Pluym et al. to cause cytotoxicity towards red blood cells (Bleumink-Pluym et al., 2013). The range of haemolysis caused by both the 488 wild-type strain and the 488 *tssC* mutant closely resembles results obtained by Bleumink-Pluym et al., with percentage haemolysis of between 1-3%. The 488 wild-type strain appeared to cause more cytotoxicity than the 488 *tssC* mutant, however these differences were not significant.

Construction of a 488 *tssB* mutant was less straightforward than for the 488 *tssC* mutant. Initially a similar strategy was followed, however transformation via electroporation of the plasmid containing *tssB* with insertion of the kanamycin resistance cassette was unsuccessful

despite attempts at optimisation. A new plasmid was constructed with replacement of the kanamycin resistance cassette with a chloramphenicol resistance cassette, which finally yielded positive clones of the *tssB* mutant after transformation.

For this study, mutant with insertion of a kanamycin resistance cassette into the *tssD* gene was constructed in the 488 strain. Mutagenesis of the genes encoding both TssBC contractile sheath components was also performed. Results presented in Chapter 4 demonstrate that mutation of *tssD* or both *tssBC* lead to complete inactivation of the T6SS. Phenotypic assays with the 488 wild-type strain, the 488 *tssD* mutant and the 488 *tssBC* double mutant indicated that mutagenesis of T6SS components resulted in reduced growth compared to the wild-type strain. Complete inactivation of the T6SS may lead to the mutant strains being less able to adapt to and survive environmental stresses. There were no significant differences in motility observed between wild-type strain and the two mutant strains.

The T6SS has been demonstrated to be involved in biofilm formation in other bacteria, with TssD/Hcp enhancing the ability of *P. aeruginosa* and *Aeromonas hydrophila* to form biofilms (Southey-Pillig et al., 2005, Sha et al., 2013). The 488 *tssD* mutant and the 488 *tssBC* double mutant displayed reduced ability to form biofilms compared to the 488 wild-type strain, supporting suggestions by a recent study that the presence of TssD also enhances the ability of *C. jejuni* to form biofilms (Noreen et al., 2018). Further work will be required to determine whether TssD is responsible for enhancing biofilm formation or if other T6SS effectors are involved.

Bacterial competition

Thus far, the *C. jejuni* T6SS has not been shown to be involved in inter- or intra-bacterial competition. Bleumink-Pluym et al. examined competition using T6SS-positive *C. jejuni* as the predator strain and T6SS-negative *C. jejuni* or *E. coli* as the prey strain, however did not find evidence of bacterial killing under their experimental conditions (Bleumink-Pluym et al., 2013). Likewise, bacterial competition data presented in this chapter also showed no indication of bacterial killing. The 488 wild-type strain did not appear to significantly kill either the 81-176 wild-type strain, the 43431 *tssD* mutant or an *E. coli* DHB10 GFP strain. The 488 wild-type strain was not used in competition against the 488 *tssB*, 488 *tssC*, 488 *tssBC* or 488 *tssD* mutants as prey strains due to the possible presence of an effector-immunity system. Bacteria harbouring the T6SS possess cognate immunity proteins that

neutralise the toxicity of effectors to prevent self-killing or the killing of sister cells (Dong et al., 2013, Yang et al., 2018). However this system has yet to be identified in *C. jejuni*.

The polysaccharide capsule of *C. jejuni* was demonstrated by Bleumink-Pluym et al. to inhibit T6SS function. Therefore the hypothesis is that removal of the polysaccharide capsule from a *C. jejuni* prey strain may enhance the ability of the T6SS to participate in bacterial killing. However, utilisation of a 11168H *kpsM* mutant strain that lacks the polysaccharide capsule as the prey strain did not appear to significantly increase the amount of killing by the 488 wild-type strain. This confirmed observations by Bleumink-Pluym et al. that killing also did not occur when an 81116 capsular polysaccharide mutant was used as the prey strain. However, it is possible that the absence of the polysaccharide capsule is required in both the predator and the prey strains for the T6SS to function in bacterial killing. Expression of capsular polysaccharide-related genes in *C. jejuni* are shown to be down-regulated during co-culture with epithelial cells (Corcionivoschi et al., 2009). Therefore, it would be expected that the surface polysaccharides of both predator and prey strains would be reduced within a host, allowing for more efficient bacterial killing via the T6SS.

It is possible that specific conditions are required for T6SS killing to occur in *C. jejuni*. Bacterial competition for this study was attempted at 37°C under microaerobic conditions; perhaps bacterial killing would be more prominent at a different temperature, under different atmospheric conditions or a different duration of co-culturing. An optimised growth medium may also be required to enhance bacterial killing. For example, an optimised *Agrobacterium* kill-triggering medium is required to observe bacterial competition between *A. tumefaciens* and *E. coli* (Santos et al., 2019). Gene expression analysis presented in Chapter 4 indicated that T6SS expression in *C. jejuni* may be modulated by the gradient of sodium deoxycholate present in the small intestine. It is possible that the presence and correct concentration of bile salts would be required in the growth medium to stimulate T6SS killing in *C. jejuni*. In addition, viscosity of the growth medium may also be important. For example, T6SS expression and sheath formation in *Vibrio fischeri* were significantly enhanced and T6SS-mediated killing was activated when the bacteria were exposed to a liquid hydrogel medium resembling a highly viscous mucoid environment (Speare et al., 2020).

The ratio of predator and prey strains may also be important. Studies examining bacterial killing use a wide range of predator-to-prey ratios, from a 1:1 ratio for competition between strains of *V. fischeri*, a 5:1 ratio for competition between *S. marcescens* and *E. coli*, up to as

high as a 30:1 ratio for competition between *A. tumefaciens* and *E. coli* (Speare et al., 2018, Lazzaro et al., 2017, Santos et al., 2019). This study used ratios of 1:1 and 5:1 as recommended by Diniz et al. for competition between *C. jejuni* strains and also a ratio of 10:1 for competition between *C. jejuni* and *E. coli* (Alcoforado Diniz et al., 2017). However, further optimisation may be required to find an ideal predator-to-prey ratio for bacterial killing by the *C. jejuni* T6SS.

Another possibility is that T6SS killing in *C. jejuni* can occur only *in vivo*. For example, intra-species killing via the type VII secretion system (T7SS) in *Staphylococcus aureus* can only be observed *in vivo* in a zebrafish model; no differences were observed in competition assays *in vitro* (Gomes and Mostowy, 2020). Competition infection experiments in a chicken model similar to one described by Pezoa et al. could be used to determine whether the *C. jejuni* T6SS is active in bacterial antagonism *in vivo* (Pezoa et al., 2014). The ability of *C. jejuni* to cause T6SS killing could also be examined in an amoebal host.

The choice of prey may also be important. It is possible that the *C. jejuni* T6SS does not target other *C. jejuni* strains or *E. coli*, rather instead the T6SS is important in killing commensal microbiota. Another possibility is that T6SS-mediated bacterial antagonism in *C. jejuni* may be strain specific. For example, the T6SS of *A. baumannii* strain M2 has been shown to be important in competition against *E. coli* and the ability of *A. baumannii* strains to outcompete *E. coli* has been well described (Carruthers et al., 2013, Weber et al., 2013). However, *A. baumannii* strains ATCC17978 and DSM30011 were found to be unable to outcompete *E. coli* (Repizo et al., 2015). The two *C. jejuni* strains utilised in this study and by Bleumink-Pluym et al. do not appear to exhibit inter- or intra-bacterial antagonism; whether this is applicable to all *C. jejuni* strains remains to be investigated (Bleumink-Pluym et al., 2013). The target might also be other organisms such as fungi or amoeba. Trunk et al. demonstrated that the *S. marcescens* T6SS deploys effectors with an anti-fungal effect (Trunk et al., 2018). The *V. cholerae* T6SS is virulent towards the amoebae of *Dictyostelium discoideum* (Zheng et al., 2011).

Alternatively, the T6SS in *C. jejuni* may not be involved in killing at all. Whilst many of the T6SSs studied thus far have a role in antagonism towards bacteria, fungi or amoeba, there are also T6SSs that do not contribute via this manner. The T6SS can instead be involved in competition for essential micronutrients that are presented in limited quantities in the environment or within a host (Chen et al., 2019). Acquisition of essential micronutrients such

as zinc, manganese and iron can provide bacteria possessing the T6SS with a significant advantage over those that do not (Wang et al., 2015, Lin et al., 2017, Si et al., 2017). Whether T6SS-positive *C. jejuni* strains achieve an advantage over T6SS-negative *C. jejuni* strains or other bacteria through this method remains an important topic to be investigated.

3.4 CONCLUSION

A number of T6SS-positive *C. jejuni* strains were obtained for this study. Genes encoding the TssBC contractile sheath and TssD needle-like components of the *C. jejuni* T6SS were mutated in the novel 488 wild-type strain to examine the roles of these components. Results from this study indicate that the T6SS is involved in the ability of *C. jejuni* to form biofilms. The T6SS has been demonstrated to have important roles in inter- and intra-bacterial competition in many bacteria. However, the results presented here suggest that the *C. jejuni* T6SS does not appear to be involved in bacterial competition against *C. jejuni* or *E. coli*.

CHAPTER FOUR: Investigation of the role of the *Campylobacter jejuni* Type VI Secretion System

4.1 INTRODUCTION

In contrast to the well-studied T6SSs of *P. aeruginosa*, *V. cholerae* and *S. marcescens*, the role of the T6SS in *C. jejuni* is not well understood. Previous studies have demonstrated the *C. jejuni* T6SS may be important in host cell adherence and invasion, colonisation of a host, bile salt stress survival and contact-dependent cytotoxicity towards red blood cells (Lertpiriyapong et al., 2012, Bleumink-Pluym et al., 2013). A recent study examined the structure of the TssD effector protein in *C. jejuni* and found that TssD is cytotoxic towards HepG2 human liver carcinoma cells (Noreen et al., 2018). However, whether the T6SS plays a role in the survival and infection of *C. jejuni* in poultry, a primary reservoir, is still unknown.

The aim of work presented in this chapter was to further characterise the role of the T6SS in *C. jejuni* interactions with host cells. The ability of the largely uncharacterised 488 wild-type strain and mutants to secrete TssD was investigated. The expression of T6SS genes was analysed in the presence of biologically relevant concentrations of bile salts found in the human small intestine. Work in this chapter also investigated an association between the T6SS and the oxidative stress response in *C. jejuni*. The role of the T6SS during interaction with host cells was explored using both *in vitro* and *in vivo* models.

4.2 RESULTS

4.2.1 Analysis of T6SS gene expression in the 488 wild-type strain using RT-PCR

Composed of interlocking TssB and TssC proteins, the contractile sheath is responsible for producing enough energy to force the TssD needle-like structure through the inner membrane, out into the extracellular space and across host membranes (Cianfanelli et al., 2016b). To initially investigate whether the *C. jejuni* 488 wild-type strain had a functional T6SS, the expression of the contractile sheath encoding genes *tssB* and *tssC* as well as the *tssD* gene was investigated using RT-PCR. T6SS genes *tssB*, *tssC* and *tssD* were all found to be expressed when the 488 wild-type strain is grown either in Brucella broth culture for 16 hours or on blood agar for 24 hours, indicating that the *C. jejuni* T6SS is produced under different growth conditions (Figure 4.1).

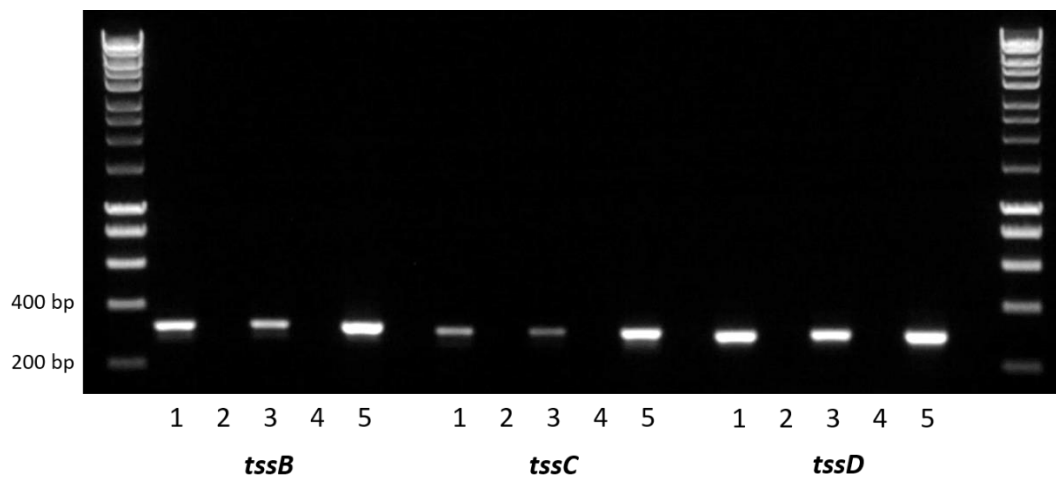


Figure 4.1. RT-PCR analysis of T6SS gene expression in the 488 wild-type strain. RNA was isolated from the 488 wild-type strain grown under different conditions. Plate cultures were grown on blood agar plates incubated for 24 hours at 37°C under microaerobic conditions. Broth cultures were grown in Brucella broth for 16 hours at 37°C with shaking at 75 rpm under microaerobic conditions. RNA was then converted to cDNA. RT-PCR was performed using *tssB*, *tssC* and *tssD* primers. The first and last lanes contain the molecular weight marker (HyperLadder 1kb, Bioline, United Kingdom). Lane 1: 488 cDNA (plate culture); Lane 2: negative control (488 cDNA from plate culture synthesised without reverse transcriptase); Lane 3: 488 cDNA (broth culture); Lane 4: negative control (488 cDNA from

broth culture synthesised without reverse transcriptase); Lane 5: positive control (488 gDNA). Expected sizes are 316 bp (*tssB*), 300 bp (*tssC*) and 287 bp (*tssD*).

4.2.2 Presence of TssD in whole cell lysates of *C. jejuni* wild-type strains

TssD is an approximately 18 kD protein that forms the needle-like structure of the T6SS and has been shown in other bacteria to be important in the secretion of effector proteins (Cianfanelli et al., 2016b). An antibody against TssD was used in Western blots to detect the presence of TssD in the whole cell lysates of *C. jejuni* wild-type strains and mutants. TssD was identified in the whole cell lysates of the T6SS-positive 488, 43431, Cj1 and Cj5 wild-type strains (Figure 4.2A). TssD was also identified in the whole cell lysate of the T6SS-positive 414 wild-type strain but in a reduced amount. In the T6SS-negative 81-176 strain, TssD was not found to be present in the whole cell lysate. The recombinant TssD protein was larger than 18 kD and this was due to the presence of a histidine tag.

In the isogenic 488 *tssB* and *tssC* mutants and the 488 *tssBC* double mutant constructed in this study, TssD was identified in the whole cell lysate (Figure 4.2B). TssD was not identified in the whole cell lysate of the isogenic 488 *tssD* mutant, but expression was partially restored in the 488 *tssD* complement strain.

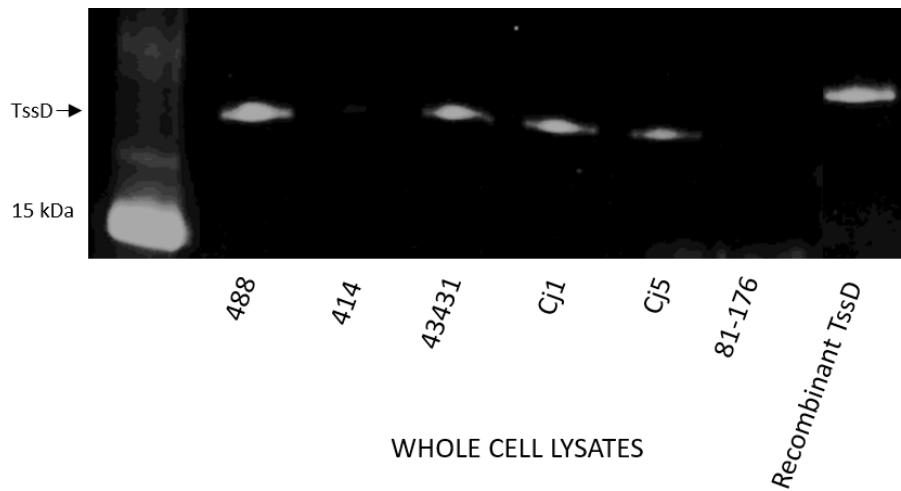
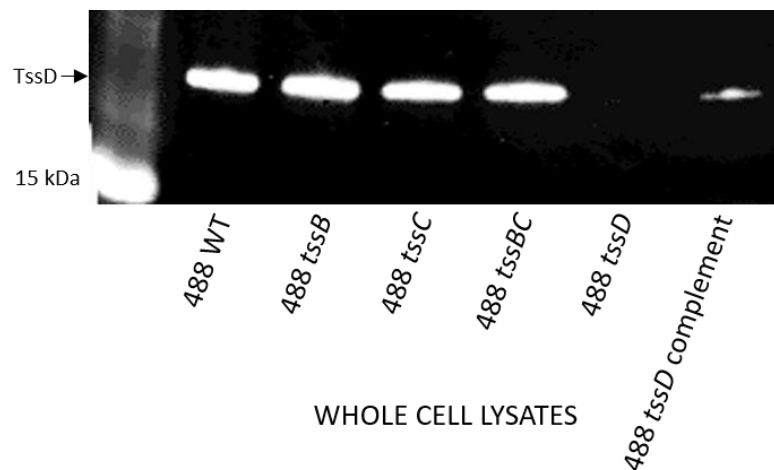
A**B**

Figure 4.2. Detection of TssD in *C. jejuni* whole cell lysates. (A) Whole cell lysate samples were prepared from 24 hour cultures of *C. jejuni* 488, 414, 43431, Cj1 and Cj5 wild-type strains grown in Brucella broth. Western blotting was performed using a TssD antibody, with a recombinant TssD protein used as a positive control. (B) Whole cell lysate samples were prepared from 16 hour cultures of *C. jejuni* 488 wild-type strain, 488 *tssB* mutant, 488 *tssC* mutant, 488 *tssBC* double mutant, 488 *tssD* mutant and 488 *tssD* complement grown in Brucella broth. 13 μ g of samples were loaded onto SDS-PAGE. Western blotting was performed using a TssD antibody, with a recombinant TssD protein used as a positive control. *C. jejuni* TssD has an estimated molecular weight of 18 kDa.

4.2.3 Secretion of TssD in *C. jejuni* wild-type strains and mutants

The secretion of TssD (Hcp) and TssI (VgrG) is considered to be a hallmark of a functional T6SS in *V. cholerae*, *P. aeruginosa* and many other bacteria with well-studied T6SSs (Pukatzki et al., 2006). In order to determine whether the T6SS in the 488 wild-type strain is functional, Western blotting was performed using a TssD antibody to detect the secretion of TssD. TssD was identified in supernatants isolated after growth of the 488 wild-type strain, indicating that this strain has a functional T6SS. TssD was absent in the supernatant isolated from the 488 *tssD* mutant. Complementation of the 488 *tssD* mutant by inserting a copy of the *tssD* gene into the pRRC plasmid and transforming this into the 488 wild-type strain restored secretion of TssD although not to the same level as the 488 wild-type strain.

488 *tssB* and *tssC* single mutants were constructed to investigate whether knocking out a single contractile sheath component would result in a non-functional T6SS. Inactivation of either *tssB* or *tssC* reduces but does not completely abolish secretion of TssD (Figure 4.3), indicating that the absence of one of the contractile sheath components does not result in a completely non-functional T6SS in *C. jejuni*. A 488 *tssBC* double mutant was also constructed to test the hypothesis that function of the *C. jejuni* T6SS is only abolished in the absence of both contractile sheath components. As hypothesised, TssD was absent in the supernatant isolated from the 488 *tssBC* double mutant, thereby demonstrating that the *C. jejuni* T6SS is not functional when the entire contractile sheath structure is absent.

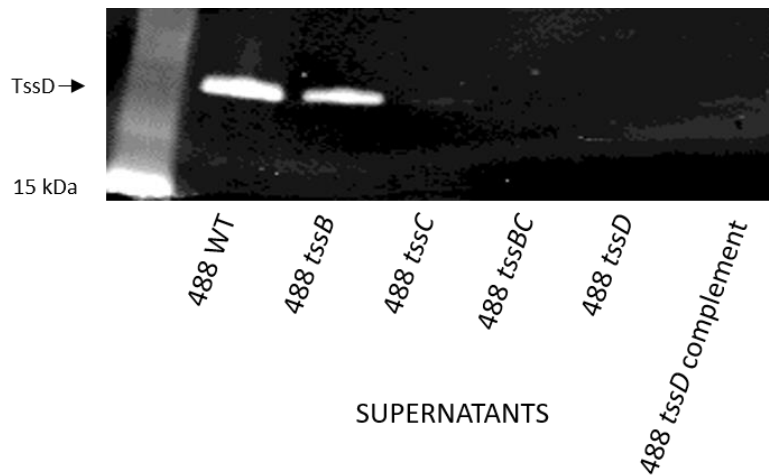


Figure 4.3. Detection of TssD in *C. jejuni* supernatants. Bacterial supernatant samples were prepared from 16 hour cultures of the *C. jejuni* 488 wild-type strain, 488 *tssB* mutant, 488 *tssC* mutant and 488 *tssBC* double mutant grown in Brucella broth. Supernatant samples were concentrated via TCA precipitation and 30 μ g of samples were loaded onto SDS-PAGE. Western blotting was performed using a *C. jejuni* TssD antibody. *C. jejuni* TssD has an estimated molecular weight of 18 kDa.

4.2.4 Presence of TssD in outer membrane vesicles from *C. jejuni* wild-type strains and mutants

Outer membrane vesicles (OMVs) play an important role in the delivery of virulence factors to host cells (Elmi et al., 2012). In *C. jejuni*, OMVs have been shown to secrete a range of virulence factors including CDT and three serine proteases – HtrA, Cj0511, and Cj1365c (Lindmark et al., 2009, Elmi et al., 2016). The relationship between the T6SS and OMVs in *C. jejuni* has yet to be investigated. The presence of TssD was detected in OMVs isolated from the 488 wild-type strain (Figure 4.4). However, TssD was absent from OMVs isolated from the 488 *tssB* mutant, 488 *tssC* mutant, 488 *tssBC* double mutant and the 488 *tssD* mutant.

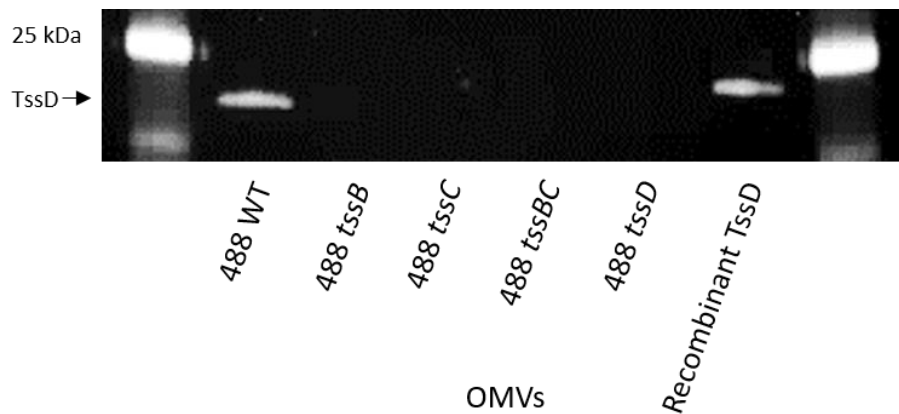


Figure 4.4. Detection of TssD in *C. jejuni* OMVs. OMV samples were isolated from 12 hour cultures of *C. jejuni* 488 wild-type strain, 488 *tssB* mutant, 488 *tssC* mutant, 488 *tssBC* double mutant and 488 *tssD* mutant grown in Brucella broth. Western blotting was performed using a *C. jejuni* TssD antibody, with a recombinant TssD protein used as a positive control. *C. jejuni* TssD has an estimated molecular weight of 18 kDa.

4.2.5 Presence of VgrG in *C. jejuni* wild-type strains

VgrG forms the sharp puncture tip of the T6SS needle (see Figure 1.11 in the Introduction) and the secretion of VgrG alongside TssD is a hallmark of a functional T6SS (Pukatzki et al., 2006). An antibody was designed against VgrG to detect the presence of VgrG in the whole cell lysates and supernatants of *C. jejuni* wild-type strains and mutants. VgrG was not detected in the whole cell lysates or supernatants (data not shown) and this was found to be due to the design of the antibody being incompatible with the *C. jejuni* strains present in our collection. Further explanation of why the VgrG antibody was incompatible with the strains is provided in the Discussion section of this chapter.

4.2.6 Analysis of the effect of sodium taurocholate on T6SS gene expression in 488 wild-type strain

Bile salts such as sodium taurocholate and sodium deoxycholate are present in bile that is secreted into the host intestine. Sodium taurocholate (ST) is a primary bile salt and has been shown to regulate OMV-mediated virulence and stimulate OMV production in *C. jejuni* (Elmi et al., 2018, Davies et al., 2019).

To determine whether T6SS expression is affected by the presence of sodium taurocholate, the 488 wild-type strain was grown in Brucella broth both with and without the addition of 0.1% (w/v) or 0.2% (w/v) sodium taurocholate, which are physiologically relevant concentrations in the human intestine (Hofmann and Hagey, 2008, Elmi et al., 2018). RT-PCR results indicated that the expression of *tssB*, *tssC* and *tssD* were not significantly altered by the presence of either 0.1% (w/v) or 0.2% (w/v) sodium taurocholate (Figure 4.5). The results for expression of *tssD* were also confirmed by qRT-PCR (Figure 4.6).

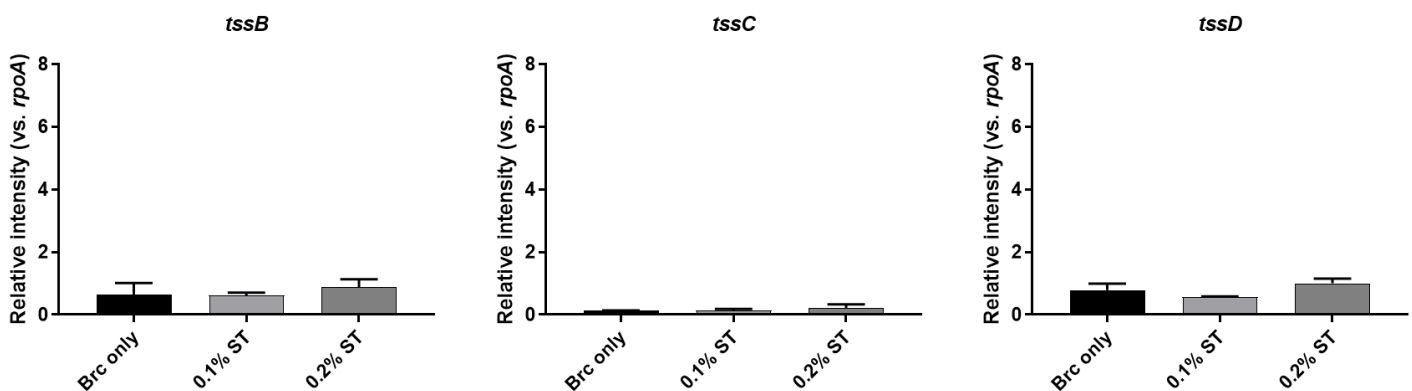


Figure 4.5. RT-PCR analysis of *tssB*, *tssC* and *tssD* expression in the 488 wild-type strain co-incubated with different concentrations of sodium taurocholate. The 488 wild-type strain was grown in Brucella broth (Brc) with or without the addition of 0.1% or 0.2% (w/v) sodium taurocholate (ST). RT-PCR analysis was performed using *tssB*, *tssC* and *tssD* primers. Data was analysed with ImageJ with *rpoA* gene as the internal control. The relative expression of *tssB*, *tssC* and *tssD* are shown.

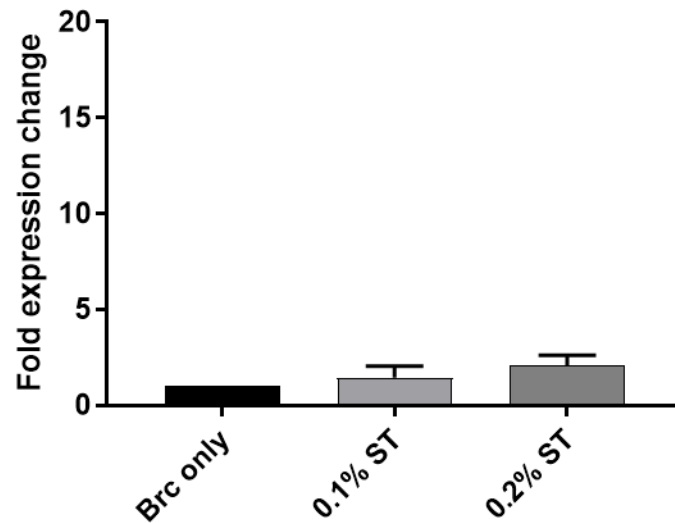


Figure 4.6. qRT-PCR analysis of *tssD* expression in the 488 wild-type strain co-incubated with different concentrations of sodium taurocholate. The 488 wild-type strain was grown in Brucella broth (Brc) with or without the addition of 0.1% or 0.2% (w/v) sodium taurocholate (ST). qRT-PCR analysis was performed using *tssD* primers. Data was analysed by the comparative C_T method with *rpoA* gene as the internal control. The relative expression of *tssD* is shown.

4.2.7 Analysis of the effect of sodium deoxycholate on T6SS gene expression in the 488 wild-type strain

Sodium deoxycholate (SDC) is a secondary bile salt and can induce virulence gene expression in *C. jejuni* (Malik-Kale et al., 2008). Bachmann et al. demonstrated that sodium deoxycholate modulates T6SS activity in *V. cholerae* (Bachmann et al., 2015) and Lertpiriyapong et al. showed that deoxycholic acid modulates *cmeA*, *tssD* (*hcp*) and *tssM* (*icmF*) expression in *C. jejuni* 43431 strain (Lertpiriyapong et al., 2012).

To determine whether T6SS expression is affected by the presence of sodium deoxycholate, the 488 wild-type strain was grown in Brucella broth both with and without the addition of 0.05% (w/v), 0.1% (w/v) or 0.2% (w/v) sodium deoxycholate, which are physiologically relevant concentrations in the human intestine (Hofmann and Hagey, 2008). RT-PCR (Figure 4.7) and qRT-PCR (Figure 4.8) results demonstrate that the expression of *tssB*, *tssC* and *tssD* appear to be significantly up-regulated in the presence of 0.1% (w/v) sodium deoxycholate and down-regulated in the presence of 0.2% (w/v) sodium deoxycholate, suggesting that the T6SS expression in *C. jejuni* may be modulated by the gradient of sodium deoxycholate present in the small intestines.

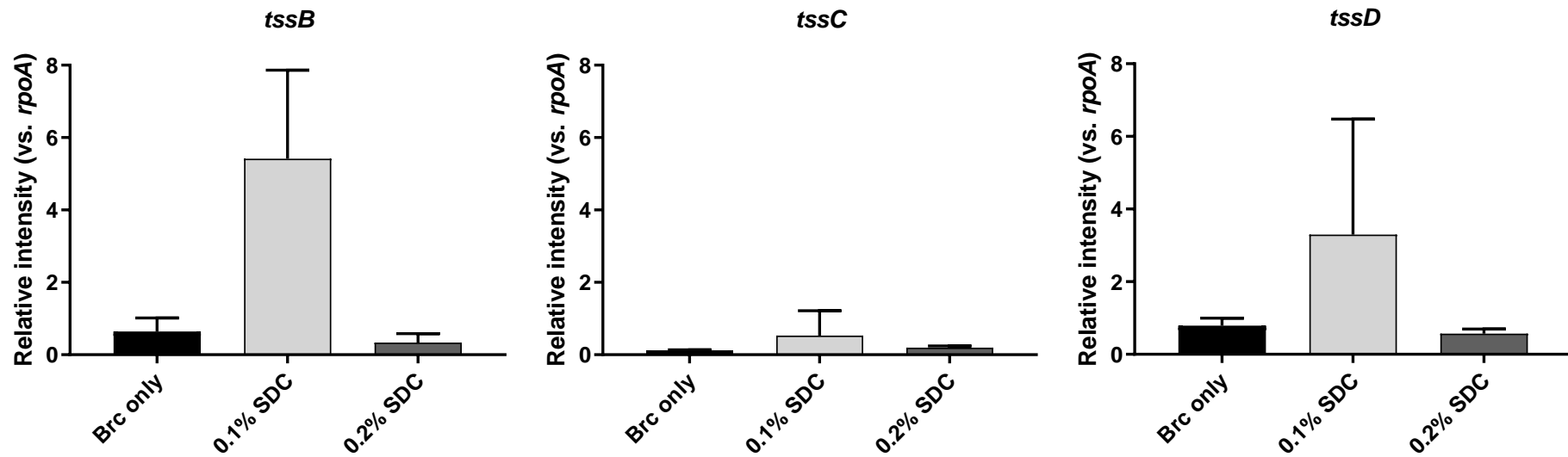


Figure 4.7. RT-PCR analysis of *tssB*, *tssC* and *tssD* expression in the 488 wild-type strain co-incubated with different concentrations of sodium deoxycholate. The 488 wild-type strain was grown in Brucella broth (Brc) with or without the addition of 0.1% or 0.2% (w/v) sodium deoxycholate (SDC). RT-PCR analysis was performed using *tssB*, *tssC* and *tssD* primers. Data was analysed with ImageJ with *rpoA* gene as the internal control. The relative expression of *tssB*, *tssC* and *tssD* are shown.

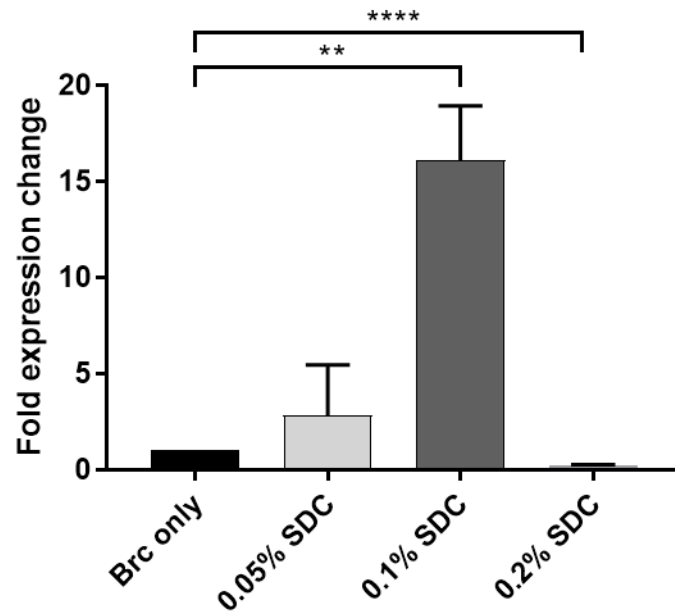


Figure 4.8. qRT-PCR analysis of *tssD* expression in the 488 wild-type strain co-incubated with different concentrations of sodium deoxycholate. The 488 wild-type strain was grown in Brucella broth (Brc) with or without the addition of 0.05%, 0.1% or 0.2% (w/v) sodium deoxycholate (SDC). qRT-PCR analysis was performed using *tssD* primers. Data was analysed by the comparative CT method with *rpoA* gene as the internal control. The relative expression of *tssD* is shown. Asterisks denote a statistically significant difference (** indicating $p \leq 0.01$, **** indicating $p \leq 0.0001$).

4.2.8 Resistance to oxidative stress of the 488 wild-type strain, 488 *tssD* mutant, 488 *tssD* complement and 81-176 wild-type strain

The T6SS has previously been linked with the oxidative stress response in *Y. pseudotuberculosis*, *B. thailandensis* and enterohemorrhagic *E. coli* (Wang et al., 2015, Si et al., 2017, Wan et al., 2017).

To investigate whether the *C. jejuni* T6SS is also associated with the oxidative stress response, the 488 wild-type strain, 488 *tssD* mutant, 488 *tssD* complement and 81-176 wild-type strain were exposed to hydrogen peroxide (H₂O₂). Following a 30 minute exposure to 50 mM H₂O₂, the 488 wild-type strain exhibited significantly greater resistance to oxidative stress killing compared to the 488 *tssD* mutant and the T6SS-negative 81-176 wild-type strain (Figure 4.9). Complementation of the 488 *tssD* mutant enhanced resistance of *C. jejuni* to oxidative stress killing.

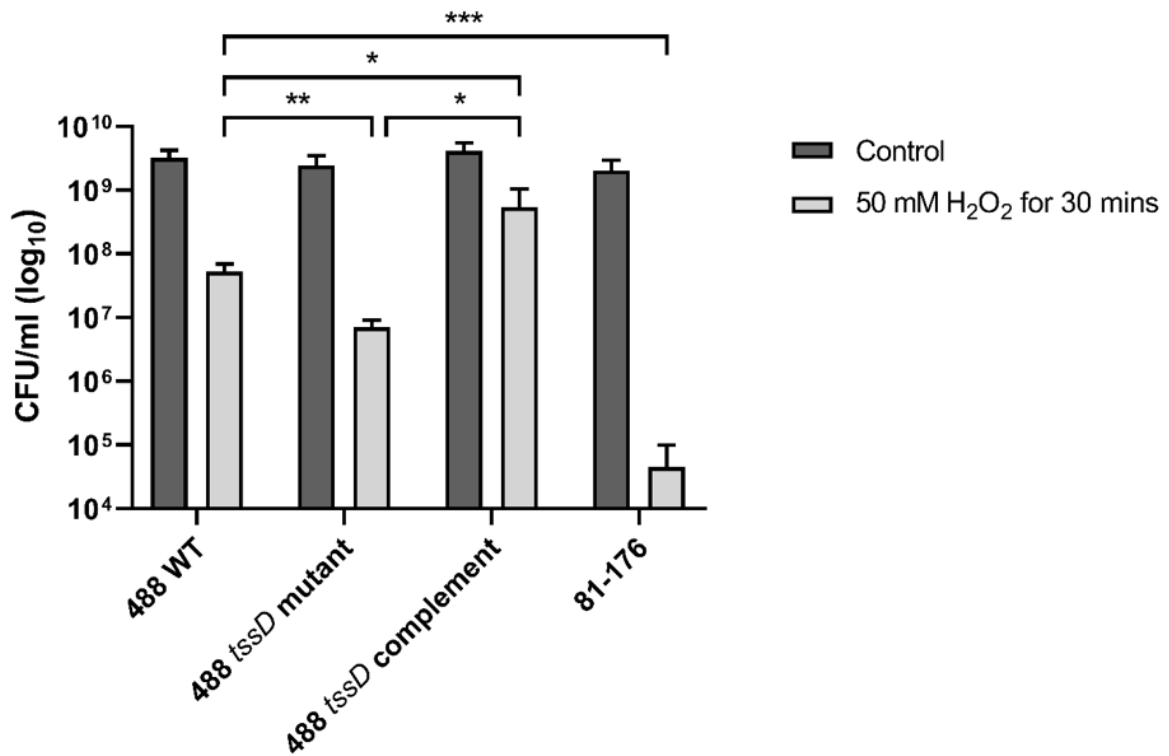


Figure 4.9. Survival of *C. jejuni* when exposed to oxidative stress. Survival of 488 wild-type strain, 488 *tssD* mutant, 488 *tssD* complement and 81-176 wild-type strain following exposure to oxidative stress. The strains were exposed to 50 mM H₂O₂ for 30 minutes, then serial dilutions were performed and plated onto blood agar plates. Plates were incubated for 48 hours at 37°C under microaerobic conditions and the CFUs/ml were counted. Asterisks denote a statistically significant difference (* indicating $p \leq 0.05$, ** indicating $p \leq 0.01$, *** indicating $p \leq 0.001$).

4.2.9 Membrane integrity of the 488 wild-type strain, 488 *tssD* mutant and 488 *tssD* complement

In order to investigate whether the increased susceptibility of the 488 *tssD* mutant to H₂O₂ is specific and not due to a potential membrane defect due to improper assembly of the T6SS in the bacterial membrane, a bile salt stress assay and antimicrobial susceptibility testing were performed.

The bile salt stress assay involved subjecting the 488 wild-type strain, 488 *tssD* mutant and 488 *tssD* complement cultured in Brucella broth to 2% (w/v) sodium taurocholate. Growth of the 488 *tssD* mutant was significantly reduced compared to the 488 wild-type strain and the 488 *tssD* complement (Figure 4.10).

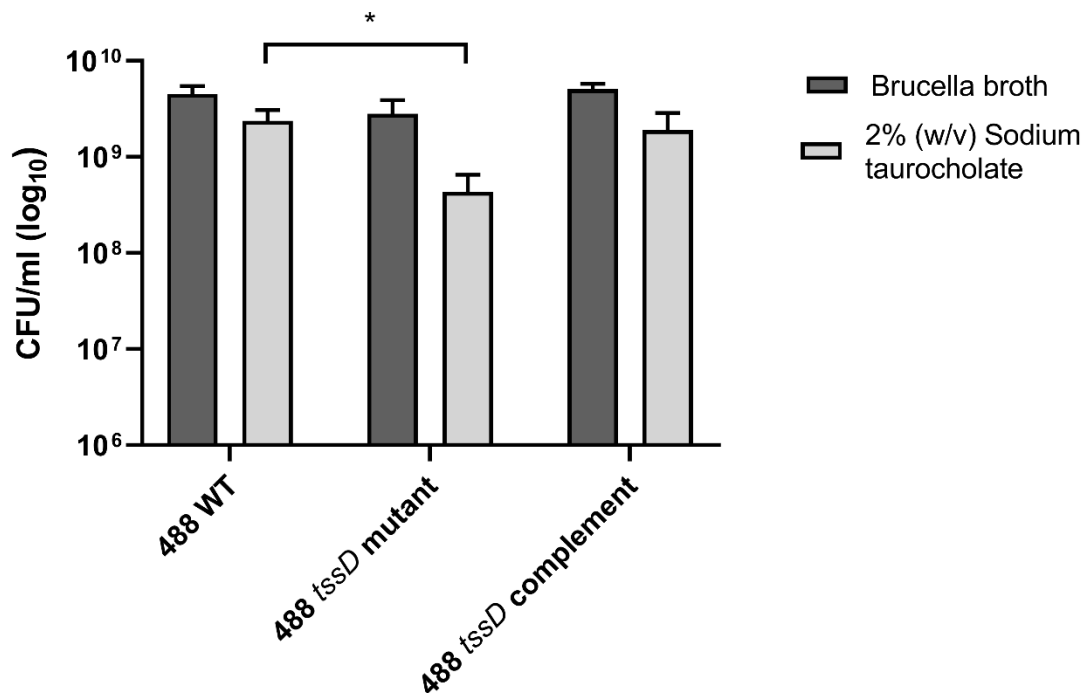


Figure 4.10. Growth of *C. jejuni* strains in presence of 2% (w/v) sodium taurocholate.

Growth of 488 wild-type strain, 488 *tssD* mutant and 488 *tssD* complement in Brucella broth with and without the addition of 2% (w/v) sodium taurocholate for 8 hours at 37°C with shaking at 75 rpm under microaerobic conditions. Serial dilutions were performed and plated onto blood agar plates. Plates were incubated for 48 hours at 37°C under microaerobic conditions and the CFUs/ml were counted. Asterisks denote a statistically significant difference (* indicating $p \leq 0.05$).

Antimicrobial susceptibility testing for the 488 wild-type strain, 488 *tssD* mutant and 488 *tssD* complement were performed through disk diffusion and broth microdilution assays. Disk diffusion assays were performed using ampicillin, amoxicillin/clavulonic acid, tetracycline and polymyxin B. A broth microdilution assay was performed using vancomycin. No differences in antimicrobial susceptibility were observed (Table 4.1), indicating that the increased susceptibility of the 488 *tssD* mutant to H₂O₂ is specific and not due to a potential membrane defect.

Table 4.1. Antimicrobial susceptibility testing.

Antibiotics	488 wild-type strain	488 <i>tssD</i> mutant	488 <i>tssD</i> complement
Ampicillin (10 µg)	S (31)	S (31)	S (31)
Amoxicillin/Clavulonic acid (30 µg)	S (30)	S (30)	S (30)
Tetracycline (30 µg)	S (40)	S (40)	S (40)
Polymyxin B (300 units)	S (20)	S (20)	S (20)
Vancomycin (MIC, µg/ml)	256	256	256

Antimicrobial susceptibility testing of 488 wild-type strain, 488 *tssD* mutant and 488 *tssD* complement. The disk diffusion assay was performed with ampicillin (10 µg), amoxicillin/clavulonic acid (2:1, 30 µg), tetracycline (30 µg), and polymyxin B (300 units) disks (Oxoid) following the method published by the European Society of Clinical Microbiology (EUCAST) (2019); zones of growth inhibition were measured in millimetres and sensitivity (S) determined based on EUCAST guidelines. Broth microdilution was performed with vancomycin (Sigma) and the minimum inhibitory concentration (MIC, µg/ml) was determined according to the method published by Wiegand et al. (2008). The experiments were performed on three independent occasions.

4.2.10 Analysis of *katA*, *sodB* and *ahpC* expression in the 488 wild-type strain and 488 *tssD* mutant using qRT-PCR

katA, *sodB* and *ahpC* encode proteins involved directly in the breakdown of reactive oxygen species (ROS). Expression of *katA*, *sodB* and *ahpC* was investigated in the 488 wild-type strain and 488 *tssD* mutant using qRT-PCR. Expression of all three genes were significantly reduced in the 488 *tssD* mutant compared to the 488 wild-type strain (Figure 4.11). This data combined with the reduced ability of the 488 *tssD* mutant to survive the effects of oxidative stress suggests that the T6SS is associated with the oxidative stress response in *C. jejuni*.

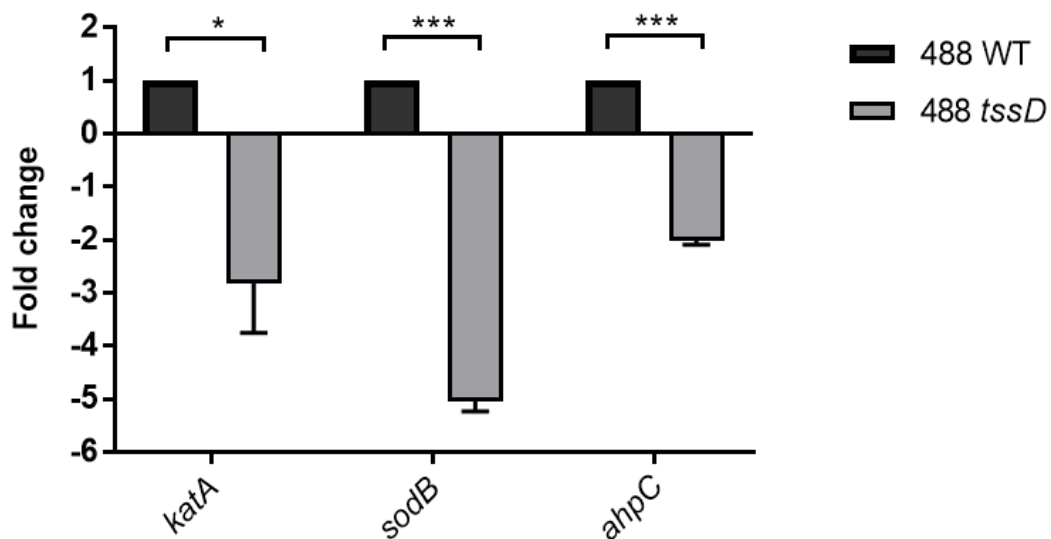


Figure 4.11. qRT-PCR analysis comparing expression of *katA*, *sodB* and *ahpC* in the 488 wild-type strain and 488 *tssD* mutant. qRT-PCR analysis was performed using *katA*, *sodB* and *ahpC* primers. Data was analysed by the comparative CT method with *gyrA* gene as the internal control (Schmittgen and Livak, 2008). The relative expression of *katA*, *sodB* and *ahpC* are shown. Asterisks denote a statistically significant difference (* indicating $p \leq 0.05$, *** indicating $p \leq 0.001$).

4.2.11 The T6SS increases *C. jejuni* cytotoxicity in the *Galleria mellonella* model of infection

The larvae of *G. mellonella* (Greater wax moth) are an established model to study the pathogenesis of *C. jejuni* (Senior et al., 2011, Gundogdu et al., 2011). In order to investigate whether the presence of a T6SS in *C. jejuni* enhances bacterial cytotoxicity, *G. mellonella* larvae were injected with *C. jejuni* strains and larvae survival examined over a duration of 5 days. Only the T6SS-positive 488 wild-type strain was cytotoxic to *G. mellonella* larvae after 24 hours post-injection (Figure 4.12). After 48 hours and 72 hours, the T6SS-negative 81-176 wild-type strain also exhibited some cytotoxicity, but at a lower level compared to the 488 wild-type strain. After 96 hours and 120 hours, cytotoxicity of the 488 *tssD* mutant was also observed but at a significantly lower level than the 488 wild-type strain, indicating that the T6SS increases *C. jejuni* cytotoxicity in the *G. mellonella* model of infection.

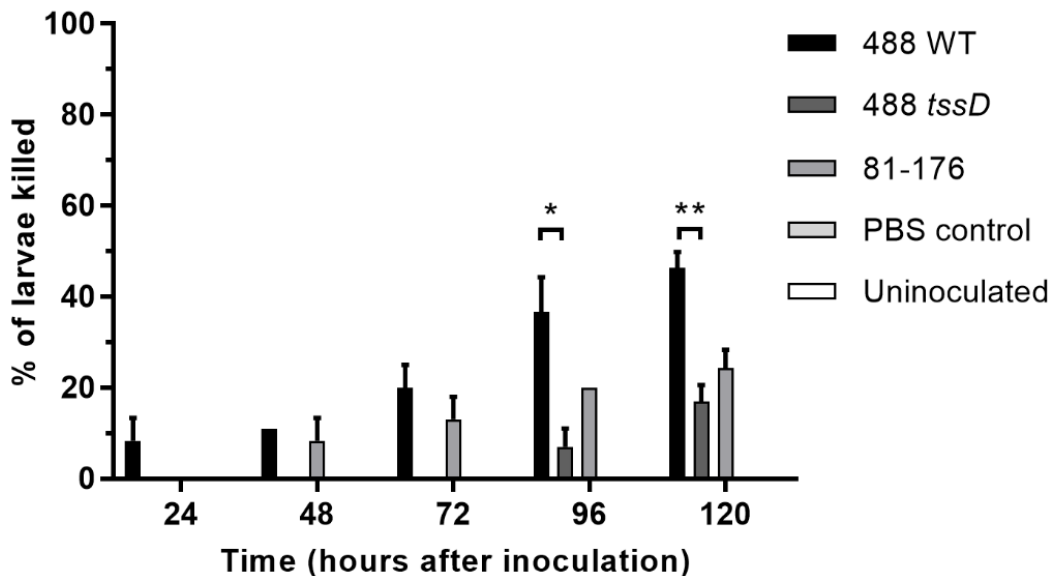
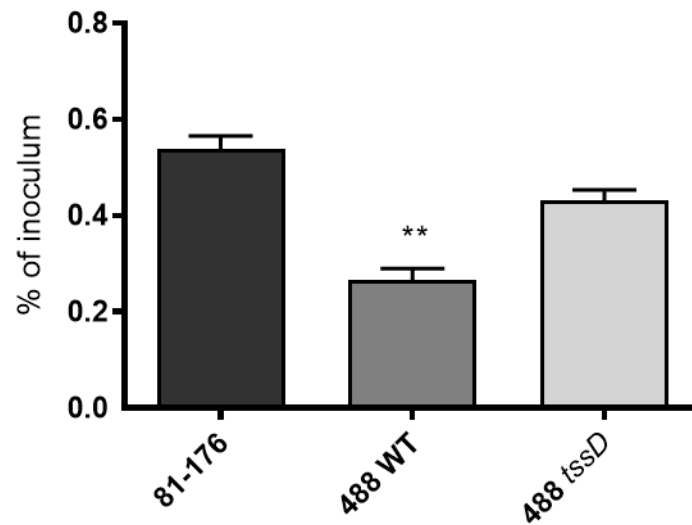


Figure 4.12. Infection of *Galleria mellonella* larvae with the 488 wild-type strain, 488 *tssD* mutant or 81-176 wild-type strain. For each bacterial strain, ten *G. mellonella* larvae were injected in the right foremost leg using a micro syringe. Controls injected with PBS only were included along with uninoculated controls. Larvae were incubated at 37°C with counts of dead larvae recorded every 24 hours over a period of 5 days. Asterisks denote a statistically significant difference (* indicating $p \leq 0.05$, ** indicating $p \leq 0.01$).

4.2.12 Interactions with and invasion of a human colonic epithelial cell line by the 488 wild-type strain, 488 *tssD* mutant and 81-176 wild-type strain

Lertpiriyapong et al. demonstrated that the T6SS of the *C. jejuni* 43431 strain is required for the adherence to and invasion of T84 human colonic epithelial cell line (Lertpiriyapong et al., 2012). This study investigated whether the presence of the T6SS enhances the ability of the *C. jejuni* 488 strain to interact with and invade the HCT-8 human colonic epithelial cell lines. The number of bacteria interacting with the HCT-8 cell line were significantly lower for the 488 wild-type strain compared to the 488 *tssD* mutant or the T6SS-negative 81-176 wild-type strain (Figure 4.13A). However, the numbers of intracellular bacteria were significantly higher for the 488 wild-type strain compared to the 488 *tssD* mutant or the 81-176 wild-type strain (Figure 4.13B).

A



B

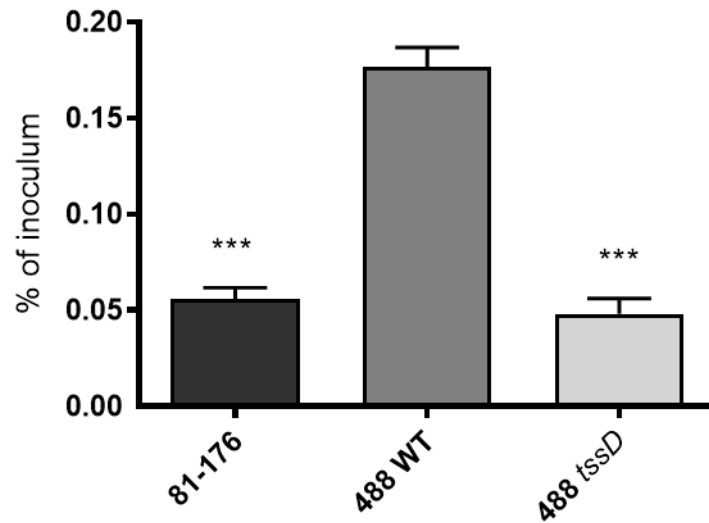


Figure 4.13. Interactions with and invasion of HCT-8 human colonic epithelial cells with the 81-176 wild-type strain, 488 wild-type strain or 488 *tssD* mutant. HCT-8 cells were infected with *C. jejuni* strains at a MOI of 1,000:1. (A) For interaction assays, infected monolayers were washed with PBS and treated with 0.1% (v/v) Triton X-100. (B) For invasion assays, infected monolayers were washed with PBS and treated with gentamicin (400 µg/ml) for 2 hours at 37°C. Cells were then washed with PBS and treated with 0.1% (v/v) Triton X-100. For both experiments, serial dilutions were then performed and plated onto blood agar plates. Plates were incubated for 48 hours at 37°C under microaerobic conditions and the CFUs/ml were counted. Asterisks denote a statistically significant difference (** indicating $p \leq 0.01$, *** indicating $p \leq 0.001$).

4.2.13 Interactions with and invasion of primary chicken intestinal epithelial cells by the 488 wild-type strain, 488 *tssD* mutant, and 81-176 wild-type strain

Recent studies suggest that the prevalence of T6SS-positive *C. jejuni* strains is on the rise in high-income countries and there are indications that T6SS-positive strains are now prevalent over T6SS-negative strains infecting chickens in farms, contaminating raw chicken sold in supermarkets, and isolated from hospital patients (Ugarte-Ruiz et al., 2015, Sima et al., 2018). To investigate whether the presence of the T6SS plays a role in the ability of *C. jejuni* to infect chickens, an *in vitro* model was used to examine the potential of *C. jejuni* to interact with to and invade primary chicken intestinal epithelial cells. The 488 wild-type strain exhibited significantly higher levels of interaction and invasion than the 488 *tssD* mutant (Figure 4.14). The T6SS-negative 81-176 wild-type strain also exhibited lower levels of interaction and invasion than the 488 wild-type strain, however these differences were not significant.

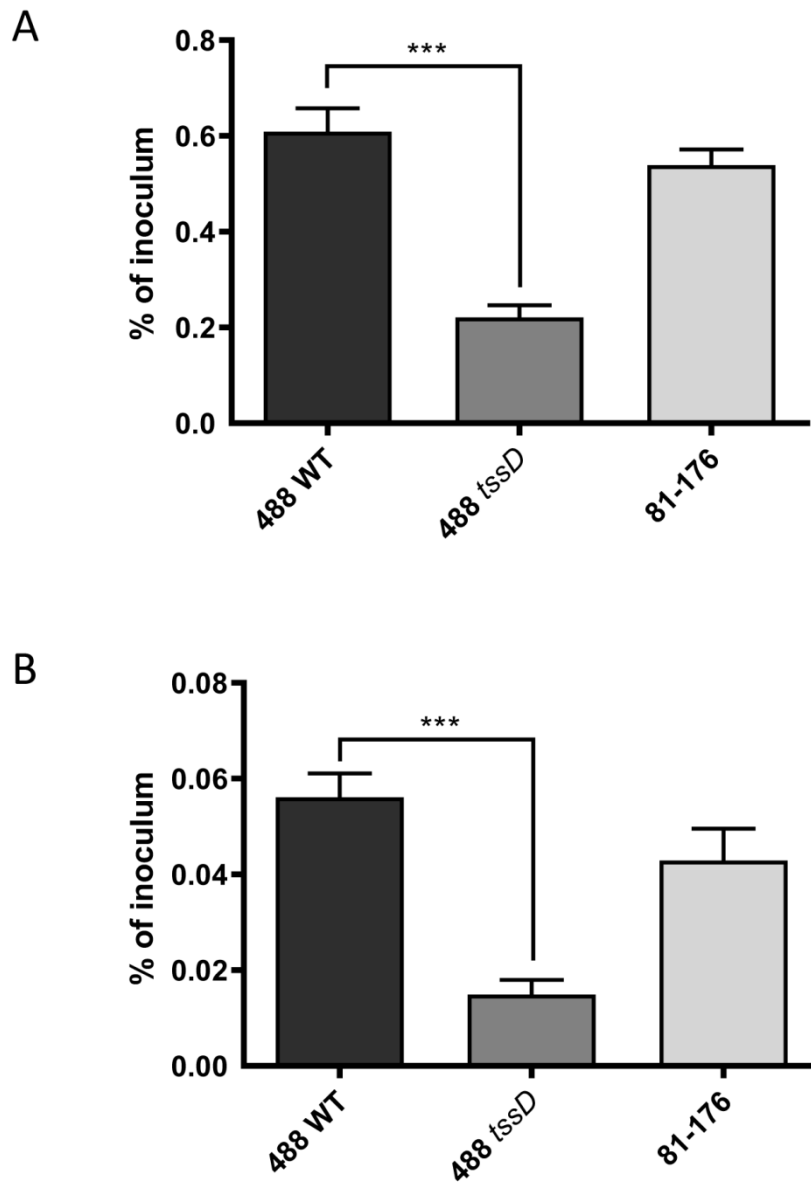


Figure 4.14. Interactions with and invasion of primary chicken intestinal cells by the 488 wild-type strain, 488 *tssD* mutant or 81-176 wild-type strain. Primary chicken intestinal cells were infected with *C. jejuni* strains at a MOI of 1,000:1. (A) For interaction assays, infected monolayers were washed with PBS and treated with 0.1% (v/v) Triton X-100 for 20 minutes at room temperature under normal atmospheric conditions. (B) For invasion assays, infected monolayers were washed with PBS and treated with gentamicin (400 $\mu\text{g/ml}$) for 2 hours at 37°C in a CO₂ incubator. Cells were then washed with PBS and treated with 0.1% (v/v) Triton X-100 for 20 minutes at room temperature under normal atmospheric conditions. For both experiments, serial dilutions were then performed and plated onto blood

agar plates. Plates were incubated for 48 hours at 37°C under microaerobic conditions and the CFUs/ml were counted. Asterisks denote a statistically significant difference (***) indicating $p \leq 0.001$).

4.2.14 Chick infection with the 488 wild-type strain, 488 *tssD* mutant, and 81-176 wild-type strain

To further investigate whether the presence of the T6SS plays a role in the ability of *C. jejuni* to infect chickens, *in vivo* infection of 15-day old Ross 308 broiler chickens was performed. At 3 days post infection, the numbers of the 488 wild-type strain detected in the caeca were significantly higher than the numbers of the 488 *tssD* mutant or 81-176 wild-type strain (Figure 4.15). Combined with the ability of T6SS to enhance both *C. jejuni* interactions with and invasion of chicken primary intestinal cells, these results indicate that the presence of the T6SS is important in enhancing the ability of *C. jejuni* to colonise chickens.

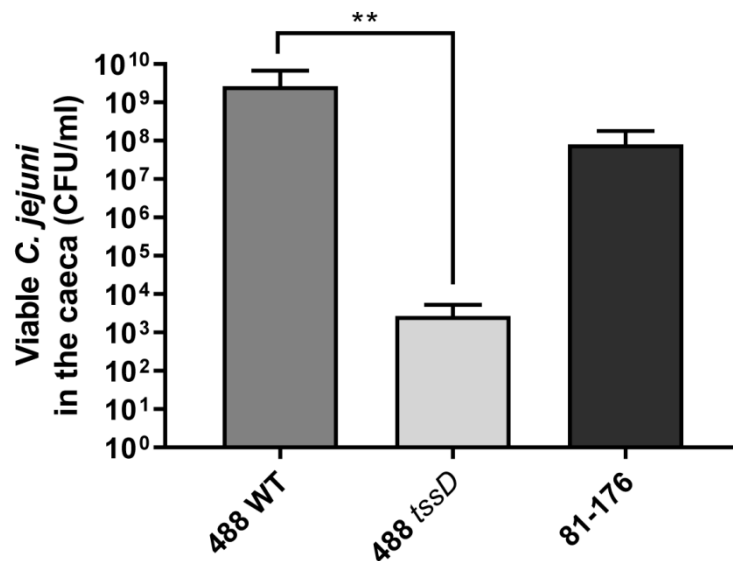


Figure 4.15. Infection of broiler chickens with the 488 wild-type strain, 488 *tssD* mutant or 81-176 wild-type strain. Ten 15-day old Ross 308 broiler chickens were inoculated with approximately 1×10^8 CFU/ml of either the 488 wild-type strain, the 488 *tssD* mutant or the 81-176 wild-type strain. Chickens were euthanised 3 days post-infection. Caecum contents were plated and counts of viable *C. jejuni* in the samples performed. Asterisks denote a statistically significant difference (** indicating $p \leq 0.01$).

4.3 DISCUSSION

The role of the T6SS in *C. jejuni* has not yet been well-elucidated in contrast to other bacteria harbouring the T6SS. Results from this study indicated that the recently isolated Brazilian 488 wild-type strain has a functional T6SS capable of secreting the TssD effector, corroborating previous studies which have shown TssD to be secreted from 43431 and 108 strains (Lertpiriyapong et al., 2012, Bleumink-Pluym et al., 2013). TssD was also found to be present in the whole cell lysates of a number of T6SS-positive strains, such as 43431, Cj1 and Cj5. However, in comparison to the other T6SS-positive strains, the 414 strain appeared to have a reduced amount of TssD in the whole cell lysate. The 414 strain is a slow-growing strain and has a vastly different gene arrangement in the T6SS cluster in comparison to the other strains.

As expected, TssD was not secreted from an isogenic 488 *tssD* mutant. Secretion of TssD was partially restored when the 488 *tssD* mutant was complemented by inserting a copy of the *tssD* gene into the pRRC plasmid (Karlyshev and Wren, 2005) and transforming into the 488 wild-type strain via a double recombination event into a non-coding spacer region of a rRNA gene cluster in the genome. This difference observed may be due to different promoters driving the expression of *tssD* in the 488 wild-type strain compared to the 488 *tssD* complement, where the *tssD* gene is now under the control of a constitutively expressed Cam^r gene promoter.

The function of the contractile sheath components TssBC has not previously been studied in *C. jejuni*. The contractile sheath of the T6SS is composed of two interlocking components – TssB/VipA and TssC/VipB – that assemble into a sheath-like structure surrounding the TssD needle-like tube (Kudryashev et al., 2015). In other bacteria, an intact contractile sheath structure is important for a fully functioning T6SS. In *V. cholerae* it has been demonstrated that removal of either TssB/VipA or TssC/VipB from the contractile sheaths resulted in a defective T6SS unable to secrete effectors (Brackmann et al., 2018, Kudryashev et al., 2015, Basler et al., 2012). In this study, we have shown that both contractile sheath genes are expressed when the 488 strain is cultured for 16 hours in Brucella broth and for 24 hours on solid blood agar plates, indicating that the *C. jejuni* T6SS contractile sheath is produced under different growth conditions. Isogenic 488 *tssB* and *tssC* mutants were constructed and were both shown to still secrete TssD at a reduced level compared to the 488 wild-type strain. The observation that the *C. jejuni* T6SS does not require both TssB and TssC components to be

present for the T6SS to be able to secrete TssD is unusual and differs from previous observations of T6SS in *V. cholerae*. This suggests that in *C. jejuni*, as long as either TssB or TssC is present, the T6SS remains capable of secreting TssD at a reduced level. However this does not suggest that the contractile sheath components in *C. jejuni* may differ from those in the T6SS model systems of *P. aeruginosa* and *V. cholerae*, rather that the contractile sheath components may be interchangeable or be able to compensate for the absence of the other component via a yet unknown process.

OMVs play an important role in the delivery of virulence factors to host cells (Elmi et al., 2012). In *C. jejuni*, OMVs have been shown to contain a range of virulence factors including the cytolethal distending toxin and proteases for delivery to the host cells (Lindmark et al., 2009, Elmi et al., 2016). Lin et al. observed that in *P. aeruginosa*, the TseF effector secreted by the H3-T6SS is incorporated into OMVs containing iron and delivered to bacterial cells (Lin et al., 2017). Previously no link has been established between the *C. jejuni* T6SS and OMVs.

In this study, Western blotting with the TssD antibody revealed the presence of the TssD component in OMVs isolated from the 488 wild-type strain. However, mutation of either the *tssB* or *tssC* genes encoding the contractile sheath components resulted in the absence of TssD from the OMVs, suggesting that the secretion of TssD within OMVs requires a fully intact and functional contractile sheath. Whether TssD is present in the OMVs of all T6SS-positive *C. jejuni* strains or whether other T6SS components are also present remains to be investigated. Proteomic analysis of highly purified OMV fractions would be able to reveal the presence of other T6SS components associated with OMVs, however the proteomic studies published to date have only studied OMVs from T6SS-negative *C. jejuni* strains (Elmi et al., 2012, Jang et al., 2014, Taheri et al., 2018, Taheri et al., 2019). The role of TssD and potentially other T6SS components in the OMVs would also need to be investigated. Treatment of OMVs with proteinase K would reveal whether the T6SS components are located on the surface or packaged inside the OMVs and would also provide a preliminary indication as to the purpose of the T6SS components associating with OMVs.

The secretion of the TssD and VgrG components is considered to be a hallmark of a functional T6SS in both *V. cholerae* and *P. aeruginosa* (Pukatzki et al., 2006). However, thus far only TssD has been shown to be secreted by the *C. jejuni* T6SS (Lertpiriyapong et al., 2012, Bleumink-Pluym et al., 2013). An antibody was designed against the *C. jejuni* 1056

VgrG amino acid sequence, following the same strategy used for the design of the TssD antibody. The TssD antibody successfully used to detect the presence of the TssD components in this study for *C. jejuni* 488, 43431, 414, Cj1 and Cj5 was designed against the *C. jejuni* 1056 TssD sequence. Therefore to maintain consistency, it was thought logical to continue designing antibodies against amino acid sequences from this strain. However, contrary to expectations VgrG was not detected in the whole cell lysates of the *C. jejuni* strains used in this study. Optimisation of various steps of the Western blot protocol, such as varying the concentrations of the primary and secondary antibodies or incubation times, were ultimately unsuccessful. Whole genome sequencing of *C. jejuni* strains in Chapter 5 has now revealed a high degree of variation in the C-terminus of VgrG amongst strains; this variation would account for the inability of the VgrG antibody to detect the presence of VgrG in *C. jejuni* 488, 43431, 414, Cj1 and Cj5. In order to detect VgrG from each strain, antibodies would have to either be designed against individual VgrG sequences from each strain. Alternatively, the VgrG sequence used for the antibody would have to be truncated to exclude the highly variable C-terminus region. Mass spectrometry data presented in Chapter 5 confirmed the presence of VgrG in the secretome of the *C. jejuni* 488 strain.

As a host metabolite, bile can modulate the global gene expression of a wide range of virulence factors in bacterial pathogens (Elmi et al., 2018). Sodium taurocholate has been shown to stimulate the production of OMVs in *C. jejuni* (Elmi et al., 2018, Davies et al., 2019). Bile salts have been demonstrated to be important in modulating T6SS activity in *V. cholerae* and the secondary bile salt sodium deoxycholate can induce virulence gene expression in *C. jejuni* (Bachmann et al., 2015, Malik-Kale et al., 2008). Lertpiriyapong et al. showed that inhibition of *C. jejuni* growth occurs at high concentrations of sodium deoxycholate; however this growth inhibition may be overcome in the presence of a T6SS (Lertpiriyapong et al., 2012).

The results from this study indicate that whilst sodium taurocholate does not alter T6SS expression in *C. jejuni*, changing concentrations of sodium deoxycholate present as *C. jejuni* moves through the small intestine could play a role in modulating the expression of the T6SS. Up-regulation of T6SS gene expression during exposure to 0.1% (w/v) sodium deoxycholate and subsequent down-regulation in T6SS gene expression during exposure to 0.2% (w/v) sodium deoxycholate would suggest that the T6SS in *C. jejuni* responds to a concentration gradient of sodium deoxycholate present in the small intestine; this indicates that the *C. jejuni*

T6SS may be activated and deactivated in specific regions as the bacteria moves up then down a concentration gradient of sodium deoxycholate in the host small intestines.

During host colonisation and infection, *C. jejuni* is exposed to conditions in the host gastrointestinal tract that present as physical and chemical stresses, including oxidative stress (Flint et al., 2016, Kim et al., 2015). Oxidative stress involves the generation of ROS that cause damage to nucleic acids, membranes and proteins of bacteria. The importance of the T6SS in countering the effects of oxidative stress has previously been shown in *Y. pseudotuberculosis*, *B. thailandensis* and enterohemorrhagic *E. coli* (Wang et al., 2015, Wan et al., 2017, Si et al., 2017). In this study, the *C. jejuni* T6SS also appears to play a role in the oxidative stress response. The genes encoding KatA, SodB and AhpC that are involved directly in the breakdown of ROS are all expressed at significantly higher levels in the 488 wild-type strain compared to the 488 *tssD* mutant. KatA is a catalase that breaks down H₂O₂ to H₂O and O₂, SodB is an iron-co-factored superoxide dismutase that detoxifies superoxide, and AhpC is an alkyl hydroperoxide reductase that scavenges endogenous H₂O₂ (Seaver and Imlay, 2001, Hwang et al., 2013, Kim et al., 2015). The 488 wild-type strain with an intact T6SS is also more resistant to the effects of oxidative stress compared to the 488 *tssD* mutant; resistance to oxidative stress was enhanced when the 488 *tssD* mutant was complemented with an intact copy of *tssD*.

The increased susceptibility of the 488 *tssD* mutant to H₂O₂ is specific and not due to a potential membrane defect due to improper assembly of the T6SS in the bacterial membrane. This was demonstrated by antimicrobial susceptibility testing which indicated no differences in antimicrobial susceptibility between the 488 wild-type strain, the 488 *tssD* mutant, and the 488 *tssD* complement, corresponding with results from a similar study by Lertpiriyapong et al. performed with the 43431 wild-type strain and *tss* mutants (Lertpiriyapong et al., 2012). Initially, the bile salt stress assay which involved subjecting the 488 wild-type strain, 488 *tssD* mutant and 488 *tssD* complement to 2% (w/v) sodium taurocholate was performed to test for any presence of membrane defects in the strains. However, this was likely not an appropriate test to distinguish membrane defects between T6SS wild-type and mutant strains, as Lertpiriyapong et al. demonstrated that T6SS mutants are more susceptible to the effects of bile salt stress; this was confirmed by the results (Figure 4.10) which showed that growth of the 488 *tssD* mutant was significantly reduced compared to the 488 wild-type strain and the 488 *tssD* complement (Lertpiriyapong et al., 2012).

We speculate that TssD positively regulates the expression of genes involved in the breakdown of ROS, and in turn this results in greater resistance to oxidative stress in strains harbouring an intact T6SS cluster. However, such an association has not been clearly demonstrated; whether regulation of a set of non-T6SS genes by the *C. jejuni* T6SS is possible and any mechanisms involved would require further investigation. A study by Weber et al. indicated that the T6SS of *Vibrio anguillarum* positively regulates the expression of the stress-response regulator RpoS, initiating a regulatory cascade that induces expression of the quorum-sensing regulator VanT (Weber et al., 2009).

A MarR family transcriptional regulator TctR was recently shown to regulate the T6SS-2 gene cluster in *B. pseudomallei* (Losada et al., 2018). Previous studies have also shown that the MarR family transcriptional regulators RrpA and RrpB are important in regulating both oxidative and aerobic stress responses in *C. jejuni* and therefore play a role in enhancing bacterial survival both in the hosts and in the environment (Gundogdu et al., 2011, Gundogdu et al., 2015, Gundogdu et al., 2016). As the results indicate that the *C. jejuni* T6SS is also associated with the oxidative stress response, it is tempting to speculate that the RrpA and RrpB regulators may in some way be linked to the T6SS; further studies will be required to investigate this hypothetical link.

Different internal controls were employed in qRT-PCR experiments examining T6SS gene expression in the presence of bile salts to that of experiments examining the expression of oxidative stress response genes. The stably expressed housekeeping gene *gyrA* was used as an internal control to examine differences in the expression of *katA*, *sodB* and *ahpC* in the 488 wild-type strain and the 488 *tssD* mutant. The *gyrA* gene, which encodes for gyrase subunit A, has been widely used as an internal control to observe the relative expression of genes in *C. jejuni* (Ritz et al., 2009, Elmi et al., 2018, Gundogdu et al., 2011, Gundogdu et al., 2015). However, Ritz et al. proposed the use of *rpoA* encoding for RNA polymerase α subunit as a suitable internal control to study stress response in *C. jejuni* (Ritz et al., 2009). The *rpoA* gene was previously used in a study by Davies et al. to examine gene expression in the presence of sodium taurocholate and was also used in this study as the internal control to examine T6SS gene expression when *C. jejuni* was cultured in the presence of bile salts (Davies et al., 2019).

Based on our data we propose that presence of the T6SS cluster in *C. jejuni* strains confers a competitive advantage to these strains within a host. *G. mellonella* is an established insect model for the study of bacterial pathogenesis (Champion et al., 2010, Senior et al., 2011,

Peleg et al., 2009). The larvae of the greater wax moth provide a convenient and inexpensive model, and upon exposure to pathogens their innate immune response resembles that of the mammalian innate immune response (Trevijano-Contador and Zaragoza, 2018).

The T6SS-positive 488 wild-type strain is more cytotoxic in the *G. mellonella* model than the T6SS-negative 81-176 wild-type strain and the 488 *tssD* mutant. This suggests that the presence of a T6SS increases the cytotoxicity of *C. jejuni* in the *G. mellonella* model of infection and secreted T6SS effectors may also be important in causing cytotoxicity to other organisms. The 81-176 strain was selected as a negative control in this study due to the absence of the T6SS in this strain. Despite lacking the T6SS, 81-176 is a hypervirulent strain capable of causing severe disease and harbours two plasmids, pTet and pVir, that play a role in increased virulence (Black et al., 1988, Bacon et al., 2000). Therefore it is important to bear in mind that any differences observed between 488 and 81-176 could in part also be due to a diversity of virulence factors in these two strains rather than just the presence or absence of the T6SS.

Previous studies have examined interactions of the *C. jejuni* T6SS with human cell lines. Lertpiriyapong et al. showed that the *C. jejuni* T6SS enhances the adherence to and invasion of *C. jejuni* to T84 human colonic epithelial cells, and Noreen et al. demonstrated that TssD is cytotoxic towards HepG2 human liver carcinoma cells (Lertpiriyapong et al., 2012, Noreen et al., 2018). However, in this study the results were inconclusive when investigating whether the presence of the T6SS enhances the ability of *C. jejuni* to interact with and invade HCT-8 human colonic epithelial cells. The 488 wild-type strain exhibited reduced interactions with the HCT-8 cell line but was also significantly more invasive than the 488 *tssD* mutant or the 81-176 wild-type strain. This was in contrast to results obtained by Lertpiriyapong et al. with T84 human colonic epithelial cells, where the 43431 wild-type strain was significantly more interactive and invasive than the 43431 *tssD* mutant (Lertpiriyapong et al., 2012). Differences between the two studies may be due to difference in behaviour between *C. jejuni* strains and also differences in the human cell lines used.

This study was the first to examine the role of T6SS of *C. jejuni* in biologically relevant models with the utilisation of a primary chicken cell line and a chicken infection model. Lertpiriyapong et al. utilised a murine model and found that a T6SS-positive strain exhibited higher levels of interaction to and invasion of RAW 264.7 macrophage cells and have a higher colonisation potential in IL-10-deficient mice (Lertpiriyapong et al., 2012). However,

it has previously been shown that *C. jejuni* does not colonise mice in the same manner as in chickens, as *C. jejuni* colonises mice at a significantly slower rate than chickens and some strains such as 81-176 do not appear to colonise mice at all (Wilson et al., 2010).

The *C. jejuni* 488 wild-type strain exhibits higher levels of interaction to and invasion of chicken cells and is also able to infect chickens at a much higher rate than the *tssD* mutant. The results indicate that the ability of *C. jejuni* to infect chickens is enhanced by the presence of the T6SS and the T6SS may be important as a colonisation factor in the natural host of *C. jejuni*. The increased ability of *C. jejuni* strains with the T6SS to infect and colonise chickens is a particular concern for the agricultural and food industries tasked with reducing *C. jejuni* load in both live chickens on farms and on raw chicken meat in the supermarket (Sima et al., 2018). From a public health perspective, the increase in T6SS-positive *C. jejuni* strains is also problematic as there are indications that strains with the T6SS may cause more severe disease in humans (Harrison et al., 2014).

4.4 CONCLUSION

This study aimed to gain a further understanding into the role of the T6SS in *C. jejuni*. The contractile sheath of the *C. jejuni* T6SS was examined and the *C. jejuni* T6SS is not functional when the entire contractile sheath structure is absent. Surprisingly, inactivation of one of the contractile sheath components did not result in a completely non-functional T6SS in *C. jejuni*; this contradicts previous findings on the contractile sheath of the *V. cholerae* T6SS and suggests that the contractile sheath machinery in *C. jejuni* may differ from that of other bacteria. Results from this study indicate that T6SS expression in *C. jejuni* is mediated by a concentration gradient of sodium deoxycholate. The importance of the T6SS in countering the effects of oxidative stress has been previously demonstrated in other bacteria, and this study was the first to establish a link between the T6SS and the oxidative stress response in *C. jejuni* (Appendix 4) (Liaw et al., 2019). The role of the *C. jejuni* T6SS in host colonisation was examined with biologically relevant models and our results suggest that the presence of the T6SS cluster in *C. jejuni* strains confers a competitive advantage to these strains within a host.

CHAPTER FIVE: Analysis of the *Campylobacter jejuni* T6SS secretome and identification of potential T6SS effectors

5.1 INTRODUCTION

The T6SS is a contractile machinery capable of delivering effector proteins to target cells. A number of bacterial effector proteins secreted by the T6SS have been identified and the types of roles these proteins can serve has been shown to be vastly diverse – from competition with microbes to survival within a host or the environment (Cianfanelli et al., 2016b, Hachani et al., 2016). Different strategies and methods have been applied to identify effector proteins secreted by the T6SS, including bioinformatic and proteomic-based approaches (Lien and Lai, 2017). The TssD component has been demonstrated to be secreted by all T6SSs and is thus far the only T6SS effector to be identified in *C. jejuni* (Lertpiriyapong et al., 2012, Bleumink-Pluym et al., 2013, Noreen et al., 2018).

The aim of this chapter was to identify effector proteins secreted via the *C. jejuni* T6SS. Whole genome sequencing of the T6SS-positive *C. jejuni* strains was performed to determine whether the complete T6SS cluster was present in these strains. Bioinformatic searches were performed to investigate whether known T6SS effector proteins found in other bacteria were also present in *C. jejuni*. Secretome profiles of the 488 wild-type strain and mutants were compared and analysed. Proteomic and bioinformatic approaches were utilised to identify proteins secreted via the *C. jejuni* T6SS and examine possible effector and immunity modules.

5.2 RESULTS

5.2.1 Bioinformatics analysis of T6SS gene clusters in the *C. jejuni* 488 and other T6SS-positive strains reveals synteny

Whole genome sequencing of *C. jejuni* 488 wild-type strain (a recent human isolate from Brazil) and *C. jejuni* wild-type strain 43431 (a human isolate from Canada) (Penner et al., 1983) was performed. *C. jejuni* wild-type strain RC039 (a chicken isolate from Northern Ireland) had been previously sequenced (Corcionivoschi et al., 2015). The presence of a single T6SS cluster was observed in all three strains. All T6SS core components were identified, however the TssH (ClpV) ATPase responsible for disassembly of the contracted sheath components is absent from the T6SS cluster of all *C. jejuni* strains sequenced thus far. The genome co-ordinates of the T6SS cluster in the *C. jejuni* 488 strain are listed in Appendix 1.

Comparisons of the 488, 43431 and RC039 genome sequences with previously published sequences for other T6SS-positive *C. jejuni* strains (Lertpiriyapong et al., 2012, Bleumink-Pluym et al., 2013) revealed a T6SS cluster that is highly conserved, sharing synteny between strains and also with other *Campylobacter* species isolated from humans and chickens (Figure 5.1). The 414 strain, isolated from a wild bank vole in the United Kingdom, has a different gene arrangement in the T6SS cluster, but the same core components are still present.

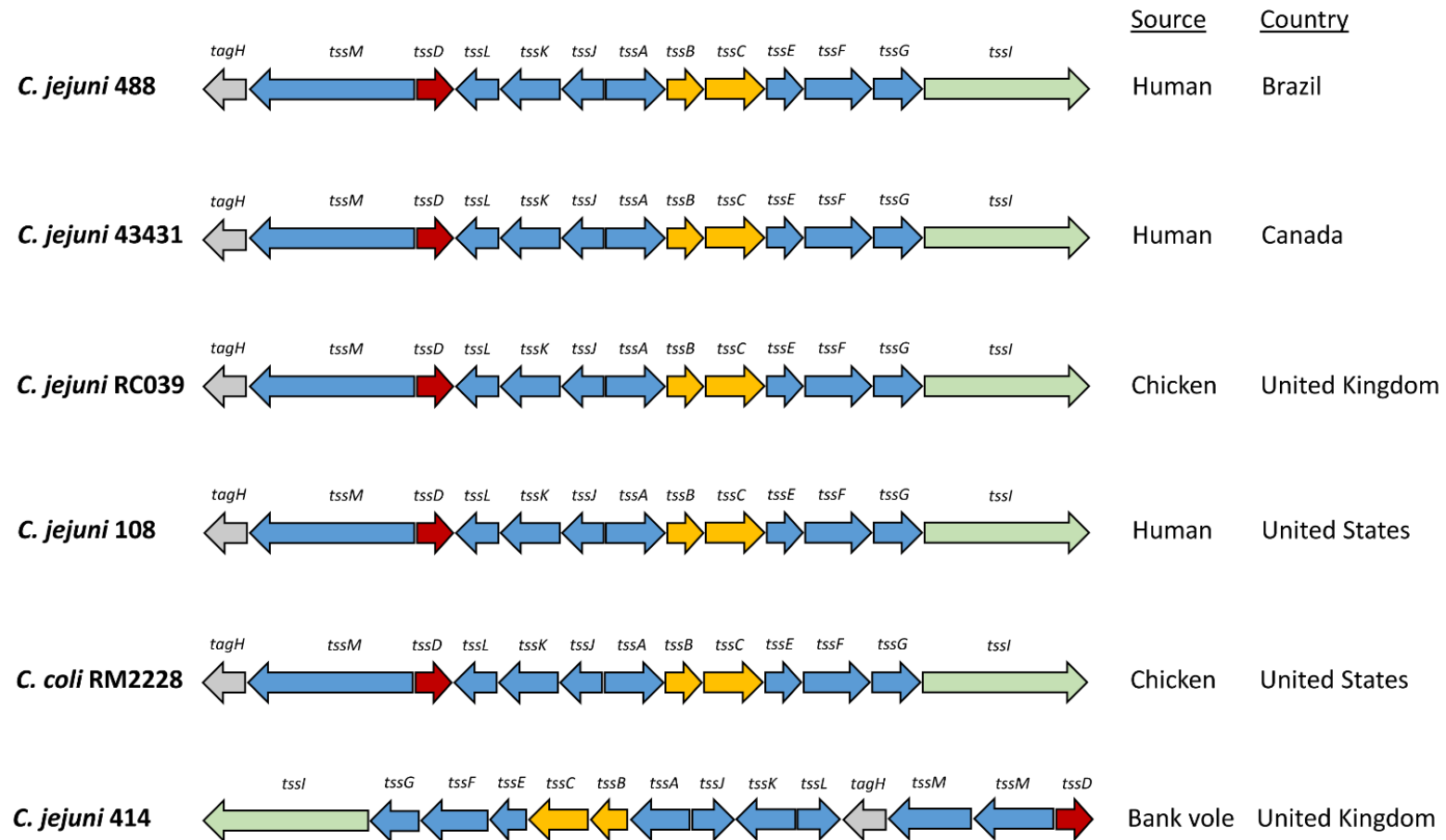


Figure 5.1. Type VI secretion system gene clusters of *C. jejuni* strains. The *C. jejuni* 488 and 43431 wild-type strains were sequenced using whole genome sequencing in this study. The genome sequence of *C. jejuni* RC039 was published by Corcionivoschi et al. (2015). The genome sequences for *C. jejuni* 108 and *C. coli* RM2228 was published by Bleumink-Pluym et al. (2013). The genome sequence for *C. jejuni* 414 was published by Lertpiriyapong et al. (2012).

5.2.2 Bioinformatics searches identified no known effector proteins in the *C. jejuni* 488 and 43431 strains

Bioinformatic searches were performed to investigate whether T6SS effector proteins found in other bacteria are present in *C. jejuni*. Effector proteins identified from the literature were searched against the genomes of the *C. jejuni* 488 and 43431 strains (Table 5.1). Amino acid sequences of known effector proteins are available in Appendix 2. However, no effector proteins were identified by these searches, at expected (E) values of 0.01 or 0.1.

A positive control using TssD from the *C. jejuni* 414 strain as the query sequence resulted in a match. However, using Hcp1 from *P. aeruginosa* PAO1 strain did not result in a match when searched against the genomes of the *C. jejuni* 488 and 43431 strains. Multiple sequence alignment of the amino acid sequences of TssD from the *C. jejuni* 488, 43431 and 414 strains against Hcp1 of *P. aeruginosa* PAO1 indicated that TssD amino acid sequences were similar between *C. jejuni* strains, but differ from the Hcp1 amino acid sequence of *P. aeruginosa* PAO1 (Figure 5.2).

Table 5.1. Bioinformatics searches for known T6SS effector proteins.

Species	Strain	T6SS Secreted Proteins	Gene Identifier	Search Performed (E0.01)	Search Performed (E0.1)
<i>Pseudomonas aeruginosa</i>	PAO1	TseF	PA2374	Not identified	Not identified
<i>Pseudomonas aeruginosa</i>	PAO1	Tse1 (Tse1)	PA1844	Not identified	Not identified
<i>Pseudomonas aeruginosa</i>	PAO1	Tse2	PA2702	Not identified	Not identified
<i>Pseudomonas aeruginosa</i>	PAO1	Tse3 (Tge1)	PA3484	Not identified	Not identified
<i>Pseudomonas aeruginosa</i>	PAO1	PldA (Tle5PA)	PA3487	Not identified	Not identified
<i>Pseudomonas aeruginosa</i>	PAO1	PldB	PA3301	Not identified	Not identified
<i>Yersinia pseudotuberculosis</i>	YPIII	YezP	YPK_3549	Not identified	Not identified
<i>Serratia marcescens</i>	DB11	Tfe1 (Ssp3)	SMDB11_1112	Not identified	Not identified
<i>Serratia marcescens</i>	DB11	Tfe2	SMDB11_1083	Not identified	Not identified
<i>Serratia marcescens</i>	DB11	Ssp1 (Tae4.1)	SMDB11_2261	Not identified	Not identified
<i>Serratia marcescens</i>	DB11	Ssp2 (Tae4.2)	SMDB11_2264	Not identified	Not identified
<i>Serratia marcescens</i>	DB11	Ssp4	SMDB11_3980	Not identified	Not identified
<i>Serratia marcescens</i>	DB11	Ssp5	SMDB11_4628	Not identified	Not identified
<i>Serratia marcescens</i>	DB11	Ssp6	SMDB11_4673	Not identified	Not identified

<i>Vibrio cholerae</i> O1 biovar El Tor chromosome I	N16961	VgrG	VC1416	Not identified	Not identified
<i>Vibrio cholerae</i> O1 biovar El Tor chromosome II	N16961	VgrG	VCA0123	Not identified	Not identified
<i>Vibrio cholerae</i> O1 biovar El Tor chromosome II	N16961	VasX	VCA0020	Not identified	Not identified
<i>Vibrio cholerae</i> O1 biovar El Tor chromosome I	N16961	TseL/Tse2VC	VC1418	Not identified	Not identified
<i>Burkholderia</i> <i>thailandensis</i> E264 chromosome II	E264	TseZ	BTH_III1884	Not identified	Not identified
<i>Salmonella enterica</i> <i>subsp. enterica</i> serovar Typhimurium	LT2	Tae4	STM0277	Not identified	Not identified
<i>Enterobacter cloacae</i> <i>subsp. cloacae</i>	ATCC 13047	Tae4	ECL_01542	Not identified	Not identified
Controls:					
<i>Campylobacter jejuni</i>	414	TssD		Identified	Identified
<i>Pseudomonas</i> <i>aeruginosa</i>	PAO1	Hcp1	PA0085	Not identified	Not identified

Bioinformatic searches were performed to identify known effector proteins found in other bacteria in *C. jejuni*. A list was generated of known effector proteins and the amino acid sequences were retrieved from GenBank then added to this list as query sequences. The sequences from this list were queried against the genome sequences of the 488, 43431 and

RC039 strains using Blastall scripts on UNIX (Camacho et al., 2009). No matches were found with expectation (E) values of 0.01 and 0.1. Positive controls were performed using TssD from *C. jejuni* 414 and Hcp1 from *P. aeruginosa* PAO1 as the query sequences.

5.2.3 Comparison of secretome profiles of the 488 wild-type strain and mutants

The secretome profiles of the 488 wild-type strain and mutants were compared via SYPRO Ruby staining of SDS-PAGE gels to determine whether there was a difference in proteins secreted into the supernatant. The results demonstrate that the secretome profiles differ between the 488 wild-type strain, 488 *tssB* mutant, 488 *tssC* mutant, 488 *tssBC* double mutant and 488 *tssD* mutant (Figure 5.3). The secretome profile also differs between the 488 wild-type strain and the RC039 wild-type strain, indicating that the secretome also varies between T6SS-positive strains.

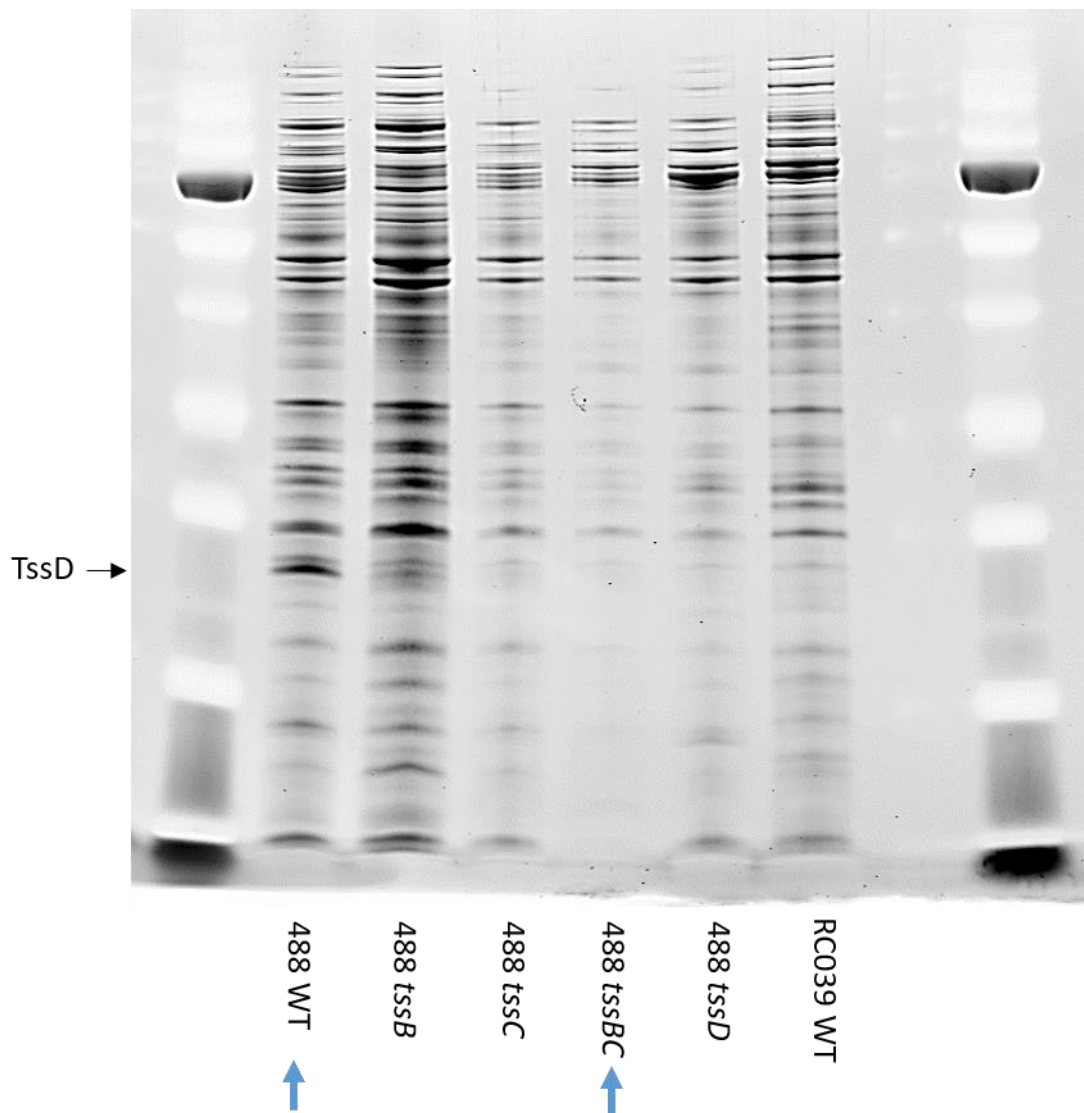


Figure 5.3. SDS-PAGE of the supernatant fractions of the 488 wild-type strain, 488 *tssB* mutant, 488 *tssC* mutant, 488 *tssBC* double mutant, 488 *tssD* mutant and the RC039 wild-type strain. Bacterial supernatant samples were prepared from 12 hour cultures of *C. jejuni* 488 wild-type strain, 488 *tssB* mutant, 488 *tssC* mutant, 488 *tssBC* double mutant, 488 *tssD* mutant and RC039 wild-type strain grown in Brucella broth. Supernatant samples were concentrated via centrifugal filters and 30 μ g of samples were loaded onto a 12% (w/v) Bis-Tris protein gel. The SDS-PAGE gel was stained with SYPRO Ruby protein gel stain and imaged on the Typhoon Trio Imager System.

5.2.4 Mass spectrometry analysis identified proteins more abundant in the secretome of the 488 wild-type strain than the 488 *tssBC* double mutant

The 488 wild-type strain and 488 *tssBC* double mutant were chosen for liquid-chromatography mass spectrometry (LC-MS) analysis to identify putative proteins secreted by the *C. jejuni* T6SS. To search for potential effector proteins in the secretome, supernatant from the 488 wild-type strain and the 488 *tssBC* contractile sheath double mutant were filtered, concentrated, then sent for mass spectrometry. Proteins found to be more abundant in the secretome of the 488 wild-type strain than the 488 *tssBC* double mutant are listed in Table 5.2. Differences were considered to be significant if the fold change was greater than 2 and the p-value was less than 0.05.

96 proteins were identified to be more abundant in the secretome of the 488 wild-type strain than the 488 *tssBC* double mutant. T6SS components TssD, TssI/VgrG, and TssC were found in the secretome of the 488 wild-type strain. ArgH (argininosuccinate lyase), Pta (phosphate acetyltransferase), AckA (acetate kinase), PstS (part of the phosphate transport system), RplU/RplQ/RplW (ribosomal proteins) were some of the proteins found to be more abundant in the secretome of the 488 wild-type strain. (Figure 5.4)

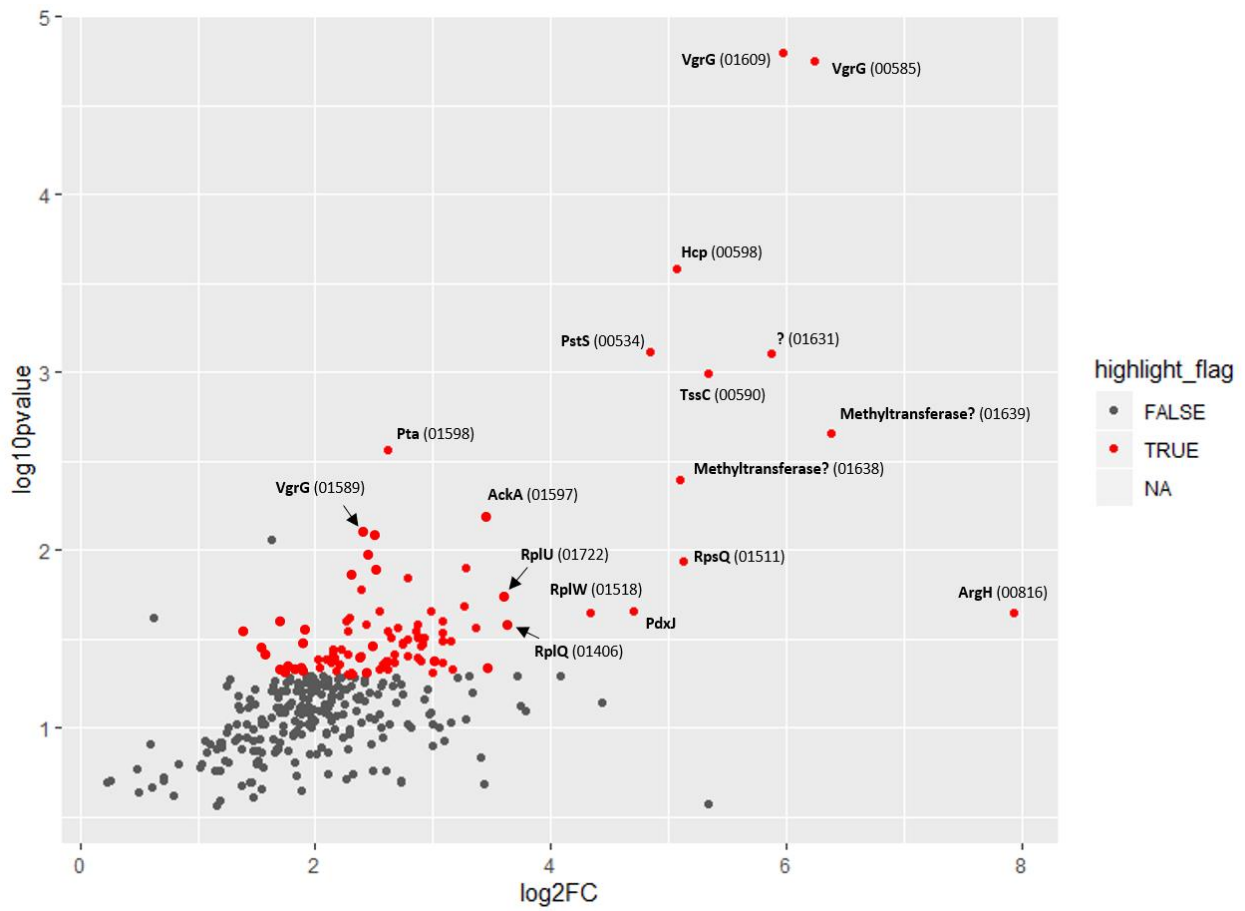


Figure 5.4. Volcano plot of comparison for the secretome of the 488 wild-type strain and the 488 *tssBC* double mutant. Points in red have a p-value < 0.05 and fold change > 2.

5.2.5 Mass spectrometry analysis identified proteins more abundant in the secretome of the 488 *tssBC* double mutant than the 488 wild-type strain

Three proteins were identified by mass spectrometry to be more abundant in the secretome of the 488 *tssBC* double mutant than the 488 wild-type strain (Table 5.3). Two of the proteins – FlgE-2 and FlgM – are associated with the flagella, whilst the remaining protein is a hypothetical protein.

Table 5.2. Proteins more abundant in secretome of the 488 wild-type strain than the 488 *tssBC* double mutant.

Accession	Max fold change	Mass	Description
488_S2_data_43_00816	244.1935513	51808	ArgH argininosuccinate lyase 735956:737338 Reverse
488_S2_data_43_01639	83.47056616	7757.9	488_S2_data_43_01639 Methyltransferase, possibly involved in O-methyl phosphoramidate capsule modification 1523764:1523958 Forward
488_S2_data_43_00585	76.0068935	66032	488_S2_data_43_00585 hypothetical protein 519097:520821 Reverse
488_S2_data_43_01609	62.94899322	35639	488_S2_data_43_01609 hypothetical protein 1494917:1495870 Reverse
488_S2_data_43_01631	58.78421605	35282	488_S2_data_43_01631 putative sugar-nucleotide epimerase/dehydratase 1516711:1517649 Forward
488_S2_data_43_00590	40.50682012	55672	TssC hypothetical protein 523808:525262 Reverse
488_S2_data_43_01511	34.88856892	9549.4	RpsQ 30S ribosomal protein S17 1390977:1391228 Reverse
488_S2_data_43_01638	34.16935181	16213	488_S2_data_43_01638 Methyltransferase, possibly involved in O-methyl phosphoramidate capsule modification 1523186:1523623 Forward
488_S2_data_43_00598	33.62245751	18764	Hcp (TssD) Major exported protein 531562:532077 Forward

488_S2_data_43_00534	28.60795242	36079	PstS putative periplasmic phosphate binding protein 471266:472261 Forward
sp Q9PN59 PDXJ_CAMJE	26.00544293	29011	Pyridoxine 5'-phosphate synthase OS=Campylobacter jejuni subsp. jejuni serotype O:2 (strain ATCC 700819 / NCTC 11168) OX=192222 GN=pdxJ PE=1 SV=1
488_S2_data_43_01518	20.17788634	10567	RplW 50S ribosomal protein L23 1394090:1394371 Reverse
488_S2_data_43_01406	12.3704681	13247	RplQ 50S ribosomal protein L17 1302702:1303055 Forward
488_S2_data_43_01722	12.09878047	11609	RplU 50S ribosomal protein L21 1620263:1620571 Forward
sp Q9PI17 RS7_CAMJE	11.03468192	17692	30S ribosomal protein S7 OS=Campylobacter jejuni subsp. jejuni serotype O:2 (strain ATCC 700819 / NCTC 11168) OX=192222 GN=rpsG PE=3 SV=1
488_S2_data_43_01597	10.87997197	44149	AckA acetate kinase 1479954:1481144 Reverse
488_S2_data_43_01517	10.25333782	30436	RplB 50S ribosomal protein L2 1393258:1394088 Reverse
sp Q9PI35 RL11_CAMJE	9.684167431	15080	50S ribosomal protein L11 OS=Campylobacter jejuni subsp. jejuni serotype O:2 (strain ATCC 700819 / NCTC 11168) OX=192222 GN=rplK PE=3 SV=1
sp Q9PM83 RS13_CAMJE	9.625129006	13735	30S ribosomal protein S13 OS=Campylobacter jejuni subsp. jejuni serotype O:2 (strain ATCC 700819 / NCTC 11168) OX=192222 GN=rpsM PE=3 SV=1
488_S2_data_43_00836	8.981338485	16130	488_S2_data_43_00836 putative lipoprotein 760383:760817 Reverse

488_S2_data_43_01404	8.899724712	23896	RpsD 30S ribosomal protein S4 1301046:1301672 Forward
488_S2_data_43_00301	8.489784978	8178.7	RpsU 30S ribosomal protein S21 262135:262332 Forward
488_S2_data_43_01318	8.481113322	14181	RpsI 30S ribosomal protein S9 1217218:1217607 Reverse
sp Q0P823 DAPD_CAMJE	8.465953263	42361	2,3,4,5-tetrahydropyridine-2,6-dicarboxylate N-succinyltransferase OS=Campylobacter jejuni subsp. jejuni serotype O:2 (strain ATCC 700819 / NCTC 11168) OX=192222 GN=dapD PE=1 SV=1
488_S2_data_43_00098	8.439571963	21650	ClpP ATP-dependent Clp protease proteolytic subunit 84290:84874 Reverse
sp Q0P9K4 DAPE_CAMJE	8.080379734	40457	Succinyl-diaminopimelate desuccinylase OS=Campylobacter jejuni subsp. jejuni serotype O:2 (strain ATCC 700819 / NCTC 11168) OX=192222 GN=dapE PE=3 SV=1
488_S2_data_43_01461	8.00558367	41378	488_S2_data_43_01461 PDZ domain protein 1349478:1350572 Forward
sp Q9PLX9 RL29_CAMJE	7.896265811	7033.5	50S ribosomal protein L29 OS=Campylobacter jejuni subsp. jejuni serotype O:2 (strain ATCC 700819 / NCTC 11168) OX=192222 GN=rpmC PE=3 SV=1
sp Q9PIB9 RISB_CAMJE	7.618855887	16686	6,7-dimethyl-8-ribityllumazine synthase OS=Campylobacter jejuni subsp. jejuni serotype O:2 (strain ATCC 700819 / NCTC 11168) OX=192222 GN=ribH PE=3 SV=1
488_S2_data_43_00876	7.498641995	72606	RpoD RNA polymerase sigma factor (sigma-70) 794056:795924 Forward

488_S2_data_43_00313	7.489120951	14930	NusB hypothetical protein 271791:272189 Reverse
sp Q9PLX0 RS10_CAMJE	7.471394517	11673	30S ribosomal protein S10 OS=Campylobacter jejuni subsp. jejuni serotype O:2 (strain ATCC 700819 / NCTC 11168) OX=192222 GN=rpsJ PE=3 SV=1
488_S2_data_43_00633	7.41285089	13682	RplS 50S ribosomal protein L19 560468:560824 Forward
488_S2_data_43_00413	7.3345153	168863	RpoC DNA-directed RNA polymerase beta' chain 357701:362254 Forward
488_S2_data_43_01441	7.317398868	49560	SdaA L-serine dehydratase 1333963:1335327 Reverse
sp Q9PI36 NUSG_CAMJE	7.280999906	20195	Transcription termination/antitermination protein NusG OS=Campylobacter jejuni subsp. jejuni serotype O:2 (strain ATCC 700819 / NCTC 11168) OX=192222 GN=nusG PE=3 SV=1
488_S2_data_43_01568	7.252706716	90065	NrdA ribonucleoside-diphosphate reductase alpha chain 1443721:1446090 Forward
sp Q0P7T9 RL6_CAMJE	6.900447804	19587	50S ribosomal protein L6 OS=Campylobacter jejuni subsp. jejuni serotype O:2 (strain ATCC 700819 / NCTC 11168) OX=192222 GN=rplF PE=3 SV=1
488_S2_data_43_01070	6.880850218	28898	488_S2_data_43_01070 putative NLPA family lipoprotein 983492:984262 Forward
488_S2_data_43_00778	6.866051233	62827	RpsA 30S ribosomal protein S1 704162:705832 Reverse
488_S2_data_43_00410	6.70197166	17685	RplJ 50S ribosomal protein L10 352586:353065 Forward

488_S2_data_43_00818	6.683313502	66062	PycB putative pyruvate carboxylase B subunit 738935:740734 Reverse
sp Q9PM80 RPOA_CAMJE	6.479239113	37686	DNA-directed RNA polymerase subunit alpha OS=Campylobacter jejuni subsp. jejuni serotype O:2 (strain ATCC 700819 / NCTC 11168) OX=192222 GN=rpoA PE=1 SV=1
488_S2_data_43_00231	6.403078306	30159	PanB 3-methyl-2-oxobutanoate hydroxymethyltransferase 197797:198621 Reverse
488_S2_data_43_01182	6.359156504	42105	488_S2_data_43_01182 hypothetical proteinc 1091010:1092080 Reverse
488_S2_data_43_00625	6.267827174	27784	488_S2_data_43_00625 hypothetical protein 555335:556051 Forward
488_S2_data_43_00189	6.144535279	35478	488_S2_data_43_00189 putative periplasmic protein 161922:162869 Reverse
488_S2_data_43_00078	6.138758089	44901	488_S2_data_43_00078 putative saccharopine dehydrogenase 64676:65881 Reverse
488_S2_data_43_01598	6.130060942	56030	Pta phosphate acetyltransferase 1481158:1482660 Reverse
488_S2_data_43_00735	6.114144253	27975	488_S2_data_43_00735 putative oxidoreductase 661666:662415 Reverse
sp Q9PLX8 RL16_CAMJE	6.07600052	16375	50S ribosomal protein L16 OS=Campylobacter jejuni subsp. jejuni serotype O:2 (strain ATCC 700819 / NCTC 11168) OX=192222 GN=rplP PE=3 SV=1

488_S2_data_43_00926	6.072175095	27562	ThiG thiazole biosynthesis protein ThiG 844696:845472 Reverse
488_S2_data_43_00621	5.939664506	17482	PurE phosphoribosylaminoimidazole carboxylase catalytic subunit 552698:553192 Forward
488_S2_data_43_00134	5.830289671	20728	Frr ribosome recycling factor 113868:114425 Reverse
488_S2_data_43_00796	5.817873511	10274	HupB hypothetical protein 720668:720964 Reverse
488_S2_data_43_00081	5.734374678	37446	CfbpA putative iron-uptake ABC transport system,periplasmic iron-binding protein 68425:69429 Reverse
488_S2_data_43_01555	5.663848776	24512	Rrc non-haem iron protein 1430848:1431495 Reverse
sp Q46124 RPOB_CAMJE	5.624640776	155915	DNA-directed RNA polymerase subunit beta OS=Campylobacter jejuni subsp. jejuni serotype O:2 (strain ATCC 700819 / NCTC 11168) OX=192222 GN=rpoB PE=3 SV=2
488_S2_data_43_00898	5.458240414	39716	LivK branched-chain amino-acid ABC transport system,periplasmic binding protein 816673:817782 Reverse
488_S2_data_43_00062	5.421005788	7476.7	RpmE 50S ribosomal protein L31 55633:55833 Reverse
488_S2_data_43_01161	5.410448199	30911	488_S2_data_43_01161 putative periplasmic protein 1075192:1076007 Forward
488_S2_data_43_01589	5.298693876	30941	488_S2_data_43_01589 hypothetical protein 1467907:1468749 Reverse
488_S2_data_43_00457	5.246842492	31208	OorB OORB subunit of 2-oxoglutarate:acceptor oxidoreductase 405780:406625 Forward

488_S2_data_43_00216	5.221903499	120894	CarB carbamoyl-phosphate synthase large chain 182611:185880 Forward
488_S2_data_43_01506	5.166612709	14733	RpsH 30S ribosomal protein S8 1389235:1389630 Reverse
488_S2_data_43_00564	4.996650559	46711	CbrR two-component response regulator 502588:503832 Forward
sp Q9PII8 RL25_CAMJE	4.956231602	19461	50S ribosomal protein L25 OS=Campylobacter jejuni subsp. jejuni serotype O:2 (strain ATCC 700819 / NCTC 11168) OX=192222 GN=rplY PE=3 SV=1
488_S2_data_43_00346	4.928538491	26921	488_S2_data_43_00346 putative oxidoreductase subunit 303966:304694 Forward
488_S2_data_43_01358	4.876997426	59132	488_S2_data_43_01358 putative periplasmic oxidoreductase 1253258:1254799 Forward
488_S2_data_43_00941	4.856558566	49397	GatA Glu-tRNA ^{Gln} amidotransferase subunit A 861047:862408 Reverse
488_S2_data_43_01249	4.826973996	26597	488_S2_data_43_01249 putative periplasmic protein 1158150:1158860 Forward
488_S2_data_43_01275	4.813547386	14646	488_S2_data_43_01275 hypothetical protein 1177925:1178302 Reverse
488_S2_data_43_01346	4.671377604	21266	488_S2_data_43_01346 putative two-component response regulator (SirA-like protein) 1241836:1242408 Reverse
488_S2_data_43_00452	4.615681531	33513	Mdh malate dehydrogenase 401376:402278 Forward

sp Q9PLY3 RL5_CAMJE	4.535371996	20214	50S ribosomal protein L5 OS=Campylobacter jejuni subsp. jejuni serotype O:2 (strain ATCC 700819 / NCTC 11168) OX=192222 GN=rpIE PE=3 SV=1
488_S2_data_43_00440	4.480225841	69596	HtpG hsp90 family heat shock protein 388125:389951 Forward
488_S2_data_43_00458	4.426148389	20123	488_S2_data_43_00458 2-oxoglutarate:acceptor oxidoreductase, gamma subunit 406622:407179 Forward
488_S2_data_43_00677	4.419019794	28661	488_S2_data_43_00677 putative NLPA family lipoprotein 604983:605759 Reverse
488_S2_data_43_01319	4.404392386	15759	RplM ribosomal protein L13 1217610:1218035 Reverse
488_S2_data_43_01050	4.267011935	39525	Tsf elongation factor TS 961960:963033 Reverse
sp P0C635 CHEY_CAMJE	4.109990056	14437	Chemotaxis protein CheY homolog OS=Campylobacter jejuni subsp. jejuni serotype O:2 (strain ATCC 700819 / NCTC 11168) OX=192222 GN=cheY PE=3 SV=1
488_S2_data_43_01315	4.047084904	131358	488_S2_data_43_01315 pyruvate-flavodoxin oxidoreductase 1211841:1215401 Reverse
sp Q0PAS1 CBF2_CAMJE	3.775069351	30518	Putative peptidyl-prolyl cis-trans isomerase Cbf2 OS=Campylobacter jejuni subsp. jejuni serotype O:2 (strain ATCC 700819 / NCTC 11168) OX=192222 GN=cbf2 PE=1 SV=1
sp O69303 EFTU_CAMJE	3.732956858	43594	Elongation factor Tu OS=Campylobacter jejuni subsp. jejuni serotype O:2 (strain ATCC 700819 / NCTC 11168) OX=192222 GN=tuf PE=3 SV=1

488_S2_data_43_01082	3.710650548	27277	488_S2_data_43_01082 putative exporting protein 997275:998000 Reverse
488_S2_data_43_00805	3.701469498	28164	Peb1A aspartate/glutamate-binding ABC transporter protein 728242:729021 Reverse
488_S2_data_43_00008	3.560557653	66481	TypA hypothetical protein 9027:10835 Reverse
488_S2_data_43_00160	3.397064694	34638	488_S2_data_43_00160 putative periplasmic solute binding protein for ABC transport system 137274:138164 Forward
488_S2_data_43_01272	3.344869917	36362	GapA glyceraldehyde 3-phosphate dehydrogenase 1175937:1176935 Reverse
sp Q9PI64 ACP_CAMJE	3.342024009	8597.8	Acyl carrier protein OS=Campylobacter jejuni subsp. jejuni serotype O:2 (strain ATCC 700819 / NCTC 11168) OX=192222 GN=acpP PE=3 SV=1
488_S2_data_43_00351	3.255421519	21066	488_S2_data_43_00351 putative periplasmic protein 308564:309136 Forward
488_S2_data_43_00347	3.252599666	63702	488_S2_data_43_00347 putative GMC oxidoreductase subunit 304696:306417 Forward
488_S2_data_43_00687	3.080810765	104926	NapA periplasmic nitrate reductase 616946:619720 Forward
488_S2_data_43_00899	2.960162315	40042	LivJ branched-chain amino-acid ABC transport system periplasmic binding protein 817804:818919 Reverse
488_S2_data_43_01136	2.924312502	63638	HydB Ni/Fe-hydrogenase large subunit 1049208:1050923 Reverse

488_S2_data_43_01023	2.623387524	10838	488_S2_data_43_01023 putative periplasmic cytochrome C 939577:939879 Forward
----------------------	-------------	-------	---

Table 5.3. Proteins more abundant in secretome of the 488 *tssBC* double mutant than the 488 wild-type strain.

Accession	Max fold change	Mass	Description
488_S2_data_43_01543	2.373566592	91029	FlgE-2 flagellar hook protein 1412549:1415119 Reverse
488_S2_data_43_01304	2.535104264	7157	FlgM hypothetical protein 1203373:1203570 Forward
488_S2_data_43_00349	2.046189201	25961	488_S2_data_43_00349 hypothetical protein 307316:308020 Reverse

5.2.6 Curation of secreted proteins

Searches were performed to determine whether the proteins identified above are genuinely secreted. The amino acid sequences of the proteins of interest were compiled and searched using the databases listed in Table 5.4 to predict protein family (Pfam), subcellular location (PSORTb and SOSUIGramN), presence of transmembrane domains (TMHMM), presence of signal peptides (SignalP), secretion method (SecretomeP and Bastion6), protein structure and domains (Phyre2) and to search for orthologues in other bacteria (BLASTp). A full list of secreted proteins and database predictions are in Appendix 3.

Table 5.4. Databases used for prediction of secreted proteins.

Database	Description	Reference
Pfam	Database of protein families.	(El-Gebali et al., 2019)
PSORTb	Protein subcellular localisation tool.	(Yu et al., 2010)
SOSUIGramN	Protein subcellular localisation tool with a focus on Gram-negative bacteria.	(Imai et al., 2008)
TMHMM	Prediction of transmembrane helices in proteins.	(Moller et al., 2001)
SignalP	Predictor for the presence of signal peptides and cleavage sites.	(Almagro Armenteros et al., 2019)
SecretomeP	Predictor for non-classically secreted proteins.	(Bendtsen et al., 2005)
Bastion6	Predictor for effectors of the T6SS.	(Wang et al., 2018)
Phyre2	Predictor of protein structure and domains.	(Kelley et al., 2015)
BLASTp	An algorithm that allows the comparison of a query sequence against a sequence database.	(Altschul et al., 1990)

5.2.7 Functional enrichment and domain analyses

Gene Ontology (GO) enrichment and Pfam domain analyses were performed to determine which biological, molecular or cellular processes are over- or under-represented in the secreted proteins from Table 5.2. GO enrichment analysis with Blast2GO indicated that translation was the only biological process significantly enriched (Table 5.5). GO enrichment analysis also identified the ribosome as a cellular location that was enriched, however this was not statistically significant; no other molecular or cellular processes were enriched. Pfam enrichment analysis did not identify any domains that were significantly enriched (Table 5.6).

Table 5.5. Gene Ontology (GO) enrichment with Blast2GO of secreted proteins.

Pfam_ID	Sorted_p_values	Gene_groups	Annotation
GO:0006412	7.00E-03	488_S2_data_43_00062, 488_S2_data_43_00134, 488_S2_data_43_00301, 488_S2_data_43_00633, 488_S2_data_43_00941, 488_S2_data_43_01318, 488_S2_data_43_01319, 488_S2_data_43_01404, 488_S2_data_43_01406, 488_S2_data_43_01506, 488_S2_data_43_01511, 488_S2_data_43_01517, 488_S2_data_43_01518, 488_S2_data_43_01722, sp Q0P7T9 RL6_CAMJE, sp Q9PI17 RS7_CAMJE, sp Q9PI35 RL11_CAMJE, sp Q9PII8 RL25_CAMJE, sp Q9PLX0 RS10_CAMJE, sp Q9PLX8 RL16_CAMJE, sp Q9PLX9 RL29_CAMJE,	Translation

		sp Q9PLY3 RL5_CAMJE, sp Q9PM83 RS13_CAMJE	
GO:0005840	4.00E-01	488_S2_data_43_00062, 488_S2_data_43_00301, 488_S2_data_43_00633, 488_S2_data_43_01318, 488_S2_data_43_01319, 488_S2_data_43_01404, 488_S2_data_43_01406, 488_S2_data_43_01506, 488_S2_data_43_01511, 488_S2_data_43_01517, 488_S2_data_43_01518, 488_S2_data_43_01722, sp Q0P7T9 RL6_CAMJE, sp Q9PI17 RS7_CAMJE, sp Q9PI35 RL11_CAMJE, sp Q9PII8 RL25_CAMJE, sp Q9PLX0 RS10_CAMJE, sp Q9PLX8 RL16_CAMJE, sp Q9PLX9 RL29_CAMJE, sp Q9PLY3 RL5_CAMJE, sp Q9PM83 RS13_CAMJE	Ribosome

Gene ontology enrichment analysis performed with Blast2GO. Processes that are functionally enriched are listed with the genes assigned to these functions along with the p-values.

Table 5.6. Pfam domain analysis of secreted proteins.

Pfam_ID	Sorted_p_values	Gene_groups	hmm name
PF01094.28	2.00E-01	488_S2_data_43_00898, 488_S2_data_43_00899	ANF_receptor
PF01558.18	2.00E-01	488_S2_data_43_00458, 488_S2_data_43_01315	POR
PF13433.6	2.00E-01	488_S2_data_43_00898, 488_S2_data_43_00899	Peripla_BP_5
PF13458.6	2.00E-01	488_S2_data_43_00898, 488_S2_data_43_00899	Peripla_BP_6
PF02775.21	5.00E-01	488_S2_data_43_00457, 488_S2_data_43_01315	TPP_enzyme_C
PF00889.19	6.00E-01	488_S2_data_43_01050, 488_S2_data_43_01050	EF_TS
PF03180.14	6.00E-01	488_S2_data_43_00677, 488_S2_data_43_01070	Lipoprotein_9
PF04561.14	6.00E-01	sp Q46124 RPOB_CAMJE, sp Q46124 RPOB_CAMJE	RNA_pol_Rpb2_2
PF00072.24	6.00E-01	sp P0C635 CHEY_CAMJE, 488_S2_data_43_00564, 488_S2_data_43_00564	Response_reg
PF00044.24	7.00E-01	488_S2_data_43_01272	Gp_dh_N
PF00140.20	7.00E-01	488_S2_data_43_00876	Sigma70_r1_2
PF00317.21	7.00E-01	488_S2_data_43_01568	Ribonuc_red_lgN
PF00374.19	7.00E-01	488_S2_data_43_01136	NiFeSe_Hases
PF00394.22	7.00E-01	488_S2_data_43_01358	Cu-oxidase
PF00572.18	7.00E-01	488_S2_data_43_01319	Ribosomal_L13
PF00731.20	7.00E-01	488_S2_data_43_00621	AIRC
PF00732.19	7.00E-01	488_S2_data_43_00347	GMC_oxred_N
PF00990.21	7.00E-01	488_S2_data_43_00564	GGDEF
PF01297.17	7.00E-01	488_S2_data_43_00160	ZnuA
PF02436.18	7.00E-01	488_S2_data_43_00818	PYC_OADA

PF02591.15	7.00E-01	488_S2_data_43_00625	zf-RING_7
PF02800.20	7.00E-01	488_S2_data_43_01272	Gp_dh_C
PF02867.15	7.00E-01	488_S2_data_43_01568	Ribonuc_red_lgC
PF02915.17	7.00E-01	488_S2_data_43_01555	Rubrerythrin
PF03313.15	7.00E-01	488_S2_data_43_01441	SDH_alpha
PF03315.15	7.00E-01	488_S2_data_43_01441	SDH_beta
PF03435.18	7.00E-01	488_S2_data_43_00078	Sacchrp_dh_NADP
PF03477.16	7.00E-01	488_S2_data_43_01568	ATP-cone
PF03724.16	7.00E-01	488_S2_data_43_00836	META
PF04264.13	7.00E-01	488_S2_data_43_00351	YceI
PF04348.13	7.00E-01	488_S2_data_43_00899	LppC
PF04539.16	7.00E-01	488_S2_data_43_00876	Sigma70_r3
PF05199.13	7.00E-01	488_S2_data_43_00347	GMC_oxred_C
PF05638.12	7.00E-01	488_S2_data_43_00598	T6SS_HCP
PF05943.12	7.00E-01	488_S2_data_43_00590	VipB
PF05954.11	7.00E-01	488_S2_data_43_00585	Phage_GPD
PF06397.12	7.00E-01	488_S2_data_43_01555	Desulfoferrod_N
PF06476.12	7.00E-01	488_S2_data_43_01275	DUF1090
PF07731.14	7.00E-01	488_S2_data_43_01358	Cu-oxidase_2
PF07732.15	7.00E-01	488_S2_data_43_01358	Cu-oxidase_3
PF09312.11	7.00E-01	488_S2_data_43_01161	SurA_N
PF10371.9	7.00E-01	488_S2_data_43_01315	EKR
PF12727.7	7.00E-01	488_S2_data_43_00534	PBP_like
PF13174.6	7.00E-01	488_S2_data_43_00189	TPR_6
PF13484.6	7.00E-01	488_S2_data_43_01315	Fer4_16
PF13509.6	7.00E-01	488_S2_data_43_00778	S1_2
PF13618.6	7.00E-01	488_S2_data_43_00346	Gluconate_2-dh3
PF15436.6	7.00E-01	488_S2_data_43_01082	PGBA_N
PF16653.5	7.00E-01	488_S2_data_43_00078	Sacchrp_dh_C
PF00163.19	7.00E-01	488_S2_data_43_01404	Ribosomal_S4
PF00177.21	7.00E-01	sp Q9PI17 RS7_CAMJE	Ribosomal_S7
PF00181.23	7.00E-01	488_S2_data_43_01517	Ribosomal_L2

PF00183.18	7.00E-01	488_S2_data_43_00440	HSP90
PF00216.21	7.00E-01	488_S2_data_43_00796	Bac_DNA_binding
PF00252.18	7.00E-01	sp Q9PLX8 RL16_CAMJE	Ribosomal_L16
PF00276.20	7.00E-01	488_S2_data_43_01518	Ribosomal_L23
PF00281.19	7.00E-01	sp Q9PLY3 RL5_CAMJE	Ribosomal_L5
PF00298.19	7.00E-01	sp Q9PI35 RL11_CAMJE	Ribosomal_L11
PF00338.22	7.00E-01	sp Q9PLX0 RS10_CAMJE	Ribosomal_S10
PF00366.20	7.00E-01	488_S2_data_43_01511	Ribosomal_S17
PF00380.19	7.00E-01	488_S2_data_43_01318	Ribosomal_S9
PF00410.19	7.00E-01	488_S2_data_43_01506	Ribosomal_S8
PF00416.22	7.00E-01	sp Q9PM83 RS13_CAMJE	Ribosomal_S13
PF00466.20	7.00E-01	488_S2_data_43_00410	Ribosomal_L10
PF00550.25	7.00E-01	sp Q9PI64 ACP_CAMJE	PP-binding
PF00562.28	7.00E-01	sp Q46124 RPOB_CAMJE	RNA_pol_Rpb2_6
PF00623.20	7.00E-01	488_S2_data_43_00413	RNA_pol_Rpb1_2
PF00639.21	7.00E-01	sp Q0PAS1 CBF2_CAMJE	Rotamase
PF00673.21	7.00E-01	sp Q9PLY3 RL5_CAMJE	Ribosomal_L5_C
PF00829.21	7.00E-01	488_S2_data_43_01722	Ribosomal_L21p
PF00831.23	7.00E-01	sp Q9PLX9 RL29_CAMJE	Ribosomal_L29
PF00871.17	7.00E-01	488_S2_data_43_01597	Acetate_kinase
PF00885.19	7.00E-01	sp Q9PIB9 RISB_CAMJE	DMRL_synthase
PF01000.26	7.00E-01	sp Q9PM80 RPOA_CAMJE	RNA_pol_A_bac
PF01029.18	7.00E-01	488_S2_data_43_00313	NusB
PF01165.20	7.00E-01	488_S2_data_43_00301	Ribosomal_S21
PF01193.24	7.00E-01	sp Q9PM80 RPOA_CAMJE	RNA_pol_L
PF01196.19	7.00E-01	488_S2_data_43_01406	Ribosomal_L17
PF01197.18	7.00E-01	488_S2_data_43_00062	Ribosomal_L31
PF01206.17	7.00E-01	488_S2_data_43_01346	TusA
PF01245.20	7.00E-01	488_S2_data_43_00633	Ribosomal_L19
PF01386.19	7.00E-01	sp Q9PII8 RL25_CAMJE	Ribosomal_L25p
PF01425.21	7.00E-01	488_S2_data_43_00941	Amidase
PF01765.19	7.00E-01	488_S2_data_43_00134	RRF

PF01855.19	7.00E-01	488_S2_data_43_01315	POR_N
PF02357.19	7.00E-01	sp Q9PI36 NUSG_CAMJE	NusG
PF02548.15	7.00E-01	488_S2_data_43_00231	Pantoate_transf
PF02787.19	7.00E-01	488_S2_data_43_00216	CPSase_L_D3
PF03118.15	7.00E-01	sp Q9PM80 RPOA_CAMJE	RNA_pol_A_CTD
PF03143.17	7.00E-01	sp O69303 EFTU_CAMJE	GTP_EFTU_D3
PF03740.13	7.00E-01	sp Q9PN59 PDXJ_CAMJE	PdxJ
PF03946.14	7.00E-01	sp Q9PI35 RL11_CAMJE	Ribosomal_L11_N
PF03947.18	7.00E-01	488_S2_data_43_01517	Ribosomal_L2_C
PF04542.14	7.00E-01	488_S2_data_43_00876	Sigma70_r2
PF04545.16	7.00E-01	488_S2_data_43_00876	Sigma70_r4
PF04560.20	7.00E-01	sp Q46124 RPOB_CAMJE	RNA_pol_Rpb2_7
PF04563.15	7.00E-01	sp Q46124 RPOB_CAMJE	RNA_pol_Rpb2_1
PF04565.16	7.00E-01	sp Q46124 RPOB_CAMJE	RNA_pol_Rpb2_3
PF04983.18	7.00E-01	488_S2_data_43_00413	RNA_pol_Rpb1_3
PF04997.12	7.00E-01	488_S2_data_43_00413	RNA_pol_Rpb1_1
PF04998.17	7.00E-01	488_S2_data_43_00413	RNA_pol_Rpb1_5
PF05000.17	7.00E-01	488_S2_data_43_00413	RNA_pol_Rpb1_4
PF05690.14	7.00E-01	488_S2_data_43_00926	ThiG
PF08659.10	7.00E-01	488_S2_data_43_00735	KR
PF09084.11	7.00E-01	488_S2_data_43_00805	NMT1
PF10385.9	7.00E-01	sp Q46124 RPOB_CAMJE	RNA_pol_Rpb2_45
PF13343.6	7.00E-01	488_S2_data_43_00081	SBP_bac_6
PF13416.6	7.00E-01	488_S2_data_43_00081	SBP_bac_8
PF13616.6	7.00E-01	sp Q0PAS1 CBF2_CAMJE	Rotamase_3
PF14693.6	7.00E-01	sp Q9PII8 RL25_CAMJE	Ribosomal_TL5_C
PF14698.6	7.00E-01	488_S2_data_43_00816	ASL_C2
PF14789.6	7.00E-01	sp Q0P823 DAPD_CAMJE	THDPS_M
PF14790.6	7.00E-01	sp Q0P823 DAPD_CAMJE	THDPS_N
PF17147.4	7.00E-01	488_S2_data_43_01315	PFOR_II
PF18291.1	7.00E-01	488_S2_data_43_00796	HU-HIG

PF02222.22	7.00E-01	488_S2_data_43_00216, 488_S2_data_43_00216	ATP-grasp
PF03144.25	7.00E-01	sp O69303 EFTU_CAMJE, 488_S2_data_43_00008	GTP_EFTU_D2
PF02786.17	7.00E-01	488_S2_data_43_00216, 488_S2_data_43_00216	CPSase_L_D2
PF00009.27	7.00E-01	sp O69303 EFTU_CAMJE, 488_S2_data_43_00008	GTP_EFTU
PF01370.21	7.00E-01	488_S2_data_43_01631, 488_S2_data_43_00735	Epimerase
PF00056.23	9.00E-01	488_S2_data_43_00452	Ldh_1_N
PF00347.23	9.00E-01	sp Q0P7T9 RL6_CAMJE	Ribosomal_L6
PF00364.22	9.00E-01	488_S2_data_43_00818	Biotin_lipoyl
PF00574.23	9.00E-01	488_S2_data_43_00098	CLP_protease
PF00682.19	9.00E-01	488_S2_data_43_00818	HMGL-like
PF01515.19	9.00E-01	488_S2_data_43_01598	PTA_PTB
PF01568.21	9.00E-01	488_S2_data_43_00687	Molybdop_binding
PF02866.18	9.00E-01	488_S2_data_43_00452	Ldh_1_C
PF04879.16	9.00E-01	488_S2_data_43_00687	Molybdop_Fe4S4
PF12849.7	9.00E-01	488_S2_data_43_00534	PBP_like_2
PF13145.6	9.00E-01	sp Q0PAS1 CBF2_CAMJE	Rotamase_2
PF13589.6	9.00E-01	488_S2_data_43_00440	HATPase_c_3

Domain enrichment analysis performed with Pfam. Genes are grouped and listed based on Pfam domains and arranged based on the p-values.

5.2.8 Multiple VgrGs identified in T6SS-positive *C. jejuni* strains

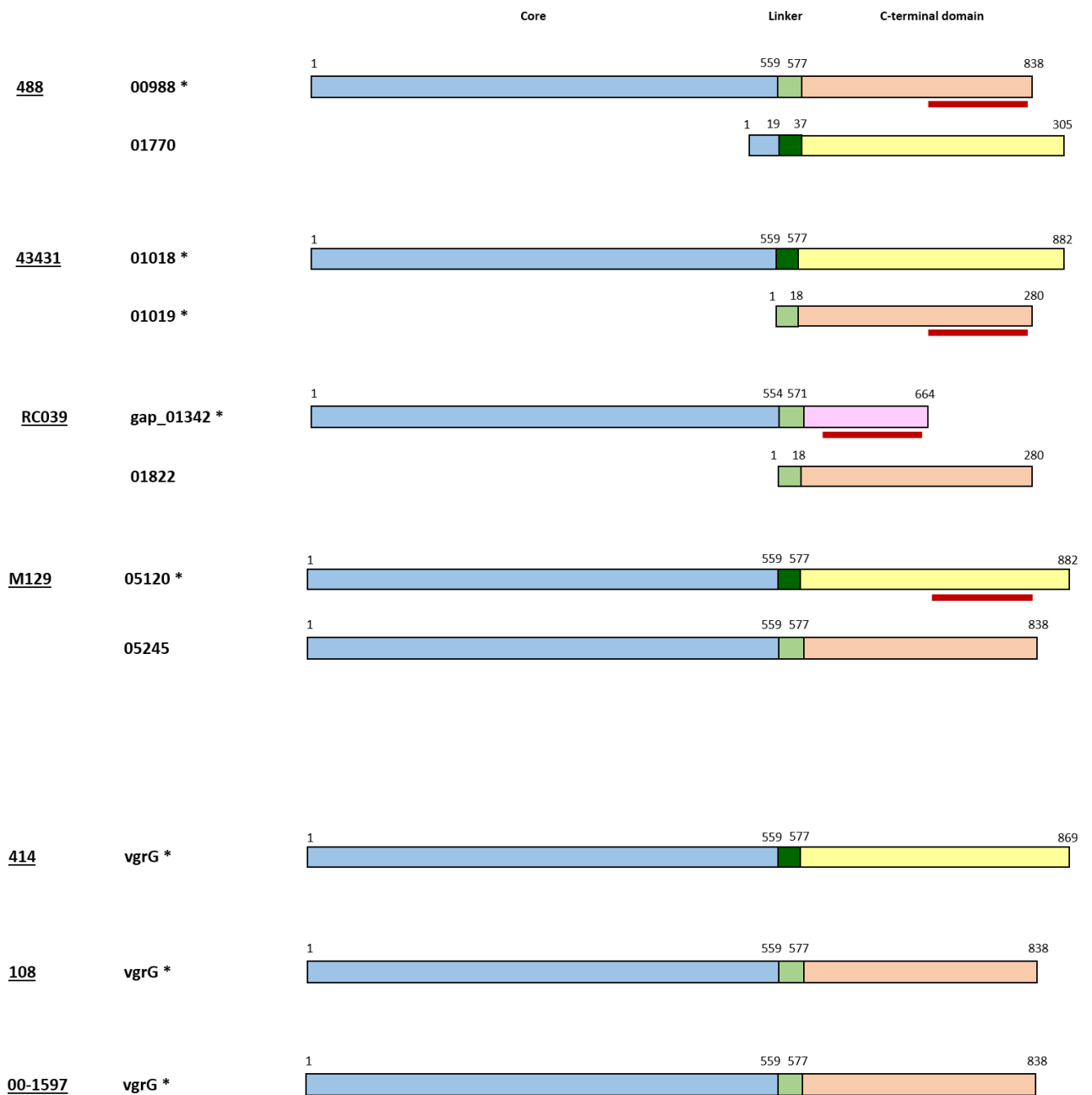
Analysis of the mass spectrometry data identified two putative VgrGs in the *C. jejuni* 488 genome sequence. Comparisons of the amino acid sequences from T6SS-positive *C. jejuni* strains revealed the presence of two VgrGs in the *C. jejuni* 488, 43431, RC039 and M129 strains (Figure 5.4). One VgrG has been identified so far in the *C. jejuni* 414, 108 and 00-1597 strains.

Three distinctive regions were observed in the VgrGs – a core region, a linker region and a C-terminal domain. Two types of VgrGs – ‘full-length’ and ‘truncated’ – were observed. Half of the VgrGs examined were full-length and contained a core region, a linker region and a C-terminal domain (Figure 5.5); VgrGs of this type are mostly associated with a T6SS cluster. Truncated VgrGs with only the linker region and the C-terminal domain (Figure 5.6) were usually located elsewhere on the genome away from a T6SS cluster, except for the *C. jejuni* 43431 strain where the truncated VgrG is directly downstream of the full-length VgrG. The *C. jejuni* M129 strain contains two full-length versions of VgrG with different C-terminal domains.

The core regions in the full-length VgrGs were 554-559 amino acids in length and appeared to be highly conserved. A linker region was consistently present in all full-length and truncated VgrGs. In the full-length VgrGs, the linker region connects the core region with the C-terminal domain. Two variations of the linker region were observed, both of which were approximately 18 amino acids in length.

The C-terminal domains of VgrGs appeared to be variable, with some possessing a gp5 domain. Two main variations were present in the majority of the VgrGs examined and the lengths vary – with one at 261 amino acids and the other at 305 amino acids. One of the VgrGs in the *C. jejuni* RC039 strain contained a shortened C-terminal domain at 93 amino acids.

Effector proteins are frequently located downstream of VgrGs in other bacteria. Some of the VgrGs identified thus far were also characterised by two genes immediately downstream resembling a potential effector-immunity module (Figure 5.7). The putative effector-immunity genes in the *C. jejuni* 488 and 43431 strains were identical in amino acid sequences (Figure 5.8). The putative effector-immunity genes were not found to be present in the genomes of T6SS-negative *C. jejuni* strains or in other bacteria.



* = Part of T6SS cluster

Gene 5

Figure 5.4. Graphical representation of VgrGs identified in *C. jejuni* strains. Sequences of VgrGs identified in *C. jejuni* strains were aligned and compared using Clustal Omega. Blue represents the conserved N-terminal core region. Light green and dark green represent the two variations for the linker region. Yellow, orange and pink represent the variable C-terminal region. An asterisk (*) denotes genes that are a part of the T6SS cluster. A red line represents presence of a gp5 domain. It should be noted that the graphical representation of the genes is an approximation and may not be exact.

Figure 5.5. Multiple sequence alignment of ‘full-length’ VgrGs identified in *C. jejuni* strains. Amino acid sequences of ‘full-length’ VgrGs identified in *C. jejuni* strains were aligned and compared using Clustal Omega. Amino acid residues were colour-coded based on physicochemical properties according to the Clustal scheme. Asterisks (*) denote identical matching of amino acids, dashes (-) denote insertion of amino acids.

```

CLUSTAL O(1.2.4) multiple sequence alignment

488_01770      VIISFLDDDDIDKPYVSGSLYNGATTMPQYNYPRYKREIATNALS YLSVVPAMIDKGLDTL 60
43431_01019   -----LYNGA-----NPSL----- 9
RC039_01822   -----LYNGA-----NPSL----- 9
                *****                               *::

488_01770      KLQENTIDYELSSINNHYLTLANSTVGV DNTNARARNEITLKN DKKEE IYILA QKDYKEE 120
43431_01019   -----VNLPFNDHQ TSLSSKTIGV---NEEGYNELT LSNIKDK EQIYLKA QKDYDEL 58
RC039_01822   -----VNLPFNDHQ TSLSSKTIGV---NEEGYNELT LSNIKDK EQIYLKA QKDYDEL 58
                :*: * :*..*:* * .. *::*:* *****: *****

488_01770      IGNNYEQTIKNNKTSEVGALYTEFITLGHMQNIIGFKNVNVGAEYLENTLLSKDTNVGLS 180
43431_01019   VQHNFTQRIILNDRKDSIVDGIYNERIKKVHTQTIDLAKNVNVGGEYLTNVGLSKDTIVGLS 118
RC039_01822   VQHNFTQRIILNDRKDSIVDGIYNERIKKVHIQTIDLAKNVNVGGEYLTNVGLSKDTIVGLS 118
                :*: * * * * * * * * * * * * * * * * * * * * * * * * * * * * * * * * * *

488_01770      NTLNVGISNEVNIQONHEEKIGNDKRVIINNNLEQDIKNDFIQRIGHNKNETIKGSYVLQ 240
43431_01019   NTLNVGVDNKVRVSKNSSEYVGENKDIEIGANQNTIIHKDEIRNVKGNKKEVVEGHYGIN 178
RC039_01822   NTLNVGVDNKVRVAKNSHEFVGENKDIEIGANQNTIIHKDEIRNVKGNKKEVVEGHYGIN 178
                *****: * * * * * * * * * * * * * * * * * * * * * * * * * * *

488_01770      TNQSIKFHSKKDLSIETNEYFKAEADDISFKAKKNCSTIADNVNIMANQESVLTAQKQI 300
43431_01019   VSDKMQVLSEKEMDYKSKDNILFTSNESIGFESDKNTSMVADNITTYAKTIHELKADSEA 238
RC039_01822   VSDKMQVLSEKEMDYKSKDNILFTSNESIGFESDKNTSMVADNITTYAKTIHELKADSEA 238
                ..::: * * * * * : : : : * * * * * * * * * * * * * * * * * * * *

488_01770      VSRVGNITITQTKDKIILQVGTIQVIIDSKGLRVKGGDLRAD 342
43431_01019   TIQVGETIINAKPDCVLIKAGGVEVIIDSNGLVVRGGELKAE 280
RC039_01822   TIQVGETIINAKPDCVLIKAGGVEVIIDSNGLVVRGGELKAE 280
                . : * * * * * . * * * * * . * * * * * * * * * * * * * * * *

```

Figure 5.6. Multiple sequence alignment of ‘truncated’ VgrGs identified in *C. jejuni* strains. Sequences of ‘truncated’ VgrGs identified in *C. jejuni* strains were aligned and compared using Clustal Omega. Amino acid residues were colour-coded based on physicochemical properties according to the Clustal scheme. Asterisks (*) denote identical matching of amino acids, dashes (-) denote insertion of amino acids.

C. jejuni 488



C. jejuni 43431



Figure 5.7. Putative effector-immunity modules identified in the *C. jejuni* 488 and 43431 strains. The *vgrG* gene and downstream genes were visualised in the genomes of *C. jejuni* 488 and 43431 strains using the Artemis genome browser. T6SS genes were annotated in purple. The genes forming putative effector-immunity modules were indicated by a red box.

A)

```
CLUSTAL O(1.2.4) multiple sequence alignment

488_00989      MNKPFYKLRFYIPCGVLVALIIFTSLTYHFLQRPLELIFWDRYYYYEKEYQNAKDMYKLF      60
43431_01020   MNKPFYKLRFYIPCGVLVALIIFTSLTYHFLQRPLELIFWDRYYYYEKEYQNAKDMYKLF      60
*****

488_00989      KSNEEFKKVFKEQNLNEELKTNQKELLNYMHHFKRDSNFMQILGLDNAYLKALRDKTSI      120
43431_01020   KSNEEFKKVFKEQNLNEELKTNQKELLNYMHHFKRDSNFMQILGLDNAYLKALRDKTSI      120
*****

488_00989      FGRKSENNLNLYFYLASNSTNLDEMNNFISIIDKYIIFINKIDTLPDTYTLMKIAFNADY      180
43431_01020   FGRKSENNLNLYFYLASNSTNLDEMNNFISIIDKYIIFINKIDTLPDTYTLMKIAFNADY      180
*****

488_00989      FLFNLVPFASSLDKNFICSIQKEQLLENMINSYERMDLLYKTKLKTEIQEMIYPAIYAT      240
43431_01020   FLFNLVPFASSLDKNFICSIQKEQLLENMINSYERMDLLYKTKLKTEIQEMIYPAIYAT      240
*****

488_00989      KKLNHFIDIAKGRNLNACGK      259
43431_01020   KKLNHFIDIAKGRNLNACGK      259
*****
```

B)

```
CLUSTAL O(1.2.4) multiple sequence alignment

488_00990      MHVENNLSPEDRQGIENYLIILNTISFLGDLNIKYNHNNAKIKNYSSGYCKYYCKIA      57
43431_01021   MHVENNLSPEDRQGIENYLIILNTISFLGDLNIKYNHNVVKIKNYSSGYCKYYCKIA      57
*****
```

Figure 5.8. Multiple sequence alignment of putative effector-immunity modules

identified in *C. jejuni* 488 and 43431 strains. A) Amino acid sequences of the putative effector proteins from *C. jejuni* 488 and 43431 strains were aligned and compared using Clustal Omega. B) Amino acid sequences of putative immunity proteins from *C. jejuni* 488 and 43431 strains were aligned and compared using Clustal Omega. Amino acid residues were colour-coded based on physicochemical properties according to the Clustal scheme. Asterisks (*) denote identical matching of amino acids, dashes (-) denote insertion of amino acids.

5.3 DISCUSSION

Whole genome sequencing

The *C. jejuni* T6SS is a functional secretory mechanism that appears distinct from the well-elucidated *P. aeruginosa* and *V. cholerae* T6SS model systems. Whole genome sequencing of a novel 488 strain and the T6SS-positive 43431 strain revealed a single T6SS cluster containing one copy of the *tssD* gene that encodes the needle-like tube of the T6SS, but also the absence of the *tssH/clpV* gene which encodes the ATPase that breaks down and recycles the TssBC contractile sheath. This is in contrast to the T6SS model systems of *P. aeruginosa* and *V. cholerae* where multiple T6SS clusters are present with differing functions. The absence of a TssH orthologue had previously been observed in other *C. jejuni* strains in two published studies (Lertpiriyapong et al., 2012, Bleumink-Pluym et al., 2013). *Burkholderia* species, *Helicobacter hepaticus*, *Francisella tularensis* and *Salmonella enterica* also appear to lack a TssH component. Despite the absence of TssH, the presence of a functional T6SS in all these organisms including *C. jejuni* suggests there must be alternate mechanisms for contractile sheath recycling. A study demonstrated in *V. cholerae* that whilst TssH is not essential, it is important in increasing the efficiency of the T6SS in inter-bacterial competition assays (Bachmann et al., 2015).

Recent studies examining the T6SS in *Francisella tularensis* and *Klebsiella pneumoniae* indicate that another member of the Clp protein family ClpB, which is an AAA⁺ ATPase involved in general protein degradation, can play a role instead of TssH/ClpV during the disassembly of contracted sheaths (Brodmann et al., 2017, Barbosa and Lery, 2019).

Intriguingly, the mass spectrometry analysis presented in this chapter identified yet another member of the Clp protein family (ClpP) in the secretome of the 488 wild-type strain, raising the possibility that contractile sheath recycling is performed by a different ATPase in *C. jejuni*. ClpP is involved in the degradation of misfolded and regulatory proteins and also has a role in biofilm formation; in addition, ClpP is required for growth of *C. jejuni* at 42°C (Cohn et al., 2007). A recent study by Lin et al. demonstrated that ClpP is important in enhancing susceptibility to T6SS killing in *A. tumefaciens* (Lin et al., 2020). Further work is required to determine whether ClpP is associated with the *C. jejuni* T6SS and plays a role in contractile sheath recycling.

Comparison of the *C. jejuni* strains sequenced in this study with previously published sequences of other *C. jejuni* strains as well as other *Campylobacter* species revealed a T6SS cluster that is very closely conserved with all core genes present in the same arrangement. *C. jejuni* 488 (human isolate from Brazil), 43431 (human isolate from Canada), 108 (human isolate from the United States), RC039 (chicken isolate from the United Kingdom) and even *C. coli* RM2228 (chicken isolate from the United States) all share the same conserved T6SS cluster. Only *C. jejuni* 414 had a different gene arrangement in the T6SS cluster. 414 is considered an environmental strain isolated from a wild bank vole in the United Kingdom (Williams et al., 2010). It is possible that agricultural intensification practices which readily facilitate passing of strains between chickens and humans could lead to these strains to share more of a conserved T6SS compared to the 414 environmental strain.

Bioinformatic searches

Bioinformatic searches in *C. jejuni* 488 and 43431 strains did not identify any known T6SS effector proteins found in other bacteria. One possibility for this is that the sequences of these effector proteins differ too much between bacteria from different genera. For example, the amino acid sequence for Hcp1 of *P. aeruginosa* PAO1 has a very low degree of similarity with the TssD sequences from any of the *C. jejuni* strains; however, we know that the TssD/Hcp component is present in both the *C. jejuni* 488 and 43431 strains. In addition, the diversity of T6SS effectors is vast and different bacteria can possess different types of T6SS effectors; therefore it is possible that none of these known effectors, apart from structural components such as TssD and VgrG, are present in *C. jejuni*.

Secretome profile comparison

Prior to mass spectrometry analysis, the secretome profiles of the 488 wild-type strain and different *tss* mutants were examined to determine if there were differences in proteins secreted between strains. Comparison of the secretome profiles revealed a number of differences between strains. Results presented in Chapter 4 demonstrated that TssD is secreted from both the 488 *tssB* mutant and the 488 *tssC* mutant though at a reduced amount, and this was further confirmed by the secretome profiles. The differences in secretome profiles between the 488 *tssB* mutant and 488 *tssC* mutant suggest mutagenesis of individual contractile sheath components impact the ability of the *C. jejuni* T6SS to secrete proteins in a

different manner; whether the two contractile sheath components have differing roles in the functioning of the T6SS should be examined. The 488 *tssBC* double mutant was subsequently chosen for comparison against the 488 wild-type strain for mass spectrometry analysis as even though TssD was still present in the whole cell fractions, mutagenesis of both components of the contractile sheath resulted in complete inactivation of the T6SS and inability of the 488 *tssBC* mutant to secrete TssD as also shown in Chapter 4.

Mass spectrometry analysis

Mass spectrometry analysis revealed an abundance of T6SS components such as TssD and VgrG in the secretome of the 488 wild-type strain. This provided further confirmation to support the findings by Lertpiriyapong et al., Bleumink-Pluym et al. and in Chapter 4 of this study that TssD is secreted into the supernatant of T6SS-positive *C. jejuni* strains (Lertpiriyapong et al., 2012, Bleumink-Pluym et al., 2013). This is also the first time that secretion of VgrG by the *C. jejuni* T6SS has been demonstrated after attempts to investigate secretion of VgrG using a VgrG antibody were unsuccessful (see Chapter 4). Interestingly, the contractile sheath component TssC was also found in the secretome; however, the other contractile sheath component TssB was not. The secretion of TssC into the *C. jejuni* supernatant requires further investigation. The presence of TssC in the secretome could potentially be due to TssC associating more strongly with TssD than TssB, allowing TssC to be secreted along with TssD.

A Proline-Alanine-Alanine-Arginine (PAAR) protein that forms the tip of the VgrG needle was not identified in the secretome of the 488 wild-type strain. Multiple copies of PAAR have been found to be present in bacteria such as *P. aeruginosa*. However, PAAR has yet to be identified in *C. jejuni*, either by mass spectrometry or by whole genome sequencing. As PAAR is a very small protein (approximately 9-10 kDa), it may be difficult to detect via mass spectrometry-based analyses.

Phosphate acetyltransferase (Pta) and acetate kinase (AckA) were both found to be more abundant in the secretome of the 488 wild-type strain than the 488 *tssBC* contractile sheath mutant. These two proteins along with Ac-CoA synthase (Acs) are crucial in the acetogenesis pathway, which is also known as the ‘acetate switch’ (Luethy et al., 2017). In the acetogenesis pathway, pyruvate is converted to acetyl-coenzyme A (Ac-CoA) by pyruvate oxidoreductase, Ac-CoA is converted to acetyl-phosphate (Ac-P) by Pta, and Ac-P is

converted to acetate and ATP by AckA. Acs converts acetate to Ac-CoA. The acetogenesis pathway influences signal transduction pathways and metabolic pathways in *C. jejuni* and mutagenesis of the genes encoding Pta and AckA results in attenuated commensal colonisation of the chicken caeca (Luethy et al., 2017).

Intriguingly, there may be a potential link between the components of the acetogenesis pathway and the regulation of oxidative stress. Ac-P has been reported to be capable of donating a phosphoryl group to two-component response regulators (Wolfe, 2010). CosR is an oxidative stress response regulator in *C. jejuni*, however thus far no histidine kinase or phosphodonor has been identified to phosphorylate CosR. Hwang et al. hypothesised that Ac-P, which is converted from Ac-CoA by Pta and converted to acetate and ATP by AckA, may be involved in phosphorylating CosR (Hwang et al., 2011). In Chapter 4 of this study, the *C. jejuni* T6SS was demonstrated to be associated with the oxidative stress response. Whether the increased abundance of Pta and AckA in the secretome of the 488 wild-type strain is involved in the enhanced oxidative stress response or whether this is due to the phosphorylation of CosR remains to be investigated.

It is also important to note that the list of secreted proteins generated from mass spectrometry analysis may not be exhaustive. The *C. jejuni* strains were grown in Brucella broth at 37°C under microaerobic conditions with shaking at 75 rpm. As such the list of secreted proteins is therefore a snapshot of the secretome under these specific conditions. It is very likely that the secretome would be different if the bacteria were cultured under different conditions, for example in minimal media, at 42°C, or with the addition of bile salts.

Functional enrichment analysis

Gene ontology enrichment and Pfam domain enrichment analyses were performed to identify which functions were enriched amongst the secreted proteins. For functional enrichment analysis, a list of secreted proteins was curated. Searches were performed on prediction databases to determine the protein family, subcellular location, presence of transmembrane domains, presence of signal peptides, secretion method, protein structure and domains, and to search for orthologues in other bacteria.

It is worth noting that the curated list includes all secreted proteins that are more abundant in the 488 wild-type strain than the 488 *tssBC* contractile sheath double mutant, including

proteins that are secreted by the T6SS, the Sec- or Tat-systems, or by other secretory methods. We attempted to identify proteins that are only secreted by the T6SS using prediction results generated from the databases mentioned above, however this could not be reliably determined. Thus far, no signal peptide has been identified in T6SS-secreted proteins, so it is likely that proteins do not require a signal peptide to be secreted directly by the T6SS. Therefore it is recommended that proteins are checked using both SignalP and SecretomeP – for non-classically secreted proteins the SecP score should be greater than 0.5 on SecretomeP, but there is also the need to ensure the proteins do not contain a signal peptide by using SignalP. However, this was further complicated by recent findings that an effector with a signal peptide was demonstrated to be secreted by the T6SS (Han et al., 2019). Therefore proteins with signal peptides should not be ruled out as secreted by the T6SS.

GO enrichment analysis indicated that translation was the only biological process significantly enriched, with no other processes determined to be enriched. Pfam enrichment analysis did not identify any domains that were significantly enriched. The lack of processes identified may be due to the small number of secreted proteins available to analyse and also the lack of genome annotation for the 488 wild-type strain.

VgrGs

A trimer of VgrG proteins form the puncturing device located at the end of the TssD needle-like tube, further sharpened by a PAAR tip (Cianfanelli et al., 2016a). VgrGs are similar to the gp27-gp5 structures of the T4 bacteriophage and also consist of two domains; the N-terminal domain is typically highly conserved whilst the C-terminal region can be highly variable and exist in either short or extended configurations (Hachani et al., 2014). The presence of multiple VgrGs has been identified in the T6SS of *E. coli*, *S. marcescens*, *A. tumefaciens*, and many others. Some of these VgrGs have been shown to be functionally redundant (Lin et al., 2019, Santos et al., 2019).

This study was the first to examine the VgrG of the *C. jejuni* T6SS, and through proteomic and bioinformatic analyses multiple VgrGs were identified in *C. jejuni* strains. The amino acid sequences of the VgrGs were compared and interestingly, two different types of VgrGs were observed – a ‘full-length’ version with a highly conserved N-terminal core region, a linker region and a C-terminal region, and also a ‘truncated’ version with only the linker region and a C-terminal region. *C. jejuni* 488, 43431 and RC039 strains all appeared to each

possess a full-length VgrG and a truncated VgrG. *C. jejuni* M129 strain possesses two full-length VgrGs and no truncated VgrG. The full-length VgrGs are more likely to be associated with the T6SS cluster, whilst the truncated VgrGs are more likely to be located elsewhere on the genome. A gp5 domain was identified in the variable C-terminal regions of some of the VgrGs. PAAR has been shown to interact with the gp5 domain in other bacteria but PAAR is not present or has not yet been identified in *C. jejuni*.

Two main variations in the C-terminal regions were observed, however there appeared to be no correlation between which variation is more likely to be associated with the full-length or the truncated VgrG. The significance of this variation and whether VgrGs possessing different C-terminal regions have differing roles remains to be investigated. In *P. aeruginosa*, recombination can result in modulation at the 3' end of the *vgrG* genes, leading to exchange of the C-terminal domain (Wood et al., 2019). Bondage et al. observed that the C-terminal variable region of the VgrGs in *Agrobacterium tumefaciens* determines the type of effector that is delivered and is also important in binding with adaptor/chaperone complexes (Bondage et al., 2016).

Further work is required to examine whether these VgrGs are functionally redundant or whether they have specialised roles. The functions of the three distinctive regions should also be investigated. A recent study by Lopez et al. demonstrated that due to a single amino acid mutation in the C-terminus, the VgrG1 in a clinical isolate of *Acinetobacter baumannii* becomes an inhibitor for the T6SS (Lopez et al., 2020). A functional T6SS does not contribute to virulence in *A. baumannii*, and the authors speculated that a mechanism to silence the T6SS may be beneficial due to the high energy expenditure required to maintain a functional T6SS.

Genes encoding putative effectors are frequently found to be associated with *vgrGs* that are located away from the T6SS cluster (De Maayer et al., 2011, Barret et al., 2011). In this study, two genes resembling a potential effector-immunity pair was observed downstream of some of the VgrGs. Interestingly, the potential effector-immunity gene pairing was located downstream of VgrGs containing the 261 amino acid C-terminal domain, regardless of whether the VgrGs were a part of or located away from the T6SS cluster. This suggests that different VgrG types, or more specifically different C-terminal domains, may be associated with the delivery of different effector proteins. Further work should compare the VgrGs and potential effector-immunity modules and analyse their prevalence amongst T6SS-positive *C.*

jejuni and *C. coli* strains with available whole genome sequences. The roles of the VgrGs and potential effector-immunity modules should also be examined.

5.4 CONCLUSION

Comparisons of the whole genome sequences of the *C. jejuni* 488 and 43431 strains with previously sequenced *C. jejuni* strains revealed a single highly conserved T6SS cluster shared between strains isolated from humans and chickens. Bioinformatics searches did not identify known T6SS effector proteins from other bacteria in *C. jejuni*. This study was the first to compare the secretome of a T6SS-positive *C. jejuni* strain with a contractile sheath mutant. Proteomic and bioinformatic analyses revealed for the first time that multiple VgrGs are present in T6SS-positive *C. jejuni* strains, and a potential effector-immunity module was also identified.

CHAPTER SIX: Final Discussion

6.1 SUMMARY

The increasing prevalence of the T6SS in recently isolated *C. jejuni* strains emphasises the need to understand the role of the T6SS in *C. jejuni* and to develop intervention strategies to combat the increase of T6SS-positive *C. jejuni* strains, especially in the poultry industry. This study aimed to examine the role of the T6SS in *C. jejuni* interactions with host and bacterial cells.

Firstly, a number of *C. jejuni* strains harbouring a complete T6SS locus were identified and a novel 488 wild-type strain was selected to be the focus of this study. Defined isogenic mutants for genes encoding the contractile sheath components TssB and TssC and the needle structure TssD were constructed in the 488 wild-type strain. Phenotypic analysis of the 488 wild-type strain and isogenic mutants was then performed, and results indicated that the T6SS is involved in the ability of *C. jejuni* to form biofilms. Whether the *C. jejuni* T6SS played a role in bacterial competition was also examined; however, the *C. jejuni* T6SS does not appear to be involved in either inter- or intra-bacterial competition under the conditions investigated in this study.

The secretion of TssD into the culture supernatant is an indication of a functional T6SS and this was demonstrated for the 488 wild-type strain. Surprisingly, inactivation of either one of the two contractile sheath components did not result in a completely non-functional T6SS in *C. jejuni*; this contradicts previous findings on the contractile sheath of the *V. cholerae* T6SS and suggests that the contractile sheath machinery in *C. jejuni* may differ from that of other bacteria. Results from this study also suggest that T6SS expression in *C. jejuni* is mediated by a concentration gradient of sodium deoxycholate. The presence of the T6SS was demonstrated to enhance the oxidative stress response in *C. jejuni*. The role of the T6SS in *C. jejuni* was further characterised during interactions with host cells, with *in vitro* and *in vivo* characterisation experiments in biologically relevant models. The results indicate that the ability of *C. jejuni* to colonise chickens is enhanced by the presence of the T6SS

Comparisons of the whole genome sequences of *C. jejuni* strains revealed a single highly conserved T6SS cluster shared between strains isolated from humans and chickens.

Bioinformatic searches did not identify known T6SS effector proteins from other bacteria in *C. jejuni*. Proteomic and bioinformatic analyses revealed for the first time that multiple

VgrGs are present in *C. jejuni* strains and a potential effector-immunity module was also identified.

6.2 FUTURE WORK

Prevalence of the C. jejuni T6SS

Recent studies demonstrating an increasing prevalence of T6SS-positive *C. jejuni* strains primarily focused on countries within Europe; a relatively small number of samples were collected from Asia in one study and the prevalence of T6SS in *C. jejuni* isolates remains unknown in the other continents. Further studies incorporating larger sample sizes from more regions from around the world are required to determine whether the increased prevalence forms part of a globally occurring pattern or is only due to a regional shift in Europe.

C. jejuni T6SS and competition with other microorganisms

The *C. jejuni* T6SS has not been shown to be involved in inter- or intra-bacterial competition thus far. It is unknown whether the lack of observable bacterial killing is due to experimental conditions or due to the complete lack of involvement of the *C. jejuni* T6SS with bacterial competition. Further work should examine bacterial competition under other conditions, examples of which include different temperatures, different atmospheric conditions, different media and growth supplements, the removal of polysaccharide capsules from both predator and prey strains, or different predator-to-prey ratios. The ability of *C. jejuni* to kill different prey should also be explored, with potential prey such as commensal gut bacteria or fungi. T6SS killing should also be examined *in vivo* in a chicken or amoeba model.

VgrGs and putative effector-immunity module

In this study, multiple VgrGs were identified in the *C. jejuni* strains studied. Further studies should examine the prevalence of the different variations and investigate whether this is significant by mutagenesis of the VgrGs and different regions within the VgrGs identified thus far. Whether these VgrGs are functionally redundant or have specialised roles should also be examined. A putative effector-immunity module was identified in the *C. jejuni* strains in this study and the role of the putative effector should also be investigated.

Identifying T6SS effectors using comparative genomics and screening platform

A comprehensive search for T6SS effectors in *C. jejuni* could incorporate diverse bioinformatic, proteomic and genomic approaches. In this study, bioinformatic and proteomic approaches were used to identify putative effectors of the *C. jejuni* T6SS. An alternative approach to identifying putative T6SS effectors is by comparative genomics. Comparative genomics was utilised by Fridman et al. to identify T6SS effector candidates in *Vibrio haemolyticus* (Fridman et al., 2020). A similar methodology could be applied to *C. jejuni*, with whole genome sequences of T6SS-positive strains compared against the sequences of T6SS-negative strains to detect genes of interest that resemble effector-immunity modules. The lack of a successful bacterial competition model has been an obstacle hindering *C. jejuni* T6SS research thus far, so the surrogate screening platform proposed by Fridman et al. could potentially provide a solution and assist in identifying effector-immunity modules.

C. jejuni T6SS and metal acquisition

The T6SS has been associated with metal acquisition, allowing bacteria possessing the T6SS to gain a fitness advantage in the competition for essential micronutrients within a host (Chen et al., 2019). Whether the *C. jejuni* T6SS plays a role in metal acquisition remains to be investigated. Interestingly, results from this study indicate that specific proteins associated with iron uptake, zinc uptake or copper efflux are more abundant in the secretome of the *C. jejuni* 488 wild-type strain than the 488 *tssBC* contractile sheath mutant. Whether these proteins are associated with the T6SS and involved in competition for metal ions within a host should be investigated. Inductively coupled plasma mass spectrometry (ICP-MS) should be utilised to examine metal content within bacterial cells. Comparison of the levels of iron, copper, manganese and zinc ions in a *C. jejuni* wild-type strain and a T6SS mutant by ICP-MS would provide a preliminary indication as to whether the *C. jejuni* T6SS is involved in the acquisition of certain metals.

C. jejuni T6SS and survival in environment

The T6SS is implicated in environmental survival and persistence; in *P. aeruginosa* and *V. cholerae*, the T6SS is associated with biofilm formation which increases the ability of the bacteria to survive in otherwise hostile environments (Chen et al., 2015, Joshi et al., 2017). The T6SS appears to be associated with enhanced biofilm formation in *C. jejuni*, but further work will be required to identify the T6SS effectors involved. Whether the enhanced ability to form biofilms will improve survival of T6SS-positive *C. jejuni* strains in the environment

will also need to be examined. Environmental changes or signals can modulate the T6SS; for example, the expression of the T6SS-2 of *B. pseudomallei* is increased during nutrient depletion (Losada et al., 2018). Studies have thus far focused on observing the *C. jejuni* T6SS under optimal growth conditions, so future work should examine the role of the T6SS when *C. jejuni* is grown in minimal media or under both aerobic and anaerobic conditions.

Visualising the C. jejuni T6SS

The T6SS has been visualised via negative electron microscopy in *P. aeruginosa* (Lossi et al., 2013) and by fluorescence microscopy in *S. marcescens* and *V. cholerae* (Gerc et al., 2015, Vettiger et al., 2017). Structures and dynamics of specific T6SS components and complexes such as the contractile sheath have also been examined in depth in enteroaggregative *E. coli* and *V. cholerae* using cryogenic electron microscopy (cryo-EM) (Rapisarda et al., 2019, Nazarov et al., 2018). In contrast, the *C. jejuni* T6SS has not been visualised and the structure has yet to be elucidated. Future work should involve examining the structure of *C. jejuni* T6SS components using cryo-EM and visualising the *C. jejuni* T6SS by fluorescence microscopy. Gaining an understanding of the structure of the contractile sheath and how the components interact may help provide an explanation as to why the individual sheath components appear to be interchangeable or be able to compensate for the absence of the other component. With fluorescence microscopy, knowledge of the role and function of the *C. jejuni* T6SS could be broadened by observing localisation and firing dynamics of the T6SS within *C. jejuni* and in interaction with other bacterial or host cells.

REFERENCES

- AGNETTI, J., SETH-SMITH, H. M. B., URSICH, S., REIST, J., BASLER, M., NICKEL, C., BASSETTI, S., RITZ, N., TSCHUDIN-SUTTER, S. & EGLI, A. 2019. Clinical impact of the type VI secretion system on virulence of *Campylobacter* species during infection. *BMC Infect Dis*, 19, 237.
- ALCOFORADO DINIZ, J., HOLLMANN, B. & COULTHURST, S. J. 2017. Quantitative Determination of Anti-bacterial Activity During Bacterial Co-culture. *Methods Mol Biol*, 1615, 517-524.
- ALMAGRO ARMENTEROS, J. J., TSIRIGOS, K. D., SONDERBY, C. K., PETERSEN, T. N., WINTHER, O., BRUNAK, S., VON HEIJNE, G. & NIELSEN, H. 2019. SignalP 5.0 improves signal peptide predictions using deep neural networks. *Nat Biotechnol*, 37, 420-423.
- ALTSCHUL, S. F., GISH, W., MILLER, W., MYERS, E. W. & LIPMAN, D. J. 1990. Basic local alignment search tool. *J Mol Biol*, 215, 403-10.
- ANG, C. W., DE KLERK, M. A., ENDTZ, H. P., JACOBS, B. C., LAMAN, J. D., VAN DER MECHE, F. G. & VAN DOORN, P. A. 2001. Guillain-Barre syndrome- and Miller Fisher syndrome-associated *Campylobacter jejuni* lipopolysaccharides induce anti-GM1 and anti-GQ1b Antibodies in rabbits. *Infect Immun*, 69, 2462-9.
- ASSEFA, S., KEANE, T. M., OTTO, T. D., NEWBOLD, C. & BERRIMAN, M. 2009. ABACAS: algorithm-based automatic contiguation of assembled sequences. *Bioinformatics*, 25, 1968-9.
- BACHMANN, V., KOSTIUK, B., UNTERWEGER, D., DIAZ-SATIZABAL, L., OGG, S. & PUKATZKI, S. 2015. Bile Salts Modulate the Mucin-Activated Type VI Secretion System of Pandemic *Vibrio cholerae*. *PLoS Negl Trop Dis*, 9, e0004031.
- BACON, D. J., ALM, R. A., BURR, D. H., HU, L., KOPECKO, D. J., EWING, C. P., TRUST, T. J. & GUERRY, P. 2000. Involvement of a plasmid in virulence of *Campylobacter jejuni* 81-176. *Infect Immun*, 68, 4384-90.
- BACON, D. J., SZYMANSKI, C. M., BURR, D. H., SILVER, R. P., ALM, R. A. & GUERRY, P. 2001. A phase-variable capsule is involved in virulence of *Campylobacter jejuni* 81-176. *Mol Microbiol*, 40, 769-77.
- BARBOSA, V. A. A. & LERY, L. M. S. 2019. Insights into *Klebsiella pneumoniae* type VI secretion system transcriptional regulation. *BMC Genomics*, 20, 506.
- BARRET, M., EGAN, F., FARGIER, E., MORRISSEY, J. P. & O'GARA, F. 2011. Genomic analysis of the type VI secretion systems in *Pseudomonas* spp.: novel clusters and putative effectors uncovered. *Microbiology*, 157, 1726-1739.
- BASLER, M., HO, B. T. & MEKALANOS, J. J. 2013. Tit-for-tat: type VI secretion system counterattack during bacterial cell-cell interactions. *Cell*, 152, 884-94.
- BASLER, M. & MEKALANOS, J. J. 2012. Type 6 secretion dynamics within and between bacterial cells. *Science*, 337, 815.

- BASLER, M., PILHOFER, M., HENDERSON, G. P., JENSEN, G. J. & MEKALANOS, J. J. 2012. Type VI secretion requires a dynamic contractile phage tail-like structure. *Nature*, 483, 182-6.
- BENDTSEN, J. D., KIEMER, L., FAUSBOLL, A. & BRUNAK, S. 2005. Non-classical protein secretion in bacteria. *BMC Microbiol*, 5, 58.
- BLACK, R. E., LEVINE, M. M., CLEMENTS, M. L., HUGHES, T. P. & BLASER, M. J. 1988. Experimental *Campylobacter jejuni* infection in humans. *J Infect Dis*, 157, 472-9.
- BLEUMINK-PLUYM, N. M., VAN ALPHEN, L. B., BOUWMAN, L. I., WOSTEN, M. M. & VAN PUTTEN, J. P. 2013. Identification of a functional type VI secretion system in *Campylobacter jejuni* conferring capsule polysaccharide sensitive cytotoxicity. *PLoS Pathog*, 9, e1003393.
- BOESZE-BATTAGLIA, K., BROWN, A., WALKER, L., BESACK, D., ZEKAVAT, A., WRENN, S., KRUMMENACHER, C. & SHENKER, B. J. 2009. Cytolethal distending toxin-induced cell cycle arrest of lymphocytes is dependent upon recognition and binding to cholesterol. *J Biol Chem*, 284, 10650-8.
- BOLGER, A. M., LOHSE, M. & USADEL, B. 2014. Trimmomatic: a flexible trimmer for Illumina sequence data. *Bioinformatics*, 30, 2114-20.
- BOLTON, D. J. 2015. *Campylobacter* virulence and survival factors. *Food Microbiol*, 48, 99-108.
- BONDAGE, D. D., LIN, J. S., MA, L. S., KUO, C. H. & LAI, E. M. 2016. VgrG C terminus confers the type VI effector transport specificity and is required for binding with PAAR and adaptor-effector complex. *Proc Natl Acad Sci U S A*, 113, E3931-40.
- BORGEAUD, S., METZGER, L. C., SCRIGNARI, T. & BLOKESCH, M. 2015. The type VI secretion system of *Vibrio cholerae* fosters horizontal gene transfer. *Science*, 347, 63-7.
- BRACKMANN, M., WANG, J. & BASLER, M. 2018. Type VI secretion system sheath inter-subunit interactions modulate its contraction. *EMBO Rep*, 19, 225-233.
- BREN, A. & EISENBACH, M. 2000. How signals are heard during bacterial chemotaxis: protein-protein interactions in sensory signal propagation. *J Bacteriol*, 182, 6865-73.
- BRODMANN, M., DREIER, R. F., BROZ, P. & BASLER, M. 2017. *Francisella* requires dynamic type VI secretion system and ClpB to deliver effectors for phagosomal escape. *Nat Commun*, 8, 15853.
- BYRNE, C. M., CLYNE, M. & BOURKE, B. 2007. *Campylobacter jejuni* adhere to and invade chicken intestinal epithelial cells in vitro. *Microbiology*, 153, 561-9.
- CAMACHO, C., COULOURIS, G., AVAGYAN, V., MA, N., PAPADOPOULOS, J., BEALER, K. & MADDEN, T. L. 2009. BLAST+: architecture and applications. *BMC Bioinformatics*, 10, 421.
- CARRUTHERS, M. D., NICHOLSON, P. A., TRACY, E. N. & MUNSON, R. S., JR. 2013. *Acinetobacter baumannii* utilizes a type VI secretion system for bacterial competition. *PLoS One*, 8, e59388.
- CARVER, T., HARRIS, S. R., BERRIMAN, M., PARKHILL, J. & MCQUILLAN, J. A. 2012. Artemis: an integrated platform for visualization and analysis of high-throughput sequence-based experimental data. *Bioinformatics*, 28, 464-9.

- CDC. 2019. *Information for Health Professionals* [Online].
<https://www.cdc.gov/campylobacter/technical.html>. [Accessed April 01 2020 2020].
- CHAMPION, O. L., KARLYSHEV, A. V., SENIOR, N. J., WOODWARD, M., LA RAGIONE, R., HOWARD, S. L., WREN, B. W. & TITBALL, R. W. 2010. Insect infection model for *Campylobacter jejuni* reveals that O-methyl phosphoramidate has insecticidal activity. *J Infect Dis*, 201, 776-82.
- CHEN, C., YANG, X. & SHEN, X. 2019. Confirmed and Potential Roles of Bacterial T6SSs in the Intestinal Ecosystem. *Front Microbiol*, 10, 1484.
- CHEN, L., ZOU, Y., SHE, P. & WU, Y. 2015. Composition, function, and regulation of T6SS in *Pseudomonas aeruginosa*. *Microbiol Res*, 172, 19-25.
- CHERRAK, Y., FLAUGNATTI, N., DURAND, E., JOURNET, L. & CASCALES, E. 2019. Structure and Activity of the Type VI Secretion System. *Microbiol Spectr*, 7.
- CIANCIOTTO, N. P. 2005. Type II secretion: a protein secretion system for all seasons. *Trends Microbiol*, 13, 581-8.
- CIANFANELLI, F. R., ALCOFORADO DINIZ, J., GUO, M., DE CESARE, V., TROST, M. & COULTHURST, S. J. 2016a. VgrG and PAAR Proteins Define Distinct Versions of a Functional Type VI Secretion System. *PLoS Pathog*, 12, e1005735.
- CIANFANELLI, F. R., MONLEZUN, L. & COULTHURST, S. J. 2016b. Aim, Load, Fire: The Type VI Secretion System, a Bacterial Nanoweapon. *Trends Microbiol*, 24, 51-62.
- COBURN, B., SEKIROV, I. & FINLAY, B. B. 2007. Type III secretion systems and disease. *Clin Microbiol Rev*, 20, 535-49.
- CODY, A. J., MCCARTHY, N. D., BRAY, J. E., WIMALARATHNA, H. M., COLLES, F. M., JANSEN VAN RENSBURG, M. J., DINGLE, K. E., WALDENSTROM, J. & MAIDEN, M. C. 2015. Wild bird-associated *Campylobacter jejuni* isolates are a consistent source of human disease, in Oxfordshire, United Kingdom. *Environ Microbiol Rep*, 7, 782-8.
- COHN, M. T., INGMER, H., MULHOLLAND, F., JORGENSEN, K., WELLS, J. M. & BRONSTED, L. 2007. Contribution of conserved ATP-dependent proteases of *Campylobacter jejuni* to stress tolerance and virulence. *Appl Environ Microbiol*, 73, 7803-13.
- COKER, A. O., ISOKPEHI, R. D., THOMAS, B. N., AMISU, K. O. & OBI, C. L. 2002. Human campylobacteriosis in developing countries. *Emerg Infect Dis*, 8, 237-44.
- COLLES, F. M., JONES, T. A., MCCARTHY, N. D., SHEPPARD, S. K., CODY, A. J., DINGLE, K. E., DAWKINS, M. S. & MAIDEN, M. C. 2008. *Campylobacter* infection of broiler chickens in a free-range environment. *Environ Microbiol*, 10, 2042-50.
- CORCIONIVOSCHI, N., CLYNE, M., LYONS, A., ELMI, A., GUNDOGDU, O., WREN, B. W., DORRELL, N., KARLYSHEV, A. V. & BOURKE, B. 2009. *Campylobacter jejuni* cocultured with epithelial cells reduces surface capsular polysaccharide expression. *Infect Immun*, 77, 1959-67.
- CORCIONIVOSCHI, N., GUNDOGDU, O., MORAN, L., KELLY, C., SCATES, P., STEF, L., CEAN, A., WREN, B., DORRELL, N. & MADDEN, R. H. 2015. Virulence

- characteristics of hcp (+) *Campylobacter jejuni* and *Campylobacter coli* isolates from retail chicken. *Gut Pathog*, 7, 20.
- CORNELIS, G. R. 2006. The type III secretion injectisome. *Nat Rev Microbiol*, 4, 811-25.
- COSTA, T. R., FELISBERTO-RODRIGUES, C., MEIR, A., PREVOST, M. S., REDZEJ, A., TROKTER, M. & WAKSMAN, G. 2015. Secretion systems in Gram-negative bacteria: structural and mechanistic insights. *Nat Rev Microbiol*, 13, 343-59.
- CRANE, J. M. & RANDALL, L. L. 2017. The Sec System: Protein Export in *Escherichia coli*. *EcoSal Plus*, 7.
- CUCCUI, J. & WREN, B. 2015. Hijacking bacterial glycosylation for the production of glycoconjugates, from vaccines to humanised glycoproteins. *J Pharm Pharmacol*, 67, 338-50.
- DAVIES, C., TAYLOR, A. J., ELMI, A., WINTER, J., LIAW, J., GRABOWSKA, A. D., GUNDOGDU, O., WREN, B. W., KELLY, D. J. & DORRELL, N. 2019. Sodium Taurocholate Stimulates *Campylobacter jejuni* Outer Membrane Vesicle Production via Down-Regulation of the Maintenance of Lipid Asymmetry Pathway. *Front Cell Infect Microbiol*, 9, 177.
- DE MAAYER, P., VENTER, S. N., KAMBER, T., DUFFY, B., COUTINHO, T. A. & SMITS, T. H. 2011. Comparative genomics of the Type VI secretion systems of *Pantoea* and *Erwinia* species reveals the presence of putative effector islands that may be translocated by the VgrG and Hcp proteins. *BMC Genomics*, 12, 576.
- DEKEYSER, P., GOSSUIN-DETRAIN, M., BUTZLER, J. P. & STERNON, J. 1972. Acute enteritis due to related vibrio: first positive stool cultures. *J Infect Dis*, 125, 390-2.
- DOLORES, J. S., AGARWAL, S., EGERER, M. & SATCHELL, K. J. 2015. Vibrio cholerae MARTX toxin heterologous translocation of beta-lactamase and roles of individual effector domains on cytoskeleton dynamics. *Mol Microbiol*, 95, 590-604.
- DONG, T. G., HO, B. T., YODER-HIMES, D. R. & MEKALANOS, J. J. 2013. Identification of T6SS-dependent effector and immunity proteins by Tn-seq in *Vibrio cholerae*. *Proc Natl Acad Sci U S A*, 110, 2623-8.
- DOUZI, B., FILLOUX, A. & VOULHOUX, R. 2012. On the path to uncover the bacterial type II secretion system. *Philos Trans R Soc Lond B Biol Sci*, 367, 1059-72.
- DOYLE, L. P. 1944. A vibrio associated with swine dysentery. *Am J Vet Res*, 4, 3-5.
- DUBOURG, A., XIA, D., WINPENNY, J. P., AL NAIMI, S., BOUZID, M., SEXTON, D. W., WASTLING, J. M., HUNTER, P. R. & TYLER, K. M. 2018. Giardia secretome highlights secreted tenascins as a key component of pathogenesis. *Gigascience*, 7, 1-13.
- DURAND, E., BERNADAC, A., BALL, G., LAZDUNSKI, A., STURGIS, J. N. & FILLOUX, A. 2003. Type II protein secretion in *Pseudomonas aeruginosa*: the pseudopilus is a multifibrillar and adhesive structure. *J Bacteriol*, 185, 2749-58.
- DURAND, E., CABBILLAU, C., CASCALES, E. & JOURNET, L. 2014. VgrG, Tae, Tle, and beyond: the versatile arsenal of Type VI secretion effectors. *Trends Microbiol*, 22, 498-507.
- DURAND, E., NGUYEN, V. S., ZOUED, A., LOGGER, L., PEHAU-ARNAUDET, G., ASCHTGEN, M. S., SPINELLI, S., DESMYTER, A., BARDIAUX, B., DUJEANCOURT, A., ROUSSEL, A., CABBILLAU, C., CASCALES, E. &

- FRONZES, R. 2015. Biogenesis and structure of a type VI secretion membrane core complex. *Nature*, 523, 555-60.
- EL-GEBALI, S., MISTRY, J., BATEMAN, A., EDDY, S. R., LUCIANI, A., POTTER, S. C., QURESHI, M., RICHARDSON, L. J., SALAZAR, G. A., SMART, A., SONNHAMMER, E. L. L., HIRSH, L., PALADIN, L., PIOVESAN, D., TOSATTO, S. C. E. & FINN, R. D. 2019. The Pfam protein families database in 2019. *Nucleic Acids Res*, 47, D427-D432.
- ELMI, A., DOREY, A., WATSON, E., JAGATIA, H., INGLIS, N. F., GUNDOGDU, O., BAJAJ-ELLIOTT, M., WREN, B. W., SMITH, D. G. E. & DORRELL, N. 2018. The bile salt sodium taurocholate induces *Campylobacter jejuni* outer membrane vesicle production and increases OMV-associated proteolytic activity. *Cell Microbiol*, 20.
- ELMI, A., NASHER, F., JAGATIA, H., GUNDOGDU, O., BAJAJ-ELLIOTT, M., WREN, B. & DORRELL, N. 2016. *Campylobacter jejuni* outer membrane vesicle-associated proteolytic activity promotes bacterial invasion by mediating cleavage of intestinal epithelial cell E-cadherin and occludin. *Cell Microbiol*, 18, 561-72.
- ELMI, A., WATSON, E., SANDU, P., GUNDOGDU, O., MILLS, D. C., INGLIS, N. F., MANSON, E., IMRIE, L., BAJAJ-ELLIOTT, M., WREN, B. W., SMITH, D. G. & DORRELL, N. 2012. *Campylobacter jejuni* outer membrane vesicles play an important role in bacterial interactions with human intestinal epithelial cells. *Infect Immun*, 80, 4089-98.
- ESCHERICH, T. 1886. Beiträge zur Kenntniss der Darmbakterien. III Über das Vorkommen van Vibrionen im Darmcanal und den Stuhlgängen der Säuglinge. *Münch. Med. Wschr*, 33, 833-835.
- EUCAST. 2019. Antimicrobial susceptibility testing: EUCAST disk diffusion method. Available: http://www.eucast.org/ast_of_bacteria/disk_diffusion_methodology/.
- FABER, E., GRIPP, E., MAURISCHAT, S., KASPERS, B., TEDIN, K., MENZ, S., ZURAW, A., KERSHAW, O., YANG, I., RAUTENSCHLEIN, S. & JOSENHANS, C. 2016. Novel Immunomodulatory Flagellin-Like Protein FlaC in *Campylobacter jejuni* and Other *Campylobacteriales*. *mSphere*, 1.
- FITZSIMONS, T. C., LEWIS, J. M., WRIGHT, A., KLEIFELD, O., SCHITTENHELM, R. B., POWELL, D., HARPER, M. & BOYCE, J. D. 2018. Identification of Novel *Acinetobacter baumannii* Type VI Secretion System Antibacterial Effector and Immunity Pairs. *Infect Immun*, 86.
- FLINT, A., BUTCHER, J. & STINTZI, A. 2016. Stress Responses, Adaptation, and Virulence of Bacterial Pathogens During Host Gastrointestinal Colonization. *Microbiol Spectr*, 4.
- FRIDMAN, C. M., KEPPEL, K., GERLIC, M., BOSIS, E. & SALOMON, D. 2020. A comparative genomics methodology reveals a widespread family of membrane-disrupting T6SS effectors. *Nat Commun*, 11, 1085.
- FSA. 2014. *New UK food poisoning figures published* [Online]. Food Standards Agency: Food Standards Agency. [Accessed 25/01 2017].
- GERC, A. J., DIEPOLD, A., TRUNK, K., PORTER, M., RICKMAN, C., ARMITAGE, J. P., STANLEY-WALL, N. R. & COULTHURST, S. J. 2015. Visualization of the *Serratia*

- Type VI Secretion System Reveals Unprovoked Attacks and Dynamic Assembly. *Cell Rep*, 12, 2131-42.
- GISH, W. & STATES, D. J. 1993. Identification of protein coding regions by database similarity search. *Nat Genet*, 3, 266-72.
- GLADMAN S, S. T. 2012. VelvetOptimiser, v2.2.5.
- GOMES, M. C. & MOSTOWY, S. 2020. The Case for Modeling Human Infection in Zebrafish. *Trends Microbiol*, 28, 10-18.
- GREEN, E. R. & MECSAS, J. 2016. Bacterial Secretion Systems: An Overview. *Microbiol Spectr*, 4.
- GUERRY, P. 2007. Campylobacter flagella: not just for motility. *Trends Microbiol*, 15, 456-61.
- GUERRY, P., EWING, C. P., SCHIRM, M., LORENZO, M., KELLY, J., PATTARINI, D., MAJAM, G., THIBAUT, P. & LOGAN, S. 2006. Changes in flagellin glycosylation affect Campylobacter autoagglutination and virulence. *Mol Microbiol*, 60, 299-311.
- GUERRY, P., POLY, F., RIDDLE, M., MAUE, A. C., CHEN, Y. H. & MONTEIRO, M. A. 2012. Campylobacter polysaccharide capsules: virulence and vaccines. *Front Cell Infect Microbiol*, 2, 7.
- GUNDOGDU, O., DA SILVA, D. T., MOHAMMAD, B., ELMI, A., MILLS, D. C., WREN, B. W. & DORRELL, N. 2015. The Campylobacter jejuni MarR-like transcriptional regulators RrpA and RrpB both influence bacterial responses to oxidative and aerobic stresses. *Front Microbiol*, 6, 724.
- GUNDOGDU, O., DA SILVA, D. T., MOHAMMAD, B., ELMI, A., WREN, B. W., VAN VLIET, A. H. & DORRELL, N. 2016. The Campylobacter jejuni Oxidative Stress Regulator RrpB Is Associated with a Genomic Hypervariable Region and Altered Oxidative Stress Resistance. *Front Microbiol*, 7, 2117.
- GUNDOGDU, O., MILLS, D. C., ELMI, A., MARTIN, M. J., WREN, B. W. & DORRELL, N. 2011. The Campylobacter jejuni transcriptional regulator Cj1556 plays a role in the oxidative and aerobic stress response and is important for bacterial survival in vivo. *J Bacteriol*, 193, 4238-49.
- HACHANI, A., ALLSOPP, L. P., ODUKO, Y. & FILLOUX, A. 2014. The VgrG proteins are "a la carte" delivery systems for bacterial type VI effectors. *J Biol Chem*, 289, 17872-84.
- HACHANI, A., LOSSI, N. S. & FILLOUX, A. 2013. A visual assay to monitor T6SS-mediated bacterial competition. *J Vis Exp*, e50103.
- HACHANI, A., WOOD, T. E. & FILLOUX, A. 2016. Type VI secretion and anti-host effectors. *Curr Opin Microbiol*, 29, 81-93.
- HAN, Y., WANG, T., CHEN, G., PU, Q., LIU, Q., ZHANG, Y., XU, L., WU, M. & LIANG, H. 2019. A Pseudomonas aeruginosa type VI secretion system regulated by CueR facilitates copper acquisition. *PLoS Pathog*, 15, e1008198.
- HARRISON, J. W., DUNG, T. T., SIDDIQUI, F., KORBRISATE, S., BUKHARI, H., TRA, M. P., HOANG, N. V., CARRIQUE-MAS, J., BRYANT, J., CAMPBELL, J. I., STUDHOLME, D. J., WREN, B. W., BAKER, S., TITBALL, R. W. & CHAMPION, O. L. 2014. Identification of possible virulence marker from Campylobacter jejuni isolates. *Emerg Infect Dis*, 20, 1026-9.

- HEISLER, D. B., KUDRYASHOVA, E., GRINEVICH, D. O., SUAREZ, C., WINKELMAN, J. D., BIRUKOV, K. G., KOTHA, S. R., PARINANDI, N. L., VAVYLONIS, D., KOVAR, D. R. & KUDRYASHOV, D. S. 2015. ACTIN-DIRECTED TOXIN. ACD toxin-produced actin oligomers poison formin-controlled actin polymerization. *Science*, 349, 535-9.
- HENDRIXSON, D. R. 2006. A phase-variable mechanism controlling the *Campylobacter jejuni* FlgR response regulator influences commensalism. *Mol Microbiol*, 61, 1646-59.
- HEPWORTH, P. J., ASHELFORD, K. E., HINDS, J., GOULD, K. A., WITNEY, A. A., WILLIAMS, N. J., LEATHERBARROW, H., FRENCH, N. P., BIRTLES, R. J., MENDONCA, C., DORRELL, N., WREN, B. W., WIGLEY, P., HALL, N. & WINSTANLEY, C. 2011. Genomic variations define divergence of water/wildlife-associated *Campylobacter jejuni* niche specialists from common clonal complexes. *Environ Microbiol*, 13, 1549-60.
- HERMANS, D., PASMANS, F., HEYNDRIKX, M., VAN IMMERSEEL, F., MARTEL, A., VAN DEUN, K. & HAESEBROUCK, F. 2012. A tolerogenic mucosal immune response leads to persistent *Campylobacter jejuni* colonization in the chicken gut. *Crit Rev Microbiol*, 38, 17-29.
- HO, B. T., DONG, T. G. & MEKALANOS, J. J. 2014. A view to a kill: the bacterial type VI secretion system. *Cell Host Microbe*, 15, 9-21.
- HOFMANN, A. F. & HAGEY, L. R. 2008. Bile acids: chemistry, pathochemistry, biology, pathobiology, and therapeutics. *Cell Mol Life Sci*, 65, 2461-83.
- HOOD, R. D., SINGH, P., HSU, F., GUVENER, T., CARL, M. A., TRINIDAD, R. R., SILVERMAN, J. M., OHLSON, B. B., HICKS, K. G., PLEMEL, R. L., LI, M., SCHWARZ, S., WANG, W. Y., MERZ, A. J., GOODLETT, D. R. & MOUGOUS, J. D. 2010. A type VI secretion system of *Pseudomonas aeruginosa* targets a toxin to bacteria. *Cell Host Microbe*, 7, 25-37.
- HOULISTON, R. S., VINOGRADOV, E., DZIECIATKOWSKA, M., LI, J., ST MICHAEL, F., KARWASKI, M. F., BROCHU, D., JARRELL, H. C., PARKER, C. T., YUKI, N., MANDRELL, R. E. & GILBERT, M. 2011. Lipooligosaccharide of *Campylobacter jejuni*: similarity with multiple types of mammalian glycans beyond gangliosides. *J Biol Chem*, 286, 12361-70.
- HUGDAHL, M. B., BEERY, J. T. & DOYLE, M. P. 1988. Chemotactic behavior of *Campylobacter jejuni*. *Infect Immun*, 56, 1560-6.
- HWANG, S., KIM, M., RYU, S. & JEON, B. 2011. Regulation of oxidative stress response by CosR, an essential response regulator in *Campylobacter jejuni*. *PLoS One*, 6, e22300.
- HWANG, S., RYU, S. & JEON, B. 2013. Roles of the superoxide dismutase SodB and the catalase KatA in the antibiotic resistance of *Campylobacter jejuni*. *J Antibiot (Tokyo)*, 66, 351-3.
- IMAI, K., ASAKAWA, N., TSUJI, T., AKAZAWA, F., INO, A., SONOYAMA, M. & MITAKU, S. 2008. SOSUI-GramN: high performance prediction for sub-cellular localization of proteins in gram-negative bacteria. *Bioinformatics*, 2, 417-21.

- JAGANNATHAN, A., CONSTANTINIDOU, C. & PENN, C. W. 2001. Roles of rpoN, fliA, and flgR in expression of flagella in *Campylobacter jejuni*. *J Bacteriol*, 183, 2937-42.
- JANG, K. S., SWEREDOSKI, M. J., GRAHAM, R. L., HESS, S. & CLEMONS, W. M., JR. 2014. Comprehensive proteomic profiling of outer membrane vesicles from *Campylobacter jejuni*. *J Proteomics*, 98, 90-8.
- JERVIS, A. J., BUTLER, J. A., WREN, B. W. & LINTON, D. 2015. Chromosomal integration vectors allowing flexible expression of foreign genes in *Campylobacter jejuni*. *BMC Microbiol*, 15, 230.
- JOHNSON, W. M. & LIOR, H. 1988. A new heat-labile cytolethal distending toxin (CLDT) produced by *Campylobacter* spp. *Microb Pathog*, 4, 115-26.
- JONES, F. S., ORCUTT, M. & LITTLE, R. B. 1931. Vibrios (*Vibrio Jejuni*, N.Sp.) Associated with Intestinal Disorders of Cows and Calves. *J Exp Med*, 53, 853-63.
- JONES, M. A., MARSTON, K. L., WOODALL, C. A., MASKELL, D. J., LINTON, D., KARLYSHEV, A. V., DORRELL, N., WREN, B. W. & BARROW, P. A. 2004. Adaptation of *Campylobacter jejuni* NCTC11168 to high-level colonization of the avian gastrointestinal tract. *Infect Immun*, 72, 3769-76.
- JOSHI, A., KOSTIUK, B., ROGERS, A., TESCHLER, J., PUKATZKI, S. & YILDIZ, F. H. 2017. Rules of Engagement: The Type VI Secretion System in *Vibrio cholerae*. *Trends Microbiol*, 25, 267-279.
- JOSHUA, G. W., GUTHRIE-IRONS, C., KARLYSHEV, A. V. & WREN, B. W. 2006. Biofilm formation in *Campylobacter jejuni*. *Microbiology*, 152, 387-96.
- JOSLIN, S. N. & HENDRIXSON, D. R. 2009. Activation of the *Campylobacter jejuni* FlgSR two-component system is linked to the flagellar export apparatus. *J Bacteriol*, 191, 2656-67.
- KAAKOUSH, N. O., CASTANO-RODRIGUEZ, N., MITCHELL, H. M. & MAN, S. M. 2015. Global Epidemiology of *Campylobacter* Infection. *Clin Microbiol Rev*, 28, 687-720.
- KAPITEIN, N., BONEMANN, G., PIETROSIUK, A., SEYFFER, F., HAUSSER, I., LOCKER, J. K. & MOGK, A. 2013. ClpV recycles VipA/VipB tubules and prevents non-productive tubule formation to ensure efficient type VI protein secretion. *Mol Microbiol*, 87, 1013-28.
- KARLYSHEV, A. V., CHAMPION, O. L., CHURCHER, C., BRISSON, J. R., JARRELL, H. C., GILBERT, M., BROCHU, D., ST MICHAEL, F., LI, J., WAKARCHUK, W. W., GOODHEAD, I., SANDERS, M., STEVENS, K., WHITE, B., PARKHILL, J., WREN, B. W. & SZYMANSKI, C. M. 2005. Analysis of *Campylobacter jejuni* capsular loci reveals multiple mechanisms for the generation of structural diversity and the ability to form complex heptoses. *Mol Microbiol*, 55, 90-103.
- KARLYSHEV, A. V., LINTON, D., GREGSON, N. A., LASTOVICA, A. J. & WREN, B. W. 2000. Genetic and biochemical evidence of a *Campylobacter jejuni* capsular polysaccharide that accounts for Penner serotype specificity. *Mol Microbiol*, 35, 529-41.
- KARLYSHEV, A. V., MCCROSSAN, M. V. & WREN, B. W. 2001. Demonstration of polysaccharide capsule in *Campylobacter jejuni* using electron microscopy. *Infect Immun*, 69, 5921-4.

- KARLYSHEV, A. V. & WREN, B. W. 2005. Development and application of an insertional system for gene delivery and expression in *Campylobacter jejuni*. *Appl Environ Microbiol*, 71, 4004-13.
- KELLEY, L. A., MEZULIS, S., YATES, C. M., WASS, M. N. & STERNBERG, M. J. 2015. The Phyre2 web portal for protein modeling, prediction and analysis. *Nat Protoc*, 10, 845-58.
- KIM, J. C., OH, E., KIM, J. & JEON, B. 2015. Regulation of oxidative stress resistance in *Campylobacter jejuni*, a microaerophilic foodborne pathogen. *Front Microbiol*, 6, 751.
- KING, E. O. 1962. The laboratory recognition of *Vibrio fetus* and a closely related vibrio isolated from cases of human vibriosis. *Annals New York Academy of Sciences*, 98, 700.
- KIRCHBERGER, P. C., UNTERWEGER, D., PROVENZANO, D., PUKATZKI, S. & BOUCHER, Y. 2017. Sequential displacement of Type VI Secretion System effector genes leads to evolution of diverse immunity gene arrays in *Vibrio cholerae*. *Sci Rep*, 7, 45133.
- KIST, M. 1986. [Who discovered *Campylobacter jejuni/coli*? A review of hitherto disregarded literature]. *Zentralbl Bakteriol Mikrobiol Hyg A*, 261, 177-86.
- KONKEL, M. E., KIM, B. J., RIVERA-AMILL, V. & GARVIS, S. G. 1999. Identification of proteins required for the internalization of *Campylobacter jejuni* into cultured mammalian cells. *Adv Exp Med Biol*, 473, 215-24.
- KONKEL, M. E., KLENA, J. D., RIVERA-AMILL, V., MONTEVILLE, M. R., BISWAS, D., RAPHAEL, B. & MICKELSON, J. 2004. Secretion of virulence proteins from *Campylobacter jejuni* is dependent on a functional flagellar export apparatus. *J Bacteriol*, 186, 3296-303.
- KORLATH, J. A., OSTERHOLM, M. T., JUDY, L. A., FORFANG, J. C. & ROBINSON, R. A. 1985. A point-source outbreak of campylobacteriosis associated with consumption of raw milk. *J Infect Dis*, 152, 592-6.
- KOROTKOV, K. V., SANDKVIST, M. & HOL, W. G. 2012. The type II secretion system: biogenesis, molecular architecture and mechanism. *Nat Rev Microbiol*, 10, 336-51.
- KOVANEN, S., ROSSI, M., POHJA-MYKRA, M., NIEMINEN, T., RAUNIO-SAARNISTO, M., SAUVALA, M., FREDRIKSSON-AHOMAA, M., HANNINEN, M. L. & KIVISTO, R. 2018. Population genetics and characterization of *Campylobacter jejuni* isolates in western jackdaws and game birds in Finland. *Appl Environ Microbiol*.
- KUDRYASHEV, M., WANG, R. Y., BRACKMANN, M., SCHERER, S., MAIER, T., BAKER, D., DIMAIO, F., STAHLBERG, H., EGELMAN, E. H. & BASLER, M. 2015. Structure of the type VI secretion system contractile sheath. *Cell*, 160, 952-962.
- LAI, C. K., CHEN, Y. A., LIN, C. J., LIN, H. J., KAO, M. C., HUANG, M. Z., LIN, Y. H., CHIANG-NI, C., CHEN, C. J., LO, U. G., LIN, L. C., LIN, H., HSIEH, J. T. & LAI, C. H. 2016. Molecular Mechanisms and Potential Clinical Applications of *Campylobacter jejuni* Cytotolethal Distending Toxin. *Front Cell Infect Microbiol*, 6, 9.
- LARA-TEJERO, M. & GALAN, J. E. 2001. CdtA, CdtB, and CdtC form a tripartite complex that is required for cytolethal distending toxin activity. *Infect Immun*, 69, 4358-65.

- LAZZARO, M., FELDMAN, M. F. & GARCIA VESCOVI, E. 2017. A Transcriptional Regulatory Mechanism Finely Tunes the Firing of Type VI Secretion System in Response to Bacterial Enemies. *mBio*, 8.
- LEE, A., O'ROURKE, J. L., BARRINGTON, P. J. & TRUST, T. J. 1986. Mucus colonization as a determinant of pathogenicity in intestinal infection by *Campylobacter jejuni*: a mouse cecal model. *Infect Immun*, 51, 536-46.
- LEE, M., JUN, S. Y., YOON, B. Y., SONG, S., LEE, K. & HA, N. C. 2012. Membrane fusion proteins of type I secretion system and tripartite efflux pumps share a binding motif for TolC in gram-negative bacteria. *PLoS One*, 7, e40460.
- LEE, P. A., TULLMAN-ERCEK, D. & GEORGIOU, G. 2006. The bacterial twin-arginine translocation pathway. *Annu Rev Microbiol*, 60, 373-95.
- LEIMAN, P. G., BASLER, M., RAMAGOPAL, U. A., BONANNO, J. B., SAUDER, J. M., PUKATZKI, S., BURLEY, S. K., ALMO, S. C. & MEKALANOS, J. J. 2009. Type VI secretion apparatus and phage tail-associated protein complexes share a common evolutionary origin. *Proc Natl Acad Sci U S A*, 106, 4154-9.
- LEO, J. C., GRIN, I. & LINKE, D. 2012. Type V secretion: mechanism(s) of autotransport through the bacterial outer membrane. *Philos Trans R Soc Lond B Biol Sci*, 367, 1088-101.
- LERTPIRIYAPONG, K., GAMAZON, E. R., FENG, Y., PARK, D. S., PANG, J., BOTKA, G., GRAFFAM, M. E., GE, Z. & FOX, J. G. 2012. *Campylobacter jejuni* type VI secretion system: roles in adaptation to deoxycholic acid, host cell adherence, invasion, and in vivo colonization. *PLoS One*, 7, e42842.
- LERTSETHTAKARN, P., OTTEMANN, K. M. & HENDRIXSON, D. R. 2011. Motility and chemotaxis in *Campylobacter* and *Helicobacter*. *Annu Rev Microbiol*, 65, 389-410.
- LI, H. & DURBIN, R. 2009. Fast and accurate short read alignment with Burrows-Wheeler transform. *Bioinformatics*, 25, 1754-60.
- LIAW, J., HONG, G., DAVIES, C., ELM, A., SIMA, F., STRATAKOS, A., STEF, L., PET, I., HACHANI, A., CORCIONIVOSCHI, N., WREN, B. W., GUNDOGDU, O. & DORRELL, N. 2019. The *Campylobacter jejuni* Type VI Secretion System Enhances the Oxidative Stress Response and Host Colonization. *Front Microbiol*, 10, 2864.
- LIEN, Y. W. & LAI, E. M. 2017. Type VI Secretion Effectors: Methodologies and Biology. *Front Cell Infect Microbiol*, 7, 254.
- LIN, H. H., YU, M., SRIRAMOJU, M. K., HSU, S. T., LIU, C. T. & LAI, E. M. 2020. A High-Throughput Interbacterial Competition Screen Identifies ClpAP in Enhancing Recipient Susceptibility to Type VI Secretion System-Mediated Attack by *Agrobacterium tumefaciens*. *Frontiers in Microbiology*, 10.
- LIN, J., ZHANG, W., CHENG, J., YANG, X., ZHU, K., WANG, Y., WEI, G., QIAN, P. Y., LUO, Z. Q. & SHEN, X. 2017. A *Pseudomonas* T6SS effector recruits PQS-containing outer membrane vesicles for iron acquisition. *Nat Commun*, 8, 14888.
- LIN, L., LEZAN, E., SCHMIDT, A. & BASLER, M. 2019. Abundance of bacterial Type VI secretion system components measured by targeted proteomics. *Nat Commun*, 10, 2584.
- LINDMARK, B., ROMPIKUNTAL, P. K., VAITKEVICIUS, K., SONG, T., MIZUNOE, Y., UHLIN, B. E., GUERRY, P. & WAI, S. N. 2009. Outer membrane vesicle-mediated

- release of cytolethal distending toxin (CDT) from *Campylobacter jejuni*. *BMC Microbiol*, 9, 220.
- LINK, A. J. & LABAER, J. 2011. Trichloroacetic acid (TCA) precipitation of proteins. *Cold Spring Harb Protoc*, 2011, 993-4.
- LOPEZ, J., LY, P. M. & FELDMAN, M. F. 2020. The Tip of the VgrG Spike Is Essential to Functional Type VI Secretion System Assembly in *Acinetobacter baumannii*. *mBio*, 11.
- LOSADA, L., SHEA, A. A. & DESHAZER, D. 2018. A MarR family transcriptional regulator and subinhibitory antibiotics regulate type VI secretion gene clusters in *Burkholderia pseudomallei*. *Microbiology*, 164, 1196-1211.
- LOSSI, N. S., MANOLI, E., FORSTER, A., DAJANI, R., PAPE, T., FREEMONT, P. & FILLOUX, A. 2013. The HsiB1C1 (TssB-TssC) complex of the *Pseudomonas aeruginosa* type VI secretion system forms a bacteriophage tail sheathlike structure. *J Biol Chem*, 288, 7536-48.
- LUETHY, P. M., HUYNH, S., RIBARDO, D. A., WINTER, S. E., PARKER, C. T. & HENDRIXSON, D. R. 2017. Microbiota-Derived Short-Chain Fatty Acids Modulate Expression of *Campylobacter jejuni* Determinants Required for Commensalism and Virulence. *mBio*, 8.
- MA, J., SUN, M., DONG, W., PAN, Z., LU, C. & YAO, H. 2017. PAAR-Rhs proteins harbor various C-terminal toxins to diversify the antibacterial pathways of type VI secretion systems. *Environ Microbiol*, 19, 345-360.
- MA, L. S., HACHANI, A., LIN, J. S., FILLOUX, A. & LAI, E. M. 2014. *Agrobacterium tumefaciens* deploys a superfamily of type VI secretion DNase effectors as weapons for interbacterial competition in planta. *Cell Host Microbe*, 16, 94-104.
- MALIK-KALE, P., PARKER, C. T. & KONKEL, M. E. 2008. Culture of *Campylobacter jejuni* with sodium deoxycholate induces virulence gene expression. *J Bacteriol*, 190, 2286-97.
- MASI, M. & WANDERSMAN, C. 2010. Multiple signals direct the assembly and function of a type 1 secretion system. *J Bacteriol*, 192, 3861-9.
- MAUE, A. C., MOHAWK, K. L., GILES, D. K., POLY, F., EWING, C. P., JIAO, Y., LEE, G., MA, Z., MONTEIRO, M. A., HILL, C. L., FERDERBER, J. S., PORTER, C. K., TRENT, M. S. & GUERRY, P. 2013. The polysaccharide capsule of *Campylobacter jejuni* modulates the host immune response. *Infect Immun*, 81, 665-72.
- MCFADYEAN, J. & STOCKMAN, S. 1913. Report of the Departmental Committee appointed by the Board of Agriculture and Fisheries to inquire into Epizootic Abortion. III. Abortion in Sheep. *In: H.M.S.O.* (ed.).
- MEUSKENS, I., SARAGLIADIS, A., LEO, J. C. & LINKE, D. 2019. Type V Secretion Systems: An Overview of Passenger Domain Functions. *Front Microbiol*, 10, 1163.
- MIYATA, S. T., KITAOKA, M., BROOKS, T. M., MCAULEY, S. B. & PUKATZKI, S. 2011. *Vibrio cholerae* requires the type VI secretion system virulence factor VasX to kill *Dictyostelium discoideum*. *Infect Immun*, 79, 2941-9.
- MOLLER, S., CRONING, M. D. & APWEILER, R. 2001. Evaluation of methods for the prediction of membrane spanning regions. *Bioinformatics*, 17, 646-53.

- MONTGOMERY, M. P., ROBERTSON, S., KOSKI, L., SALEHI, E., STEVENSON, L. M., SILVER, R., SUNDARARAMAN, P., SINGH, A., JOSEPH, L. A., WEISNER, M. B., BRANDT, E., PRARAT, M., BOKANYI, R., CHEN, J. C., FOLSTER, J. P., BENNETT, C. T., FRANCOIS WATKINS, L. K., AUBERT, R. D., CHU, A., JACKSON, J., BLANTON, J., GINN, A., RAMADUGU, K., STANEK, D., DEMENT, J., CUI, J., ZHANG, Y., BASLER, C., FRIEDMAN, C. R., GEISSLER, A. L., CROWE, S. J., DOWELL, N., DIXON, S., WHITLOCK, L., WILLIAMS, I., JHUNG, M. A., NICHOLS, M. C., DE FIJTER, S. & LAUGHLIN, M. E. 2018. Multidrug-Resistant *Campylobacter jejuni* Outbreak Linked to Puppy Exposure - United States, 2016-2018. *MMWR Morb Mortal Wkly Rep*, 67, 1032-1035.
- MOUGOUS, J. D., CUFF, M. E., RAUNSER, S., SHEN, A., ZHOU, M., GIFFORD, C. A., GOODMAN, A. L., JOACHIMIAK, G., ORDONEZ, C. L., LORY, S., WALZ, T., JOACHIMIAK, A. & MEKALANOS, J. J. 2006. A virulence locus of *Pseudomonas aeruginosa* encodes a protein secretion apparatus. *Science*, 312, 1526-30.
- NATALE, P., BRUSER, T. & DRIESSEN, A. J. 2008. Sec- and Tat-mediated protein secretion across the bacterial cytoplasmic membrane--distinct translocases and mechanisms. *Biochim Biophys Acta*, 1778, 1735-56.
- NAZAROV, S., SCHNEIDER, J. P., BRACKMANN, M., GOLDIE, K. N., STAHLBERG, H. & BASLER, M. 2018. Cryo-EM reconstruction of Type VI secretion system baseplate and sheath distal end. *EMBO J*, 37.
- NEWELL, D. G. & FEARNLEY, C. 2003. Sources of *Campylobacter* colonization in broiler chickens. *Appl Environ Microbiol*, 69, 4343-51.
- NOREEN, Z., JOBICHEN, C., ABBASI, R., SEETHARAMAN, J., SIVARAMAN, J. & BOKHARI, H. 2018. Structural basis for the pathogenesis of *Campylobacter jejuni* Hcp1, a structural and effector protein of the Type VI Secretion System. *FEBS J*.
- NOTHAFT, H. & SZYMANSKI, C. M. 2013. Bacterial protein N-glycosylation: new perspectives and applications. *J Biol Chem*, 288, 6912-20.
- OCHSNER, U. A., SNYDER, A., VASIL, A. I. & VASIL, M. L. 2002. Effects of the twin-arginine translocase on secretion of virulence factors, stress response, and pathogenesis. *Proc Natl Acad Sci U S A*, 99, 8312-7.
- PARK, S. F. 2002. The physiology of *Campylobacter* species and its relevance to their role as foodborne pathogens. *Int J Food Microbiol*, 74, 177-88.
- PARKER, C. T., GILBERT, M., YUKI, N., ENDTZ, H. P. & MANDRELL, R. E. 2008. Characterization of lipooligosaccharide-biosynthetic loci of *Campylobacter jejuni* reveals new lipooligosaccharide classes: evidence of mosaic organizations. *J Bacteriol*, 190, 5681-9.
- PELEG, A. Y., JARA, S., MONGA, D., ELIOPOULOS, G. M., MOELLERING, R. C., JR. & MYLONAKIS, E. 2009. *Galleria mellonella* as a model system to study *Acinetobacter baumannii* pathogenesis and therapeutics. *Antimicrob Agents Chemother*, 53, 2605-9.
- PENNER, J. L., HENNESSY, J. N. & CONGI, R. V. 1983. Serotyping of *Campylobacter jejuni* and *Campylobacter coli* on the basis of thermostable antigens. *Eur J Clin Microbiol*, 2, 378-83.

- PEZOA, D., BLONDEL, C. J., SILVA, C. A., YANG, H. J., ANDREWS-POLYMERIS, H., SANTIVIAGO, C. A. & CONTRERAS, I. 2014. Only one of the two type VI secretion systems encoded in the *Salmonella enterica* serotype Dublin genome is involved in colonization of the avian and murine hosts. *Vet Res*, 45, 2.
- PHE 2017a. Campylobacter data 2008 to 2017. In: ENGLAND, P. H. (ed.). <https://www.gov.uk/government/publications/campylobacter-infection-annual-data/campylobacter-data-2008-to-2017>.
- PHE 2017b. Travel-associated Campylobacter infections: 2014. In: ENGLAND, P. H. (ed.). <https://www.gov.uk/government/publications/travel-associated-campylobacter-infections>.
- PIKE, B. L., GUERRY, P. & POLY, F. 2013. Global Distribution of Campylobacter jejuni Penner Serotypes: A Systematic Review. *PLoS One*, 8, e67375.
- POLY, F., EWING, C., GOON, S., HICKEY, T. E., ROCKABRAND, D., MAJAM, G., LEE, L., PHAN, J., SAVARINO, N. J. & GUERRY, P. 2007. Heterogeneity of a Campylobacter jejuni protein that is secreted through the flagellar filament. *Infect Immun*, 75, 3859-67.
- POLY, F., THREADGILL, D. & STINTZI, A. 2004. Identification of Campylobacter jejuni ATCC 43431-specific genes by whole microbial genome comparisons. *J Bacteriol*, 186, 4781-95.
- PRESTON, A., MANDRELL, R. E., GIBSON, B. W. & APICELLA, M. A. 1996. The lipooligosaccharides of pathogenic gram-negative bacteria. *Crit Rev Microbiol*, 22, 139-80.
- PUKATZKI, S., MA, A. T., STURTEVANT, D., KRASTINS, B., SARRACINO, D., NELSON, W. C., HEIDELBERG, J. F. & MEKALANOS, J. J. 2006. Identification of a conserved bacterial protein secretion system in *Vibrio cholerae* using the *Dictyostelium* host model system. *Proc Natl Acad Sci U S A*, 103, 1528-33.
- RAPISARDA, C., CHERRAK, Y., KOOPER, R., SCHMIDT, V., PELLARIN, R., LOGGER, L., CASCALES, E., PILHOFER, M., DURAND, E. & FRONZES, R. 2019. In situ and high-resolution cryo-EM structure of a bacterial type VI secretion system membrane complex. *EMBO J*, 38.
- REICHOW, S. L., KOROTKOV, K. V., HOL, W. G. & GONEN, T. 2010. Structure of the cholera toxin secretion channel in its closed state. *Nat Struct Mol Biol*, 17, 1226-32.
- REPIZO, G. D., GAGNE, S., FOUCAULT-GRUNENWALD, M. L., BORGES, V., CHARPENTIER, X., LIMANSKY, A. S., GOMES, J. P., VIALE, A. M. & SALCEDO, S. P. 2015. Differential Role of the T6SS in *Acinetobacter baumannii* Virulence. *PLoS One*, 10, e0138265.
- RINGEL, P. D., HU, D. & BASLER, M. 2017. The Role of Type VI Secretion System Effectors in Target Cell Lysis and Subsequent Horizontal Gene Transfer. *Cell Rep*, 21, 3927-3940.
- RITZ, M., GARENAUX, A., BERGE, M. & FEDERIGHI, M. 2009. Determination of *rpoA* as the most suitable internal control to study stress response in *C. jejuni* by RT-qPCR and application to oxidative stress. *J Microbiol Methods*, 76, 196-200.
- ROBINSON, D. A. 1981. Infective dose of *Campylobacter jejuni* in milk. *Br Med J (Clin Res Ed)*, 282, 1584.

- ROSALES-REYES, R., SKELDON, A. M., AUBERT, D. F. & VALVANO, M. A. 2012. The Type VI secretion system of Burkholderia cenocepacia affects multiple Rho family GTPases disrupting the actin cytoskeleton and the assembly of NADPH oxidase complex in macrophages. *Cell Microbiol*, 14, 255-73.
- RUSSELL, A. B., HOOD, R. D., BUI, N. K., LEROUX, M., VOLLMER, W. & MOUGOUS, J. D. 2011. Type VI secretion delivers bacteriolytic effectors to target cells. *Nature*, 475, 343-7.
- RUSSELL, A. B., LEROUX, M., HATHAZI, K., AGNELLO, D. M., ISHIKAWA, T., WIGGINS, P. A., WAI, S. N. & MOUGOUS, J. D. 2013. Diverse type VI secretion phospholipases are functionally plastic antibacterial effectors. *Nature*, 496, 508-12.
- RUSSELL, A. B., PETERSON, S. B. & MOUGOUS, J. D. 2014. Type VI secretion system effectors: poisons with a purpose. *Nat Rev Microbiol*, 12, 137-48.
- S, A. 2010. FastQC. <http://www.bioinformatics.babraham.ac.uk/projects/fastqc/>, v0.11.2. <http://www.bioinformatics.babraham.ac.uk/projects/fastqc/>.
- SAINATO, R., ELGENDY, A., POLY, F., KUROIWA, J., GUERRY, P., RIDDLE, M. S. & PORTER, C. K. 2018. Epidemiology of Campylobacter Infections among Children in Egypt. *Am J Trop Med Hyg*, 98, 581-585.
- SALIH, O., HE, S., PLANAMENTE, S., STACH, L., MACDONALD, J. T., MANOLI, E., SCHERES, S. H. W., FILLOUX, A. & FREEMONT, P. S. 2018. Atomic Structure of Type VI Contractile Sheath from Pseudomonas aeruginosa. *Structure*, 26, 329-336 e3.
- SANA, T. G., FLAUGNATTI, N., LUGO, K. A., LAM, L. H., JACOBSON, A., BAYLOT, V., DURAND, E., JOURNET, L., CASCALES, E. & MONACK, D. M. 2016. Salmonella Typhimurium utilizes a T6SS-mediated antibacterial weapon to establish in the host gut. *Proc Natl Acad Sci U S A*, 113, E5044-51.
- SANA, T. G., HACHANI, A., BUCIOR, I., SOSCIA, C., GARVIS, S., TERMINE, E., ENGEL, J., FILLOUX, A. & BLEVES, S. 2012. The second type VI secretion system of Pseudomonas aeruginosa strain PAO1 is regulated by quorum sensing and Fur and modulates internalization in epithelial cells. *J Biol Chem*, 287, 27095-105.
- SANA, T. G., LUGO, K. A. & MONACK, D. M. 2017. T6SS: The bacterial "fight club" in the host gut. *PLoS Pathog*, 13, e1006325.
- SANTIN, Y. G., DOAN, T., LEBRUN, R., ESPINOSA, L., JOURNET, L. & CASCALES, E. 2018. In vivo TssA proximity labelling during type VI secretion biogenesis reveals TagA as a protein that stops and holds the sheath. *Nat Microbiol*, 3, 1304-1313.
- SANTOS, M. N. M., CHO, S. T., WU, C. F., CHANG, C. J., KUO, C. H. & LAI, E. M. 2019. Redundancy and Specificity of Type VI Secretion vgrG Loci in Antibacterial Activity of Agrobacterium tumefaciens 1D1609 Strain. *Front Microbiol*, 10, 3004.
- SCHMITTGEN, T. D. & LIVAK, K. J. 2008. Analyzing real-time PCR data by the comparative C(T) method. *Nat Protoc*, 3, 1101-8.
- SCHNEIDER, C. A., RASBAND, W. S. & ELICEIRI, K. W. 2012. NIH Image to ImageJ: 25 years of image analysis. *Nat Methods*, 9, 671-5.
- SCHWARZ, S., HOOD, R. D. & MOUGOUS, J. D. 2010. What is type VI secretion doing in all those bugs? *Trends Microbiol*, 18, 531-7.
- SCHWARZ, S., SINGH, P., ROBERTSON, J. D., LEROUX, M., SKERRETT, S. J., GOODLETT, D. R., WEST, T. E. & MOUGOUS, J. D. 2014. VgrG-5 is a

- Burkholderia type VI secretion system-exported protein required for multinucleated giant cell formation and virulence. *Infect Immun*, 82, 1445-52.
- SCOTLAND, H. P. 2019. Annual summary of Campylobacter infections, 2018. In: SCOTLAND, H. P. (ed.). <https://www.hps.scot.nhs.uk/web-resources-container/annual-summary-of-campylobacter-infections-2018>.
- SEAVER, L. C. & IMLAY, J. A. 2001. Alkyl hydroperoxide reductase is the primary scavenger of endogenous hydrogen peroxide in Escherichia coli. *J Bacteriol*, 183, 7173-81.
- SEBALD, M. & VÉRON, M. 1963. Teneur en bases de l'ADN et classification des vibrions. *Ann Inst Pasteur*, 105, 897-910.
- SEEMANN, T. 2014. Prokka: rapid prokaryotic genome annotation. *Bioinformatics*, 30, 2068-2069.
- SENIOR, N. J., BAGNALL, M. C., CHAMPION, O. L., REYNOLDS, S. E., LA RAGIONE, R. M., WOODWARD, M. J., SALGUERO, F. J. & TITBALL, R. W. 2011. Galleria mellonella as an infection model for Campylobacter jejuni virulence. *J Med Microbiol*, 60, 661-9.
- SHA, J., ROSENZWEIG, J. A., KOZLOVA, E. V., WANG, S., EROVA, T. E., KIRTLEY, M. L., VAN LIER, C. J. & CHOPRA, A. K. 2013. Evaluation of the roles played by Hcp and VgrG type 6 secretion system effectors in Aeromonas hydrophila SSU pathogenesis. *Microbiology*, 159, 1120-1135.
- SHENKER, B. J., WALKER, L. P., ZEKAVAT, A., DLAKIC, M. & BOESZEBATTAGLIA, K. 2014. Blockade of the PI-3K signalling pathway by the Aggregatibacter actinomycetemcomitans cytolethal distending toxin induces macrophages to synthesize and secrete pro-inflammatory cytokines. *Cell Microbiol*, 16, 1391-404.
- SHNEIDER, M. M., BUTH, S. A., HO, B. T., BASLER, M., MEKALANOS, J. J. & LEIMAN, P. G. 2013. PAAR-repeat proteins sharpen and diversify the type VI secretion system spike. *Nature*, 500, 350-3.
- SI, M., WANG, Y., ZHANG, B., ZHAO, C., KANG, Y., BAI, H., WEI, D., ZHU, L., ZHANG, L., DONG, T. G. & SHEN, X. 2017. The Type VI Secretion System Engages a Redox-Regulated Dual-Functional Heme Transporter for Zinc Acquisition. *Cell Rep*, 20, 949-959.
- SIDDIQUI, F., CHAMPION, O., AKRAM, M., STUDHOLME, D., EQANI, S. A., WREN, B. W., TITBALL, R. & BOKHARI, H. 2015. Molecular detection identified a type six secretion system in Campylobacter jejuni from various sources but not from human cases. *J Appl Microbiol*, 118, 1191-8.
- SIMA, F., STRATAKOS, A. C., WARD, P., LINTON, M., KELLY, C., PINKERTON, L., STEF, L., GUNDOGDU, O., LAZAR, V. & CORCIONIVOSCHI, N. 2018. A Novel Natural Antimicrobial Can Reduce the in vitro and in vivo Pathogenicity of T6SS Positive Campylobacter jejuni and Campylobacter coli Chicken Isolates. *Front Microbiol*, 9, 2139.
- SKARP, C. P. A., HANNINEN, M. L. & RAUTELIN, H. I. K. 2016. Campylobacteriosis: the role of poultry meat. *Clin Microbiol Infect*, 22, 103-109.
- SKIRROW, M. B. 1977. Campylobacter enteritis: a "new" disease. *Br Med J*, 2, 9-11.

- SMITH, T. & TAYLOR, M. S. 1919. Some morphological and biological characters of Spirilla (*Vibrio foetus* n.sp.) associated with disease of fetal membranes in cattle. *J Exp Med*, 30, 299-311.
- SONG, Y. C., JIN, S., LOUIE, H., NG, D., LAU, R., ZHANG, Y., WEERASEKERA, R., AL RASHID, S., WARD, L. A., DER, S. D. & CHAN, V. L. 2004. FlaC, a protein of *Campylobacter jejuni* TGH9011 (ATCC43431) secreted through the flagellar apparatus, binds epithelial cells and influences cell invasion. *Mol Microbiol*, 53, 541-53.
- SOUTHEY-PILLIG, C. J., DAVIES, D. G. & SAUER, K. 2005. Characterization of temporal protein production in *Pseudomonas aeruginosa* biofilms. *J Bacteriol*, 187, 8114-26.
- SPEARE, L., CECERE, A. G., GUCKES, K. R., SMITH, S., WOLLENBERG, M. S., MANDEL, M. J., MIYASHIRO, T. & SEPTER, A. N. 2018. Bacterial symbionts use a type VI secretion system to eliminate competitors in their natural host. *Proc Natl Acad Sci U S A*, 115, E8528-E8537.
- SPEARE, L., SMITH, S., SALVATO, F., KLEINER, M. & SEPTER, A. N. 2020. Environmental Viscosity Modulates Interbacterial Killing during Habitat Transition. *mBio*, 11.
- SUAREZ, G., SIERRA, J. C., EROVA, T. E., SHA, J., HORNEMAN, A. J. & CHOPRA, A. K. 2010. A type VI secretion system effector protein, VgrG1, from *Aeromonas hydrophila* that induces host cell toxicity by ADP ribosylation of actin. *J Bacteriol*, 192, 155-68.
- SZWEDZIAK, P. & PILHOFER, M. 2019. Bidirectional contraction of a type six secretion system. *Nat Commun*, 10, 1565.
- SZYMANSKI, C. M., LOGAN, S. M., LINTON, D. & WREN, B. W. 2003. *Campylobacter*-a tale of two protein glycosylation systems. *Trends Microbiol*, 11, 233-8.
- SZYMANSKI, C. M., YAO, R., EWING, C. P., TRUST, T. J. & GUERRY, P. 1999. Evidence for a system of general protein glycosylation in *Campylobacter jejuni*. *Mol Microbiol*, 32, 1022-30.
- TACK, D. M., MARDER, E. P., GRIFFIN, P. M., CIESLAK, P. R., DUNN, J., HURD, S., SCALLAN, E., LATHROP, S., MUSE, A., RYAN, P., SMITH, K., TOBIN-D'ANGELO, M., VUGIA, D. J., HOLT, K. G., WOLPERT, B. J., TAUXE, R. & GEISSLER, A. L. 2019. Preliminary Incidence and Trends of Infections with Pathogens Transmitted Commonly Through Food - Foodborne Diseases Active Surveillance Network, 10 U.S. Sites, 2015-2018. *MMWR Morb Mortal Wkly Rep*, 68, 369-373.
- TAHERI, N., FALLMAN, M., WAI, S. N. & FAHLGREN, A. 2019. Accumulation of virulence-associated proteins in *Campylobacter jejuni* Outer Membrane Vesicles at human body temperature. *J Proteomics*, 195, 33-40.
- TAHERI, N., MAHMUD, A., SANDBLAD, L., FALLMAN, M., WAI, S. N. & FAHLGREN, A. 2018. *Campylobacter jejuni* bile exposure influences outer membrane vesicles protein content and bacterial interaction with epithelial cells. *Sci Rep*, 8, 16996.

- TANG, J. Y., BULLEN, N. P., AHMAD, S. & WHITNEY, J. C. 2018. Diverse NADase effector families mediate interbacterial antagonism via the type VI secretion system. *J Biol Chem*, 293, 1504-1514.
- THIBAULT, P., LOGAN, S. M., KELLY, J. F., BRISSON, J. R., EWING, C. P., TRUST, T. J. & GUERRY, P. 2001. Identification of the carbohydrate moieties and glycosylation motifs in *Campylobacter jejuni* flagellin. *J Biol Chem*, 276, 34862-70.
- THOLOZAN, J. L., CAPPELIER, J. M., TISSIER, J. P., DELATTRE, G. & FEDERIGHI, M. 1999. Physiological characterization of viable-but-nonculturable *Campylobacter jejuni* cells. *Appl Environ Microbiol*, 65, 1110-6.
- THOMAS, C., HILL, D. J. & MABEY, M. 1999. Morphological changes of synchronized *Campylobacter jejuni* populations during growth in single phase liquid culture. *Lett Appl Microbiol*, 28, 194-8.
- THOMAS, S., HOLLAND, I. B. & SCHMITT, L. 2014. The Type 1 secretion pathway - the hemolysin system and beyond. *Biochim Biophys Acta*, 1843, 1629-41.
- TING, S. Y., BOSCH, D. E., MANGIAMELI, S. M., RADEY, M. C., HUANG, S., PARK, Y. J., KELLY, K. A., FILIP, S. K., GOO, Y. A., ENG, J. K., ALLAIRE, M., VEESLER, D., WIGGINS, P. A., PETERSON, S. B. & MOUGOUS, J. D. 2018. Bifunctional Immunity Proteins Protect Bacteria against FtsZ-Targeting ADP-Ribosylating Toxins. *Cell*, 175, 1380-1392 e14.
- TOSKA, J., HO, B. T. & MEKALANOS, J. J. 2018. Exopolysaccharide protects *Vibrio cholerae* from exogenous attacks by the type 6 secretion system. *Proc Natl Acad Sci U S A*, 115, 7997-8002.
- TREVIJANO-CONTADOR, N. & ZARAGOZA, O. 2018. Immune Response of *Galleria mellonella* against Human Fungal Pathogens. *J Fungi (Basel)*, 5.
- TROISFONTAINES, P. & CORNELIS, G. R. 2005. Type III secretion: more systems than you think. *Physiology (Bethesda)*, 20, 326-39.
- TRUNK, K., PELTIER, J., LIU, Y. C., DILL, B. D., WALKER, L., GOW, N. A. R., STARK, M. J. R., QUINN, J., STRAHL, H., TROST, M. & COULTHURST, S. J. 2018. The type VI secretion system deploys antifungal effectors against microbial competitors. *Nat Microbiol*, 3, 920-931.
- TSENG, T. T., TYLER, B. M. & SETUBAL, J. C. 2009. Protein secretion systems in bacterial-host associations, and their description in the Gene Ontology. *BMC Microbiol*, 9 Suppl 1, S2.
- TSIRIGOTAKI, A., DE GEYTER, J., SOSTARIC, N., ECONOMOU, A. & KARAMANOU, S. 2017. Protein export through the bacterial Sec pathway. *Nat Rev Microbiol*, 15, 21-36.
- UGARTE-RUIZ, M., STABLER, R. A., DOMINGUEZ, L., PORRERO, M. C., WREN, B. W., DORRELL, N. & GUNDOGDU, O. 2014. Prevalence of Type VI Secretion System in Spanish *Campylobacter jejuni* Isolates. *Zoonoses Public Health*.
- UGARTE-RUIZ, M., STABLER, R. A., DOMINGUEZ, L., PORRERO, M. C., WREN, B. W., DORRELL, N. & GUNDOGDU, O. 2015. Prevalence of Type VI Secretion System in Spanish *Campylobacter jejuni* Isolates. *Zoonoses Public Health*, 62, 497-500.

- VEGGE, C. S., BRONSTED, L., LI, Y. P., BANG, D. D. & INGMER, H. 2009. Energy taxis drives *Campylobacter jejuni* toward the most favorable conditions for growth. *Appl Environ Microbiol*, 75, 5308-14.
- VETTIGER, A., WINTER, J., LIN, L. & BASLER, M. 2017. The type VI secretion system sheath assembles at the end distal from the membrane anchor. *Nat Commun*, 8, 16088.
- WALLDEN, K., RIVERA-CALZADA, A. & WAKSMAN, G. 2010. Type IV secretion systems: versatility and diversity in function. *Cell Microbiol*, 12, 1203-12.
- WAN, B., ZHANG, Q., NI, J., LI, S., WEN, D., LI, J., XIAO, H., HE, P., OU, H. Y., TAO, J., TENG, Q., LU, J., WU, W. & YAO, Y. F. 2017. Type VI secretion system contributes to Enterohemorrhagic *Escherichia coli* virulence by secreting catalase against host reactive oxygen species (ROS). *PLoS Pathog*, 13, e1006246.
- WANG, J., YANG, B., LEIER, A., MARQUEZ-LAGO, T. T., HAYASHIDA, M., ROCKER, A., ZHANG, Y., AKUTSU, T., CHOU, K. C., STRUGNELL, R. A., SONG, J. & LITHGOW, T. 2018. Bastion6: a bioinformatics approach for accurate prediction of type VI secreted effectors. *Bioinformatics*, 34, 2546-2555.
- WANG, T., SI, M., SONG, Y., ZHU, W., GAO, F., WANG, Y., ZHANG, L., ZHANG, W., WEI, G., LUO, Z. Q. & SHEN, X. 2015. Type VI Secretion System Transports Zn²⁺ to Combat Multiple Stresses and Host Immunity. *PLoS Pathog*, 11, e1005020.
- WEBER, B., HASIC, M., CHEN, C., WAI, S. N. & MILTON, D. L. 2009. Type VI secretion modulates quorum sensing and stress response in *Vibrio anguillarum*. *Environ Microbiol*, 11, 3018-28.
- WEBER, B. S., MIYATA, S. T., IWASHIKI, J. A., MORTENSEN, B. L., SKAAR, E. P., PUKATZKI, S. & FELDMAN, M. F. 2013. Genomic and functional analysis of the type VI secretion system in *Acinetobacter*. *PLoS One*, 8, e55142.
- WIEGAND, I., HILPERT, K. & HANCOCK, R. E. 2008. Agar and broth dilution methods to determine the minimal inhibitory concentration (MIC) of antimicrobial substances. *Nat Protoc*, 3, 163-75.
- WIGLEY, P. 2015. Blurred Lines: Pathogens, Commensals, and the Healthy Gut. *Front Vet Sci*, 2, 40.
- WILLIAMS, N. J., JONES, T. R., LEATHERBARROW, H. J., BIRTLES, R. J., LAHUERTA-MARIN, A., BENNETT, M. & WINSTANLEY, C. 2010. Isolation of a novel *Campylobacter jejuni* clone associated with the bank vole, *Myodes glareolus*. *Appl Environ Microbiol*, 76, 7318-21.
- WILSON, D. L., RATHINAM, V. A. K., QI, W. H., WICK, L. M., LANDGRAF, J., BELL, J. A., PLOVANICH-JONES, A., PARRISH, J., FINLEY, R. L., MANSFIELD, L. S. & LINZ, J. E. 2010. Genetic diversity in *Campylobacter jejuni* is associated with differential colonization of broiler chickens and C57BL/6J IL10-deficient mice. *Microbiology-Sgm*, 156, 2046-2057.
- WOLFE, A. J. 2010. Physiologically relevant small phosphodonors link metabolism to signal transduction. *Curr Opin Microbiol*, 13, 204-9.
- WOOD, T. E., HOWARD, S. A., FORSTER, A., NOLAN, L. M., MANOLI, E., BULLEN, N. P., YAU, H. C. L., HACHANI, A., HAYWARD, R. D., WHITNEY, J. C., VOLLMER, W., FREEMONT, P. S. & FILLoux, A. 2019. The *Pseudomonas*

- aeruginosa T6SS Delivers a Periplasmic Toxin that Disrupts Bacterial Cell Morphology. *Cell Rep*, 29, 187-201 e7.
- YANG, X., LONG, M. & SHEN, X. 2018. Effector(-)Immunity Pairs Provide the T6SS Nanomachine its Offensive and Defensive Capabilities. *Molecules*, 23.
- YOUNG, K. T., DAVIS, L. M. & DIRITA, V. J. 2007. Campylobacter jejuni: molecular biology and pathogenesis. *Nat Rev Microbiol*, 5, 665-79.
- YOUNG, N. M., BRISSON, J. R., KELLY, J., WATSON, D. C., TESSIER, L., LANTHIER, P. H., JARRELL, H. C., CADOTTE, N., ST MICHAEL, F., ABERG, E. & SZYMANSKI, C. M. 2002. Structure of the N-linked glycan present on multiple glycoproteins in the Gram-negative bacterium, Campylobacter jejuni. *J Biol Chem*, 277, 42530-9.
- YU, N. Y., WAGNER, J. R., LAIRD, M. R., MELLI, G., REY, S., LO, R., DAO, P., SAHINALP, S. C., ESTER, M., FOSTER, L. J. & BRINKMAN, F. S. 2010. PSORTb 3.0: improved protein subcellular localization prediction with refined localization subcategories and predictive capabilities for all prokaryotes. *Bioinformatics*, 26, 1608-15.
- ZERBINO, D. R. & BIRNEY, E. 2008. Velvet: algorithms for de novo short read assembly using de Bruijn graphs. *Genome Res*, 18, 821-9.
- ZHENG, J., HO, B. & MEKALANOS, J. J. 2011. Genetic analysis of anti-amoebae and anti-bacterial activities of the type VI secretion system in Vibrio cholerae. *PLoS One*, 6, e23876.
- ZHENG, J., MENG, J., ZHAO, S., SINGH, R. & SONG, W. 2008. Campylobacter-induced interleukin-8 secretion in polarized human intestinal epithelial cells requires Campylobacter-secreted cytolethal distending toxin- and Toll-like receptor-mediated activation of NF-kappaB. *Infect Immun*, 76, 4498-508.
- ZOUED, A., BRUNET, Y. R., DURAND, E., ASCHTGEN, M. S., LOGGER, L., DOUZI, B., JOURNET, L., CABBILLAU, C. & CASCALES, E. 2014. Architecture and assembly of the Type VI secretion system. *Biochim Biophys Acta*, 1843, 1664-73.
- ZOUED, A., DURAND, E., BRUNET, Y. R., SPINELLI, S., DOUZI, B., GUZZO, M., FLAUGNATTI, N., LEGRAND, P., JOURNET, L., FRONZES, R., MIGNOT, T., CABBILLAU, C. & CASCALES, E. 2016. Priming and polymerization of a bacterial contractile tail structure. *Nature*, 531, 59-63.

APPENDICES

Appendix 1: *C. jejuni* 488 strain genome coordinates

TSS System	Coordinates
TssA	525818..527047
TssB	525264..525749
TssC	523808..525262
TssD	531562..532077
TssE	523413..523805
TssF	522589..523416
TssG	520972..521265
TssH	529563..530219
TssI	520821..519097
TssJ	527048..527473
TssK	527483..528880
TssL	528877..529683
TssM	530216..531526

Appendix 2: Amino acid sequences of known T6SS effector proteins

Species	Strain	T6SS Secreted Proteins	Gene Identifier	Search Performed (e0.01)	Search Performed (e0.1)	Amino Acid Sequence
<i>Pseudomonas aeruginosa</i>	PAO1	TseF	PA2374	Not identified	Not identified	MAASGKLDLVRGDSHLAGNLLDGSLEGPLRIDEHDR PQASLGYRQGQLHGASTLFHPNGKVSAQLAFVDGKL HGPASFHAAEGWLQRKAHYRNGLLHGEAFNYFANG QVAEREHYRDGVRDGVYQRFHGNGQLAFDGRYLNG QLLDGAQPFADDGRPLDSEGKPMARWRWWWTRLA EP
<i>Pseudomonas aeruginosa</i>	PAO1	Tse1 (Tse1)	PA1844	Not identified	Not identified	MDSLDQCIVNACKNSWDKSYLAGTPNKDNCSEGFVQS VAAELGVPMPRGNANAMVDGLEQSWTKLASGAEAA QKAAQGFLVIAGLKGRTYGHVAVVISGPLYRQKYPM CWCGSIAGAVGQSQGLKSVGQVWNRTDRDLNYYV YSLASCSLPRAS
<i>Pseudomonas aeruginosa</i>	PAO1	Tse2	PA2702	Not identified	Not identified	MSYDYEKTSLLTYRAVFKANYDGDVGRYLHPDKEL AEAAEVAPLLHPTFDSPTPGVVPARAPDIVAGRDGLY APDTGGTSVFDRAVLRRADGDFVIPDGTDIPDLKV KQDSYNKRLQATHYTIMPAKPMYREVLMLGQLDNFV RNAIRRQWEKARGL
<i>Pseudomonas aeruginosa</i>	PAO1	Tse3 (Tge1)	PA3484	Not identified	Not identified	MTATSDLIESLISYSWDDWQVTRQEARRVIAAIRNDN VPDATIAALDKSGSLIKLFQRVGPELARSLIASIAGRT TMQRYQARNALIRSLINNPLGTQTDNWIYFPTITFFDI CADLADAAGRLGFAAAGATGVASQAIQGPFSGVGAT GVNPTDLPSIAFGDQLKLLNKDPATVTKYSNPLGDLG AYLSQLSPQDKLNQAQTLVGQPISLTFPDA YPGNPPSR AKVMSAAARKYDLTPQLIGAILAEQRDQTRDEDAK DYQAAVSIKSANTSIGLGQVVVSTAIKYELFTDLLGQP VRRGLSRKAVATLLASDEFNIFATARYIRYVANLASQ QDLRKLKTRGAFPSIDLRAYAGNPRNWRDNRVRL ASEYTSRPWDDNLSPGWPMFVDDAYATFLDPGMRFP

<i>Pseudomonas aeruginosa</i>	PAO1	PldA (Tle5PA)	PA3487	Not identified	Not identified	MLQKKPYNGLHEKELNQINQQDGPCVAISAPGCFIK GSLNFSEKRAGNRVRFFTTGRDYFSDLASALDSASSSI FITGWQVNYDVLLDGRRLWQCLRQALERSPALKVY VMPWLSPSGSLGTYDFETMLAVFQLNAGLEGGARAF CTPAIQQSDMQGLGVAFSHHQKSVVIDNRIGYVGGID LAYGRRDDNDFSLDASGRRGNDAYNPGLPHLGWMA EDEHVSSMGLMMATLFDLSRPLASLTLHAPTLRLSPF PHIAASDEPLLSIPLAPSRARALNGAAYLSDLFRSPML PSLQWLGRAYNSSKEGLDEGFERLDALRRQMVASSIR AIANLIADNLDALPIEPELERRLRAWLEELRTAALNLP EALRIKSLLLINQWMSETELGQVLTLSIGKGFEDIPQN LSGKAGELAGSLFWTLHRLMQARAGGHQQPYRYLD EAPQPLASPDNARLAADQPRMPWQDVHCRIEGPSVY DLARNFIDRWNGQQAYLAKTPALQDTALVRSALAEAV MKWLNLSAAAAGLENYLDEKRNLRLELDPPTPCWIN APEQLPQEPEVRRGGMTVQVLRSAARMLEQEQAQR LGAGVNLPLQVGVSTEGVQSNCKDAMLLAISGAQQF IYIENQFFQSEFGKEGEVFKDLPLSGPMASLRDVGSLR RDFVVRIRLEEALQQRDLWLLDWAEEVEKIAQEPGTEA RQFLKSMAMWGVNAQGWLTHKLGEAQHGLLNEIG EALARRIERAIQREHPFHVYL VLPVHPEGALNVPNIM HQVHLTQQSLVFGEQSLVKRIQRQMALKALEGKSDP AQAREIIRKRDARGRPVYEQQDWSRYLTLNLRRTWA VLGGRVVTEQIYVHSKLLIADDRVAILGSANINDRSL QGERDSELAVMVRDSEPLTVRLDGKNDIAIVGKAIHQ LRVNLWKKHFGLSQGGGFVKPASELSAYLSIPAAQE AWEAIQTLAKENTRAYERTFNFIQNISQTQLQTPPEP PKGFEFGFPASIWPTWAYRKPGE LRAGGQLMEPMPY QEIFWRSSNLTSVKTFPPPNGVSGFITALPTS WTRGER NDSGLNLSILAHQDSRSLPTQVAMNGDSSAQGKHRT
<i>Pseudomonas aeruginosa</i>	PAO1	PldB	PA3301	Not identified	Not identified	MPAAAYWLPASDETPLYTRHWPSATAVGAVMLSHG MAEHAGRYERLAAALNAAGYHFY AIDQRGHGRTAE ADELGHFADQGGWGKVVGD LASLNHHIRQQHPELPI FLLGHSMGSYISMA YLLHHSCSLQGAILSGSNYQPQA LYRIARLIARFERWRQGPLGKSALIDFLSFGSFKAFK

						PNRTAFDWLSRDPQEVDRYVADPLCGFRCSNQLWVD LLGGLADITPPTHRLRQIDADLPLLIIGGERDPVSQGKRL GDLADALRGAGLRQVTLKTYPEARHELFFNESNRDAV TQDLIDWLEQALRHRRDHSTKERT
<i>Yersinia pseudotuberculosis</i>	YPIII	YezP	YPK_3549	Not identified	Not identified	MSKITTVDALPSVPVETSADAFNVVTLDAPIMRGNTTI TQITVKNPNTGALRGAKLQALLDQDQDVALIRVLPRT TPNLTVPINNLEPADIYALSQALALFFLPNSVRSDFLT A
<i>Serratia marcescens</i>	DB11	Tfe1 (Ssp3)	SMDB11_11 12	Not identified	Not identified	MHWLNFKRYKSDVAKQAVPPHLNAAEFARHYADKP QTDTEEYLSLSGEMCWDVAVLCAHRSGALSKAKYK QLWQTVFDKQYKHFVSPDDTEIRTMADMLRAPQGC IGIFSLRDAAAPRLHAMIPTGAGFAAGNKNLCIGVG GAVGWENLNLARDLRWQPEGFLRQGDNEVLRIFYR PFPA
<i>Serratia marcescens</i>	DB11	Tfe2	SMDB11_10 83	Not identified	Not identified	MPLVDGIIRGDRGSEPSRWQHASTKPLITLTHHTIP WNCLRNWVWGLVAGQHWNALDEFMNLIGVPNRAE VITQIKNKNLQDRDGLHTLVWQGWNVIEGPGNEYR AQGDDPGENFDGWSGKGMSTNQQATLQQVNVLYQ VMAPLGSRALDAARQAPNISAEASVLQRTIKQTRPT LRGKEPIRWQEDMWHQVQPGKEAKHFARWDTKPV WRKRLHSDLAQAG
<i>Serratia marcescens</i>	DB11	Ssp1 (Tae4.1)	SMDB11_22 61	Not identified	Not identified	MKPLYRQLKSSHYSSDYSSPGYLAAEAVYAEIGYELD TLLKQNPYANTCAVRMSLALLKTGISFKGRLPIKKG AYKGTIEPGAKLLADQLHRSSSFGKAKIFFNAPDAE KGIGNKKGVVFFNKITNYDGGHIDLIEPENSLTCHSH CYFNCKEVVFWELS
<i>Serratia marcescens</i>	DB11	Ssp2 (Tae4.2)	SMDB11_22 64	Not identified	Not identified	MSRPSFQQAQWQRFSEINVDITDVGKKIGGNVGLNIEL GVNDPLQGFTNACAIRMSYTLNYSFGKVERGAWKTV SGKDKNWIYRVRDIINFLNYKFGKPKTIKNPTPSDF SKDKGILVFTVPGWINDASGHATLWNGTTCSDHCFYF KSNEASIWLLK
<i>Serratia marcescens</i>	DB11	Ssp4	SMDB11_39 80	Not identified	Not identified	MKTAFSTPFGSPEDDLTNAEFARLLGNTGVQEFYRDI NLQALQDSLDCSLAFHGVGIIFSDGQNSFLVRPTQHT GYSNASQVTHVVISKTVAHTSRVAATNLSEALSKPS VSKELASAALSCGTLLVSVFLLASGSVAVPFTGGTSS

						AVAYLGYAGMAASALQCGNGLYRVNKLVDGKGD LAQLDSEQWYIATSTVLDVISLASAGAALKEATMTYR AMRRISARKATEWLKSMRPRSERKRLTENIIRAENPGIS NNVLKEMVKNGLYPKRYPTETAIQNGLRQQLHSALNN ALTFVGSIGSGLSAPVNVKTTGQYFVGMQKLPQMV R
<i>Serratia marcescens</i>	DB11	Ssp5	SMDB11_46 28	Not identified	Not identified	MANEDELRIALSPVQLAAVLSDESVEGETLSNRLG GLGLAGGVVELMGAGVLCYAPDPTFITKVGCVVGT HSLDSIKAASNQMITGHPTTTDTYQSAVLLAQTGAD RETAYNVGLTVDIAVPFVAFAGAVGAARVASVRMGR VKLVEHESVSGKYPGGHTLARHINIAPEALITRLARRP KLIIASTFRSVKEAEKYVSITVKANRADIVNWMKYA SPGSRLSVYHNFKESVGYGVLRGSTDVYQCHRVGVV IEFTRYNGKPYFILSAFPAR
<i>Serratia marcescens</i>	DB11	Ssp6	SMDB11_46 73	Not identified	Not identified	MAKGAKEIAQEMANAVNSKSNFFGGFIEGAISFPVDI GYLAYDFINTDNRSINRYDTERMLRLIKAGLANQHSL TKIVKLVVDEYLKKVDVDKVKRWVEKSGSKIAGR VSNQVLMVNLGAVLSERVVIRLATGYALTSLLTLGA MNSRAIHTSRQLRQRNPEIYDNLRRAGNLDLLYFLVE PKTKPFEQAIEIWRKNRGEFDRITELFFEKVSK
<i>Vibrio cholerae</i> O1 biovar El Tor chromosome I	N16961	VgrG	VC1416	Not identified	Not identified	MATLAYSIEVEGLEDETLVVRGFHGGESLSNSVFLGQ ACYGFRYEVQLASRVSNLTAEQMVDKRAELKLYRNS QLVQRVHGIVRAFSQGDIGHHTFYQLTLVPALERLS LRHNSRIFQKQTVPEILSILLQEMGINDYAFALKRDGV QREFCVQYRESIDIDFLHRLAAEEGLVYSFVHEAGKHT LYFSDASDLSKLPEPIPNALVGGGAIDTPYIHGLTYR TQAEVSEVQLKDYSFKKPAYSFLQTVQGTELDYQQT RYQHFDAPGRYKDDVNGAAFSQIRLDYLRRHAHTAT GQSNEPLL RAGYKFDLQEHLDPAMNRDWWVVSINHQ GEQPQALQEDGGSGATTYSNQFSLIPGHLHWRAEPQP KPQVDGPMIATVVGPEGEEIFCDEHGRVKIHFWDY SNGNEQSSCWVRVSQGWAGSQYGFIAIPRIGHEVIVE FLNGDPDQPIITGRTYHATNTPPYTLPEHKTKTVLRTE THQGEFNFELSFEDQAGKEQIYLHAQKDFDGLIENDH TTVIRHDHHLTVENDQFTQIKHNQHLTVEWESREAVT

						<p>GEQVLSIEGSLHVKTGKVVVNEAGTEIHVKAGQKVV IEAGSEITVKAGGSFVKVDPAGVHLSGALVNLNSGGS AGSGSGFGGAMPALPGGLEPAVALAPPQTISYQALLQ AEQANVPAVKVCPLAAQEATPAVNSITPPPPPIAPPM APPQIMNPQPTANAQPNLGRSTKATPDFPTHFPKSSI GIENELAGLVVAMPANSAQKFGYVKSAAQGDALFMLT KDMNQGSYQRPPSLQDGKNYQNWQHTVELVSYPC EMDDKAAVETRKQAMLWLATHFTTHIDQSNHQPLA PIQSEDGRFVIEITNAKHVIAAGNGISAESQGQTITMTP SGQQATVGVAAGGFGTSATPELRLLESAPWYQKSLK SQFASLTSANLDDKELAAANVFAYLTSIYLKTAELAK KFGIYINEWDPMSEQITPNANGLTDPKVKNAWEILPR TKPSKIVEILSKSDAKAVMKHIKPQLQSRYSLSKNV FQYFQDGGEVAGHGINNATVGDKHSPAILFEFRTV PNELQSYLPKTESTTKSEVKLLDQFDPMKRKTVIQQV ESLVQNSGDAFDKQWYQSYRDSMNQPPVKNACKIASA NQKAQWVKEHNPQEWQRHIA</p>
<i>Vibrio cholerae</i> O1 biovar El Tor chromosome II	N16961	VgrG	VCA0123	Not identified	Not identified	<p>MARLQFQLKVDGLEDESLVVRGFEGQESLSDSVWRC EPCYGFYQVDLASALSNLTAEQFVDQTAHLTILRDG QVVQQINGIVRQLSKGDTGHRHTFYSLTLVPALERLS LRNSNRIFQQQSVPEIISILLQEMGIEDYAFALKRECAQ REFCVQYRETDLQFLHRIAEEGLVYSHLHEAQKHTL LFTDSSDSQPKLAKVPYNALAGGEINLPYVVDLQFK TTAQVSHTELKDYSFKKPAYGFTQRTQGKDIAQQP NYEHFDAPGRYKDDANGKAQFSQIRLEYLRDALLAD AKSDEPLLAGVRFDLQDHLDHAMNRDVLVQANH QGTQPQALQEEGGSGATTYSNQLKLIPAHITWRARPC AKPQVDGPMIATVVGPGGEEIYCDNFRVVKVHFPWD RYSSSNEKSSCWVRVAQEWAGSQYGSMAIPRVGHEV IVSFLNGDPDQPIITGRTYHATNTAPYALPDHKTKTVL RTETHQGGYNELSFEDQAGSEQILLHAQKDWALIE HDHTEVIRHDQHLTVDNDRFTRIQRNQHLTVEGEVRS KIALDSSHEVGASLQHKVGQRIAVEAGKEISLKSAGKI VVEAGAELTLKAGGSFVKVDAGGVHLVGPAINLNAG GSAGSGSAYGGQLAAAPRMLAQAKPVAELVQPDIAA</p>

						SMQSGAARVIDVASLPTMMPSSANNTANDEPVAAEK TPERILKSDLLKPSDELEKLAKRQASAYRQGNHSDEV KLLQEALIKLGFDLGKAGADGDFGSKTKTAIEQFQKS YQPSHQTHPSYSIGAVDGIVGKGTLLALDEALMDGW VYENNIYQIWPLGKTSEKYESAGRGPVISTGNGDYG GASYGCMSSNLGVVQKYIQSSKFKEFFSGLNPATK EFNVVWQDIASRYPQEFREEQHOFIKRTHYDIQIGHLR GKGLLFEHNRAAVHDLIWSTSVQFGGRTNLIFNALNG QNMESMTDKDIILVQDYKLVNTERLFKSSPSWWSDL KKRAVSEKKALLELEIDGLEVDIK
<i>Vibrio cholerae</i> O1 biovar El Tor chromosome II	N16961	VasX	VCA0020	Not identified	Not identified	MSNPNQAAKTGQTNDANPASACPFKQPLIGIIPVRY AFDVYDDQGQALHPLPKADRQWKGQFSIKQRSYTLR QLRDGWL YVYDETAKTLEHEYEVVGGCKLTKIDWSDD EANKPOTHERGSKGESKSCLLYPAQHTLSIGYAHQRWT WRVCEHMRSNTSSRHAVMRKVSLKQFESNGTHPHA HFAQYLEDYVADIGTPAEQDIFKDTCTPSLPVEKSEEA VKGTEFKFVADKAVVSSSDYLQDLPEQNCGLFVALN DPLADVSDLFVTFTTQVAKRTKAIGDETQQHKMQMA ELTRTLGRIRLEEKEIPDFVKQDPIRILELERAITEYCAT AKLAEIESHHLASEGHSPSGNYALMQQQAEQKLAEL KTLYRFEPTSAQMRKWRKKDNSFIDEVRWADLDNFL VEHYTELKGLDEQIKQHYAQFMSAFNQLGLDLLFG MDNQDEVQAYLLALTSQFLVVVTQVNHDEKSLEIL KKDLSFDSPKNLMALASTGFSLQANQAINNHQGFST AFLSTSNPSDMVAFATAIANWDTFTGDERIQEKAWFK RWIEPAQSSFGALQKAVANQAKESWQAVMELLFPYQ NQPKGGTPSLLANLRLLLVESLVREEAVLQHNPKYA AELKQFETKLNAILQEMNDALELKPGNVSPKNHQIAT AQSAQRKLGQLSSELPMMMLTLKNQAAMNTFQQSV NEKLSALSKNVKTSSASVSQKLGGLGGLLFALNLWN TMTVLENIRYKVAQYPSWNPFPKNPALGEAIYATGNTI VVAGAISAGRAWVTIAEQGLLDRTLKNALNTTKVLG TKDALKTFAKSIALVATVGMIA SALETWESWGKFND SSKTDLERFGYLLKAGATGAQGIIFYIQFFTLGSGIGG PSIAAISAGWMLAGFAVIGIVYLIGVILTNVFKRSELEI

						WLSKSTWVGKESAHWPVVGKELTELEHLLHRPSLRLSQ VTQRKAAQWMDSGSLQWQLELTPDYLGKQTIGLQI TRLPAQPAYYQPQREAVTPILINEQQGKWSIEDNQPV YRITLGGSEKDTVGVCV ALPLRWGKELSLKFYASGTR AGELDLQSAEANDIATRNLVVGKG
<i>Vibrio cholerae</i> O1 biovar El Tor chromosome I	N16961	TseL/Tse2V C	VC1418	Not identified	Not identified	MDSFNVCVQCNPENWLELEFRSENDEPIDGLLVTIT NQSAPSNTYTQTTSSGKVLFGKIAAGEWRASVSQASL L TEVEKYASRKEGQESPVKKRAAAELDAADKDTKQY RFTTIGDFWDEAPKDEFLLQKQHKGIDVNASAEKAGFR LSHNQTYVFEIKALRSYMPVIIDTDEFNLVNSYTFALL SKLAYATNDFNRDDGKTIDNQGAISTVISQLKRKERP TYSGDLQAKWLEEIPYSKALSAQYYAEDDVGSEGYI IFNDELAIGVRGTEPYFQSKKPPVDNTKFKIIKAASG MAAVIADKIESATDSPGMKDLITDLDAQIAPEEFGG TYVHRGFYQYTMALLSLMEKDLGLHKIKKFFYCCGHS LGGAGALLISALIKDSYHPPVLRLYTYGMPRVGRSF VERYQNILHYRHVNNHDLVPQIPTVWMNTDVSEGFH VLDVFKSRVDLMRKMLTDDDDDNQHHGHLSQLLT YNSNNQVLLTPKQTQVTMLDLANLATNDSVAMVDG LSDASIVEHGMEQYIPNLFEQLTALSDESMLMVHYQRA ISALEQEIATLQQSYLTVKQAWIESIGNGTPTMNIGRL MSEMHSINKLIENRNKIRGELRQIVSDPQRMPATKFLI SQQTLPEIKVQIR
<i>Burkholderia thailandensis</i> E264 chromosome II	E264	TseZ	BTH_II1884	Not identified	Not identified	MIDPKEIFAACNNAHQYGQDASGSMAPFMD SIPNLS TASSSNASNLIGNVQEVGSKMLEHMSSIKSAVDKQV MIHQDNQQRQKTYDFNVDMRDLRPTNAVGFPEEMPS IFFAPFRTGK
<i>Salmonella enterica subsp. enterica</i> serovar Typhimurium	LT2	Tae4	STM0277	Not identified	Not identified	MNRPSFNEAWLAFRKNHNSVADVSGSIIGGNVGNIT GGYFQNACPIRMSYVLNATGFPIARNSPYAKVSGADN KFYIYRVNDMIDYLTHTMGKPDIVNPNPKQSDFIGKK GIIVVKGHGWSNARGHVTLWNGSICSDQCHLLNDPD NGPFVPEVGTWILP
<i>Enterobacter cloacae subsp. cloacae</i>	ATCC 13047	Tae4	ECL_01542	Not identified	Not identified	MSHMRPAFGAAWNRFKEVNVNVEQVKGKLLGGKVQ HNIDAGIFKNACPIRMSYVLNYCGIPVPSNSKYATVTG SDKKRYMFRVKDMIAFLPTVLGKADISVSSPTPAQFA

						GKQGIIFTGHGWLDATGHVTLWNGNICSDDCCHFLGS PGNGSFIPTNATFWSLK
Controls						
<i>Campylobacter jejuni</i>	414	TssD		Identified	Identified	MAEPAFIKIEGSTQGLISSGASTEASIGNRYKSGHEDEI MAQEVSHIVTVPVDQQSGQPSGQRVHKPFSFTCSLNK SVPLLYNALTKGERLPTVEVHWFRTATSGGSEHFFTT KLEDAIITNIELIMPNAQETSNHDKTELLKVSMSYRKV VWEHTAAGTSGSDDWREGKA
<i>Pseudomonas aeruginosa</i>	PAO1	Hcp1	PA0085	Not identified	Not identified	MAVDMFIKIGDVKGESKDKTHAEEIDVLAWSWGMS QSGSMHMGGGGGAGKVVNVQDLSFTKYIDKSTPNLM MACSSGKHYPQAKLTIRKAGGENQVEYLII TLKEVLVSSVSTGGSGGEDRLTENVTLNFAQVQVDY QPQKADGAKDGGPVKYGWNIRQNVQA

Appendix 3: List of secreted proteins and database predictions

Accession	Max fold change	Mass	Description	Pfam Accession	Pfam	PSORTb localisation	SOSUI GramN	TMH MM	SignalP	Secretome P	NCSP	Bastion6
488_S2_d ata_43_00 816	244.193 5513	51808	ArgH - Argininosuccinate lyase	Lyase_1	Lyase	Cytoplasmic	Cytoplasmic	No	Other	0.171654	No	No
488_S2_d ata_43_01 639	83.4705 6616	7757.9	Methyltransferase , possibly involved in O-methyl phosphoramidate capsule modification	N/A	N/A	Unknown	Cytoplasmic	No	Other	0.082292	No	No (0.302)
488_S2_d ata_43_00 585	76.0068 935	66032	TssI - Hypothetical protein	Phage_GPD	Phage late control gene D protein (GPD)	Cytoplasmic	Extracellular	No	Other	0.296262	No	Predicted

488_S2_d ata_43_01 609	62.9489 9322	35639	Partial TssI - Hypothetical protein	N/A	N/A	Unknown	Extracellular	No	Other	0.918480	Yes	Predicted
488_S2_d ata_43_01 631	58.7842 1605	35282	Putative sugar- nucleotide epimerase/ dehydratase	Epimerase	NAD dependent epimerase/deh ydratase family	Cytoplasmic	Cytoplasmic	No	Other	0.791848	Yes	No
488_S2_d ata_43_00 590	40.5068 2012	55672	TssC	VipB	Type VI secretion protein, EvpB/VC_A0 108, tail sheath	Cytoplasmic	Cytoplasmic	No	Other	0.119204	No	Predicted
488_S2_d ata_43_01 511	34.8885 6892	9549.4	RpsQ - 30S ribosomal protein S17	Ribosomal_S 17	Ribosomal protein S17	Cytoplasmic	Cytoplasmic	No	Other	0.141659	No	No
488_S2_d ata_43_01 638	34.1693 5181	16213	Methyltransferase , possibly involved in O- methyl phosphoramidate	Methyltransf _11	Methyltransfer ase domain	Cytoplasmic	Cytoplasmic	No	Other	0.601788	Yes	No (0.419)

			capsule modification									
488_S2_d ata_43_00 598	33.6224 5751	18764	TssD - Major exported protein	T6SS_HCP	Type VI secretion system effector, Hcp	Extracellular	Cytoplasmic	No	Other	0.877335	Yes	Predicted
488_S2_d ata_43_00 534	28.6079 5242	36079	PstS -Putative periplasmic phosphate binding protein	PBP_like_2	PBP superfamily domain	Cytoplasmic Membrane	Periplasmic	No	Signal peptide (Sec/SPI)	0.877371	No	No (0.376)
sp Q9PN59 PDXJ_CAMJE	26.0054 4293	29011	PdxJ -Pyridoxine 5'-phosphate synthase	PdxJ	Pyridoxal phosphate biosynthesis protein PdxJ	Cytoplasmic	Cytoplasmic	No	Other	0.132487	No	No
488_S2_d ata_43_01 518	20.1778 8634	10567	RplW - 50S ribosomal protein L23	Ribosomal_L 23	Ribosomal protein L23	Unknown	Cytoplasmic	No	Other	0.605801	Yes	No
488_S2_d ata_43_01 406	12.3704 681	13247	RplQ - 50S ribosomal protein L17	Ribosomal_L 17	Ribosomal protein L17	Cytoplasmic	Cytoplasmic	No	Other	0.211134	No	No

488_S2_d ata_43_01 722	12.0987 8047	11609	RplU - 50S ribosomal protein L21	Ribosomal_L 21p	Ribosomal prokaryotic L21 protein	Cytoplasmic	Cytoplasmic	No	Other	0.361758	No	No
sp Q9PI1 7 RS7_C AMJE	11.0346 8192	17692	RspG - 30S ribosomal protein S7	Ribosomal_S 7	Ribosomal protein S7p/S5e	Cytoplasmic	Cytoplasmic	No	Other	0.175321	No	No
488_S2_d ata_43_01 597	10.8799 7197	44149	AckA -Acetate kinase	Acetate_kina se	Acetokinase family	Cytoplasmic	Cytoplasmic	No	Other	0.054970	No	No
488_S2_d ata_43_01 517	10.2533 3782	30436	RplB - 50S ribosomal protein L2	Ribosomal_L 2_C	Ribosomal Proteins L2, C-terminal domain	Cytoplasmic	Cytoplasmic	No	Other	0.599870	Yes	No
sp Q9PI3 5 RL11_C AMJE	9.68416 7431	15080	RplK - 50S ribosomal protein L11	Ribosomal_L 11_N	Ribosomal protein L11, N-terminal domain	Cytoplasmic	Cytoplasmic	No	Other	0.886168	Yes	No
sp Q9PM 83 RS13_ CAMJE	9.62512 9006	13735	RpsM - 30S ribosomal protein S13	Ribosomal_S 13	Ribosomal protein S13/S18	Cytoplasmic	Cytoplasmic	No	Other	0.180351	No	No

488_S2_d ata_43_00 836	8.98133 8485	16130	Putative lipoprotein	META	META domain	Extracellular	Extracellular	No	Lipoprote in signal peptide (Sec/SPII)	0.923234	No	Predicted
488_S2_d ata_43_01 404	8.89972 4712	23896	RpsD - 30S ribosomal protein S4	Ribosomal_S 4	Ribosomal protein S4/S9 N-terminal domain	Cytoplasmic	Cytoplasmic	No	Other	0.404652	No	No
488_S2_d ata_43_00 301	8.48978 4978	8178.7	RpsU - 30S ribosomal protein S21	Ribosomal_S 21	Ribosomal protein S21	Unknown	Cytoplasmic	No	Other	0.254100	No	No
488_S2_d ata_43_01 318	8.48111 3322	14181	RpsI - 30S ribosomal protein S9	Ribosomal_S 9	Ribosomal protein S9/S16	Cytoplasmic	Cytoplasmic	No	Other	0.835155	Yes	No
sp Q0P82 3 DAPD_ CAMJE	8.46595 3263	42361	DapD - 2,3,4,5- tetrahydropyridin e-2,6- dicarboxylate N- succinyltransferas e	THDPS_N	Tetrahydrodipi colinate N- succinyltransfe rase N- terminal	Cytoplasmic	Cytoplasmic	No	Other	0.050470	No	No

488_S2_d ata_43_00 098	8.43957 1963	21650	ClpP - ATP- dependent Clp protease proteolytic subunit	CLP_proteas e	Clp protease	Cytoplasmic	Cytoplasmic	No	Other	0.087461	No	No
sp Q0P9K 4 DAPE_ CAMJE	8.08037 9734	40457	DapE - Succinyl- diaminopimelate desuccinylase	Peptidase_M 20	Peptidase family M20/M25/M4 0	Unknown (May have multiple localization sites)	Cytoplasmic	No	Other	0.046269	No	No
488_S2_d ata_43_01 461	8.00558 367	41378	PDZ domain protein	PDZ_2	PDZ domain	Unknown	Cytoplasmic	No	Signal peptide (Sec/SPI)	0.346831	No	No (0.304)
sp Q9PL X9 RL29 _CAMJE	7.89626 5811	7033.5	RpmC - 50S ribosomal protein L29	Ribosomal_L 29	Ribosomal L29 protein	Unknown	Cytoplasmic	No	Other	0.532839	No	No
sp Q9PIB 9 RISB_C AMJE	7.61885 5887	16686	RibH - 6,7- dimethyl-8- ribityllumazine synthase	DMRL_synt hase	6,7-dimethyl- 8- ribityllumazin e synthase	Cytoplasmic	Cytoplasmic	No	Other	0.213581	No	No

488_S2_d ata_43_00 876	7.49864 1995	72606	RpoD - RNA polymerase sigma factor (sigma-70)	Sigma70_r3	Sigma-70 region 3	Cytoplasmic	Cytoplasmic	No	Other	0.064334	No	No
488_S2_d ata_43_00 313	7.48912 0951	14930	NusB - Hypothetical protein	NusB	NusB family	Unknown	Cytoplasmic	No	Other	0.083896	No	No
sp Q9PL X0 RS10_ CAMJE	7.47139 4517	11673	RpsJ - 30S ribosomal protein S10	Ribosomal_S 10	Ribosomal protein S10p/S20e	Cytoplasmic	Unknown	No	Other	0.152039	No	No
488_S2_d ata_43_00 633	7.41285 089	13682	RplS - 50S ribosomal protein L19	Ribosomal_L 19	Ribosomal protein L19	Cytoplasmic	Cytoplasmic	No	Other	0.451000	No	No
488_S2_d ata_43_00 413	7.33451 53	16886 3	RpoC - DNA- directed RNA polymerase beta' chain	RNA_pol_R pb1_1	RNA polymerase Rpb1, domain 1	Cytoplasmic	Cytoplasmic	No	Other	0.049420	No	No
488_S2_d ata_43_01 441	7.31739 8868	49560	SdaA - L-serine dehydratase	SDH_alpha	Serine dehydratase alpha chain	Cytoplasmic	Cytoplasmic	No	Other	0.078285	No	No

sp Q9PI36 NUSG_CAMJE	7.280999906	20195	NusG - Transcription termination/antitermination protein	NusG	Transcription termination factor nusG	Cytoplasmic	Cytoplasmic	No	Other	0.109427	No	No
488_S2_data_43_01568	7.252706716	90065	NrdA - Ribonucleoside-diphosphate reductase alpha chain	Ribonuc_red_lgC	Ribonucleotide reductase, barrel domain	Cytoplasmic	Cytoplasmic	No	Other	0.055854	No	No
sp Q0P7T9 RL6_CAMJE	6.900447804	19587	RplF - 50S ribosomal protein L6	Ribosomal_L6	Ribosomal protein L6	Cytoplasmic	Cytoplasmic	No	Other	0.506899	Yes	No
488_S2_data_43_01070	6.880850218	28898	Putative NLPA family lipoprotein	Lipoprotein_9	NLPA lipoprotein	Cytoplasmic Membrane	Outer membrane	No	Signal peptide (Sec/SPI)	0.142080	No	No
488_S2_data_43_00778	6.866051233	62827	RpsA - 30S ribosomal protein S1	S1	S1 RNA binding domain	Cytoplasmic	Cytoplasmic	No	Other	0.043040	No	No
488_S2_data_43_00410	6.70197166	17685	RplJ - 50S ribosomal protein L10	Ribosomal_L10	Ribosomal protein L10	Cytoplasmic	Cytoplasmic	No	Other	0.239061	No	No

488_S2_d ata_43_00 818	6.68331 3502	66062	PycB - Putative pyruvate carboxylase B subunit	PYC_OADA	Conserved carboxylase domain	Cytoplasmic	Cytoplasmic	No	Other	0.060848	No	No
sp Q9PM 80 RPOA _CAMJE	6.47923 9113	37686	RpoA - DNA- directed RNA polymerase subunit alpha	RNA_pol_A _CTD	Bacterial RNA polymerase, alpha chain C terminal domain	Cytoplasmic	Cytoplasmic	No	Other	0.051470	No	No
488_S2_d ata_43_00 231	6.40307 8306	30159	PanB - 3-methyl- 2-oxobutanoate hydroxymethyltra nsferase	Pantoate_tra nsf	Ketopantoate hydroxymethy ltransferase	Cytoplasmic	Cytoplasmic	No	Other	0.083587	No	No
488_S2_d ata_43_01 182	6.35915 6504	42105	Hypothetical protein	N/A	N/A	Cytoplasmic	Cytoplasmic	No	Other	0.107183	No	No
488_S2_d ata_43_00 625	6.26782 7174	27784	Hypothetical protein	zf-RING_7	C4-type zinc ribbon domain	Cytoplasmic	Cytoplasmic	No	Other	0.167418	No	No

488_S2_d ata_43_00 189	6.14453 5279	35478	Putative periplasmic protein	TPR_6	Tetratricopepti de repeat	Outer Membrane	Outer membrane	No	Signal peptide (Sec/SPI)	0.954636	No	No (0.499)
488_S2_d ata_43_00 078	6.13875 8089	44901	Putative saccharopine dehydrogenase	Sacchrp_dh_ C	Saccharopine dehydrogenase C-terminal domain	Cytoplasmic	Unknown	No	Other	0.053131	No	No
488_S2_d ata_43_01 598	6.13006 0942	56030	Pta Phosphate acetyltransferase	PTA_PTB	Phosphate acetyl/butaryl transferase	Cytoplasmic	Cytoplasmic	No	Other	0.077883	No	No
488_S2_d ata_43_00 735	6.11414 4253	27975	Putative oxidoreductase	adh_short	Short chain dehydrogenase	Cytoplasmic	Cytoplasmic	No	Other	0.122652	No	No
sp Q9PL X8 RL16 _CAMJE	6.07600 052	16375	RplP - 50S ribosomal protein L16	Ribosomal_L 16	Ribosomal protein L16p/L10e	Cytoplasmic	Unknown	No	Other	0.348435	No	No
488_S2_d ata_43_00 926	6.07217 5095	27562	ThiG - Thiazole biosynthesis protein	ThiG	Thiazole biosynthesis protein ThiG	Cytoplasmic	Cytoplasmic	No	Other	0.227186	No	No

488_S2_d ata_43_00 621	5.93966 4506	17482	PurE - Phosphoribosyla minoimidazole carboxylase catalytic subunit	AIRC	AIR carboxylase	Unknown	Unknown	No	Other	0.370778	No	No
488_S2_d ata_43_00 134	5.83028 9671	20728	Frr - Ribosome recycling factor	RRF	Ribosome recycling factor	Cytoplasmic	Cytoplasmic	No	Other	0.946776	Yes	No
488_S2_d ata_43_00 796	5.81787 3511	10274	HupB - Hypothetical protein	Bac_DNA_b inding	Bacterial DNA-binding protein	Cytoplasmic	Cytoplasmic	No	Other	0.963833	Yes	No
488_S2_d ata_43_00 081	5.73437 4678	37446	CfbpA - Putative iron-uptake ABC transport system, periplasmic iron- binding protein	SBP_bac_6	Bacterial extracellular solute-binding protein	Periplasmic	Periplasmic	No	Lipoprote in signal peptide (Sec/SPII)	0.241625	No	No
488_S2_d ata_43_01 555	5.66384 8776	24512	Rrc - Non-haem iron protein	Rubrerythrin	Rubrerythrin	Cytoplasmic	Cytoplasmic	No	Other	0.054968	No	No

sp Q46124 RPOB_CAMJE	5.624640776	155915	RpoB - DNA-directed RNA polymerase subunit beta	RNA_pol_Rpb2_6	RNA polymerase Rpb2, domain 6	Cytoplasmic	Cytoplasmic	No	Other	0.044786	No	No
488_S2_data_43_00898	5.458240414	39716	LivK - Branched-chain amino-acid ABC transport system, periplasmic binding protein	Peripla_BP_6	Periplasmic binding protein	Periplasmic	Unknown	No	Signal peptide (Sec/SPI)	0.896673	No	No
488_S2_data_43_00062	5.421005788	7476.7	RpmE - 50S ribosomal protein L31	Ribosomal_L31	Ribosomal protein L31	Cytoplasmic	Cytoplasmic	No	Other	0.769982	Yes	No
488_S2_data_43_01161	5.410448199	30911	Putative periplasmic protein	SurA_N	SurA N-terminal domain	Unknown	Periplasmic	Yes (1)	Signal peptide (Sec/SPI)	0.785163	No	No
488_S2_data_43_01589	5.298693876	30941	Hypothetical protein	N/A	N/A	Cytoplasmic	Extracellular	No	Other	0.895900	Yes	Predicted

488_S2_d ata_43_00 457	5.24684 2492	31208	OorB - OORB subunit of 2- oxoglutarate:acce ptor oxidoreductase	TPP_enzyme _C	Thiamine pyrophosphate enzyme, C- terminal TPP binding domain	Cytoplasmic	Inner membrane	No	Other	0.136350	No	No
488_S2_d ata_43_00 216	5.22190 3499	12089 4	CarB - Carbamoyl- phosphate synthase large chain	CPSase_L_D 2	Carbamoyl- phosphate synthase L chain, ATP binding domain	Unknown (May have multiple localization sites)	Cytoplasmic	No	Lipoprote in signal peptide (Sec/SPII)	0.050163	No	No
488_S2_d ata_43_01 506	5.16661 2709	14733	RpsH - 30S ribosomal protein S8	Ribosomal_S 8	Ribosomal protein S8	Cytoplasmic	Cytoplasmic	No	Other	0.054023	No	No
488_S2_d ata_43_00 564	4.99665 0559	46711	CbrR - Two- component response regulator	GGDEF	Diguanylate cyclase, GGDEF domain	Cytoplasmic	Cytoplasmic	No	Other	0.068998	No	No

sp Q9PII8 RL25_C AMJE	4.95623 1602	19461	RplY - 50S ribosomal protein L25	Ribosomal_T L5_C	Ribosomal protein TL5, C-terminal domain	Cytoplasmic	Cytoplasmic	No	Other	0.174995	No	No
488_S2_d ata_43_00 346	4.92853 8491	26921	Putative oxidoreductase subunit	Gluconate_2- dh3	Gluconate 2- dehydrogenase subunit 3	Unknown	Extracellular	Yes (1)	TAT signal peptide (Tat/SPI)	0.477355	No	Predicted
488_S2_d ata_43_01 358	4.87699 7426	59132	Putative periplasmic oxidoreductase	Cu- oxidase_3	Multicopper oxidase	Unknown (May have multiple localization sites)	Cytoplasmic	No	TAT signal peptide (Tat/SPI)	0.076536	No	No
488_S2_d ata_43_00 941	4.85655 8566	49397	GatA - Glu- tRNAGln amidotransferase subunit A	Amidase	Amidase	Cytoplasmic	Cytoplasmic	No	Other	0.527952	Yes	No
488_S2_d ata_43_01 249	4.82697 3996	26597	Putative periplasmic protein	Thioredoxin_ 2	Thioredoxin- like domain	Unknown	Outer membrane	No	Signal peptide (Sec/SPI)	0.883255	No	No

488_S2_d ata_43_01 275	4.81354 7386	14646	Hypothetical protein	DUF1090	Protein of unknown function (DUF1090)	Unknown (May have multiple localization sites)	Cytoplasmic	No	Signal peptide (Sec/SPI)	0.086298	No	No
488_S2_d ata_43_01 346	4.67137 7604	21266	Putative two- component response regulator (SirA-like protein)	TusA	Sulfurtransfera se TusA	Cytoplasmic	Cytoplasmic	No	Other	0.037584	No	No
488_S2_d ata_43_00 452	4.61568 1531	33513	Mdh - Malate dehydrogenase	Ldh_1_N	Ldh_1_N lactate/malate dehydrogenase , NAD binding domain	Cytoplasmic	Cytoplasmic	No	Other	0.333802	No	No
sp Q9PL Y3 RL5_ CAMJE	4.53537 1996	20214	RplE - 50S ribosomal protein L5	Ribosomal_L 5_C	Ribosomal_L5 _C ribosomal L5P family C- terminus	Cytoplasmic	Cytoplasmic	No	Other	0.088174	No	No

488_S2_d ata_43_00 440	4.48022 5841	69596	HtpG - Hsp90 family heat shock protein	HSP90	Hsp90 protein	Cytoplasmic	Cytoplasmic	No	Other	0.107919	No	No
488_S2_d ata_43_00 458	4.42614 8389	20123	2- oxoglutarate:acce ptor oxidoreductase, gamma subunit	POR	Pyruvate ferredoxin/flav odoxin oxidoreductase	Cytoplasmic	Unknown	No	Other	0.066759	No	No
488_S2_d ata_43_00 677	4.41901 9794	28661	Putative NLPA family lipoprotein	Lipoprotein_ 9	NLPA lipoprotein	Cytoplasmic Membrane	Outer membrane	Yes (1)	Signal peptide (Sec/SPI)	0.073417	No	No
488_S2_d ata_43_01 319	4.40439 2386	15759	RplM - Ribosomal protein L13	Ribosomal_L 13	Ribosomal protein L13	Cytoplasmic	Cytoplasmic	No	Other	0.433091	No	No
488_S2_d ata_43_01 050	4.26701 1935	39525	Tsf - Elongation factor TS	EF_TS	Elongation factor TS	Cytoplasmic	Cytoplasmic	No	Other	0.071952	No	No
sp POC63 5 CHEY_ CAMJE	4.10999 0056	14437	CheY Chemotaxis protein homolog	Response_re g	Response regulator receiver domain	Cytoplasmic	Cytoplasmic	No	Other	0.051263	No	No

488_S2_d ata_43_01 315	4.04708 4904	13135 8	Pyruvate- flavodoxin oxidoreductase	POR_N	Pyruvate flavodoxin/ferr edoxin oxidoreductase , thiamine diP- bdg	Cytoplasmic	Outer membrane	No	Other	0.193227	No	No (0.381)
sp QOPAS 1 CBF2_ CAMJE	3.77506 9351	30518	Cbf2 - Putative peptidyl-prolyl cis-trans isomerase	Rotamase_3	PPIC-type PPIASE domain	Outer Membrane	Periplasmic	Yes (1)	Signal peptide (Sec/SPI)	0.897606	No	No
sp O6930 3 EFTU_ CAMJE	3.73295 6858	43594	TuF - Elongation factor Tu	GTP_EFTU	Elongation factor Tu GTP binding domain	Cytoplasmic	Cytoplasmic	No	Other	0.050281	No	No
488_S2_d ata_43_01 082	3.71065 0548	27277	Putative exporting protein	PGBA_N	Plasminogen- binding protein pgbA N-terminal	Cytoplasmic	Periplasmic	No	Signal peptide (Sec/SPI)	0.078143	No	No
488_S2_d ata_43_00 805	3.70146 9498	28164	Peb1A - Aspartate/glutama te-binding ABC	SBP_bac_3	Bacterial extracellular solute-binding	Periplasmic	Periplasmic	No	Signal peptide (Sec/SPI)	0.563937	No	No

			transporter protein		proteins, family 3							
488_S2_d ata_43_00 008	3.56055 7653	66481	TypA - Hypothetical protein	GTP_EFTU	Elongation factor Tu GTP binding domain	Cytoplasmic Membrane	Cytoplasmic	No	Other	0.044885	No	No
488_S2_d ata_43_00 160	3.39706 4694	34638	Putative periplasmic solute binding protein for ABC transport system	ZnuA	Zinc-uptake complex component A periplasmic	Periplasmic	Periplasmic	No	Signal peptide (Sec/SPI)	0.096911	No	No
488_S2_d ata_43_01 272	3.34486 9917	36362	GapA - Glyceraldehyde 3-phosphate dehydrogenase	Gp_dh_C	Glyceraldehyd e 3-phosphate dehydrogenase , C-terminal domain	Cytoplasmic	Unknown	No	Other	0.073504	No	No
sp Q9PI6 4 ACP_C AMJE	3.34202 4009	8597.8	AcpP – Acyl carrier protein	PP-binding	Phosphopantet heine attachment site	Cytoplasmic	Cytoplasmic	No	Other	0.045986	No	No

488_S2_d ata_43_00 351	3.25542 1519	21066	Putative periplasmic protein	YceI	YceI-like domain	Unknown	Periplasmic	No	Signal peptide (Sec/SPI)	0.822586	No	No (0.427)
488_S2_d ata_43_00 347	3.25259 9666	63702	Putative GMC oxidoreductase subunit	GMC_oxred _C	GMC oxidoreductase	Unknown	Extracellular	No	Other	0.950808	Yes	Predicted
488_S2_d ata_43_00 687	3.08081 0765	10492 6	NapA - Periplasmic nitrate reductase	Molybdopterin	Molybdopterin oxidoreductase	Periplasmic	Periplasmic	No	TAT signal peptide (Tat/SPI)	0.751225	No	Predicted
488_S2_d ata_43_00 899	2.96016 2315	40042	LivJ - Branched- chain amino-acid ABC transport system periplasmic binding protein	Peripla_BP_ 6	Periplasmic binding protein	Periplasmic	Periplasmic	No	Signal peptide (Sec/SPI)	0.551509	No	No
488_S2_d ata_43_01 136	2.92431 2502	63638	HydB - Ni/Fe- hydrogenase large subunit	NiFeSe_Hases	Nickel- dependent hydrogenase	Cytoplasmic Membrane	Unknown	No	Other	0.397239	No	No

488_S2_d ata_43_01 023	2.62338 7524	10838	Putative periplasmic cytochrome C	Cytochrom_ C	Cytochrome c	Periplasmic	Periplasmic	Yes (1)	Signal peptide (Sec/SPI)	0.300833	No	No
------------------------------	-----------------	-------	---	-----------------	--------------	-------------	-------------	------------	--------------------------------	----------	----	----



The *Campylobacter jejuni* Type VI Secretion System Enhances the Oxidative Stress Response and Host Colonization

Janie Liaw¹, Geunhye Hong¹, Cadi Davies¹, Abdi Elmi¹, Filip Sima², Alexandros Stratakos², Lavinia Stef³, Ioan Pet³, Abderrahman Hachani^{1,4}, Nicolae Corcionivoschi^{2,3}, Brendan W. Wren¹, Ozan Gundogdu¹ and Nick Dorrell^{1*}

¹ Faculty of Infectious and Tropical Diseases, London School of Hygiene & Tropical Medicine, London, United Kingdom,

² Bacteriology Branch, Veterinary Sciences Division, Agri-Food and Biosciences Institute, Belfast, United Kingdom,

³ Bioengineering of Animal Science Resources, Banat University of Agricultural Sciences and Veterinary Medicine – King

Michael the I of Romania, Timisoara, Romania, ⁴ The Peter Doherty Institute for Infection and Immunity, Department of Microbiology and Immunology, University of Melbourne, Melbourne, VIC, Australia

OPEN ACCESS

Edited by:

Ignacio Arechaga,
University of Cantabria, Spain

Reviewed by:

Carlos J. Blondel,
Andres Bello University, Chile
Ina Attree,
Centre National de la Recherche
Scientifique (CNRS), France

*Correspondence:

Nick Dorrell
nick.dorrell@lshtm.ac.uk

Specialty section:

This article was submitted to
Microbial Physiology and Metabolism,
a section of the journal
Frontiers in Microbiology

Received: 28 March 2019

Accepted: 26 November 2019

Published: 17 December 2019

Citation:

Liaw J, Hong G, Davies C, Elmi A, Sima F, Stratakos A, Stef L, Pet I, Hachani A, Corcionivoschi N, Wren BW, Gundogdu O and Dorrell N (2019) The *Campylobacter jejuni* Type VI Secretion System Enhances the Oxidative Stress Response and Host Colonization. *Front. Microbiol.* 10:2864. doi: 10.3389/fmicb.2019.02864

The role of the Type VI secretion system (T6SS) in *Campylobacter jejuni* is poorly understood despite an increasing prevalence of the T6SS in recent *C. jejuni* isolates in humans and chickens. The T6SS is a contractile secretion machinery capable of delivering effectors that can play a role in host colonization and niche establishment. During host colonization, *C. jejuni* is exposed to oxidative stress in the host gastrointestinal tract, and in other bacteria the T6SS has been linked with the oxidative stress response. In this study, comparisons of whole genome sequences of a novel human isolate 488 with previously sequenced strains revealed a single highly conserved T6SS cluster shared between strains isolated from humans and chickens. The presence of a functional T6SS in the 488 wild-type strain is indicated by expression of T6SS genes and secretion of the effector TssD. Increased expression of oxidative stress response genes *katA*, *sodB*, and *ahpC*, and increased oxidative stress resistance in 488 wild-type strain suggest T6SS is associated with oxidative stress response. The role of the T6SS in interactions with host cells is explored using *in vitro* and *in vivo* models, and the presence of the T6SS is shown to increase *C. jejuni* cytotoxicity in the *Galleria mellonella* infection model. In biologically relevant models, the T6SS enhances *C. jejuni* interactions with and invasion of chicken primary intestinal cells and enhances the ability of *C. jejuni* to colonize chickens. This study demonstrates that the *C. jejuni* T6SS provides defense against oxidative stress and enhances host colonization, and highlights the importance of the T6SS during *in vivo* survival of T6SS-positive *C. jejuni* strains.

Keywords: campylobacter, type 6 secretion system, oxidative stress, chicken colonization, catalase, superoxide dismutase

INTRODUCTION

Campylobacter jejuni, a Gram-negative microaerophilic bacteria, is the leading cause of bacterial foodborne gastroenteritis worldwide. *C. jejuni* infection in humans can lead to diarrhea, vomiting, abdominal pain, fever, with symptoms generally appearing 2–5 days following exposure to an infectious dose as low as 500–900 bacteria (Robinson, 1981; Kaakoush et al., 2015). Disease

presentation can vary depending on geographical region, with infections in low- and middle-income countries typically presenting with watery, non-inflammatory diarrhea whilst infections in high income countries display more severe disease, presenting with bloody inflammatory diarrhea (Coker et al., 2002). Campylobacteriosis is generally self-limiting, however, around 1 in 1,000 cases can develop severe auto-immune complications such as Guillain-Barré syndrome or Miller Fisher syndrome (Ang et al., 2001).

Campylobacter jejuni is most commonly transmitted through the handling and consumption of raw or undercooked poultry, but can also be spread through unpasteurized milk, contaminated water and cross contamination with other foods (Young et al., 2007; Kaakoush et al., 2015). *C. jejuni* colonizes chickens and other avian species and an estimated 70% of raw chicken sold in supermarkets in the United Kingdom will be contaminated with *C. jejuni* (Kaakoush et al., 2015). *C. jejuni* was previously regarded as a harmless commensal in the digestive tract of chickens, but recent studies indicate that colonization by *C. jejuni* is not asymptomatic, resulting in weight loss and slow growth of the infected poultry (Hermans et al., 2012; Wigley, 2015). The spread of *C. jejuni* through chicken flocks in farms can have a vast economic impact on the poultry industry and an increased spread of *C. jejuni* in chickens can subsequently affect the rates of infection in humans (Newell and Fearnley, 2003; Skarp et al., 2016).

During host colonization and infection, *C. jejuni* is exposed to conditions in the host gastrointestinal tract that present as physical and chemical stresses, including oxidative stress (Kim et al., 2015; Flint et al., 2016). Oxidative stress involves the generation of reactive oxygen species (ROS) that cause damage to nucleic acids, membranes and proteins of bacteria. In order to survive in this hostile environment, *C. jejuni* must defend against oxidative stress with enzymes that degrade ROS, such as SodB (superoxide dismutase), KatA (catalase), and AhpC (hydroperoxide reductase) (Kim et al., 2015). Regulation of the *C. jejuni* oxidative stress response is controlled by multiple regulatory mechanisms involving PerR, Fur and CosR to respond to fluctuating levels of ROS. Two MarR-type transcriptional regulators, RrpA and RrpB, also play a role in oxidative stress response regulation (Gundogdu et al., 2015).

The Type VI Secretion System (T6SS) is a contact-dependent secretion machinery capable of delivering effector proteins to both prokaryotic and eukaryotic cells. First identified in *Vibrio cholerae* and *Pseudomonas aeruginosa*, the T6SS has since been found to be present in 25% of Gram-negative bacterial species (Mougous et al., 2006; Pukatzki et al., 2006). The structure of the T6SS resembles an inverted bacteriophage tail with homologous components. The T6SS consists of 13 core components (TssA-TssM) and accessory proteins such as the T6SS-associated gene (Tag) proteins (see Table 1). A functioning T6SS complex requires essential components such as the baseplate (TssEFGK), a membrane-anchoring structure (TssJLM), a contractile sheath (TssBC) wrapped around a needle-like tube (TssD) and a puncture tip (TssI) further sharpened by a spike (TagD) (Cianfanelli et al., 2016). Composed of interlocking TssB and TssC components, the contractile sheath

TABLE 1 | Components of the bacterial Type VI Secretion System.

TSS system	Orthologs	Putative function/location
TssA	VasJ/ImpA	Docks to membrane complex, recruits baseplate complex, initiates/coordinates polymerization of TssD with sheath
TssB	VipA/ImpB	Contractile sheath
TssC	VipB/ImpC	Contractile sheath
TssD	Hcp	Secreted tube, effector
TssE	HsiF	Baseplate
TssF	VasA/ImpG	Baseplate
TssG	VasB/ImpH	Baseplate
TssH	ClpV/VasG	AAA+ATPase, sheath recycling
TssI	VgrG	Expelled spike, effector
TssJ	VasD/Lip/SciN	Membrane complex
TssK	VasE/ImpJ	Baseplate
TssL	IcmH/DotU/VasF	Membrane complex
TssM	IcmF/VasK	Membrane complex
TagD	PAAR	Tip of expelled spike

is responsible for producing enough energy to force the TssD needle-like structure through the inner membrane out into the extracellular space and puncture a host membrane to deliver effector proteins (Cianfanelli et al., 2016; Salih et al., 2018). The extended contractile sheath is broken down and the components recycled by the TssH ATPase for further sheath assembly (Kapitein et al., 2013).

Delivery of effector proteins by the T6SS to target cells can exert a number of effects including colonization and niche establishment (Kapitein and Mogk, 2014; Ma et al., 2014; Drebes Dorr and Blokesch, 2018). T6SS effectors can target and eliminate bacterial and fungal competitors and also affect eukaryotic host cells (Murdoch et al., 2011; Trunk et al., 2018). To prevent self-intoxication by effector proteins, bacteria with the T6SS possess immunity proteins to neutralize the effects of the toxins (Kirchberger et al., 2017; Ringel et al., 2017; Fitzsimons et al., 2018). In competition with prokaryotic targets, T6SS can act either defensively or offensively; for example, the T6SS of *V. cholerae* and *Serratia marcescens* are offensive, apparently firing constantly and indiscriminately into the surrounding space, whilst the defensive T6SS of *P. aeruginosa* reacts only when fired upon in a "tit-for-tat" response (Gerc et al., 2015). T6SS effectors can subvert host cell processes by manipulating the host cytoskeleton, hindering host defense mechanisms, modulating the host inflammatory response and modifying host membrane structure (Hachani et al., 2016).

The T6SS can also defend against the production of ROS through secretion of effectors. For example, the T6SS-4 of *Yersinia pseudotuberculosis* secretes the effector YezP, which is able to bind to and sequester zinc ions and protect the bacteria from the effects of oxidative stress (Wang et al., 2015). The T6SS-4 of *Burkholderia thailandensis* also secretes effectors TseM for the uptake of manganese ions and TseZ for the uptake of zinc ions to mitigate the effects of oxidative stress. Similarly, enterohemorrhagic *Escherichia coli* secretes a T6SS effector, KatN, which facilitates survival of the bacteria in macrophages through decreasing the level of intracellular ROS (Wan et al., 2017).

Studies examining the prevalence of the T6SS in *C. jejuni* in Asia and Europe found a large variation in prevalence between regions. Harrison et al. (2014) observed in 2014 that up to 70% of isolates from chickens and humans in Vietnam were positive for the T6SS, whilst approximately only 3% of similar isolates from the United Kingdom were T6SS-positive. A further study in 2015 examining chicken isolates in Spain found a prevalence of 14%, whilst another study found that 28.8% of chicken isolates in Northern Ireland were T6SS-positive (Corcionivoschi et al., 2015; Ugarte-Ruiz et al., 2015). Other *Campylobacter* species can also carry the T6SS; the same study in Northern Ireland observed that 56.1% of *C. coli* found in retail chickens were T6SS-positive (Corcionivoschi et al., 2015). However, the large variation in prevalence may be due to differences in sample sizes, sample sources and in detection methods. Recent data suggests that the T6SS is becoming increasingly prevalent in *C. jejuni* strains, with indications that T6SS-positive strains are becoming more prevalent than T6SS-negative strains infecting chickens in farms, on raw poultry in supermarkets and even in hospital patients in the United Kingdom (Carmel Kelly, Agri-Food and Biosciences Institute, Personal Communication). A recent study in 2018 examining the presence of *C. jejuni* in wild birds of Finland observed that 49% of western jackdaw isolates and 72% of mallard duck isolates were T6SS-positive (Kovanen et al., 2018). This emphasizes the need to understand the role of the T6SS in *C. jejuni* and to develop intervention strategies to combat the rise of T6SS-positive *C. jejuni* strains (Sima et al., 2018).

In contrast to *V. cholerae* and *P. aeruginosa*, the role of the T6SS in *C. jejuni* is poorly understood. To date, only one *C. jejuni* T6SS cluster expressing a single TssD has been identified, compared to *P. aeruginosa* and *Yersinia pseudotuberculosis* which both possess multiple T6SS clusters exhibiting different functions (Lertpiriyapong et al., 2012). The structure of the *C. jejuni* T6SS is yet to be solved and TssD is thus far the only effector protein identified to be secreted by the *C. jejuni* T6SS (Lertpiriyapong et al., 2012; Bleumink-Pluym et al., 2013). Previous studies have demonstrated the *C. jejuni* T6SS may be important in host cell adherence and invasion, colonization, survival in bile salts and contact-dependent cytotoxicity toward red blood cells (Lertpiriyapong et al., 2012; Bleumink-Pluym et al., 2013). A recent study examined the structure of the TssD effector in *C. jejuni* and found that TssD is cytotoxic toward HepG2 human liver carcinoma cells (Noreen et al., 2018). However, whether the T6SS plays a role in the survival and infection of *C. jejuni* in poultry, a primary reservoir in humans is still unknown.

In this study, we investigated the role of the *C. jejuni* T6SS through whole genome sequencing of a T6SS-positive 488 wild-type strain (a recent human isolate from Brazil). We also sequenced the T6SS-positive 43431 wild-type strain (a human isolate from Canada) (Penner et al., 1983). We constructed defined isogenic mutants for genes encoding the contractile sheath components TssBC and needle structure TssD in the 488 wild-type strain and performed *in vitro* and *in vivo* characterization experiments in biologically relevant models. Our findings indicate that a functional T6SS is present in the *C. jejuni* 488 wild-type strain and the presence of

the T6SS is important in defending against oxidative stress and enhancing *in vivo* survival, potentially thereby allowing strains harboring the T6SS to colonize and dominate in specific niches within a host.

RESULTS

Bioinformatic Analysis of T6SS Gene Clusters in *C. jejuni* 488 and Other T6SS-Positive Wild-Type Strains Reveals Synteny

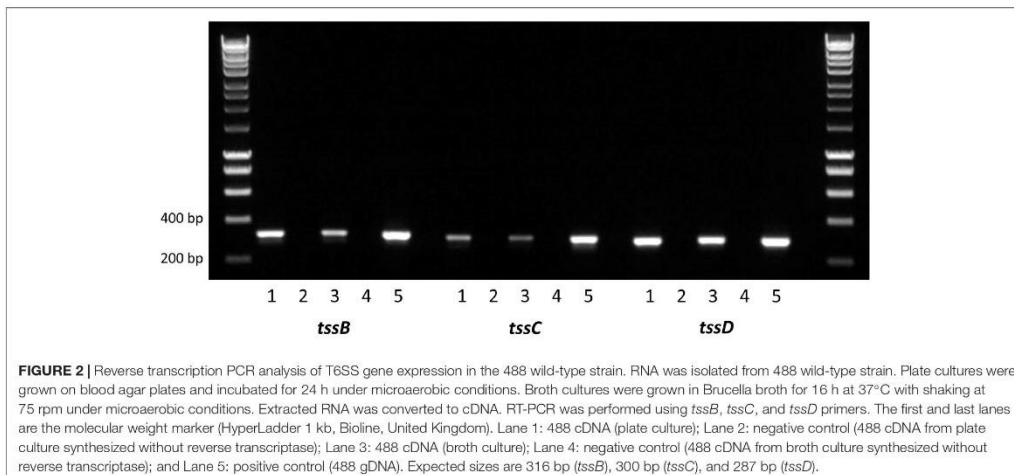
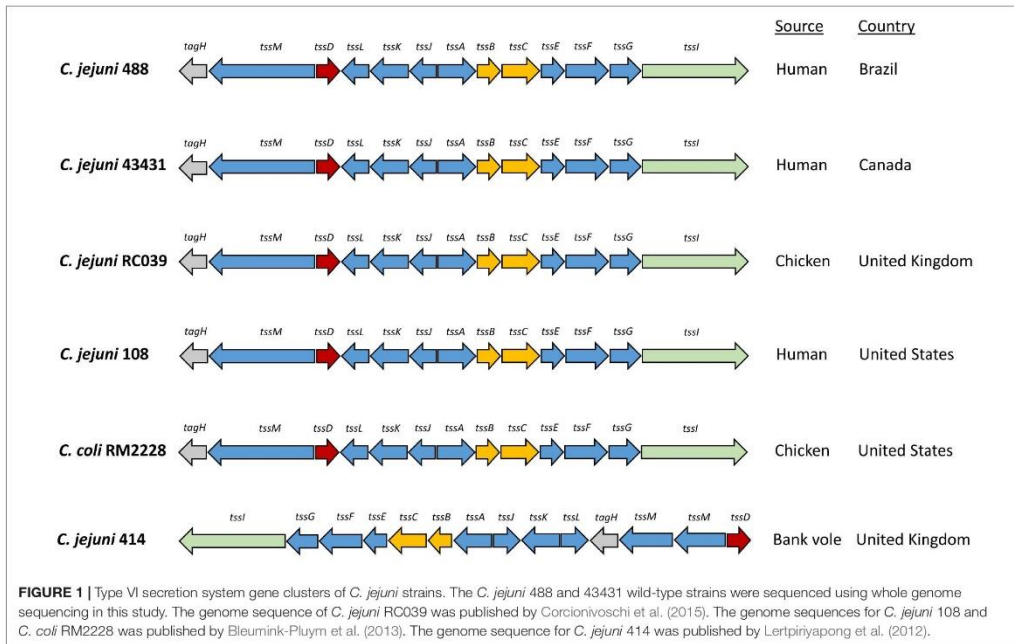
Whole genome sequencing of *C. jejuni* 488 wild-type strain (a recent human isolate from Brazil) and *C. jejuni* wild-type strain 43431 (a human isolate from Canada) (Penner et al., 1983) was performed. *C. jejuni* wild-type strain RC039 (a chicken isolate from Northern Ireland) was previously sequenced (Corcionivoschi et al., 2015). The presence of a single T6SS cluster was observed in all three strains. All T6SS core components were identified, however, the TssH (ClpV) ATPase responsible for disassembly of the contractile sheath components is absent from the T6SS cluster of all *C. jejuni* strains sequenced thus far. The genome coordinates of the T6SS cluster in the *C. jejuni* 488 strain is listed in **Supplementary Table S1**. Comparisons of the 488, 43431, and RC039 genome sequences with previously published sequences for other T6SS-positive *C. jejuni* strains (Lertpiriyapong et al., 2012; Bleumink-Pluym et al., 2013) revealed a T6SS cluster that is highly conserved, sharing synteny between strains and also with other *Campylobacter* species isolated from humans and chickens (**Figure 1**). The 414 strain, isolated from wild bank voles in the United Kingdom, has a different gene arrangement in the T6SS cluster, but the same core components are still present.

T6SS Genes *tssB*, *tssC* *tssD* Are Expressed in the 488 Wild-Type Strain

Composed of interlocking TssB and TssC proteins, the contractile sheath is responsible for producing enough energy to force the TssD needle-like structure through the inner membrane out into the extracellular space and across host membranes (Cianfanelli et al., 2016). To investigate whether the *C. jejuni* 488 wild-type strain has a functional T6SS, the expression of the contractile sheath genes *tssB* and *tssC* as well as the *tssD* gene was investigated using RT-PCR. *tssB*, *tssC* *tssD* were all found to be expressed when the 488 wild-type strain is grown both in broth culture for 16 h and on blood agar for 24 h, indicating that the *C. jejuni* T6SS contractile sheath is produced under different growth conditions (**Figure 2**).

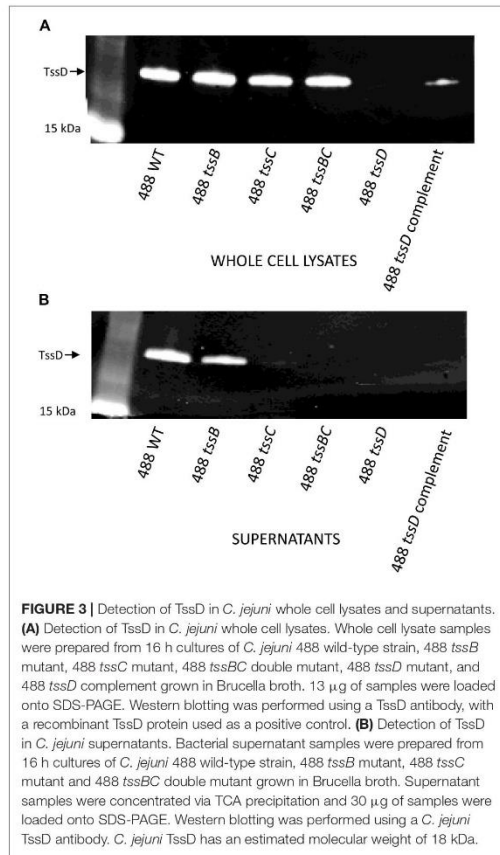
C. jejuni 488 Wild-Type Strain Has a Functional T6SS That Secretes TssD

Previous studies have used the secretion of TssD as evidence that the T6SS is functional in *C. jejuni* (Lertpiriyapong et al., 2012; Bleumink-Pluym et al., 2013). In order to determine whether the T6SS in the 488 wild-type strain is functional,



Western blotting was performed using a TssD antibody to detect the secretion of TssD. TssD is an approximately 18 kD protein that makes up the needle-like structure of the T6SS and has been shown in other bacteria to be important in the secretion of effector proteins (Cianfanelli et al., 2016). TssD is

present in the whole cell lysate (Figure 3A) and also secreted into the supernatant of the 488 wild-type strain (Figure 3B), indicating that this strain has a functional T6SS. TssD is absent from both whole cell lysate and supernatant from the 488 *tssD* mutant.



Inactivation of Individual Contractile Sheath Components Does Not Abolish *C. jejuni* T6SS Function

488 *tssB* and *tssC* single mutants were constructed to investigate whether knocking out a contractile sheath component would result in a non-functional T6SS. Inactivation of either *tssB* or *tssC* reduces but does not completely abolish secretion of TssD (Figure 3B), indicating that the absence of one of the contractile sheath components does not result in a completely non-functional T6SS in *C. jejuni*. A 488 *tssBC* double mutant was also constructed to test the hypothesis that function of the *C. jejuni* T6SS is only abolished in the absence of both contractile sheath components. As hypothesized, TssD was present in the whole cell lysate but absent from the supernatant of the 488 *tssBC* double mutant, thereby demonstrating that the *C. jejuni* T6SS is not functional when the entire contractile sheath structure is missing.

T6SS in *C. jejuni* Is Associated With the Oxidative Stress Response

The T6SS has previously been linked with the oxidative stress response in *Y. pseudotuberculosis*, *B. thailandensis*, and enterohemorrhagic *E. coli* (Wang et al., 2015; Si et al., 2017; Wan et al., 2017). To investigate whether the *C. jejuni* T6SS is also associated with the oxidative stress response, the 488 wild-type strain, 488 *tssD* mutant and 81–176 wild-type strain were exposed to hydrogen peroxide (H_2O_2). Following 30 min exposure to 50 mM H_2O_2 , the 488 wild-type strain exhibited significantly greater resistance to oxidative stress killing compared to the 488 *tssD* mutant and the 81–176 wild-type strain (Figure 4A). In order to investigate whether the increased susceptibility of the 488 *tssD* mutant to H_2O_2 is specific and not due to a potential membrane defect due to improper assembly of the T6SS in the bacterial membrane, antimicrobial susceptibility testing for the 488 wild-type strain, 488 *tssD* mutant and 488 *tssD* complement were performed. Disk diffusion assays were performed using ampicillin, amoxicillin/clavulanic acid, tetracycline and polymyxin B. A broth microdilution assay was performed using vancomycin. No differences in antimicrobial susceptibility were observed (Supplementary Table S2).

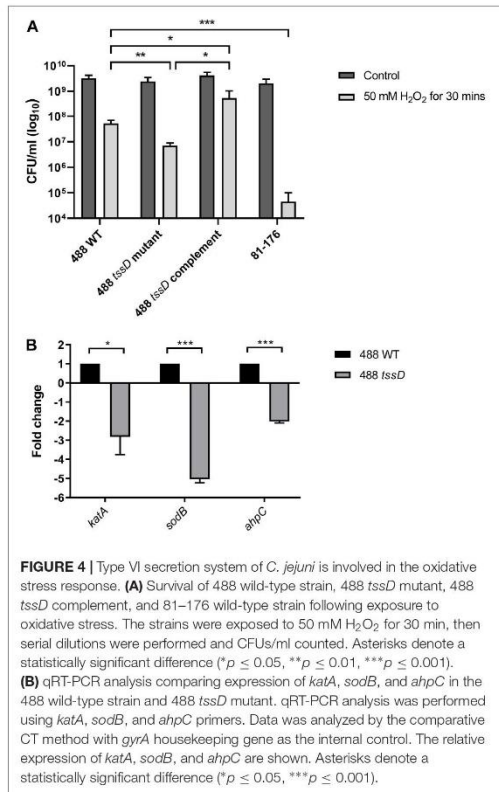
kata, *sodB*, and *ahpC* encode proteins involved directly in the breakdown of ROS. Expression of *kata*, *sodB*, and *ahpC* was investigated in the 488 wild-type strain and 488 *tssD* mutant using qRT-PCR. Expression of all three genes were significantly reduced in the 488 *tssD* mutant compared to the 488 wild-type strain. This data combined with the increased ability of the 488 wild-type strain to survive the effects of oxidative stress suggest that the T6SS is associated with the oxidative stress response in *C. jejuni* (Figure 4B).

T6SS Increases *C. jejuni* Cytotoxicity in the *Galleria mellonella* Model of Infection

The larvae of *G. mellonella* (Greater wax moth) are an established model to study the pathogenesis of *C. jejuni* (Senior et al., 2011). In order to investigate whether the presence of a T6SS in *C. jejuni* enhances bacterial cytotoxicity, *G. mellonella* larvae were injected with *C. jejuni* strains and larvae survival examined over a duration of 5 days. Only the T6SS-positive 488 wild-type strain was cytotoxic to *G. mellonella* larvae after 24 h post-injection (Figure 5). The T6SS-negative 81–176 wild-type strain also exhibited some cytotoxicity, but at a lower level compared to the 488 wild-type strain after 48 and 72 h. After 96 and 120 h, cytotoxicity of the 488 *tssD* mutant was also observed but at a significantly lower level than the 488 wild-type strain.

T6SS Enhances Both *C. jejuni* Interactions With and Invasion of Chicken Primary Intestinal Cells

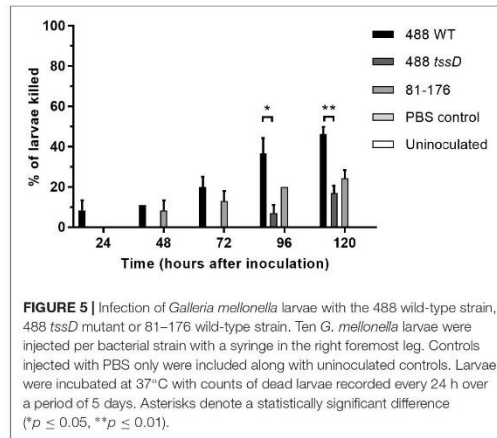
Recent studies suggest that the prevalence of T6SS-positive *C. jejuni* strains is on the rise in high-income countries and there are indications that T6SS-positive strains are now prevalent over T6SS-negative strains infecting chickens in farms, on raw chicken in supermarkets and in hospital patients (Ugarte-Ruiz et al., 2015; Sima et al., 2018). To investigate whether the presence of the



T6SS plays a role in the ability of *C. jejuni* to infect chickens, an *in vitro* model was used to examine the potential of *C. jejuni* to adhere to and invade chicken primary intestinal cells. The 488 wild-type strain exhibited significantly higher levels of adherence and invasion than the 488 *tssD* mutant. The T6SS-negative 81-176 wild-type strain also exhibited lower levels of adherence and invasion than the 488 wild-type strain, however, these differences were not significant (Figure 6).

T6SS Enhances the Ability of *C. jejuni* to Infect Chickens

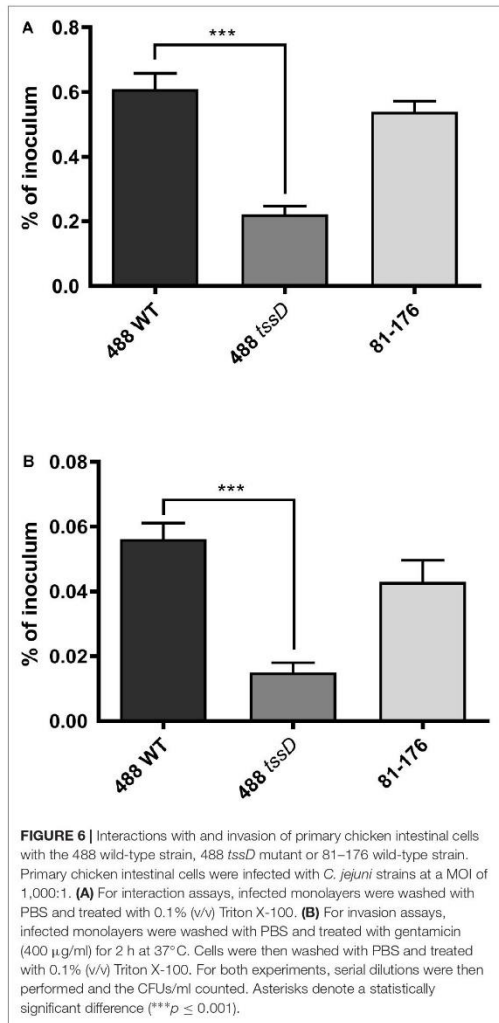
To further investigate whether the presence of the T6SS plays a role in the ability of *C. jejuni* to infect chickens, chicken infection studies were performed. An identical pattern was observed after *in vivo* infection of 15-day old Ross 308 broiler chickens, where at 3 days post-infection the numbers of the 488 wild-type strain detected in the caeca were significantly higher than the numbers of the 488 *tssD* mutant or 81-176 wild-type strain (Figure 7). These results indicate that the presence of the T6SS is important in enhancing the ability of *C. jejuni* to colonize chickens.



DISCUSSION

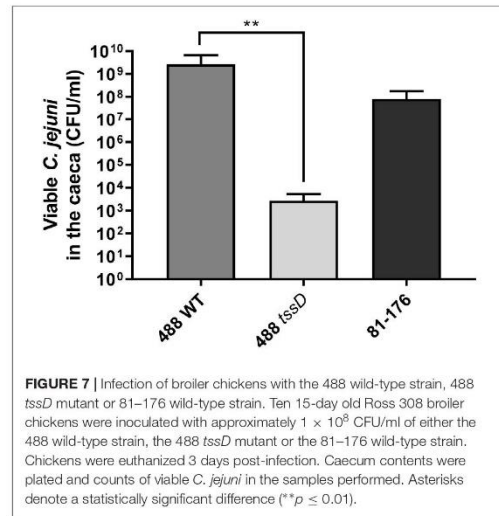
The *C. jejuni* T6SS is a functional secretory mechanism that appears distinct from the well-elucidated *P. aeruginosa* and *V. cholerae* T6SS model systems. Whole genome sequencing of a novel 488 strain and the T6SS-positive 43431 strain revealed a single T6SS cluster containing one copy of the *tssD* gene that encodes the needle-like tube of the T6SS, but the absence of *tssH* which encodes the ATPase that breaks down and recycles the TssBC contractile sheath. This is in contrast to the T6SS model systems of *P. aeruginosa* and *V. cholerae* where multiple T6SS clusters are present with differing functions. The absence of a *tssH* ortholog had previously been observed in other *C. jejuni* strains in other studies (Lertpiriyapong et al., 2012; Bleumink-Pluym et al., 2013). *Burkholderia* species, *Helicobacter hepaticus*, *Francisella tularensis*, and *Salmonella enterica* also appear to lack a TssH component. Despite the absence of TssH, the presence of a functional T6SS in all these organisms including *C. jejuni* suggests there may be alternate mechanisms for contractile sheath recycling. In *V. cholerae* a study demonstrated that whilst TssH is not essential, it is important in increasing the efficiency of the T6SS in inter-bacterial competition assays (Bachmann et al., 2015).

Comparison of the *C. jejuni* strains sequenced in this study with previously published sequences of other *C. jejuni* strains as well as other *Campylobacter* species revealed a T6SS cluster that is very closely conserved with all core genes present in the same arrangement. *C. jejuni* 488 (human isolate from Brazil), 43431 (human isolate from Canada), 108 (human isolate from the United States), RC039 (chicken isolate from the United Kingdom), and even *C. coli* RM2228 (chicken isolate from the United States) all share the same conserved T6SS cluster. Only *C. jejuni* 414 had a different gene arrangement in the T6SS cluster. 414 is an environmental strain, isolated from a wild bank vole in the United Kingdom (Williams et al., 2010). It is possible that agricultural intensification practices which readily facilitate



passing of strains between chickens and humans could lead to these strains to share more of a conserved T6SS compared to the 414 environmental strain.

Further investigations indicated that the novel 488 strain has a functional T6SS capable of secreting the TssD effector, corroborating previous studies which have shown TssD to be secreted from 43431 and 108 strains (Lertpiriyapong et al., 2012; Bleumink-Pluyem et al., 2013). However, the contractile sheath components TssBC and their function had not previously been studied in *C. jejuni*. In other bacteria, an intact contractile sheath structure is important for a fully functioning T6SS as removal



of either TssB/VipA or TssC/VipB from the contractile sheaths described in *V. cholerae* result in a defective T6SS unable to secrete effectors (Basler et al., 2012; Kudryashev et al., 2015; Brackmann et al., 2018). In this study we have shown that both contractile sheath genes are expressed when the 488 strain is cultured in broth and on solid plates. Isogenic 488 *tssB* and *tssC* mutants were constructed and shown to still be able to secrete TssD at a reduced level compared to the wild-type strain. The observation that the *C. jejuni* T6SS does not require both TssB and TssC components to be present for the T6SS to be able to secrete TssD is unusual and differs from previous observations of the T6SS in *V. cholerae*. This suggests that in *C. jejuni*, as long as either TssB or TssC is present, the T6SS remains capable of secreting TssD at a reduced level. However, this does not suggest that the contractile sheath components in *C. jejuni* may differ from those in the T6SS model systems of *P. aeruginosa* and *V. cholerae*, rather that the contractile sheath components may be interchangeable or be able to compensate for the absence of the other component via a yet unknown process.

The importance of the T6SS in countering the effects of oxidative stress has previously been shown in *Y. pseudotuberculosis*, *B. thailandensis*, and enterohemorrhagic *E. coli* (Wang et al., 2015; Si et al., 2017; Wan et al., 2017). In this study, we show that the *C. jejuni* T6SS also appears to play a role, with the genes that encode Kata, SodB, and AhpC that are involved directly in the breakdown of ROS all expressed at significantly higher levels in the 488 wild-type strain compared to the 488 *tssD* mutant. The 488 wild-type strain with an intact T6SS is also more resistant to the effects of oxidative stress compared to the 488 *tssD* mutant. We speculate that TssD positively regulates the expression of genes involved in the breakdown of ROS, and in turn this results in greater resistance to oxidative stress in strains harboring an intact T6SS cluster.

A MarR family transcriptional regulator TctR was recently shown to regulate the T6SS-2 gene cluster in *B. pseudomallei* (Losada et al., 2018). Previous studies have also shown that the MarR family transcriptional regulators RrpA and RrpB are important in regulating both oxidative and aerobic stress responses in *C. jejuni* and therefore play a role in enhancing bacterial survival both in the hosts and in the environment (Gundogdu et al., 2011, 2015, 2016). As our results indicate that the *C. jejuni* T6SS is also associated with the oxidative stress response, it is tempting to speculate that the RrpA and RrpB regulators may in some way be linked to the T6SS. Further studies will be required to investigate this hypothetical link.

Based on our data we propose that presence of the T6SS cluster in *C. jejuni* strains also confers a competitive advantage to these strains within a host. The T6SS-positive 488 wild-type strain is more cytotoxic in the *G. mellonella* model than the T6SS-negative 81-176 wild-type strain and the 488 *tssD* mutant. This suggests that the presence of a T6SS increases the cytotoxicity of *C. jejuni* in the *G. mellonella* model of infection and secreted T6SS effectors may also be important in causing cytotoxicity to other organisms. The 81-176 strain was selected as a negative control in this study due to the absence of the T6SS in this strain. Despite lacking the T6SS, 81-176 is a hypervirulent strain capable of causing severe disease and harbors two plasmids, pTet and pVir, that play a role in increased virulence (Black et al., 1988; Bacon et al., 2000). Therefore, any differences observed between 488 and 81-176 could potentially be due to a diversity of virulence factors in these two strains rather than the presence or absence of the T6SS.

This study is the first to examine the role of T6SS of *C. jejuni* in a biologically relevant model. Lertpiriyapong et al. (2012) utilized a murine model and found that a T6SS-positive strain to be more interactive with and invasive in RAW 264.7 macrophage cells and have a higher colonization potential in IL-10-deficient mice. However, it has previously been shown that *C. jejuni* does not colonize mice in the same manner as in chickens, as *C. jejuni* colonizes mice at a significantly slower rate than chickens and some strains such as 81-176 do not appear to colonize mice at all (Wilson et al., 2010). The *C. jejuni* 488 wild-type strain exhibits higher levels of adherence to and invasion of chicken cells and is also able to infect chickens at a much higher rate than the *tssD* mutant. The results indicate that the ability of *C. jejuni* to infect chickens is enhanced by the presence of the T6SS and the T6SS may be important as a colonization factor in the natural host of *C. jejuni*. The increased ability of *C. jejuni* strains with the T6SS to infect and colonize chickens is a particular concern for the agricultural and food industries tasked with reducing *C. jejuni* load in both live chickens on farms and on raw chicken meat in the supermarket (Sima et al., 2018). From a public health perspective, the rise of T6SS in *C. jejuni* is also problematic as there are indications that strains with the T6SS may cause more severe disease in humans (Harrison et al., 2014).

In summary, in this study we confirmed the presence of a single T6SS cluster among several *C. jejuni* strains and confirmed that the functional T6SS is capable of secreting the TssD effector. Our results indicated that the *C. jejuni* T6SS is involved in the oxidative stress response. Using *in vitro* and *in vivo* models we demonstrated the increased ability of T6SS-positive *C. jejuni*

to colonize the natural avian host. Our findings highlight the importance of further understanding the function of the T6SS present in an expanding population of *C. jejuni*, the potential importance of the T6SS in colonization and niche establishment in different hosts and the potential for T6SS-positive *C. jejuni* strains to cause more severe disease in both chickens and humans.

MATERIALS AND METHODS

Bacterial Strains and Growth Conditions

Campylobacter jejuni strains used in this study are listed in **Supplementary Table S3**. *C. jejuni* strains were grown at 37°C under microaerobic conditions (85% N₂, 15% CO₂, 5% O₂) in a variable atmosphere chamber (Don Whitley Scientific, United Kingdom). Unless otherwise stated, *C. jejuni* were grown either on Columbia agar with 7% (v/v) horse blood (TCS Biosciences, United Kingdom) with the addition of Skirrow *Campylobacter* selective supplement or in Brucella broth (BD Diagnostics, United Kingdom). *E. coli* strains listed in **Supplementary Table S4** were grown on lysogeny broth (LB) agar plates or in LB broth at 37°C. The appropriate antibiotics were added as required at concentrations of 50 µg/ml kanamycin, 100 µg/ml ampicillin or 10 µg/ml chloramphenicol for *C. jejuni* growth, with the concentration of chloramphenicol for *E. coli* growth increased to 50 µg/ml. All reagents were obtained from Oxoid (United Kingdom) unless otherwise stated.

Whole Genome Sequencing

Genome sequencing of the *C. jejuni* 488 and 43431 (Poly et al., 2004) wild-type strains was performed as previously described by Ugarte-Ruiz et al. (2014). Briefly, sequencing was performed using the Illumina MiSeq 2 × 301 bp paired-end sequencing. To analyze the data quality, FastQC was used (Simon, 2010) followed by read trimming using Trimmomatic (v0.32) (leading' and "trailing" setting of 3, a "sliding window" setting of 4:20 and a "minlength" of 36 nucleotides) (Bolger et al., 2014). Reads were mapped using BWA-MEM (v0.7.7-r441) against the genome sequence of *C. jejuni* NCTC 11168 (AL111168) (Li and Durbin, 2009). Assembly on unmapped regions was performed using Velvet Optimizer (v2.2.5) using n50 optimization (Zerbino and Birney, 2008; Gladman and Seemann, 2012). Contigs were ordered against *C. jejuni* NCTC 11168 (AL111168) strains using ABACAS (v1.3.1) (Assefa et al., 2009). Genome annotation was performed using Prokka (Seemann, 2014). Genomes were visualized using Artemis and ACT software (Carver et al., 2012). T6SS ORFs were identified using BLAST (Altschul et al., 1990; Gish and States, 1993). The 488 and 43431 genome sequences were uploaded to the EBI ENA database (Accession number PRJEB31331).

Reverse Transcription PCR (RT-PCR) and Quantitative Real-Time PCR (qRT-PCR) Analyses

Total RNA was isolated using PureLink RNA Mini Kit (Thermo Fisher Scientific) from *C. jejuni* cultures grown for 16 h at

37°C with shaking at 75 rpm under microaerobic conditions in Brucella broth. TURBO DNA-free kit (Thermo Fisher Scientific) was used to remove DNA contamination and RNA was converted to cDNA using the SuperScript III First-Strand Synthesis System (Thermo Fisher Scientific). Reverse transcription PCR (RT-PCR) was performed according to the manufacturer's instructions with primers listed in **Supplementary Table S5**. Quantitative real-time PCR (qRT-PCR) was performed using primers listed in **Supplementary Table S5**, with SYBR Green Master Mix (Applied Biosystems, United Kingdom) on the ABI 7500 Real-Time PCR System machine (Applied Biosystems). qRT-PCR data was analyzed by the comparative C_T method with *gyrA* housekeeping gene as an internal control (Ritz et al., 2002; Schmittgen and Livak, 2008).

Construction of *tssB*, *tssC*, *tssD* Mutants and *tssBC* Double Mutant

Campylobacter jejuni mutants were constructed as previously described (Gundogdu et al., 2011). Briefly, the appropriate gene specific primers (see **Supplementary Table S5**) were used to amplify the gene of interest from *C. jejuni* genomic DNA. PCR products were cloned into a pGEM-T Easy vector (Promega, United Kingdom) and transformed into *E. coli* XL2-Blue if the unique restriction site was *Bam*HI or *Bgl*II. *E. coli* SCS110 were used if the restriction site was *Bcl*I. If none of these sites were present, inverse PCR mutagenesis was used to introduce a *Bgl*II site (Gundogdu et al., 2015). Plasmid DNA was digested with *Bam*HI, *Bcl*I, or *Bgl*II, a kanamycin or chloramphenicol resistance cassette was inserted and the resulting construct transformed into *E. coli*. Successful constructs were transformed into *C. jejuni* by electroporation and positive clones were confirmed by PCR and Sanger sequencing. For construction of a *C. jejuni tssBC* double mutant, the plasmid DNA construct used for the *C. jejuni tssC* mutant was transformed into *C. jejuni tssB* mutant by electroporation.

Preparation of Whole Cell Lysates and Supernatants for Protein Secretion Assays

Campylobacter jejuni strains from 24 h plate cultures were inoculated to OD₆₀₀ 0.1 in Brucella broth and incubated at 37°C with shaking at 75 rpm under microaerobic conditions until late log phase. The broth cultures were centrifuged at 4,000 rpm at 4°C for 30 min to separate the pellet and the supernatant.

To prepare a whole cell lysate sample, a pellet was re-suspended in PBS and sonicated for 10 min on high setting using a Bioruptor (Diagenode, Belgium). Sonicated samples were centrifuged at 13,000 rpm for 5 min and the resulting supernatant was added to 2X Laemmli sample buffer (Sigma-Aldrich, United Kingdom) then boiled at 95°C for 10 min, followed by centrifugation at 13,000 rpm for 5 min. To prepare a supernatant sample, supernatant was filtered through a 0.2 µm-pore-size filter (Millipore, United Kingdom) to remove remaining cells and the titrate was concentrated using an Amicon Ultra-15 centrifugal filter (10 kDa) (Millipore). Trichloroacetic acid (TCA) precipitation with acetone washes was performed to

further concentrate the samples as described previously (Link and LaBaer, 2011). Following acetone washes, the pellet was re-suspended in 2X Laemmli sample buffer and boiled at 95°C for 10 min, followed by centrifugation at 13,000 rpm for 5 min.

SDS-PAGE and Western Blot Analysis

BCA assay was performed to determine protein concentration in samples. 13 µg of whole cell lysate samples and 30 µg of supernatant samples were loaded along with PAGERuler Plus Pre-stained Protein Ladder (Thermo Fisher Scientific, United Kingdom) onto NuPAGE Bis-Tris gel (12%) (Thermo Fisher Scientific) with MOPS running buffer (Thermo Fisher Scientific). Membrane transfer was performed using the iBlot 2 Dry Blotting System (Thermo Fisher Scientific). The membrane was blocked with 2% (w/v) milk overnight at 4°C, incubated with the TssD antibody in phosphate buffered saline with 0.1% (v/v) Tween-20 (PBS-T) for 1 h at room temperature, washed with PBS-T then incubated with the secondary goat anti-rabbit antibody in PBS-T for 1 h at room temperature. The membrane was washed twice with PBS-T, once with PBS scanned using the Odyssey Imaging System (LI-COR Biosciences, United Kingdom).

TssD Antibody Production

The polyclonal anti-TssD antibody was produced by Capra Science Antibodies AB (Sweden). The *tssD* gene cloned into an expression vector and recombinant TssD protein was isolated and purified. For production of the TssD antiserum, purified TssD was immunized into a rabbit. Two boosts with the antigen were performed, followed by the first bleed. A further boost with the antigen was performed followed by the second bleed; the process was repeated for a third bleed. Antiserum collected from the third bleed was affinity purified using a peptide-coupled column for the anti-TssD antibody.

Oxidative Stress Assay

Campylobacter jejuni from 24 h plate cultures were re-suspended in PBS, the OD₆₀₀ was measured and the suspension adjusted with PBS to OD₆₀₀ 1.0. Bacterial suspensions were exposed to 50 mM H₂O₂ for 30 min at 37°C stationary under microaerobic conditions. Serial dilutions were performed and dilutions plated onto blood agar plates. Plates were incubated at 37°C under microaerobic conditions and colonies counted after 48 h.

Antimicrobial Susceptibility Assays

The disk diffusion assays were performed with ampicillin (10 µg), amoxicillin/clavulanic acid (2:1, 30 µg), tetracycline (30 µg) or polymyxin B (300 units) disks (Oxoid) following the methodology published by the European Society of Clinical Microbiology (EUCAST) (EUCAST, 2019). Zones of growth inhibition were measured in millimeters and sensitivity (S) determined based on the EUCAST guidelines. Broth microdilution assays were performed with vancomycin (Sigma) and the minimum inhibitory concentration (MIC, µg/ml) was determined according to the methodology published by Wiegand et al. (2008).

Galleria mellonella Model of Infection

Galleria mellonella larvae were purchased from Livefoods Direct (United Kingdom). Bacterial cells harvested from 24 h plate cultures were re-suspended in PBS and OD₆₀₀ adjusted to 0.1. Ten *G. mellonella* larvae per bacterial strain were injected with 10 µl bacterial suspension with a micro syringe (Hamilton, Switzerland) in the right foremost leg. Controls injected with PBS or not injected were also prepared. Larvae were incubated at 37°C, with counts of dead larvae recorded every 24 h for 5 days.

Chicken Cell Interaction and Invasion Assays

Isolation of chicken intestinal primary cells (Byrne et al., 2007) as well as interaction and invasion assays (Corcionivoschi et al., 2009) were performed as described previously. Briefly, biopsies from sections of small intestines from 6 to 12 week-old broiler chickens (Cobb 500) were placed in primary cell culture medium and primary cells were isolated. *C. jejuni* strains were grown for 24 h on Muller-Hinton agar under microaerobic conditions. Bacterial cells were washed and resuspended in tissue culture medium to an OD₆₀₀ of 0.4, then added to chicken intestinal primary cells grown in tissue culture plates to yield a multiplicity of infection of 1000:1. Plates were centrifuged and incubated for 3 h at 37°C in a microaerophilic environment. For interaction assays, infected monolayers were washed with PBS and treated with 0.1% v/v Triton X-100. Serial dilutions were performed and the CFUs/ml were enumerated. For invasion assays, infected monolayers were washed with PBS and treated with gentamicin (400 µg/ml) for 2 h at 37°C. Cells were then washed with PBS and treated with 0.1% v/v Triton X-100. Serial dilutions were performed and the CFUs/ml were enumerated.

Chicken Infection Assay

Thirty male broiler chickens (Ross 308) were housed in isolation units on wood shaving bedding. The temperature in the isolation unit was kept between 22–25°C and thermostatically controlled. Broilers were fed *ad libitum* with a standard diet. *C. jejuni* strains were grown on Muller Hinton plates for 24 h under microaerobic conditions and resuspended in sterile distilled water. At 15 days old, ten broilers were inoculated with approximately 1×10^8 CFU/ml of either the 488 wild-type strain, the 488 *issD* mutant or the 81–176 wild-type strain. The different batches of infected broilers were kept separated in sterile isolation units. After 3 days of infection, broilers were euthanized and *C. jejuni* was enumerated by analyzing the cecum content using the ISO17025 methodology for plate counting. All broilers were confirmed using cloacal swabs as being *Campylobacter* free at the

time of infection. These experiments were performed in triplicate on three separate occasions.

Statistical Analysis

All experiments were performed with at least three biological replicates and three technical replicates, unless otherwise stated. Statistical analyses were performed using GraphPad Prism 7 (GraphPad Software, United States) and data were presented as mean ± SEM. Results were compared using unpaired *t*-test with **p* ≤ 0.05, ***p* ≤ 0.01, ****p* ≤ 0.001.

DATA AVAILABILITY STATEMENT

The genome sequence datasets generated for this study can be found in EBI ENA, PRJEB31331.

ETHICS STATEMENT

The experiments were performed according to the legislation in place (Law 471/2002 and government ordinance 437/2002) and under the supervision of National Sanitary Veterinary Agency. The Ethics Committee of Banat University of Agricultural Sciences and Veterinary Medicine – King Michael I of Romania approved this work.

AUTHOR CONTRIBUTIONS

OG and ND conceived the study with input from AH and NC. JL, GH, CD, AE, FS, AS, and OG performed the experiments and contributed to this manuscript. JL, OG, and ND wrote the manuscript with significant input from LS, IP, NC, and BW.

FUNDING

The authors gratefully acknowledge the support of the Biotechnology and Biological Sciences Research Council Institute Strategic Programme BB/R012504/1 constituent project BBS/E/F/000PR10349. AH was supported by H2020-MSCA Global Fellowship grant 657766.

SUPPLEMENTARY MATERIAL

The Supplementary Material for this article can be found online at: <https://www.frontiersin.org/articles/10.3389/fmicb.2019.02864/full#supplementary-material>

REFERENCES

- Altschul, S. F., Gish, W., Miller, W., Myers, E. W., and Lipman, D. J. (1990). Basic local alignment search tool. *J. Mol. Biol.* 215, 403–410. doi: 10.1006/jmbi.1990.9999
- Ang, C. W., De Klerk, M. A., Endtz, H. P., Jacobs, B. C., Laman, J. D., van der Meche, F. G., et al. (2001). Guillain-Barre syndrome- and miller fisher syndrome-associated campylobacter *jejuni* lipopolysaccharides induce anti-GM1 and anti-GQ1b antibodies in rabbits. *Infect. Immun.* 69, 2462–2469. doi: 10.1128/IAI.69.4.2462-2469.2001

- Assefa, S., Keane, T. M., Otto, T. D., Newbold, C., and Berriman, M. (2009). ABACAS: algorithm-based automatic contiguation of assembled sequences. *Bioinformatics* 25, 1968–1969. doi: 10.1093/bioinformatics/btp347
- Bachmann, V., Kostiuk, B., Unterwiesing, D., Diaz-Satizabal, L., Ogg, S., and Pukatzki, S. (2015). Bile salts modulate the mucin-activated type VI secretion system of pandemic *Vibrio cholerae*. *PLoS Negl. Trop. Dis.* 9:e0004031. doi: 10.1371/journal.pntd.0004031
- Bacon, D. J., Alm, R. A., Burr, D. H., Hu, L., Kopecko, D. J., Ewing, C. P., et al. (2000). Involvement of a plasmid in virulence of *Campylobacter jejuni* 81-176. *Infect. Immun.* 68, 4384–4390. doi: 10.1128/iai.68.8.4384-4390.2000
- Basler, M., Pilhofer, M., Henderson, G. P., Jensen, G. J., and Mekalanos, J. J. (2012). Type VI secretion requires a dynamic contractile phage tail-like structure. *Nature* 483, 182–186. doi: 10.1038/nature10846
- Black, R. E., Levine, M. M., Clements, M. L., Hughes, T. P., and Blaser, M. J. (1988). Experimental *Campylobacter jejuni* infection in humans. *J. Infect. Dis.* 157, 472–479. doi: 10.1093/infdis/157.3.472
- Bleumink-Pluym, N. M., van Alphen, L. B., Bouwman, L. I., Wosten, M. M., and van Putten, J. P. (2013). Identification of a functional type VI secretion system in *Campylobacter jejuni* conferring capsule polysaccharide sensitive cytotoxicity. *PLoS Pathog.* 9:e1003393. doi: 10.1371/journal.ppat.1003393
- Bolger, A. M., Lohse, M., and Usadel, B. (2014). Trimmomatic: a flexible trimmer for Illumina sequence data. *Bioinformatics* 30, 2114–2120. doi: 10.1093/bioinformatics/btu170
- Brackmann, M., Wang, J., and Basler, M. (2018). Type VI secretion system sheath inter-subunit interactions modulate its contraction. *EMBO Rep.* 19, 225–233. doi: 10.15252/embr.201744416
- Byrne, C. M., Clyne, M., and Bourke, B. (2007). *Campylobacter jejuni* adhere to and invade chicken intestinal epithelial cells in vitro. *Microbiology* 153(Pt 2), 561–569. doi: 10.1099/mic.0.2006/000711-710
- Carver, T., Harris, S. R., Berriman, M., Parkhill, J., and McQuillan, J. A. (2012). Artemis: an integrated platform for visualization and analysis of high-throughput sequence-based experimental data. *Bioinformatics* 28, 464–469. doi: 10.1093/bioinformatics/btr703
- Cianfanelli, F. R., Monlezun, L., and Coulthurst, S. J. (2016). Aim, load, fire: the type VI secretion system, a bacterial Nanoweapon. *Trends Microbiol.* 24, 51–62. doi: 10.1016/j.tim.2015.10.005
- Coker, A. O., Isokpehi, R. D., Thomas, B. N., Amisu, K. O., and Obi, C. I. (2002). Human campylobacteriosis in developing countries. *Emerg. Infect. Dis.* 8, 237–244. doi: 10.3201/eid0803.010233
- Corcionivoschi, N., Clyne, M., Lyons, A., Elmi, A., Gundogdu, O., Wren, B. W., et al. (2009). *Campylobacter jejuni* cocultured with epithelial cells reduces surface capsular polysaccharide expression. *Infect. Immun.* 77, 1959–1967. doi: 10.1128/IAI.01239-1238
- Corcionivoschi, N., Gundogdu, O., Moran, L., Kelly, C., Scates, P., Stef, L., et al. (2015). Virulence characteristics of hcp (+) *Campylobacter jejuni* and *Campylobacter coli* isolates from retail chicken. *Gut Pathog.* 7:20. doi: 10.1186/s13099-015-0067-z
- Drebes Dorr, N. C., and Blokesch, M. (2018). Bacterial type VI secretion system facilitates niche domination. *Proc. Natl. Acad. Sci. U.S.A.* 115, 8855–8857. doi: 10.1073/pnas.1812776115
- EUCAST (2019). *Antimicrobial Susceptibility Testing: EUCAST Disk Diffusion Method*. Available at: http://www.eucast.org/ast_of_bacteria/disk_diffusion_methodology/ (accessed May 10, 2019).
- Fitzsimons, T. C., Lewis, J. M., Wright, A., Kleifeld, O., Schittenhelm, R. B., Powell, D., et al. (2018). Identification of novel *Acinetobacter baumannii* Type VI secretion system antibacterial effector and immunity pairs. *Infect. Immun.* 86:e00297-18. doi: 10.1128/IAI.00297-18
- Flint, A., Butcher, J., and Stintzi, A. (2016). Stress responses, adaptation, and virulence of bacterial pathogens during host gastrointestinal colonization. *Microbiol. Spectr.* 4:VMBF-0007-2015. doi: 10.1128/microbiolspec.VMBF-0007-2015
- Gerc, A. J., Diepold, A., Trunk, K., Porter, M., Rickman, C., Armitage, J. P., et al. (2015). Visualization of the *Serratia* Type VI secretion system reveals unprovoked attacks and dynamic assembly. *Cell Rep.* 12, 2131–2142. doi: 10.1016/j.celrep.2015.08.053
- Gish, W., and States, D. J. (1993). Identification of protein coding regions by database similarity search. *Nat. Genet.* 3, 266–272. doi: 10.1038/ng0393-266
- Gladman, S., and Seemann, T. (2012). *Velvet Optimiser*, v2.2.5.
- Gundogdu, O., da Silva, D. T., Mohammad, B., Elmi, A., Mills, D. C., Wren, B. W., et al. (2015). The *Campylobacter jejuni* MarR-like transcriptional regulators RrpA and RrpB both influence bacterial responses to oxidative and aerobic stresses. *Front. Microbiol.* 6:724. doi: 10.3389/fmicb.2015.00724
- Gundogdu, O., da Silva, D. T., Mohammad, B., Elmi, A., Wren, B. W., van Vliet, A. H., et al. (2016). The *Campylobacter jejuni* oxidative stress regulator RrpB is associated with a genomic hypervariable region and altered oxidative stress resistance. *Front. Microbiol.* 7:2117. doi: 10.3389/fmicb.2016.02117
- Gundogdu, O., Mills, D. C., Elmi, A., Martin, M. J., Wren, B. W., and Dorrell, N. (2011). The *Campylobacter jejuni* transcriptional regulator Cj1556 plays a role in the oxidative and aerobic stress response and is important for bacterial survival in vivo. *J. Bacteriol.* 193, 4238–4249. doi: 10.1128/JB.05189-5111
- Hachani, A., Wood, T. E., and Filloux, A. (2016). Type VI secretion and anti-host effectors. *Curr. Opin. Microbiol.* 29, 81–93. doi: 10.1016/j.mib.2015.11.006
- Harrison, J. W., Dung, T. T., Siddiqui, F., Korbrisar, S., Bukhari, H., Tra, M. P., et al. (2014). Identification of possible virulence marker from *Campylobacter jejuni* isolates. *Emerg. Infect. Dis.* 20, 1026–1029. doi: 10.3201/eid2006.130635
- Hermans, D., Pasmans, F., Heyndrickx, M., Van Immerseel, F., Martel, A., Van Deun, K., et al. (2012). A tolerogenic mucosal immune response leads to persistent *Campylobacter jejuni* colonization in the chicken gut. *Crit. Rev. Microbiol.* 38, 17–29. doi: 10.3109/1040841X.2011.615298
- Kaakoush, N. O., Castano-Rodriguez, N., Mitchell, H. M., and Man, S. M. (2015). Global epidemiology of *Campylobacter* infection. *Clin. Microbiol. Rev.* 28, 687–720. doi: 10.1128/CMR.00006-15
- Kapitein, N., Bonemann, G., Pietrosiuk, A., Seyffer, F., Hauser, I., Locker, J. K., et al. (2013). ClpV recycles VipA/VipB tubules and prevents non-productive tubule formation to ensure efficient type VI protein secretion. *Mol. Microbiol.* 87, 1013–1028. doi: 10.1111/mmi.12147
- Kapitein, N., and Mogk, A. (2014). Type VI secretion system helps find a niche. *Cell Host Microb.* 16, 5–6. doi: 10.1016/j.chom.2014.06.012
- Kim, J. C., Oh, E., Kim, J., and Jeon, B. (2015). Regulation of oxidative stress resistance in *Campylobacter jejuni*, a microaerophilic foodborne pathogen. *Front. Microbiol.* 6:751. doi: 10.3389/fmicb.2015.00751
- Kirchberger, P. C., Unterwiesing, D., Provenzano, D., Pukatzki, S., and Boucher, Y. (2017). Sequential displacement of Type VI secretion system effector genes leads to evolution of diverse immunity gene arrays in *Vibrio cholerae*. *Sci. Rep.* 7:45133. doi: 10.1038/srep45133
- Kovanen, S., Rossi, M., Pohja-Mykka, M., Nieminen, T., Raunio-Saarnisto, M., Sauvala, M., et al. (2018). Population genetics and characterization of *Campylobacter jejuni* isolates in western jackdaws and game birds in Finland. *Appl. Environ. Microbiol.* 85:e02365-18. doi: 10.1128/AEM.02365-18
- Kudryashev, M., Wang, R. Y., Brackmann, M., Scherer, S., Maier, T., Baker, D., et al. (2015). Structure of the type VI secretion system contractile sheath. *Cell* 160, 952–962. doi: 10.1016/j.cell.2015.01.037
- Lertpiriyapong, K., Gamazon, E. R., Feng, Y., Park, D. S., Pang, J., Botka, G., et al. (2012). *Campylobacter jejuni* type VI secretion system: roles in adaptation to deoxycholic acid, host cell adherence, invasion, and in vivo colonization. *PLoS One* 7:e42842. doi: 10.1371/journal.pone.0042842
- Li, H., and Durbin, R. (2009). Fast and accurate short read alignment with burrows-wheeler transform. *Bioinformatics* 25, 1754–1760. doi: 10.1093/bioinformatics/btp324
- Link, A. J., and LaBaer, J. (2011). Trichloroacetic acid (TCA) precipitation of proteins. *Cold Spring Harb. Protoc.* 2011, 993–994. doi: 10.1101/pdb.prot5651
- Losada, L., Shea, A. A., and DeShazer, D. (2018). A MarR family transcriptional regulator and subinhibitory antibiotics regulate type VI secretion gene clusters in *Burkholderia pseudomallei*. *Microbiology* 164, 1196–1211. doi: 10.1099/mic.0.000697
- Ma, L. S., Hachani, A., Lin, J. S., Filloux, A., and Lai, E. M. (2014). *Agrobacterium tumefaciens* deploys a superfamily of type VI secretion DNase effectors as weapons for interbacterial competition in planta. *Cell Host Microb.* 16, 94–104. doi: 10.1016/j.chom.2014.06.002
- Mougous, J. D., Cuff, M. E., Raunser, S., Shen, A., Zhou, M., Gifford, C. A., et al. (2006). A virulence locus of *Pseudomonas aeruginosa* encodes a protein secretion apparatus. *Science* 312, 1526–1530. doi: 10.1126/science.1128393
- Murdoch, S. L., Trunk, K., English, G., Fritsch, M. J., Pourkarimi, E., and Coulthurst, S. J. (2011). The opportunistic pathogen *Serratia marcescens* utilizes

- type VI secretion to target bacterial competitors. *J. Bacteriol.* 193, 6057–6069. doi: 10.1128/JB.05671-5611
- Newell, D. G., and Fearnley, C. (2003). Sources of *Campylobacter* colonization in broiler chickens. *Appl. Environ. Microbiol.* 69, 4343–4351. doi: 10.1128/aem.69.8.4343-4351.2003
- Noreen, Z., Jobichen, C., Abbasi, R., Seetharaman, J., Sivaraman, J., and Bokhari, H. (2018). Structural basis for the pathogenesis of *Campylobacter jejuni* Hcp1, a structural and effector protein of the Type VI Secretion System. *FEBS J.* 285, 4060–4070. doi: 10.1111/febs.14650
- Penner, J. L., Hennessy, J. N., and Congi, R. V. (1983). Serotyping of *Campylobacter jejuni* and *Campylobacter coli* on the basis of thermostable antigens. *Eur. J. Clin. Microbiol.* 2, 378–383. doi: 10.1007/bf02019474
- Poly, F., Threadgill, D., and Stintzi, A. (2004). Identification of *Campylobacter jejuni* ATCC 43431-specific genes by whole microbial genome comparisons. *J. Bacteriol.* 186, 4781–4795. doi: 10.1128/JB.186.14.4781-4795.2004
- Pukatzki, S., Ma, A. T., Sturtevant, D., Krastins, B., Sarracino, D., Nelson, W. C., et al. (2006). Identification of a conserved bacterial protein secretion system in *Vibrio cholerae* using the *Dictyostelium* host model system. *Proc. Natl. Acad. Sci. U.S.A.* 103, 1528–1533. doi: 10.1073/pnas.0510322103
- Ringel, P. D., Hu, D., and Basler, M. (2017). The role of Type VI secretion system effectors in target cell lysis and subsequent horizontal gene transfer. *Cell Rep.* 21, 3927–3940. doi: 10.1016/j.celrep.2017.12.020
- Ritz, M., Garenaux, A., Berge, M., and Federighi, M. (2002). Determination of *rpoA* as the most suitable internal control to study stress response in *C. jejuni* by RT-qPCR and application to oxidative stress. *J. Microbiol. Methods* 76, 196–200. doi: 10.1016/j.mimet.2008.10.014
- Robinson, D. A. (1981). Infective dose of *Campylobacter jejuni* in milk. *Br. Med. J.* 282:1584. doi: 10.1136/bmj.282.6276.1584
- Salih, O., He, S., Planamente, S., Stach, L., MacDonald, J. T., Manoli, E., et al. (2018). Atomic structure of Type VI contractile sheath from *Pseudomonas aeruginosa*. *Structure* 26, 329–336.e3. doi: 10.1016/j.str.2017.12.005
- Schmittgen, T. D., and Livak, K. J. (2008). Analyzing real-time PCR data by the comparative C(T) method. *Nat. Protoc.* 3, 1101–1108. doi: 10.1038/nprot.2008.73
- Seemann, T. (2014). Prokka: rapid prokaryotic genome annotation. *Bioinformatics* 30, 2068–2069. doi: 10.1093/bioinformatics/btu153
- Senior, N. J., Bagnall, M. C., Champion, O. L., Reynolds, S. E., La Ragione, R. M., Woodward, M. J., et al. (2011). *Galleria mellonella* as an infection model for *Campylobacter jejuni* virulence. *J. Med. Microbiol.* 60(Pt 5), 661–669. doi: 10.1099/jmm.0.026658-26650
- Si, M., Wang, Y., Zhang, B., Zhao, C., Kang, Y., Bai, H., et al. (2017). The Type VI secretion system engages a Redox-regulated dual-functional heme transporter for zinc acquisition. *Cell Rep.* 20, 949–959. doi: 10.1016/j.celrep.2017.06.081
- Sima, F., Stratakos, A. C., Ward, P., Linton, M., Kelly, C., Pinkerton, L., et al. (2018). A novel natural antimicrobial can reduce the *in vitro* and *in vivo* Pathogenicity of T6SS positive *Campylobacter jejuni* and *Campylobacter coli* chicken isolates. *Front. Microbiol.* 9:2139. doi: 10.3389/fmicb.2018.02139
- Simon, A. (2010). *FastQC*. Available at: <http://www.bioinformatics.babraham.ac.uk/projects/fastqc/>, v0.11.2 (accessed March 5, 2018).
- Skarp, C. P. A., Hanninen, M. L., and Rautelin, H. I. K. (2016). *Campylobacteriosis*: the role of poultry meat. *Clin. Microbiol. Infect.* 22, 103–109. doi: 10.1016/j.cmi.2015.11.019
- Trunk, K., Peltier, J., Liu, Y. C., Dill, B. D., Walker, L., Gow, N. A. R., et al. (2018). The type VI secretion system deploys antifungal effectors against microbial competitors. *Nat. Microbiol.* 3, 920–931. doi: 10.1038/s41564-018-0191-x
- Ugarte-Ruiz, M., Stabler, R. A., Dominguez, L., Porrero, M. C., Wren, B. W., Dorrell, N., et al. (2014). Prevalence of Type VI secretion system in spanish *Campylobacter jejuni* isolates. *Zoonoses Public Health* 62, 497–500. doi: 10.1111/zph.12176
- Ugarte-Ruiz, M., Stabler, R. A., Dominguez, L., Porrero, M. C., Wren, B. W., Dorrell, N., et al. (2015). Prevalence of type VI secretion system in spanish *Campylobacter jejuni* isolates. *Zoonoses Public Health* 62, 497–500. doi: 10.1111/zph.12176
- Wan, B., Zhang, Q., Ni, J., Li, S., Wen, D., Li, J., et al. (2017). Type VI secretion system contributes to Enterohemorrhagic *Escherichia coli* virulence by secreting catalase against host reactive oxygen species (ROS). *PLoS Pathog.* 13:e1006246. doi: 10.1371/journal.ppat.1006246
- Wang, T., Si, M., Song, Y., Zhu, W., Gao, F., Wang, Y., et al. (2015). Type VI Secretion system transports Zn²⁺ to combat multiple stresses and host immunity. *PLoS Pathog.* 11:e1005020. doi: 10.1371/journal.ppat.1005020
- Wiegand, I., Hilpert, K., and Hancock, R. E. (2008). Agar and broth dilution methods to determine the minimal inhibitory concentration (MIC) of antimicrobial substances. *Nat. Protoc.* 3, 163–175. doi: 10.1038/nprot.2007.521
- Wigley, P. (2015). Blurred lines: pathogens, commensals, and the healthy Gut. *Front. Vet. Sci.* 2:40. doi: 10.3389/fvets.2015.00040
- Williams, N. J., Jones, T. R., Leatherbarrow, H. J., Birtles, R. J., Lahuerta-Marin, A., Bennett, M., et al. (2010). Isolation of a novel *Campylobacter jejuni* clone associated with the bank vole, *Myodes glareolus*. *Appl. Environ. Microbiol.* 76, 7318–7321. doi: 10.1128/AEM.00511-10
- Wilson, D. L., Rathinam, V. A. K., Qi, W. H., Wick, L. M., Landgraf, J., Bell, J. A., et al. (2010). Genetic diversity in *Campylobacter jejuni* is associated with differential colonization of broiler chickens and C57BL/6J IL10-deficient mice. *Microbiology* 156, 2046–2057. doi: 10.1099/mic.0.035717-35710
- Young, K. T., Davis, L. M., and Dirita, V. J. (2007). *Campylobacter jejuni*: molecular biology and pathogenesis. *Nat. Rev. Microbiol.* 5, 665–679. doi: 10.1038/nrmicro1718
- Zerbino, D. R., and Birney, E. (2008). Velvet: algorithms for de novo short read assembly using de Bruijn graphs. *Genome Res.* 18, 821–829. doi: 10.1101/gr.074492.107

Conflict of Interest: The authors declare that the research was conducted in the absence of any commercial or financial relationships that could be construed as a potential conflict of interest.

Copyright © 2019 Liaw, Hong, Davies, Elmi, Sima, Stratakos, Stef, Pet, Hachani, Corcionivoschi, Wren, Gundogdu and Dorrell. This is an open-access article distributed under the terms of the Creative Commons Attribution License (CC BY). The use, distribution or reproduction in other forums is permitted, provided the original author(s) and the copyright owner(s) are credited and that the original publication in this journal is cited, in accordance with accepted academic practice. No use, distribution or reproduction is permitted which does not comply with these terms.